



Hart, Jaynee E. (2018) *Biochemical and genetic approaches to modulate phototropin photoreceptor sensitivity*. PhD thesis.

<https://theses.gla.ac.uk/30991/>

Copyright and moral rights for this work are retained by the author

A copy can be downloaded for personal non-commercial research or study, without prior permission or charge

This work cannot be reproduced or quoted extensively from without first obtaining permission from the author

The content must not be changed in any way or sold commercially in any format or medium without the formal permission of the author

When referring to this work, full bibliographic details including the author, title, awarding institution and date of the thesis must be given

Enlighten: Theses

<https://theses.gla.ac.uk/>  
[research-enlighten@glasgow.ac.uk](mailto:research-enlighten@glasgow.ac.uk)

**BIOCHEMICAL AND GENETIC APPROACHES TO  
MODULATE PHOTOTROPIN PHOTORECEPTOR  
SENSITIVITY**

By: Jaynee E. Hart

Thesis submitted for the degree of Doctor of Philosophy

College of Medical, Veterinary & Life Sciences

School of Life Sciences

University of Glasgow

October, 2018

© Jaynee Hart, 2018

## Abstract

The necessity of light for plants to sustain their autotrophic lifestyle has made the optimization of growth to maximize light capture a crucial strategy for survival in light-limiting environments. Increases in light capture can be achieved through alterations in plant architecture, such as modifications to leaf position and stem length. Responses to the light environment are mediated by a network of photoreceptor proteins, which sense specific wavelengths of light and respond to light excitation by initiating signaling. Higher plants respond to red and far-red light through the phytochrome family, blue light through cryptochromes, the zeaxanthin family, and phototropins, and UV-B light through the UV RESISTANCE LOCUS 8 photoreceptor. Of these photoreceptor proteins, the phototropins (phots) are perhaps the most closely tied to photosynthetic efficiency. Higher plant phots, phot1 and phot2, mediate leaf expansion to maximize the surface area available for light capture as well as control movement and positioning responses, such as petiole inclination, movement towards more favorable light conditions through phototropism, and, at a cellular level, chloroplast movement. Furthering the role of phots in optimizing responses upstream of photosynthesis, phot1 and phot2 also control stomatal opening in response to blue light, allowing the uptake of carbon dioxide into the leaf for fixation into sugars. In general, these responses are redundantly coordinated by both phot1 and phot2, with phot1 acting as the primary sensor due to its greater sensitivity. Because of the profound effect phots have on photosynthetic competence, the studies presented here examine phot1 with the goal of understanding the physiological role of phot1 sensitivity in plants and explore the possibility that enhancing phot1 sensitivity could increase plant growth.

Phots consist of two N-terminal light sensing LOV (Light, Oxygen or Voltage) domains, LOV1 and LOV2, coupled to a serine/threonine kinase domain at the C-terminus. Each of the LOV domains bind a flavin mononucleotide (FMN) chromophore that allows these domains to perceive blue light. In darkness, FMN is non-covalently bound within each of the LOV domains, which repress the activity of the kinase domain. When FMN is excited by blue light, a covalent bond is formed between a conserved cysteine residue present within each LOV domain and FMN. LOV2 specifically is coupled to the kinase domain through two alpha helices, J $\alpha$  and A' $\alpha$ , which become disordered following the formation of the covalent photoadduct. The unfolding of these alpha helices relieves repression of the kinase domain, initiating signaling. The onset of phot1 signaling is characterized by phot1 autophosphorylation and the dephosphorylation of the phot1 signaling partner NON-PHOTOTROPIC HYPOCOTYL 3 (NPH3). Over time, the covalent photoadduct decays and

phot1 returns to its inactive dark state, completing the photocycle. The chemistry of the phot1 photocycle *in vitro* is understood in detail, but its downstream signaling following activation remains relatively elusive, with only a handful of signaling partners and phosphorylation substrates identified. For the sensitivity of phot1 to be thoroughly explored, how the phot1 photocycle affects plant growth as well as how phot1 activity is modulated by signaling partners needed to be addressed. Therefore, a biochemical approach was used to introduce mutations within LOV2 to slow its dark reversion to prolong signaling and investigate how this modulates phot1 sensitivity *in vitro* and *in planta*, and, secondly, a genetic strategy was employed to uncover whether any signaling processes can modulate phot1 sensitivity in plants.

Compared to other photoreceptors that receive blue light through LOV domains, dark reversion of phot1 following a light stimulus is relatively fast, with the lit state lasting only approximately 15 minutes, while other LOV domains remain activated for many hours. To generate slow photocycle mutants of phot1, previous characterizations of slow photocycling LOV domains were exploited to engineer the phot1 photocycle to have a slower dark reversion by introducing mutations into LOV2. To study the photocycle *in vitro*, the phot1 light-sensing module consisting of the LOV1 and LOV2 domains (LOV1+LOV2) was heterologously expressed and purified from *E. coli* and the photocycle was measured spectrophotometrically. Using this approach, 13 LOV2 variants were generated and examined to identify slow photocycle mutants. Three mutations in LOV2, N476L, V478I, and L558I, were found to slow the LOV1+LOV2 photocycle *in vitro*. Following identification, these mutations were introduced into full-length phot1 expressed heterologously in insect cells to verify the autophosphorylation activity of each mutant.

Following the characterization of the candidate slow photocycle mutants *in vitro*, each phot1 photocycle mutant was examined *in planta* in a *phot1phot2* double mutant background to see whether possession of a slow photocycle increased phot1 sensitivity. Of the three candidate mutations, V478I and L558I were verified as possessing a slow dark reversion through the phosphorylation status of NPH3. NPH3 is dephosphorylated in a phot1-dependent manner following light treatment; it was found that in the presence of wild-type phot1, the phosphorylated form of NPH3 is recovered around one hour following a return to darkness after phot1 stimulation by blue light. By contrast, the dephosphorylated state of NPH3 was sustained in phot1-V478I and -L558I for a substantially longer period of time, consistent with a slow phot1 photocycle and prolonged phot1 activation in these mutants. Surprisingly, it was found that these mutants were less sensitive than wild-type phot1 for

phototropism in response to low intensity light treatments. Furthermore, biomass accumulation was not increased in the *phot1-L558I* mutant under growth conditions consisting of very low light. While the photocycle mutants did not exhibit increased sensitivity or growth in response to continuous light treatments, evidence from collaborators indicated that *phot1-L558I* is more efficient than wild-type *phot1* for the chloroplast accumulation response following brief pulses of blue light. While the role of the *phot1* photocycle under continuous irradiation remained unclear, this enhanced chloroplast accumulation response implies that the *phot1* photocycle is important for its sensitivity to brief irradiations. Unlike *phot1*, further work with *phot2* later indicated that introducing a slow photocycle mutation to *phot2* LOV2 can significantly increase growth in a *phot1phot2* mutant background under continuous low light.

To investigate other factors that may affect *phot1* sensitivity, a genetic screen was undertaken in an attempt to identify suppressors of *phot1* activity. The LOV2Kinase (L2K) transgenic line, which expresses a truncated version of *phot1* in a *phot1phot2* double mutant background, was previously found to be unable to respond to low-intensity blue light, though it can mediate *phot1* responses when the light intensity is increased. Because L2K possesses this conditional phenotype, random mutations were introduced into the genome of L2K-expressing plants and a screen was established to identify mutants that were able to respond to low-intensity light with the hypothesis that those mutations could lie within suppressors of *phot1* activity, allowing L2K to signal under circumstances where it ordinarily could not. Using this approach, three independent candidate suppressor mutants were identified that had increased sensitivity for the petiole positioning response under low light. One suppressor mutant was identified as a novel allele of the phytochrome B red light receptor, the second is likely to be a mutant of the transcription factor SQUAMOSA PROMOTOR BINDING LIKE 14, and the identity of the third candidate suppressor is still not known, though it overexpressed the L2K protein. These candidate suppressors may represent novel modulators of *phot1* activity and possible mechanisms for how these candidate suppressors may act on *phot1* activity are discussed.

In summary, both the biochemical and genetic approaches yielded mutants with increased sensitivity for *phot1*-mediated responses, enabling a more detailed understanding of how *phot1* sensitivity influences its activity and plant growth. This lays the groundwork for extending the increased sensitivity observed in response to pulses in the photocycle mutants to responses other *phot1*-mediated responses, and for integrating new models of suppression of *phot1* activity into our framework for *phot1* activation and signaling.

# Table of Contents

<b>Abstract</b> .....	<b>2</b>
<b>List of Tables</b> .....	<b>9</b>
<b>List of Figures</b> .....	<b>10</b>
<b>Accompanying Material</b> .....	<b>13</b>
<b>Acknowledgements</b> .....	<b>14</b>
<b>Author's Declaration</b> .....	<b>15</b>
<b>Abbreviations</b> .....	<b>16</b>
<b>Chapter 1 Photoperception and Sensitivity of <i>Arabidopsis</i> Photoreceptors</b> .....	<b>19</b>
1.1 <i>Light is an environmental signal in addition to an energy source</i> .....	19
1.2 <i>Introduction to plant photoreceptor families</i> .....	20
1.2.1 Phytochromes .....	20
1.2.2 Cryptochromes.....	23
1.2.3 UV-RESISTANCE LOCUS 8 .....	26
1.2.4 Zeirupe family photoreceptors.....	27
1.2.5 Phototropins .....	30
1.3 <i>Modulating photoreceptor sensitivity</i> .....	43
1.3.1 Photoreceptor overexpression.....	43
1.3.2 Constitutively active photoreceptor variants.....	44
1.3.3 Targeting photoreceptor sensitivity through photocycles.....	45
1.4 <i>Project aims</i> .....	47
<b>Chapter 2 Materials and Methods</b> .....	<b>49</b>
2.1 <i>Materials used in this study</i> .....	49
2.2 <i>DNA isolation</i> .....	49
2.2.1 Plasmid DNA isolation .....	49
2.2.2 Genomic DNA isolation from <i>Arabidopsis</i> .....	49
2.3 <i>DNA cloning and manipulation</i> .....	50
2.3.1 DNA agarose gel electrophoresis .....	50
2.3.2 Gel purification.....	51
2.3.3 Primer design .....	51
2.3.4 Polymerase chain reaction (PCR) .....	51
2.3.5 DNA digestion.....	54
2.3.6 DNA ligation .....	55
2.3.7 Cloning techniques.....	55
2.3.8 DNA sequencing.....	60
2.4 <i>RNA isolation</i> .....	60
2.5 <i>Isolation of whole protein extracts</i> .....	60
2.5.1 Isolation of whole protein extracts from <i>Arabidopsis</i> seedlings .....	60
2.5.2 Isolation of whole protein extracts from mature plants .....	60
2.5.3 Isolation of soluble protein extracts from Sf9 insect cells .....	61
2.6 <i>Determination of protein content</i> .....	61
2.6.1 Bradford assay.....	61
2.6.2 Absorbance at 450 nanometers.....	61
2.7 <i>Protein electrophoresis and Western Blotting</i> .....	62

2.7.1 SDS-Polyacrylamide gel electrophoresis (SDS-PAGE) .....	62
2.7.2 Coomassie staining and gel drying .....	62
2.7.3 Western blotting .....	62
2.8 <i>Sequence alignment</i> .....	64
2.9 <i>Bacterial transformation and growth</i> .....	64
2.9.1 Generation of chemically competent <i>E. coli</i> .....	64
2.9.2 Transformation of chemically competent <i>E. coli</i> .....	64
2.9.3 Generation of electrocompetent <i>Agrobacterium tumefaciens</i> cells.....	65
2.9.4 Transformation of <i>Agrobacterium</i> by electroporation .....	65
2.10 <i>Heterologous expression and purification of proteins in E. coli</i> .....	65
2.10.1 Heterologous protein expression in <i>E. coli</i> .....	65
2.10.2 Affinity chromatography purification of proteins .....	66
2.10.3 TEV cleavage of the 6xHis tag from LOV2 .....	67
2.10.4 Size exclusion chromatography.....	68
2.11 <i>NMR spectroscopy</i> .....	68
2.12 <i>UV-Vis spectroscopy</i> .....	68
2.12.1 Generation of dark absorption spectra .....	69
2.12.2 Generation of light-minus-dark absorption spectra.....	69
2.12.3 Calculation of percent photoproduct remaining.....	69
2.13 <i>Culture and transfection of Sf9 insect cells</i> .....	69
2.13.1 Culture of Sf9 cells.....	69
2.13.2 Transfection of Sf9 cells to express phot1 .....	70
2.14 <i>Autophosphorylation assays</i> .....	71
2.15 <i>Arabidopsis growth</i> .....	72
2.15.1 Plant materials .....	72
2.15.2 <i>Arabidopsis</i> growth conditions.....	72
2.15.3 Surface sterilization of seeds.....	72
2.15.4 Isolation of microsomal membranes from <i>Arabidopsis</i> .....	73
2.16 <i>Generation of transgenic Arabidopsis</i> .....	73
2.16.1 <i>Arabidopsis</i> transformation by floral dip .....	73
2.16.2 Selection of transformants.....	74
2.17 <i>Screen for suppressors of LOV2Kinase</i> .....	75
2.18 <i>Physiological evaluation of Arabidopsis</i> .....	75
2.18.1 Phototropism .....	75
2.18.2 Leaf flattening .....	76
2.18.3 Chloroplast accumulation .....	76
2.18.4 Petiole positioning .....	77
2.18.5 Fresh and dry weight determination.....	77
2.18.6 Hypocotyl elongation .....	77
2.18.7 Phot1 modulation of gravity sensing .....	77
2.19 <i>Use of BiFC to probe phot1 dimerization</i> .....	78
<b>Chapter 3 Modifying the Phot1 Photocycle <i>in vitro</i></b> .....	<b>80</b>
3.1 <i>Introduction</i> .....	80
3.2 <i>Results</i> .....	81
3.2.1 Characterization of the wild-type LOV1+LOV2 photocycle .....	81
3.2.2 Addition of the Zeitlupe-family FAD loop to LOV1+LOV2 .....	83
3.2.3 Mutagenesis of LOV1+LOV2 based on a naturally occurring slow photocycling LOV domain .....	86
3.2.4 Photocycle mutations within the flavin binding pocket of LOV2 .....	88
3.2.5 Substitutions on the LOV2 surface .....	94
3.2.6 Combination of slow photocycle mutations in LOV1+LOV2.....	98
3.2.7 Photocycle mutants selected for further study.....	100

3.2.8 <i>In vitro</i> autophosphorylation assays indicate photocycle mutant functionality in full-length phot1 .....	101
3.3 Discussion .....	102
3.3.1 The ztl-family FAD loop insertion abolishes photoreactivity in LOV2 .....	102
3.3.2 The LOV1+LOV2 photocycle can be effectively altered with point mutations.....	103
3.3.3 Surface substitutions slow the photocycle as much as substitutions within the FMN binding pocket .....	105
3.3.4 The photocycle mutants in full-length phot1 are functional <i>in vitro</i> .....	106
<b>Chapter 4 Investigating the Phot1 Photocycle <i>in planta</i> .....</b>	<b>107</b>
4.1 Introduction .....	107
4.2 Results.....	108
4.2.1 Expression of photocycle mutants of phot1 <i>in planta</i> .....	108
4.2.2 The phot1 photocycle mutants are biochemically active.....	109
4.2.3 The photocycle mutants complement phot1-mediated responses <i>in planta</i> .....	111
4.2.4 NPH3 phosphorylation status confirms the slow photocycle of phot1-V478I and -L558I .....	116
4.2.5 Phototropism of the photocycle mutant lines across multiple fluence rates does not indicate increased sensitivity .....	118
4.2.6 The phot1-L558I photocycle mutants do not accumulate more biomass than phot1-GFP under low light.....	119
4.2.7 Structural probe of low functionality in variants of V478 .....	120
4.2.8 Dimerization is not perturbed in phot1-V478I or -V478L in the light <i>in planta</i> .....	125
4.2.9 Determining the region of phot1 dimerization .....	127
4.3 Discussion .....	130
4.3.1 The photocycles of V478I and L558I are slow <i>in planta</i> as well as <i>in vitro</i> .....	131
4.3.2 The photocycle mutants are functional to varying degrees.....	132
4.3.3 The chemical shift of W553 in LOV2-V478L upon light exposure does not appear to underpin the low functionality of phot1-V478L.....	134
4.3.4 Dimerization of phot1 .....	134
4.3.5 Phot1 sensitivity and the photocycle .....	136
<b>Chapter 5 Identification of Putative Suppressors of Phot1 activity .....</b>	<b>138</b>
5.1 Introduction .....	138
5.2 Results.....	140
5.2.1 L2K requires intense light to drive phototropism .....	140
5.2.2 An EMS screen for altered petiole identified three potential suppressor mutants of L2K .....	142
5.2.3 Rosette phenotypes and biomass accumulation of the EMS mutants.....	145
5.2.4 The 24B and 24C mutants have increased sensitivity for phototropism .....	147
5.2.5 The 24C mutant is vertically oriented under low blue light .....	148
5.2.6 The 24C mutant overexpresses the L2K protein .....	152
5.2.7 L2K is an active kinase in the 24C mutant background .....	154
5.2.8 The 24C and 21D mutants have a long hypocotyl phenotype specific to red light .....	156
5.2.9 The 24C and 21D mutants both encode the same mutant allele of <i>PHYB</i> .....	158
5.2.10 Inheritance of the suppressor phenotypes .....	160
5.2.11 Genomic deep sequencing of 24B and 24C yields candidate suppressor SNPs .....	162
5.3 Discussion .....	164
5.3.1 The isolated mutants may act as suppressors of phot1 activity .....	164
5.3.2 24C and 21D are <i>PHYB</i> mutants .....	166
5.3.3 The 24C mutant overexpresses L2K protein .....	170
5.3.4 The role of NPH3 in phot1 signal transduction .....	172
5.3.5 Candidate suppressors in the 24B and 24C backgrounds .....	173
<b>Chapter 6 General Discussion.....</b>	<b>176</b>
6.1 Introduction .....	176
6.2 Phot sensitivity and the photocycle .....	176

6.3 Examination of <i>phot1</i> -V478L functionality .....	185
6.4 Suppressors of <i>phot1</i> .....	189
6.4.1 Possible signal integration between <i>phyB</i> and <i>phot1</i> .....	192
6.5 Perspectives on <i>phot1</i> sensitivity .....	193
<b>Appendix to Chapter 3 .....</b>	<b>195</b>
<b>Appendix to Chapter 4 .....</b>	<b>196</b>
<b>Appendix to Chapter 5 .....</b>	<b>200</b>
<b>Appendix to Chapter 6 .....</b>	<b>206</b>
<b>List of References .....</b>	<b>209</b>

## List of Tables

<b>Table 2.1:</b> Mutagenic primers for PCR.	<b>53</b>
<b>Table 2.2:</b> qPCR primers used in this study.	<b>54</b>
<b>Table 2.3:</b> Expression constructs and the associated cloning primers or sources.	<b>58</b>
<b>Table 2.4:</b> Genomic DNA primers.	<b>59</b>
<b>Table 2.5:</b> Antibodies used in this study.	<b>63</b>
<b>Table 3.1:</b> Dark recovery half-lifetimes for all photocycle mutants in this study.	<b>100</b>
<b>Table 5.1</b> Petiole positioning in F <sub>1</sub> seedlings from the crosses between the L2K transgenic line and the EMS mutants.	<b>160</b>
<b>Table 5.2:</b> Petiole positioning in F <sub>2</sub> seedlings from crosses between the L2K transgenic line and the EMS mutants.	<b>161</b>
<b>Table 5.3:</b> Segregation of petiole positioning and hypocotyl elongation in F <sub>2</sub> seedlings from crosses between the L2K transgenic line and 24C mutants.	<b>162</b>
<b>Table 5.4:</b> Candidate genes for suppressors in the 24B mutant.	<b>163</b>
<b>Table 5.5:</b> Candidate genes for suppressors in the 24C mutant.	<b>163</b>

## List of Figures

<b>Figure 1.1:</b> Plant phytochrome domain structure and activity.	<b>22</b>
<b>Figure 1.2:</b> Plant cryptochrome domain structure and activity.	<b>25</b>
<b>Figure 1.3:</b> UVR8 activity.	<b>27</b>
<b>Figure 1.4:</b> Ztl family domain structure and activity.	<b>29</b>
<b>Figure 1.5:</b> Phot light sensing and activation.	<b>32</b>
<b>Figure 1.6:</b> Phot signal pathways for leaf flattening and positioning.	<b>35</b>
<b>Figure 1.7:</b> Phot signal pathway for phototropism.	<b>38</b>
<b>Figure 1.8:</b> Phot1 interacts with the NRL proteins NCH1 and RPT2 to bring about chloroplast accumulation.	<b>40</b>
<b>Figure 1.9:</b> Phot signal pathway for stomatal opening.	<b>42</b>
<b>Figure 3.1:</b> Photochemistry of wild-type LOV1+LOV2.	<b>82</b>
<b>Figure 3.2:</b> Addition of the nine amino acid ztl family FAD loop insertion to LOV2 in LOV1+LOV2.	<b>84</b>
<b>Figure 3.3:</b> Photoreactivity of ztl-i.	<b>86</b>
<b>Figure 3.4:</b> Photochemistry of T520R, a substitution based on a slow-recovering LOV domain.	<b>88</b>
<b>Figure 3.5:</b> Photochemistry of substitutions facing FMN: N511S and L558I.	<b>90</b>
<b>Figure 3.6:</b> Photochemistry of V478 substitutions facing FMN.	<b>92</b>
<b>Figure 3.7:</b> Photochemistry of substitutions facing FMN: L558I.	<b>93</b>
<b>Figure 3.8:</b> Photochemistry of amino acid substitutions on the LOV2 surface	<b>95</b>
<b>Figure 3.9:</b> Photochemistry of histidine substitutions on the LOV2 surface	<b>97</b>
<b>Figure 3.10:</b> Photochemistry of combinatorial substitutions.	<b>99</b>
<b>Figure 3.11:</b> Dark recovery kinetics of photocycle mutants selected for further study.	<b>101</b>
<b>Figure 3.12:</b> Autophosphorylation activity of the photocycle mutants <i>in vitro</i> .	<b>102</b>
<b>Figure 4.1:</b> Phot1 expression construct and phot1 protein expression in T <sub>3</sub> transgenic lines.	<b>109</b>
<b>Figure 4.2:</b> Electrophoretic mobility shifts of phot1-GFP and NPH3 in the photocycle mutants.	<b>110</b>
<b>Figure 4.3:</b> Leaf flattening of the photocycle mutants.	<b>112</b>
<b>Figure 4.4:</b> Chloroplast accumulation of the photocycle mutants.	<b>113</b>
<b>Figure 4.5:</b> Petiole positioning of photocycle mutants.	<b>114</b>
<b>Figure 4.6:</b> Phototropism of the photocycle mutants.	<b>115</b>

<b>Figure 4.7:</b> NPH3 phosphorylation status is altered in the photocycle mutants.	<b>117</b>
<b>Figure 4.8:</b> Phototropism of the photocycle mutants across varying fluence rates.	<b>119</b>
<b>Figure 4.9:</b> There is no gain in fresh weight accumulation in the L558I slow photocycle mutant under low light relative to phot1-GFP.	<b>120</b>
<b>Figure 4.10:</b> Comparison of V478I and V478L functionality <i>in planta</i> .	<b>122</b>
<b>Figure 4.11:</b> NMR and size exclusion chromatography analysis of LOV2-V478L.	<b>124</b>
<b>Figure 4.12:</b> Phot1-V478I and -V478L can dimerize.	<b>126</b>
<b>Figure 4.13:</b> The truncated phot1 protein LOV2Kinase can dimerize.	<b>128</b>
<b>Figure 4.14:</b> Dimerization pattern of LOV1+LOV2 and the phot1 kinase domain.	<b>130</b>
<b>Figure 5.1:</b> Phototropic responses of the L2K transgenic line.	<b>141</b>
<b>Figure 5.2:</b> L2K requires high intensity blue light to trigger NPH3 dephosphorylation.	<b>142</b>
<b>Figure 5.3:</b> Three EMS mutants of L2K have enhanced petiole positioning under low intensity light.	<b>143</b>
<b>Figure 5.4:</b> The L2K protein is wild-type in the 24B, 24C, and 21D mutants.	<b>144</b>
<b>Figure 5.5:</b> Rosette phenotypes and fresh and dry weights of the EMS mutants.	<b>146</b>
<b>Figure 5.6:</b> The 24B and 24C mutants show increased sensitivity to blue light.	<b>148</b>
<b>Figure 5.7:</b> Gravitropism is altered by differential sensitivity in the EMS mutants.	<b>151</b>
<b>Figure 5.8:</b> The 24C mutant has increased L2K protein and transcript levels.	<b>153</b>
<b>Figure 5.9:</b> Light-induced turnover of the L2K protein in the 24C mutant background is not altered.	<b>154</b>
<b>Figure 5.10:</b> The L2K protein 24C mutant background shows <i>in vitro</i> kinase activity.	<b>155</b>
<b>Figure 5.11:</b> The 24C and 21D mutants have long hypocotyls in red light.	<b>157</b>
<b>Figure 5.12:</b> <i>PHYB</i> is mutated in the 24C and 21D mutants.	<b>159</b>
<b>Figure 6.1:</b> NPH3 phosphorylation and fresh weight accumulation in the phot2-V392L transgenic lines.	<b>180</b>
<b>Figure 6.2:</b> Illustration of the compromise between increasing phot sensitivity and introducing functional defects.	<b>183</b>
<b>Figure 6.3:</b> Position of V478 within LOV2.	<b>187</b>

- Figure 6.4:** Possible mechanisms of suppression in the 24C and 24B suppressor mutants. **191**
- Figure 6.5:** Hypothesized mechanisms for phy and phot1 interactions. **193**

## **Accompanying Material**

The data from the sequencing of the EMS mutants performed in Chapter 5 is deposited in the European Nucleotide Archive (Accession number: PRJEB29381).

## Acknowledgements

I would like to thank everyone who contributed to my PhD, especially those who aided in my training and development as a scientist. In particular, my supervisor, Professor John Christie, was an excellent mentor and was always available for chats about science. Professor Kevin Folta got me hooked on plant photobiology as my undergraduate supervisor, believed I could be a scientist, and has supported me ever since. It has also been a pleasure to work closely with Dr. Stuart Sullivan on my PhD project, whose contributions and perspectives helped propel the project and made my work better. Dr. Jan Petersen patiently helped and trained me during the early days of my work, for which I am very grateful. Conversations with Dr. Noriyuki Suetsugu were always illuminating and helpful. Likewise, everyone else in the Brian Lab have been both labmates and friends to me over the past four years. Joint lab meetings with Dr. Eirini Kaiserli and her lab were also immensely helpful in grounding my work. For the work on the photocycle, our collaborator and friend Dr. Justyna Łabuz helped with analysis of our mutants. For my genetic screen, I would like to thank Dr. Bobby Brown for performing the EMS mutagenesis and establishing the F<sub>2</sub> population and Dr. Graham Hamilton at Glasgow Polyomics for analyzing the deep sequencing data. I feel massive amounts of gratitude to the Gatsby Foundation for supporting my work, training me, and enabling me to come to the UK to conduct my PhD on the research I love.

I could not have gotten this far without the unwavering support of my dad, whose love and kindness are the foundation of my achievements and the person I have become. The additional support of my sister, mom, and the Yarn Cake Knit-Nighters cannot be overstated; in particular, I want to thank very stable geniuses Dr. Vicki Henderson and Dr. Gillian Borland for helping me maintain my sanity and keeping me in the wool. Gillian also kindly assisted in proofreading this thesis. Dr. Jonathan Schnabel, Bob Rooney, and Georgia Kirby were always available for thesis- and life-related discussions and always made me feel better. My sincerest gratitude belongs to these people and to all the others who enabled my work.

## **Author's Declaration**

I declare that, except where explicit reference is made to the contribution of others, this thesis is the result of my own work and has not been submitted for any other degree at the University of Glasgow or any other institution.

Jayne Hart

Signature:

## Abbreviations

A table of abbreviations used in this thesis follows:

ABCB19	ATB BINDING CASSETTE B19
ADO	ADAGIO
AHA1	H <sup>+</sup> -ATPASE 1
<sup>32</sup> P-ATP	Adenosine 5'- $\gamma$ - <sup>32</sup> P-triphosphate
35S	Cauliflower mosaic virus 35S promoter
BIC	BLUE LIGHT INHIBITOR OF CRYPTOCHROME
BIFC	Bimolecular Fluorescence Complementation
BHP1	BLUE LIGHT DEPENDENT H <sup>+</sup> -ATPASE PHOSPHORYLATION 1
BSA	Bovine serum albumin
BLUS1	BLUE LIGHT SIGNALING 1
CBC1	CONVERGENCE OF BLUE LIGHT AND CO <sub>2</sub> 1
CCT	Cryptochrome C-terminal Domain
cDNA	Complementary DNA
CDF	CYCLING DOF FACTOR
CHS	CHALCONE SYNTHASE
CHUP	CHLOROPLAST UNUSUAL POSITIONING
CIB	CRYPTOCHROME-INTERACTING BASIC HELIX LOOP HELIX
CO	CONSTANS
CO <sub>2</sub>	Carbon dioxide
COP	Constitutively photomorphogenic
cry	Cryptochrome
CUL	CULLIN
D6PK	D6 PROTEIN KINASE
DASH	<i>Drosophila</i> , <i>Arabidopsis</i> , <i>Synechocystis</i> , Human homology domain
dH <sub>2</sub> O	Distilled water
dNTPs	Deoxyribonucleotide triphosphates
DNA	Deoxyribonucleic acid
DR5	Synthetic auxin response element
ELF3	EARLY FLOWERING 3
EMS	Ethyl methane sulfonate
FAD	Flavin adenine dinucleotide
FBP	F-Box protein
fkf1	Flavin-binding, kelch repeat, F-box 1
fkf1-i	phot1 LOV1+LOV2 encompassing the fkf1 insertion
FMN	Flavin mononucleotide
FT	FLOWERING LOCUS T

GAF	cGMP-specific and -regulated cyclic nucleotide phosphodiesterase, Adenylyl cyclase and FhIA homology domain
GFP	Green fluorescent protein
GI	GIGANTEA
GUS	$\beta$ -glucuronidase
HKRD	Histidine Kinase Related Domain
HY5	ELONGATED HYPOCOTYL 5
HSQC	Heteronuclear Single Quantum Coherence
IPTG	Isopropyl $\beta$ -D-galactopyranoside
KAC	KINESIN-LIKE PROTEIN FOR ACTIN-BASED CHLOROPLAST MOVEMENT
kDa	Kilodaltons
LHCB	LIGHT HARVESTING CHLOROPHYLL BINDING
L2K	LOV2KINASE
LKP2	LOV Kelch Protein 2
LOV	Light, Oxygen or Voltage sensitive
mg	milligram
ml	milliliter
MTHF	Methenyltetrahydrofolate
NCH1	NRL PROTEIN FOR CHLOROPLAST MOVEMENT 1
nm	Nanometres
NMR	Nuclear magnetic resonance
NPH	NONPHOTOTROPIC HYPOCOTYL
NRL	NPH3/RPT2-like
OD	Optical density
p1-GFP	phot1 tagged C-terminally with GFP
<i>p1p2</i>	<i>phot1-5 phot2-1</i> double mutant
P <sub>FR</sub>	Far-red absorbing, biologically active phytochrome
P <sub>R</sub>	Red absorbing, inactive phytochrome
PAS	Per/Arnt/Sim
PCH1	PERIODIC CONTROL OF HYPOCOTYL
PCR	Polymerase chain reaction
phot	Phototropin
PHR	Photolyase Homology Region
phy	Phytochrome
PIF	PHYTOCHROME INTERACTING FACTOR
PIN	PIN-FORMED
PKS	PHYTOCHROME KINASE SUBSTRATE
PP1	PROTEIN PHOSPHATASE 1
PP2A	PROTEIN PHOSPHATASE 2A
PPK	PHOTOACTIVATED PROTEIN KINASE
PRR5	PSEUDO RESPONSE REGULATOR 5
RBCL	RIBULOSE BISPHOSPHATE CARBOXYLASE LARGE CHAIN
RNA	Ribonucleic acid
RPT	ROOT PHOTOTROPISM

RUP	REPRESSOR OF UV-B PHOTOMORPHOGENESIS
SAS	Shade Avoidance Syndrome
SCF	SKP1–CUL1–FBP (SKP, CULLIN, F BOX PROTEIN)
SDS	Sodium dodecyl sulfate
SDS-PAGE	SDS-polyacrylamide gel electrophoresis
Sf9	<i>Spodoptera frugiperda</i> cell line
SLAC1	SLOW ANION CHANNEL ASSOCIATED 1
SLAH1	SLOW ANION CHANNEL HOMOLOGUE 1
SNP	Single Nucleotide Polymorphism
SPA	SUPPRESSOR OF PHYTOCHROME A
SPL	SQUAMOSA PROMOTER BINDING LIKE
SR	Short and Raised
T-DNA	Transfer-DNA
TOC1	TIMING OF CAB 1
UV	Ultra-violet
UVR8	UV-RESISTANCE LOCUS 8
v/v	volume/volume
VVD	Vivid
w/v	weight/volume
WCC	White Collar Complex
YFP	Yellow Fluorescent Protein
YHB	Constitutively active phyB with the Y276H mutation
ztl	zeitlupe
ztl-i	phot1 LOV1+LOV2 encompassing the fkf1 insertion

# Chapter 1 Photoperception and Sensitivity of *Arabidopsis* Photoreceptors

## 1.1 Light is an environmental signal in addition to an energy source

Though light perception in plants is often considered with respect to the photosynthetic apparatus, the necessity of light capture for plant survival has engendered the evolution of a sophisticated network of photoreceptors that respond to ambient light as a signal (Li and Mathews, 2016). This network of photoreceptors has partly specialized in the evasion of suboptimal light conditions. The phototropin (phot) blue light photoreceptors (Christie, 2007; Christie *et al.*, 2015) are especially elegantly tuned for this purpose and can initiate directional growth, termed phototropism, toward more favorable light environments. Additionally, phot1 control petiole angle (Inoue *et al.*, 2008), triggering petiole inclination to optimize light capture, and chloroplast positioning (Jarillo *et al.*, 2001; Kagawa *et al.*, 2001; Sakai *et al.*, 2001; Kasahara, Kagawa, *et al.*, 2002), re-localizing chloroplasts within cells to either increase light capture or avoid damaging irradiation. In another mechanism evolved to escape low-intensity light, shaded conditions initiate a series of responses called Shade Avoidance Syndrome (SAS), which also leads to raised petioles, in addition to rapid elongation of the primary stem to attempt to overtop the neighboring plants producing the shade. SAS is mediated by both the red/far-red perceiving phytochrome family of photoreceptors (phys; Franklin and Quail, 2010), and the blue light responsive cryptochromes (crys; Chaves *et al.*, 2011).

Aside from modulating growth habit to enhance light capture, photoreceptors are crucial for plant development from the moment seedlings emerge from the soil. Phys (Franklin and Quail, 2010), crys (Chaves *et al.*, 2011), and the UV-perceiving protein UV RESISTANCE LOCUS 8 (UVR8; Jenkins, 2017) act together to activate the transcriptional programs that initiate photomorphogenesis, which entails inhibition of hypocotyl elongation and the development of chloroplasts, leading to photosynthetic competence. Light is also important for appropriate plant development as they mature. Photoreceptors, including phys, crys, and the blue light perceiving Zeitzlupe family (ztl; Ito, Song and Imaizumi, 2012), facilitate estimation of daylength and the time of year in order to flower at an optimal time (Song, Ito and Imaizumi, 2013). All of these processes require complex coordination in order to manage development and optimize growth for a particular light environment. Taken

together, light perception by photoreceptor proteins has a profound impact on growth and development, making comprehension of these proteins crucial to understanding plant physiology generally, as well as potentially providing targets for engineering plants to grow more efficiently in agricultural settings.

## 1.2 Introduction to plant photoreceptor families

### 1.2.1 Phytochromes

The red/far-red perceiving phytochrome photoreceptors are present in a diverse set of organisms, including bacteria, fungi, and plants (Li *et al.*, 2015A). The phytochromes are the best-characterized family of plant photoreceptors due to the far-reaching effects they have on physiological responses. Light sensing by phy impacts plant development through their roles in germination, photomorphogenesis and hypocotyl growth, plant architecture, and flowering time, and contribute to optimizing growth in response to the environment through temperature sensing, neighbor detection, and SAS (Franklin and Quail, 2010). Phys were recently found to be thermosensors, with their activity for responses such as inhibition of hypocotyl elongation controlled partly by temperature as well as light (thermomorphogenesis; Jung *et al.*, 2016; Legris *et al.*, 2016). This broad control of plant growth habit makes phy key regulators of plant physiology.

Phytochromes (phys) A, B, and C are present in most seed plants; *Arabidopsis* encodes five phytochrome genes, *PHYA* to *PHYE* (Sharrock and Quail, 1989; Mathews and Sharrock, 1996). Phylogenetically, *PHYA* and *PHYC* are related to each other, while *PHYB* and *PHYD* share a large degree of sequence identity and form their own clade with *PHYE* (Mathews, 2010). In darkness, phytochromes (phys) exist in their inactive, red light absorbing form, termed P<sub>R</sub> (Rockwell, Su and Lagarias, 2006). Once illuminated with red light, the receptors become biologically active. The phy lit state absorbs far-red wavelengths most optimally and are therefore designated to be in the P<sub>FR</sub> state (Rockwell, Su and Lagarias, 2006). The active P<sub>FR</sub> form converts back to P<sub>R</sub> through both far-red irradiation and thermal reversion such that the pool of phy exists in a photoequilibrium of the P<sub>R</sub> and P<sub>FR</sub> states *in planta* (Rockwell, Su and Lagarias, 2006). In an exception to this general model, phyA is distinguished from the other phys due to its activity in response to continuous irradiation with far-red light (Nagatani, Reed and Chory, 1993; Parks and Quail, 1993; Whitelam *et al.*, 1993; Yanovsky, Casal and Whitelam, 1995; Hennig, Buche and Schafer, 2000), and because it is light-labile, becoming rapidly degraded with continuous red light treatment

(Clough and Vierstra, 1997; Hennig, Buche and Schafer, 2000). By contrast, the other phys are relatively stable in continuous red light (Somers *et al.*, 1991; Sharrock and Clack, 2002), with phyB present as the dominant phy in light-grown plants (Smith, 2000; Sharrock and Clack, 2002). This complex interplay between individual phys and their partially divergent roles, particularly between phyA and phyB, allows for powerful coordination that enables plants to respond appropriately to a wide array of light conditions (Franklin and Quail, 2010).

### 1.2.1.1 Phytochrome activation and signal transduction

Plant phytochromes can be divided into two regions: an N-terminal photosensory unit, consisting of the PAS, GAF, and PHY (Per, Arnt, Sim; cGMP phosphodiesterase, adenylate cyclase, FhLA; phytochrome) domains, with the GAF domain binding the phytochromobilin chromophore (Lagarias and Rapoport, 1980; Rockwell, Su and Lagarias, 2006), and a C-terminal unit made up of two tandem PAS domains, PAS1 and PAS2, followed by a histidine kinase related domain (Rockwell, Su and Lagarias, 2006; Figure 1.1A). While expression of the PAS/GAF/PHY region of phyB *in planta* is sufficient to complement phy responses, the C-terminal region has been shown to be mostly important for regulating phy activity (Wagner and Quail, 1995; Chen, Schwab and Chory, 2003; Matsushita, Mochizuki and Nagatani, 2003; Oka *et al.*, 2004), though the phyB C-terminus expressed on its own *in planta* retains a small degree of activity for hypocotyl growth inhibition (Qiu *et al.*, 2017).

Upon light perception, phys translocate from the cytoplasm to the nucleus, which is the primary site of phy activity (Sakamoto and Nagatani, 1996; Hisada *et al.*, 2000; Kircher *et al.*, 2002; Huq, Al-Sady and Quail, 2003). Within the nucleus, phys localize to small loci called photobodies (Kircher *et al.*, 1999; Yamaguchi *et al.*, 1999). The exact role of photobodies in phy function is not understood, though their formation is important for efficient signaling and full complementation of phy-mediated responses (Chen, Schwab and Chory, 2003; Matsushita, Mochizuki and Nagatani, 2003). What is known about phy nuclear action is that phy activation controls transcriptional programs through PHYTOCHROME INTERACTING FACTOR (PIF) basic helix-loop-helix transcription factors (reviewed in Leivar and Monte, 2014; Figure 1.1B). Phy light activation leads to phosphorylation of both the phys themselves as well as PIFs, leading to rapid turnover of both proteins (Figure 1.1B; Al-Sady *et al.*, 2006; Shen *et al.*, 2007, 2008; Ni *et al.*, 2014). Though there is some evidence that the phytochromes themselves are kinases and are responsible for the phosphorylation of both themselves and the PIFs (Fankhauser *et al.*, 1999; Shin *et al.*, 2016), new findings suggest that this phosphorylation cascade is primarily mediated through

PHOTOACTIVATED PROTEIN KINASES (PPKs; Figure 1.1B; Ni *et al.*, 2017). In either case, the degradation of PIFs leads to transcriptional repression of PIF target genes, which generally promote a “dark growth” or skotomorphogenic developmental program, allowing the initiation of phy-mediated responses such as photomorphogenesis (Leivar and Monte, 2014). Many of the alterations in transcription resulting from phy activity lead to changes to the biosynthesis and transport of plant hormones, particularly auxin, which produce the downstream effects on plant growth (Halliday and Fankhauser, 2003; Halliday, Martínez-García and Josse, 2009). Through this deceptively simple signaling mechanism, phys exert their control on plant growth and development.

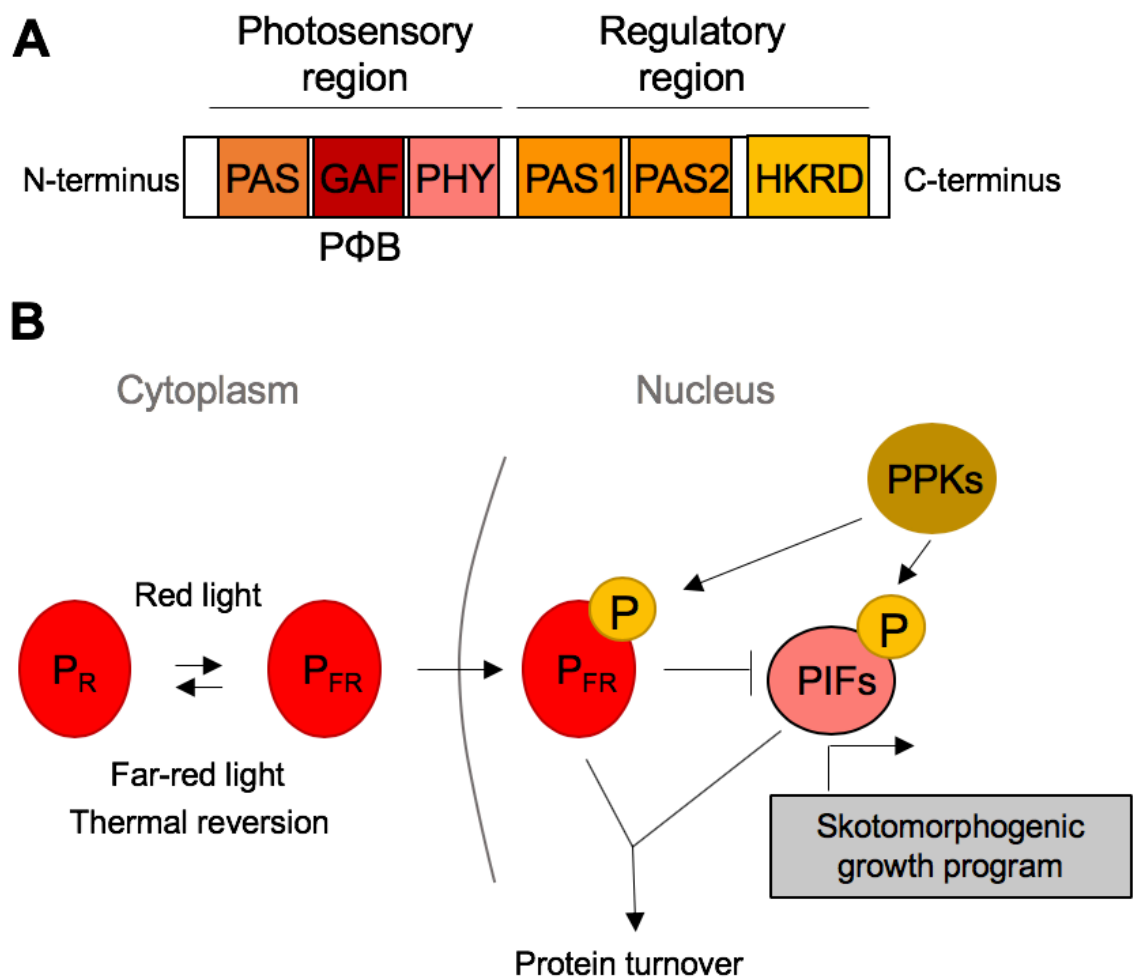


**Figure 1.1: Plant phytochrome domain structure and activity.** **A.** Phytochrome domains. The phy N-terminus is the portion of the protein that senses light and consists of a PAS domain, a GAF domain where the phytochromobilin (PΦB) chromophore binds, and a PHY domain. The C-terminus regulates activity of the protein and has two tandem PAS domains, PAS1 and PAS2, followed by a histidine kinase related domain (HKRD). **B.** Phytochrome light sensing and activity. Phytochrome is translated in its biologically inactive P<sub>R</sub> form and converts to its active P<sub>FR</sub> form upon perception of red light. The P<sub>FR</sub> form can convert back to P<sub>R</sub> either following irradiation with far-red light or thermal reversion. Activated phy translocates to the nucleus, where it interacts with PIFs to inhibit the transcription of genes involved in skotomorphogenic, or dark growth, development. This phy/PIF interaction leads to phosphorylation by PPKs and the turnover of both phys and PIFs. Arrows indicate activation, and lines ending in another perpendicular line indicate inhibition.

## 1.2.2 Cryptochromes

Of the three UV-A/blue light perceiving photoreceptor families present in *Arabidopsis*, the cryptochrome (cry) family perhaps plays the most diverse set of roles, affecting plant development from emergence from the soil to flowering time (Christie *et al.*, 2015; Wang *et al.*, 2018). Crys are descended from DNA-repairing bacterial photolyases, and bear some homology to those enzymes, though the activity of some plant and animal crys has diverged into light signaling and maintenance of the circadian clock (Chaves *et al.*, 2011). There are three CRY genes in *Arabidopsis*: *CRY1* to *CRY3* (Chaves *et al.*, 2011). While cry1 and cry2 are canonical plant photoreceptors and act primarily in the nucleus (Cashmore *et al.*, 1999; Guo *et al.*, 1999), cry3 localizes to chloroplasts and mitochondria and seems to show activity for repair of single stranded DNA (Kleine, Lockhart and Batschauer, 2003; Selby and Sancar, 2006). Cry1 and cry2 act cooperatively to promote photomorphogenesis and de-etiolation in monochromatic blue light (Ahmad and Cashmore, 1993; Lin *et al.*, 1998) but show divergent functions in the cry1 mediation of SAS as well as thermomorphogenesis (Keller *et al.*, 2011; Ma *et al.*, 2016; Pedmale *et al.*, 2016), and the profound effect cry2 specifically has on flowering time (Guo *et al.*, 1998; H. Liu *et al.*, 2008; L.J. Liu *et al.*, 2008). In a regulatory mechanism comparable to phyA and phyB, cry1 is light stable and present in light-grown plants, while cry2 is light labile (Ahmad *et al.*, 1998; Lin *et al.*, 1998). Through the activity of both cry1 and cry2, plant blue light perception can coordinate both development and environmental responses.

### 1.2.2.1 Cryptochrome activation and signaling

Cry1 and cry2 are made up of two domains: an N-terminal photolyase homology region (PHR), and a C-terminal cryptochrome extension (CCT; Figure 1.2A; Chaves *et al.*, 2011; Christie *et al.*, 2015). Both proteins bind two chromophores within the PHR domain: a UV-A absorbing methenyltetrahydrofolate (MTHF), and a UV-A/blue light receiving flavin adenine dinucleotide (FAD; Figure 1.2A; Chaves *et al.*, 2011; Christie *et al.*, 2015). The FAD chromophore is fully oxidized in the dark (Chaves *et al.*, 2011). When excited by light, FAD is reduced to the neutral radical FADH<sup>•</sup>, leading to activation of the protein (Chaves *et al.*, 2011). There is some debate regarding the electron transfer that facilitates reduction of the FAD chromophore. Both cry1 and cry2 possess a conserved triad of tryptophans that are hypothesized by some to act as the electron donors for this process (Chaves *et al.*, 2011; Christie *et al.*, 2015). In the case of the *Drosophila* cryptochrome (Lin *et al.*, 2018) and in one report for cry1 (Zeugner *et al.*, 2005), mutation of these tryptophans to residues that

cannot participate in redox chemistry attenuates or eliminates the reduction of FAD *in vitro* and eliminates downstream signaling *in vivo*. Mutation of these residues in cry2, however, did not appear to abolish cry2 activity *in planta*, though in some cases cry2 became constitutively active (Li *et al.*, 2011). Contradicting the previous finding that *Arabidopsis* cry1 is not active when the tryptophan triad is mutated (Zeugner *et al.*, 2005), a later study reported that cry1 with these tryptophan mutations retained activity, making it similar to cry2 in this sense (Gao *et al.*, 2015). These latter two findings would indicate a photoreduction channel in *Arabidopsis* crys that does not involve the tryptophans. Regardless of the mechanism of electron transfer, the reduced FAD chromophore thermally reverts back to its oxidized state over time, completing its photocycle (Banerjee *et al.*, 2007). Interestingly, in addition to dark reversion, illumination of cry in its lit state with green light further reduces the flavin radical to FADH<sup>-</sup>, which also inactivates cry and possibly has implications for the role of cry1 in shade conditions, where green light is enriched relative to other wavelengths (Bouly *et al.*, 2007; Sellaro *et al.*, 2010; Ahmad, 2016). With hypotheses regarding the cry photocycle remaining hotly contested, undoubtedly further information regarding its mechanism and biological significance will continue to emerge.

In the cry dark state, the PHR and CCT domains are closely coordinated (Christie *et al.*, 2015; Wang *et al.*, 2018). Upon light excitation, the cry CCT is extensively phosphorylated by the PPKs and possibly other kinases, causing a conformational change that pushes the CCT away from the PHR (Christie *et al.*, 2015; Liu *et al.*, 2017; Wang *et al.*, 2018). This conformational change initiates homodimerization, which is required for cry function (Sang *et al.*, 2005; Rosenfeldt *et al.*, 2008), and allows for interaction with signaling partners (Chaves *et al.*, 2011; Christie *et al.*, 2015). In a negative feedback loop, cry activation induces the transcription of BLUE LIGHT INHIBITOR OF CRYPTOCHROME (BIC) 1 and 2 proteins, which physically interact with cry2 to inhibit its dimerization, negatively affecting the activity of both cry1 and cry2 for inhibition of hypocotyl elongation and flowering time (Figure 1.2B; Wang *et al.*, 2016, 2017).

The signal resulting from light sensing in cry1 and cry2 is transduced through alterations in transcription through two separate mechanisms. In the first, crys physically interact with the COP/SPA (CONSTITUITIVELY PHOTOMORPHOGENIC/SUPPRESSOR OF PHYTOCHROME A) ubiquitylation machinery to inhibit proteolysis of transcriptional activators of photomorphogenic growth (Figure 1.2B; Wang *et al.*, 2018). Perhaps the most important of these transcription factors is ELONGATED HYPOCOTYL (HY5), which is a master regulator of plant development following light exposure (Gangappa and Botto, 2016).

In the other mechanism, both crys physically interact with CRYPTOCHROME INTERACTING BASIC HELIX LOOP HELIX (CIB) and PIF transcription factors to modulate their activity (Figure 1.2B; H. Liu *et al.*, 2008; Liu *et al.*, 2013; Ma *et al.*, 2016; Pedmale *et al.*, 2016). Through this mechanism, cry2 controls flowering by positively regulating transcription of the florigen *FLOWERING LOCUS T* (*FT*) through its interaction with the CIB transcription factors (H. Liu *et al.*, 2008; Liu *et al.*, 2013). With both of these means to influence transcriptional programs, crys can exert their activity over a diverse set of plant physiological responses.

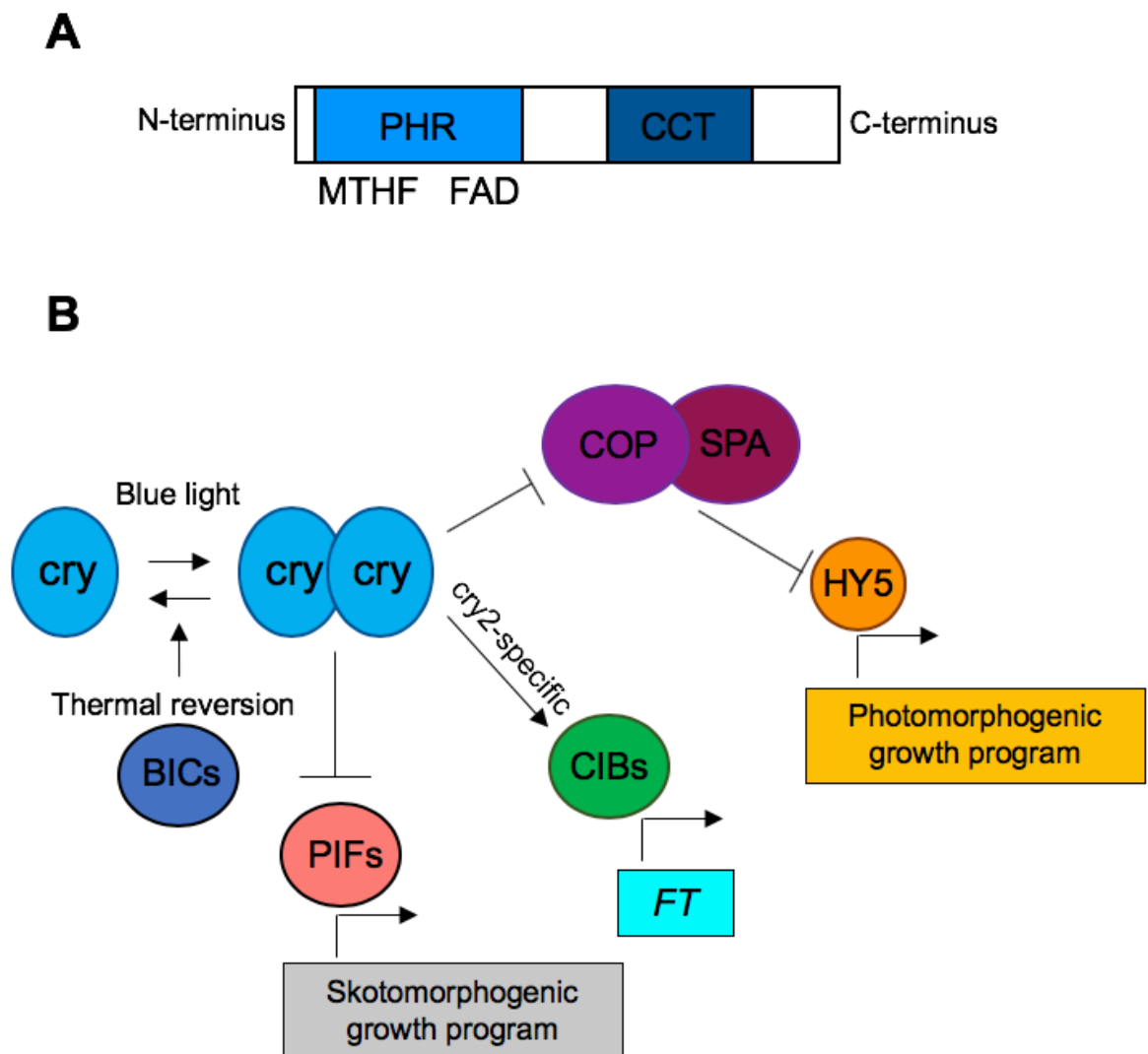


**Figure 1.2: Plant cryptochrome domain structure and activity.** **A.** Cryptochrome domains. Cry1 and cry2 each have an N-terminal photolyase homology region (PHR) domain, which binds the methenyltetrahydrofolate (MTHF) and (FAD) chromophores and senses light, and a cryptochrome C-terminal extension (CCT) domain, which is the binding site for many cry-interacting proteins. **B.** Cryptochrome light sensing and activity. Photoactivation leads to cry dimerization, which is inhibited by the BIC proteins. Crys interact with PIF and CIB transcription factors to inhibit or modulate their activity, respectively. Crys also influence transcription by inhibiting the proteolytic turnover of transcription factors by the COP/SPA complex. Arrows indicate activation, and lines ending in another perpendicular line indicate inhibition.

### 1.2.3 UV-RESISTANCE LOCUS 8

The UV-RESISTANCE LOCUS 8 (UVR8) photoreceptor modulates both photomorphogenesis and defense responses following its perception of UV-B light (Jenkins, 2017; Demarsy, Goldschmidt-Clermont and Ulm, 2018). Unlike the other photoreceptors discussed here, UVR8 does not bind a chromophore to enable light sensing. Instead, UV-B absorption is an intrinsic feature of this protein, occurring through a conserved series of tryptophan residues (Rizzini *et al.*, 2011; Christie *et al.*, 2012; Di Wu *et al.*, 2012). Prior to excitation, UVR8 exists as an inactive homodimer (Rizzini *et al.*, 2011). The UV-B absorbing tryptophans are located at the dimer interface, and their excitation by UV light causes a conformational change that makes the UVR8 homodimer dissociate and become a biologically active monomer (Figure 1.3; Christie *et al.*, 2012; Di Wu *et al.*, 2012). Similar to the negative feedback mechanism of the inhibition of cry2 dimerization by BIC proteins, UVR8 activation leads to transcription of the REPRESSOR OF UV-B PHOTOMORPHOGENESIS (RUP) proteins, RUP1 and RUP2, which facilitate the re-dimerization of UVR8, causing its inactivation (Figure 1.3; Gruber *et al.*, 2010). In another parallel to crys, activated UVR8 physically interacts with the COP1 complex to modulate the stability of transcription factors, most notably HY5, to enable photomorphogenic development (Brown *et al.*, 2005; Oravecz *et al.*, 2006). However, unlike the interaction between COP/SPA and crys, the interaction with UVR8 changes COP/SPA activity to positively modulate HY5 stability under UV-B irradiation through an unknown mechanism (Oravecz, 2006; Favory *et al.*, 2009; Huang *et al.*, 2013). UVR8 also can cause accumulation of protective pigments, which allay damage caused by UV irradiation, through modulating transcription of CHALCONE SYNTHASE (CHS; Jenkins, 2017; Demarsy, Goldschmidt-Clermont and Ulm, 2018). Interestingly, UVR8 activity has also been linked to repression of SAS and, along with cry1, to the sensing of sun flecks, which are brief moments of full sunlight to which plants grown under canopy shade are occasionally exposed (Hayes *et al.*, 2014; Moriconi *et al.*, 2018). Recently, UVR8 was additionally shown to be involved in thermomorphogenesis through an indirect effect on PIF4 abundance (Hayes *et al.*, 2017). Additionally, UVR8 activity is continually associated with new transcription factors (as in Liang *et al.*, 2018), which is likely to expand our understanding of its role in plant development and defense.

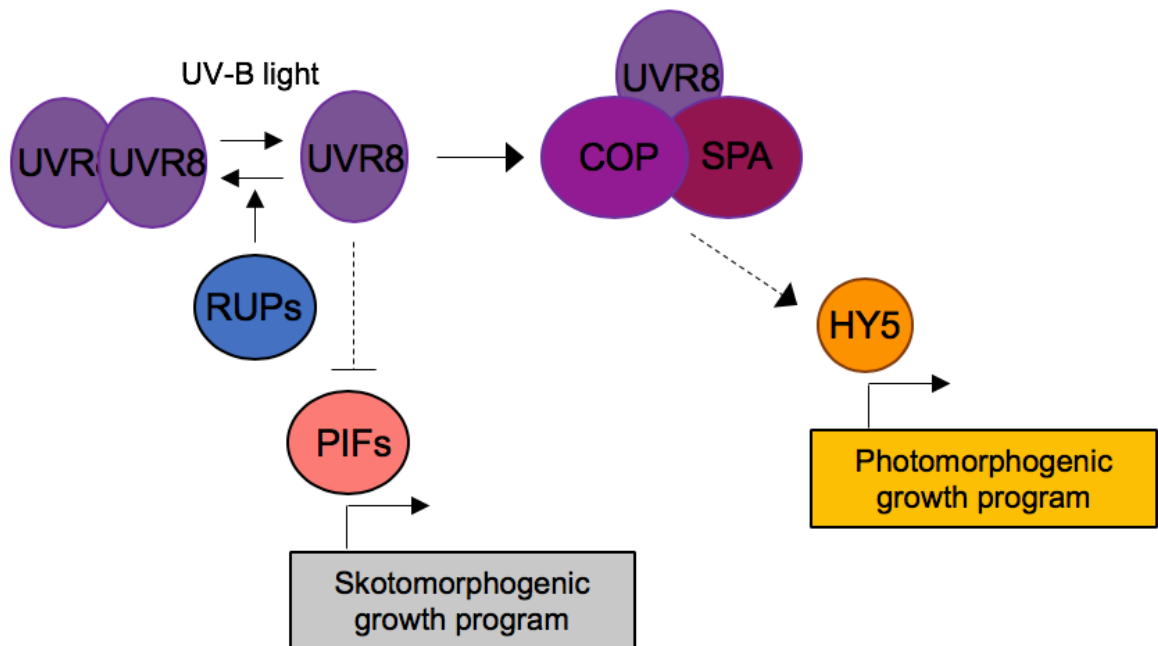


**Figure 1.3: UVR8 activity.** UVR8 exists as an inactive homodimer in the dark, and monomerizes to become active following excitation by UV-B light. This monomerization is inhibited by the activity of the RUP proteins, which facilitate re-dimerization. UVR8 primarily acts with the COP/SPA complex to stabilize the HY5 transcription factor. UVR8 activity can also indirectly inhibit the activity of PIF transcription factors. Arrows indicate activation, lines ending in another perpendicular line indicate inhibition, and broken lines indicate indirect or relationships that are not yet fully understood.

### 1.2.4 Zeitlupe family photoreceptors

The related UV-A/blue light photoreceptors zeitlupe (*ztl*), LOV-kelch protein 2 (*lkp2*), and flavin-binding kelch repeat f-box 1 (*fkf1*) share roles in the maintenance of circadian rhythms and in flowering time (Ito, Song and Imaizumi, 2012; Christie *et al.*, 2015). Each member of the *ztl* family contains an N-terminal Light, Oxygen, or Voltage sensing (LOV) domain followed by an F-box domain and C-terminal kelch repeats (Figure 1.4A). Protein/protein interactions are mediated through the LOV domain and kelch repeats, while the F-box domain confers E3 ubiquitin ligase activity within an SCF (Skp, Cullin, F-box containing) protein complex (Ito, Song and Imaizumi, 2012; Christie *et al.*, 2015). The LOV domain has a further role in gating these activities through light sensing (Imaizumi *et al.*, 2003; Ito, Song and Imaizumi, 2012; Christie *et al.*, 2015). LOV domains are a part of the PAS domain superfamily, and are ubiquitous light sensing modules in bacteria, fungi, and plants (Briggs, 2007; Glantz *et al.*, 2016). The *ztl* family LOV domains encompass a flavin mononucleotide (FMN) chromophore (Figure 1.4A; Imaizumi *et al.*, 2003). When FMN is excited by blue light, a covalent bond is formed between the FMN and a conserved cysteine within the LOV domain that translates to the activity of the F-box domain through an unknown mechanism (Imaizumi *et al.*, 2003; Christie *et al.*, 2015).

While all three of the *ztl* family photoreceptors are involved in circadian clock oscillations and flowering time, *ztl* seems to have specialized in maintenance of the circadian clock (Somers *et al.*, 2000) whereas *fkf1* acts primarily on flowering (Nelson *et al.*, 2000; Imaizumi *et al.*, 2003; Imaizumi *et al.*, 2005). *Lkp2* is relatively poorly characterized; *lkp2* mutants do not show any strong phenotypes, though it was found that *LKP2* overexpression had effects both on diurnal rhythms and flowering time, demonstrating that it does contribute in some way to the same responses as *ztl* and *fkf1* (Kiyosue and Wada, 2000; Schultz *et al.*, 2001; Imaizumi *et al.*, 2003; Baudry *et al.*, 2010). *Ztl* acts in the circadian clock by targeting the clock components PSEUDO RESPONSE REGULATOR 5 (PRR5) and TIMING OF CAB EXPRESSION (TOC1) for turnover in the evening (Figure 1.4C; Más *et al.*, 2003; Kiba *et al.*, 2007; Fujiwara *et al.*, 2008). Alteration of flowering time by this photoreceptor family is through modulating the stability of the transcription factor CONSTANS (CO; Valverde *et al.*, 2004).

As previously mentioned, the transcription of *FT* is the final committed step that leads to the transition to flowering in plants (Turck, Fornara and Coupland, 2008). One of the most important transcription factors in this process is CO; because CO can directly activate the transcription of *FT*, its mRNA and protein levels are tightly regulated (Turck, Fornara and Coupland, 2008). *Fkf1* interacts with the protein GIGANTEA (GI), which binds to the *fkf1* LOV domain following light activation, to stabilize CO protein by inhibiting the activity of the COP/SPA complex, which targets CO for turnover (Figure 1.4B; Lee *et al.*, 2017). *Fkf1* also positively modulates *CO* transcript by targeting the CYCLING DOF FACOR (CDF) proteins, which inhibit the transcription of *CO* by occupying its promoter, for degradation (Figure 1.4B; Imaizumi, 2005; Fornara *et al.*, 2009). The role of *ztl* in the clock impacts flowering by targeting CO for degradation in the morning; interestingly, this *ztl* response is dependent on GI binding, demonstrating that GI can be both a positive and negative regulator of flowering through differentially modulating CO stability at different times of day (Figure 1.4B; Song *et al.*, 2014). Through this complex set of protein/protein interactions that leads to either stabilization or degradation of target interactors, the *ztl* family of photoreceptors modulate day length sensing as well as flowering time.

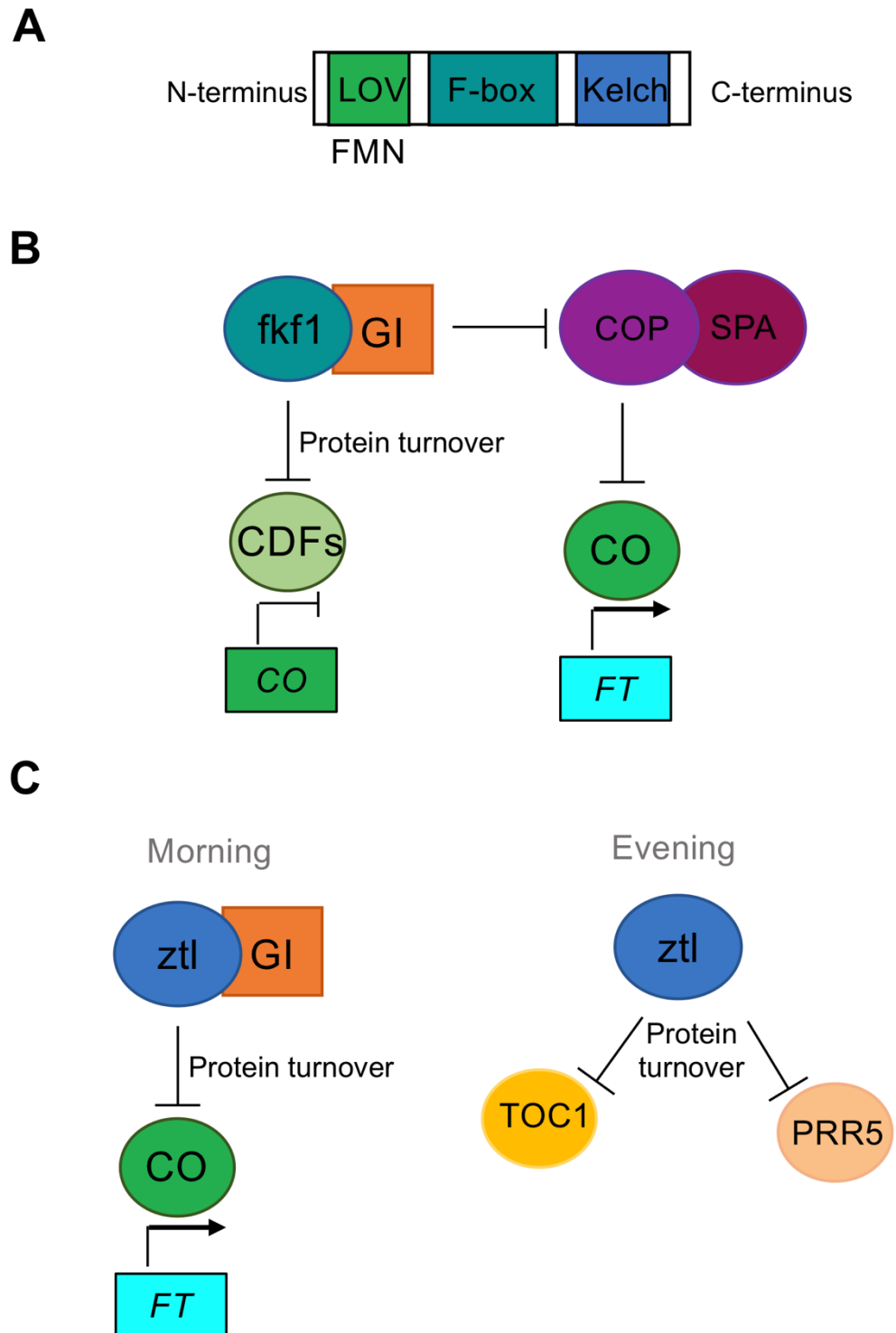


**Figure 1.4: Ztl family domain structure and activity.** **A.** Domains of *ztl*, *fkl1*, and *lkp2*. Each photoreceptor has an N-terminal LOV domain, which binds the flavin mononucleotide (FMN) chromophore, followed by an F-box domain, and kelch repeats **B.** *Fkl1* activity. *Fkl1* interacts with GI through its LOV domain to modulate CO abundance. *Fkl1* stabilizes CO by directly inhibiting the COP/SPA complex and promotes *CO* transcription by targeting the CDF proteins, which prevent *CO* transcription by binding to its promoter, for degradation. **C.** *Ztl* activity. *Ztl* interacts with GI through its LOV domain to target CO for turnover in the morning. In the evening, *ztl* maintains circadian rhythmicity by marking TOC1 and PRR5 for degradation in a GI-independent manner. Arrows indicate activation, and lines ending in another perpendicular line indicate inhibition.

## 1.2.5 Phototropins

The UV-A/blue light sensing phototropin (phot) photoreceptors are present in green algae and land plants (Li *et al.*, 2015B). In seed plants, the ancestral phot underwent a duplication, resulting in phot1 and phot2 (Li *et al.*, 2015B). Unlike the other photoreceptors introduced in this chapter, phototropins are light-responsive kinases and function outside of the nucleus, making them unique modulators of plant physiology (Christie *et al.*, 2015). Phot activity is primarily related to efficient positioning of plant organs and organelles to maximize light capture for photosynthesis by controlling leaf flatness, petiole positioning, phototropism, and chloroplast movement (Spalding and Folta, 2005; Christie *et al.*, 2015). The idea that these responses can relate to photosynthetic capability is supported by the finding that phototropins are crucial for normal plant development and biomass accumulation in low blue light conditions (Takemiya *et al.*, 2005). Phot activity also acts upstream of photosynthesis by controlling blue light mediated stomatal opening, which allows for the uptake of the carbon dioxide that is fixed during photosynthesis (Kinoshita *et al.*, 2001). Though it is less well-established, phot1 has been shown to be involved in destabilization of *LHCB* and *RBCL* mRNA transcripts, genes that are intimately connected to chloroplast development and photosynthesis, respectively (Folta and Kaufman, 2003); supporting these findings, phot1 was recently identified in a proteomics screen for non-canonical RNA-binding proteins in etiolated seedlings (Reichel *et al.*, 2016). Though land plant phototropins seem to have a more indirect effect on the photosynthetic machinery, the single phot from the green alga *Chlamydomonas reinhardtii* was found to protect photosystem II in high light conditions by inducing the expression of a gene involved in photoprotection (Petroustos *et al.*, 2016). Taken together, these responses clearly demonstrate the importance of phototropins in photosynthetic competence through increasing light capture and controlling stomatal opening.

### 1.2.5.1 Phot light sensing and activation

Both phot1 and phot2 are characterized by two tandem LOV domains at the N-terminus, LOV1 and LOV2, followed by a serine/threonine kinase domain (Christie *et al.*, 2015). Prior to illumination, it is thought that the LOV domains physically interact with the kinase domain to repress its activity (Figure 1.5; Harper, Christie and Gardner, 2004; Oide *et al.*, 2016; Takakado *et al.*, 2017). Each LOV domain receives blue light through a flavin mononucleotide (FMN) chromophore. As introduced for the ztl family LOV domains, when FMN is excited, a covalent bond forms between the C4a of FMN and a conserved cysteine

residue within each of the LOV domains (Figure 1.5; Salomon *et al.*, 2000; Briggs, 2007; Christie *et al.*, 2015). Though both LOV1 and LOV2 act as light sensors, LOV2 is accompanied by two alpha helices, J $\alpha$  and A' $\alpha$ , that sit on the outside of the LOV2 beta sheet core and become disordered following the formation of the covalent photoadduct (Figure 1.5; Harper, Christie and Gardner, 2004; Zayner, Antoniou and Sosnick, 2012; Halavaty and Moffat, 2013). Photoadduct formation is hypothesized to translate to unfolding of the  $\alpha$  helices through the conformational change of a conserved glutamine within LOV2, Q575, which flips to change its hydrogen bonding partner after the covalent photoadduct is formed (Nozaki *et al.*, 2004; Jones *et al.*, 2007; Nash *et al.*, 2008; Peter, Dick and Baeurle, 2010). When the alpha helices are released, kinase activity is de-repressed and phot1 signaling begins (Figure 1.5; Harper, Christie and Gardner, 2004; Oide *et al.*, 2016; Takakado *et al.*, 2017). This photocycle completes when the covalent adduct thermally decays, returning the protein to its dark, inactive state (Briggs, 2007; Christie *et al.*, 2015).

Upon activation by light and release of the repression of the kinase domain, phot1 undergoes autophosphorylation (Christie *et al.*, 1998; Christie *et al.*, 2002). This autophosphorylation activity is required for the transduction of phot signal, as mutation to autophosphorylation sites within the activation loop of both phot1 and phot2 to alanine eliminates activity (Inoue *et al.*, 2008A; Inoue *et al.*, 2011). Further solidifying the importance of LOV2 in phot1 activation, light sensing in LOV2, but not LOV1, is necessary and sufficient for the induction of this autophosphorylation activity (Christie *et al.*, 2002; Cho *et al.*, 2007). In another early signaling event, the phot1-interacting protein NON-PHOTOTROPIC HYPOCOTYL 3 (NPH3), which physically associates with phot1 and is required for the transduction of some phot1 responses, is dephosphorylated in a phot1-dependent manner following phot1 activation (Motchoulski and Liscum, 1999; Pedmale and Liscum, 2007; Tsuchida-Mayama *et al.*, 2008).

In the dark state, both phot1 and NPH3 are associated with the plasma membrane (Sakamoto and Briggs, 2002; Haga *et al.*, 2015). Following light perception, phot1 dimerizes and partially internalizes from the plasma membrane into the cytoplasm in a manner dependent upon its kinase activity (Sakamoto and Briggs, 2002; Kaiserli *et al.*, 2009; Xue *et al.*, 2018). Phot2 internalizes from the plasma membrane as well, with a small pool of phot2 associating with the chloroplast outer membrane and Golgi apparatus (Kong *et al.*, 2006, 2013). Likewise, NPH3 is internalized, but instead makes small clusters in the cytoplasm before eventually recycling back to the plasma membrane (Haga *et al.*, 2015). Interestingly, though the exact function of NPH3 is not understood, NPH3 is reported to have E3 ubiquitin ligase

activity and target phot1 for mono- and multiubiquitination (Roberts *et al.*, 2011). Because phosphorylation followed by ubiquitination often precedes re-localization of proteins from the plasma membrane, it is possible that NPH3 is playing a role in phot internalization (Roberts *et al.*, 2011; Dubeaux and Vert, 2017). However, the functional significance of these re-localization events following light activation, if any, is not known (Haga *et al.*, 2015; Liscum, 2016): anchoring phot1 to the plasma membrane through myristylation and farnesylation did not alter phot1 activity (Preuten *et al.*, 2015). Though the purpose of internalization is not understood, the noted changes in phosphorylation are required for phot activity. The early steps of phot activity following light sensing are marked by receptor autophosphorylation and dimerization, NPH3 dephosphorylation, and internalization of phot and NPH3 from the plasma membrane.

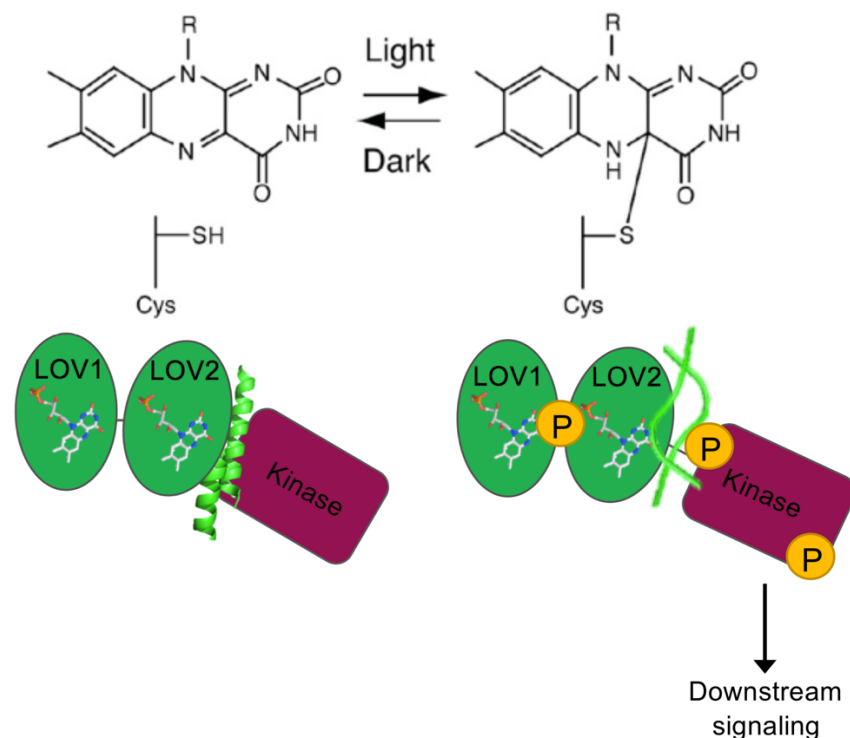


**Figure 1.5: Phot light sensing and activation.** Phots undergo a photocycle within their LOV domains wherein the flavin mononucleotide chromophore (FMN), which is bound within each LOV domain, becomes excited by blue light, leading to the formation of a covalent bond between FMN and a conserved cysteine within each LOV domain. This covalent bond formation triggers a conformational change that causes the alpha helices accompanying LOV2 to become disordered, releasing repression of the kinase domain and causing autophosphorylation, initiating downstream signaling.

### 1.2.5.2 Differential roles and sensitivity between phot1 and phot2

Between phot1 and phot2, phot1 is the most light sensitive and can signal over a wide range of fluence rates, whereas phot2 requires higher light intensities to drive phot responses (Sakai *et al.* 2001). This is thought to be partly due to differences between the phot1 and

phot2 photocycles: the lifetime of the photoadduct of phot1 is longer than that of phot2, which has the consequence that under a given light intensity, a greater proportion of the pool of phot1 protein is active and signaling relative to phot2 (Christie *et al.*, 2002; Kasahara *et al.*, 2002). Consistent with the idea that the phot2 photocycle limits its sensitivity, domain-swapping experiments that added the LOV1+LOV2 region of phot1 to the C-terminus of phot2 and expressed this chimeric phot on the phot2 promoter showed increased sensitivity for phot responses that was comparable in activity under low light to wild-type phot1 (Aihara *et al.*, 2008). Another factor in the differential sensitivity of phot1 and phot2 is protein expression. Phot1 is very highly expressed in etiolated seedlings, making it the dominant of the two in early development (Christie and Murphy, 2013). However, phot1 is slightly light labile, and is mostly turned over within hours of continuous irradiation of moderate to high intensity light, making phot1 somewhat less dominant in established, light-grown plants (Sakamoto and Briggs, 2002; Sullivan *et al.*, 2010). By contrast, phot2 expression is induced by light and remains stable under moderate and high intensity light conditions (Kanegae *et al.*, 2000; Jarillo *et al.*, 2001; Kagawa *et al.*, 2001; Kong *et al.*, 2006). These variations in sensitivity and protein levels establish phot1 as crucial for early development and response to low-light conditions, whereas phot2 acts as a high light sensor.

Phot1 and phot2 are functionally redundant in many cases, but each photoreceptor also plays specific roles that are not performed by the other. Phot1 and phot2 both mediate phototropism, leaf flattening, petiole positioning, chloroplast accumulation and stomatal opening (Christie *et al.*, 2015). Consistent with its role as a high light sensor, phot2 primarily mediates the chloroplast avoidance response, in which chloroplasts move to the anticlinal walls of the cell to prevent absorption of potentially damaging levels of irradiation (Jarillo *et al.*, 2001; Kagawa *et al.*, 2001; Kasahara *et al.*, 2002). The activity of phot2 specifically is also implicated in the development of palisade mesophyll cells in moderate blue light conditions (Kozuka *et al.*, 2011). Aside from its discrete role in mediating phot responses under low light, phot1-specific responses include rapid inhibition of hypocotyl elongation following initial blue light exposure in etiolated seedlings (Folta and Spalding, 2001; Folta *et al.*, 2003) and mRNA destabilization (Folta and Kaufman, 2003). The interplay of slightly differing roles as well as a distinctive range of sensitivities between phot1 and phot2 allows for a broad spectrum of responsiveness as well as finely tuned regulation of these responses.

### 1.2.5.3 Phot activity for leaf flatness and positioning

Both *phot1* and *phot2* have a strong effect on leaf development and orientation. From the time that the first *phot1phot2* double mutant was generated, it was observed that these mutants exhibited curled leaves that did not seem to be fully expanded (Sakai *et al.*, 2001; Sakamoto and Briggs, 2002). Further study showed that *phot1* and *phot2* both controlled leaf flattening in a fluence rate dependent manner and that phot-mediated leaf expansion was important for biomass accumulation in light-limiting conditions (Takemiya *et al.*, 2005; Inoue *et al.*, 2008B). In addition to leaf expansion, photos exert control over leaf positioning by regulating petiole angle (Inoue *et al.*, 2008B; de Carbonnel *et al.*, 2010). In light-limiting conditions, the angle of petioles relative to the horizontal increases in a phot-dependent manner in young plants, changing leaf position (Inoue *et al.*, 2008B; de Carbonnel *et al.*, 2010). In the absence of phot activity, petioles are constitutively downward sloping (Inoue *et al.*, 2008B; de Carbonnel *et al.*, 2010). These responses are thought to increase light capture for photosynthesis in the leaves, and indeed, it was found that mutants impaired in petiole positioning and leaf flattening show reduced photosynthetic activity and biomass accumulation (de Carbonnel *et al.*, 2010).

The pathways underlying leaf flattening and positioning are not fully understood. It has been shown that, as for many *phot1* responses, NPH3 is required (Inoue *et al.*, 2008B; de Carbonnel *et al.*, 2010). ROOT PHOTOTROPISM 2 (RPT2), an NPH3-related protein in the NPH3 AND RPT2 LIKE (NRL) family (Sakai *et al.*, 2000), has also been shown to be important for both leaf flattening and positioning (Harada *et al.*, 2013). Likewise, a second set of proteins, members of the PHYTOCHROME KINASE SUBSTRATE (PKS) family, are required for transduction of phot activity for these responses (de Carbonnel *et al.*, 2010). Single *pks* mutations have relatively minor impacts on leaf flattening and positioning, but when mutants of *pks1*, *pks2*, and *pks4* were combined with *nph3* (*nph3pks1pks2pks4* quadruple mutants), leaf flattening was completely abrogated under high light, leading to plants that resembled *phot1phot2* mutants in both appearance and extent of biomass accumulation (de Carbonnel *et al.*, 2010). The relationship between PKS and NRL proteins is not currently understood, but they seem to work cooperatively in phot signal transduction (Figure 1.6; Christie *et al.*, 2018)

There is a connection, however, between NRL and PKS proteins and auxin transport. When the *PKS2* promoter was used to drive the expression of the GUS ( $\beta$ -glucuronidase) reporter, staining showed that *PKS2* localizes to the outer lamina of mature leaves, overlapping with

the *DR5* auxin reporter, perhaps indicating a role for auxin transport in the leaf flatness response (de Carbonnel *et al.*, 2010). Similarly, there is evidence to indicate that NPH3 is involved in lateral auxin transport to produce directional growth, making it feasible that NPH3 also influences auxin transport to mediate leaf flattening (Haga *et al.*, 2005; Wan *et al.*, 2012). Interestingly, it was also reported that phyB acts through NPH3 to suppress phot-mediated leaf flattening, providing evidence that multiple light signaling pathways are likely to converge in mediating auxin flux for this response (Kozuka *et al.*, 2013). Furthering the connection between leaf flattening and auxin, D6 PROTEIN KINASES (D6PKs), which are involved in auxin transport (Zourelidou *et al.*, 2009), have been shown to contribute to leaf flatness (Willige *et al.*, 2013). Further investigation may help elucidate the significance of PKS and NPH3/RPT2 co-action as well as the involvement of auxin and provide more information on how phot activation relates to specific signaling pathways.

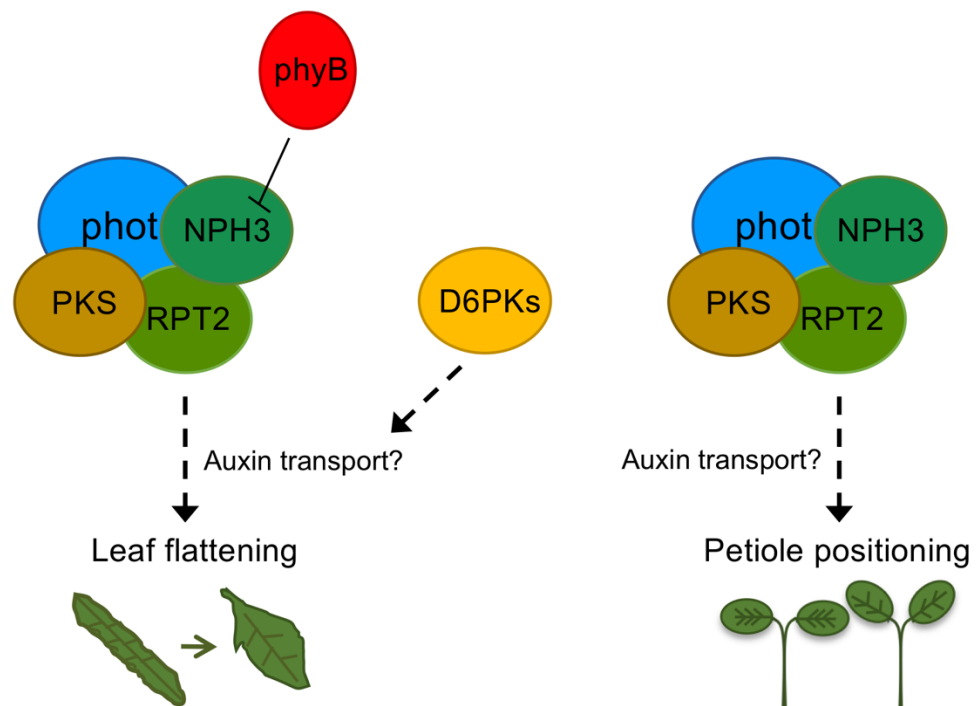


**Figure 1.6: Phot signal pathways for leaf flattening and positioning.** Phot1 acts with its signaling partners NPH3, RPT2, and members of the PKS family to regulate leaf flattening and positioning, possibly through modulating auxin flux (indicated by broken lines). Components that may be specific to leaf flattening include phyB, which negatively regulates NPH3, and D6PKs, which are involved in auxin transport.

#### 1.2.5.4 Phot activity for phototropism

Phototropism is defined by directional growth in response to a lateral light stimulus. While shoots and aboveground plant organs move toward the light stimulus, a response termed positive phototropism, roots undergo negative phototropism by moving away from the light (Christie and Murphy, 2013). Shoot phototropism occurs in three steps: there is first-positive

phototropism, in which phototropism occurs in response to brief irradiations with blue light and obeys reciprocity, with the degree of bending corresponding to the number of photons received in a linear fashion, followed by a refractory period during which no phototropism occurs, and finally second positive phototropism, which no longer obeys reciprocity, and is characterized by robust curvatures in response to continuous unilateral light treatment (Christie and Murphy, 2013). Though it has not been shown that the ability to undergo phototropism confers greater fitness to plants through optimizing light capture, it is expected that this response is beneficial for plants grown under canopies, where light conditions frequently change, and is useful for taking advantage of canopy gaps providing valuable sunlight (Goyal *et al.*, 2016).

In shoots, phototropism is the result of differential cell growth: cells elongate or divide more rapidly in the shaded portion of the stem, while the growth in lit portion remains the same, resulting in curvature in the direction of the light stimulus (Christie and Murphy, 2013). This change in growth rate on the shaded side is widely believed to be due to changing auxin flux within the shoot, with polar auxin transport temporarily halted while auxin moves laterally from the illuminated to the shaded side of the shoot (Friml *et al.*, 2002; Christie *et al.*, 2011; Ding *et al.*, 2011). Activated phot1 creates a phosphorylation gradient across the hypocotyl, dictating the direction of phototropic curvature and perhaps also the direction of lateral auxin transport (Salomon, Zacherl and Rüdiger, 1997; Christie and Murphy, 2013). After phosphorylation by phot1 in a blue light dependent manner, the auxin efflux transporter ATP BINDING CASSETTE B19 (ABCB19) is inhibited in its polar auxin transport activity (Figure 1.7; Christie *et al.*, 2011). Following this inhibition, a lateral auxin gradient is formed by the action of D6PKs to re-localize PIN-FORMED (PIN) auxin transporters from the tops and bottoms of cells to the sides in order to redirect auxin flux from polar to lateral movement (Figure 1.7; Friml *et al.*, 2002; Christie *et al.*, 2011; Willige *et al.*, 2013; Haga *et al.*, 2018). To bring this about, it is likely that the D6PKs phosphorylate the PINs to trigger their re-localization (Willige *et al.*, 2013). How phot activation is linked to the kinase activity of D6PKs is not yet understood; however, supporting this re-localization model, the *d6pk0123* quadruple mutant and the *pin137* triple mutant are severely deficient in phototropic curvature (Willige *et al.*, 2013; Haga *et al.*, 2018). This intricate control of auxin flux following phot establishment of a light gradient leads to the asymmetric growth that produces phototropism.

In addition to the auxin transport machinery, other proteins have been implicated in the regulation of phototropism. As for phot1 activity for leaf flattening and petiole positioning, the combined actions of NPH3, RPT2, and multiple members of the PKS family are required

for full phototropic responsiveness (Figure 1.7; Motchoulski and Liscum, 1999; Sakai *et al.*, 2000; Lariguet *et al.*, 2006), with NPH3 being absolutely required for any phototropic curvature to occur (Motchoulski and Liscum, 1999). Signal transduction for phot2-mediated phototropism requires NPH3 (Zhao *et al.*, 2018) and PKS proteins (Kami *et al.*, 2014) and is likely to be similar to that of phot1, though this pathway is not as well-established (Figure 1.7). Of these phot interacting proteins, phot1 is reported to phosphorylate PKS4 (Demarsy *et al.*, 2012). While *pks4* mutants have relatively small phototropic defects, PKS4 does seem to positively modulate phototropism in etiolated seedlings (Demarsy *et al.*, 2012; Schumacher *et al.*, 2018). Following this phosphorylation event, however, it seems that PKS4 becomes a negative regulator of phototropism in higher light conditions (Schumacher *et al.*, 2018). No phot2-mediated phosphorylation events have been connected with phototropism as yet, but it has been found that the dephosphorylation activity of PROTEIN PHOSPHATASE 2A (PP2A) inhibits phot2-mediated phototropism by reducing the extent of its autophosphorylation following blue light treatment (Tseng and Briggs, 2010). The combined action of the phot-interacting proteins NPH3, RPT2, and PKS in phototropism is likely to be related to the changes in auxin transport discussed above, though the evidence for this hypothesis is not yet definitive (Haga *et al.*, 2005; de Carbonnel *et al.*, 2010; Kami *et al.*, 2014).

PhyA and phyB are also required for full phototropic responsiveness in etiolated seedlings, and pre-treatment of seedlings with red light prior to the onset of phototropism enhances curvature (Briggs and Chon, 1966; Parks, Quail and Hangarter, 1996; Janoudi *et al.*, 1997; Kami *et al.*, 2012; Sullivan *et al.*, 2016). PhyA, and partly phyB, are hypothesized to inhibit the gravitropic pathway in order to allow full phototropic curvature toward the light stimulus (Figure 1.7; Kim *et al.*, 2011). Supporting this model, in seedlings grown vertically under monochromatic blue light, it seems that this release of gravitropic growth causes seedlings to become randomly oriented unless active phototropism is present to maintain upward growth through phototropism (Lariguet and Fankhauser, 2004). Potentially presenting a new model for phot/phy interactions for phototropism, phyB was found to suppress phototropism in high red:far-red ratios in de-etiolated seedlings, supporting a role for phototropism in SAS (Figure 1.7; Goyal *et al.*, 2016). How this finding fits in with the framework of phy activity to enhance phototropism in etiolated seedlings has not yet been reconciled. Aside from the input of phy activity, phototropism is enhanced in de-etiolated seedlings in both curvature and kinetics of the response relative to etiolated seedlings, indicating that other factors positively modulate phototropism after the development of photosynthetic capability (Hart and Macdonald, 1981; Hasegawa *et al.*, 1987). What those factors may be is the subject of ongoing research,

and more suppressors and enhancers of phot-mediated phototropism in addition to components involved in lateral auxin transport are likely to be found.

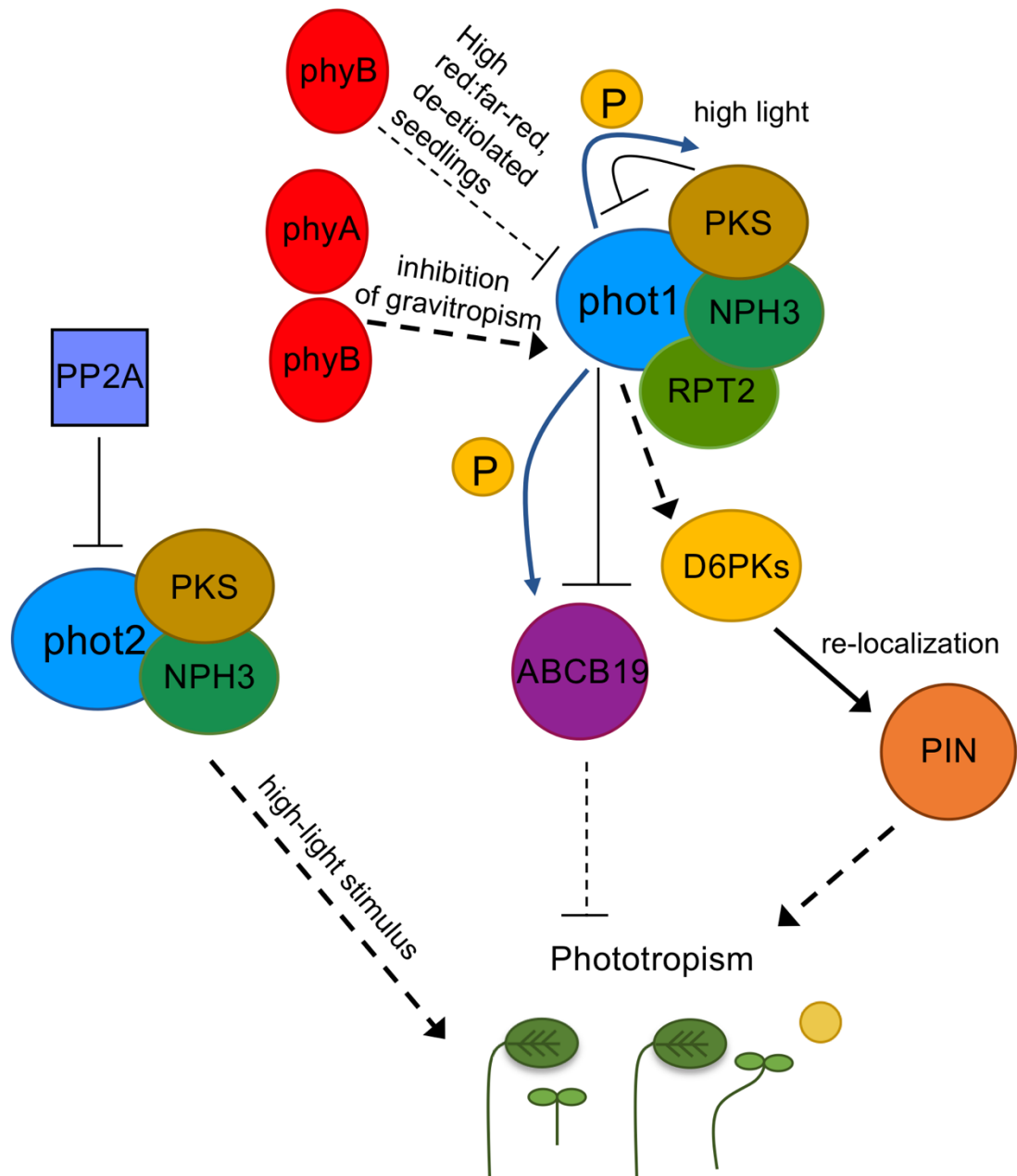


**Figure 1.7: Phot signal pathway for phototropism.** Under most light conditions, phot1-mediated phototropism depends on phot1 interaction with NPH3, RPT2, and PKS family members. At higher light, phot2 interacts with NPH3 and PKS proteins to transduce the signal for phototropism. The phosphatase PP2A negatively regulates phot2 autophosphorylation and activity for phototropism. For phot1, its activation eventually leads to the phosphorylation of the auxin efflux transporter ABCB19, which inhibits its activity. Phot activity for phototropism also leads to the redistribution of PIN proteins through D6PKs, which along with inhibition of ABCB19, promotes lateral auxin transport to produce the asymmetric growth that leads to phototropic curvature. Phot1 also is reported to phosphorylate PKS4, which in turn inhibits phototropism in high light conditions. This process is enhanced by phyA and phyB inhibition of gravitropic growth. In de-etiolated seedlings grown in high red:far-red ratios (non-shaded conditions), phyB seems to inhibit phototropism. Arrows indicate activation, lines ending in another perpendicular line indicate inhibition, and broken lines indicate indirect relationships or those that are not yet fully understood.

### 1.2.5.5 Phot activity for chloroplast movement

As described above, while both *phot1* and *phot2* mediate the chloroplast accumulation response, *phot2* is the dominant receptor for chloroplast avoidance. It is hypothesized that chloroplast accumulation to maximize light capture in low and moderate light intensities is crucial for optimizing photosynthesis (Suetsugu and Wada, 2012). Conversely, an intact chloroplast avoidance response is clearly required to mitigate damage to leaves and the photosystems in intense light conditions (Kasahara *et al.*, 2002). These movement responses seem to be mediated by specialized actin filaments that associate with the chloroplasts, which both anchor chloroplasts to the plasma membrane and differentially polymerize on the sides of the chloroplasts in order to facilitate movement (Wada and Kong, 2018). How phot activity leads to chloroplast movement responses is not understood, though interestingly phot signal transduction for chloroplast accumulation is redundantly mediated by RPT2 and another NRL family member, NRL PROTEIN FOR CHLOROPLAST MOVEMENT 1 (NCH1; Figure 1.8; Suetsugu *et al.*, 2016) even though chloroplast positioning does not involve auxin flux. The protein CHLOROPLAST UNUSUAL POSITIONING 1 (CHUP1) may play a key role in chloroplast movement (Wada and Kong, 2018). Chloroplasts in *chup1* mutants are detached from the plasma membrane and lie along the bottom surface of the cell (Oikawa *et al.*, 2003; Oikawa *et al.*, 2008). Additionally, *chup1* mutants may be deficient in actin polymerization, preventing any chloroplast movement from occurring (Schmidt Von Braun and Schleiff, 2008; Wada and Kong, 2018). Other components of chloroplast movement responses have also been identified, such as KINESIN-LIKE PROTEIN FOR ACTIN BASED CHLOROPLAST MOVEMENT (KAC), which contains a kinesin-like motor domain that may enable chloroplast movement, though its exact role is not understood (Suetsugu *et al.*, 2010), and THRUMIN1, which bundles the actin filaments coming off chloroplasts and appears to be required for the maintenance of these filaments over time (Whippo *et al.*, 2011; for a complete review of proteins involved in actin-mediated chloroplast positioning see Wada and Kong, 2018). Whether any of these proteins are substrates of phot kinase activity is of interest, in addition to how photos provide the directionality for these movements.

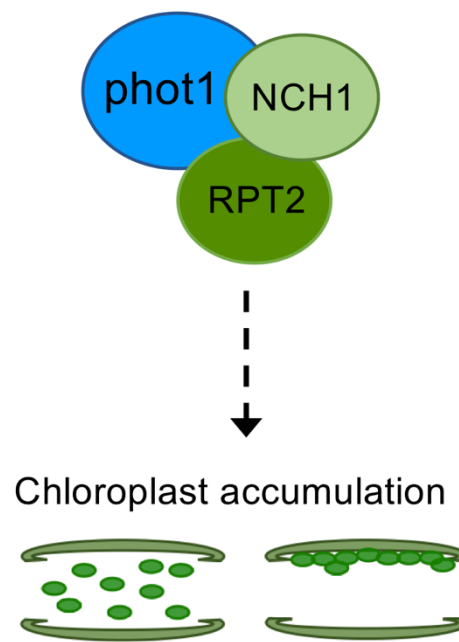


**Figure 1.8: Phot1 interacts with the NRL proteins NCH1 and RPT2 to bring about chloroplast accumulation.** How the signal from phot1/NCH1/RPT2 causes chloroplast accumulation is not fully understood and is therefore indicated with a broken line.

#### 1.2.5.6 Phot activity for stomatal opening

Stomatal opening represents the closest link in higher plants between phot activity and photosynthesis by utilizing blue light sensing by phot1 as a signal to induce stomatal opening and allow for the uptake of carbon dioxide (Inoue, Takemiya and Shimazaki, 2010; Inoue and Kinoshita, 2017). Unlike other phot-mediated responses, phot activity for stomatal opening does not appear to require the activity of NRL family members, though there are conflicting reports regarding whether RPT2 is involved in this process (Inada *et al.*, 2004; Tsutsumi *et al.*, 2013; Suetsugu *et al.*, 2016; Christie *et al.*, 2017). Though the pathway for phot-induced stomatal opening is perhaps the best-described phot signaling pathway, some important gaps in understanding remain (Inoue, Takemiya and Shimazaki, 2010; Inoue and Kinoshita, 2017). The well-established components of the pathway are that phot blue light sensing and autophosphorylation in guard cells leads to activation of PROTEIN PHOSPHATASE 1 (PP1) to somehow bring about the phosphorylation of the second to last threonine in the H<sup>+</sup>-ATPase isoform AHA1 by an unknown kinase, leading AHA1 to pump H<sup>+</sup> ions out of the guard cell and hyperpolarize the plasma membrane (Figure 1.9; Inoue, Takemiya and Shimazaki, 2010; Inoue and Kinoshita, 2017). This hyperpolarization triggers the activity of inward-rectifying potassium channels, eventually increasing the turgor pressure within guard cells, causing the swelling that opens the stomatal pore (Inoue, Takemiya and Shimazaki, 2010; Inoue and Kinoshita, 2017).

Phot1 activity is in part translated into stomatal opening by the kinase BLUE LIGHT SIGNALING 1 (BLUS1; Takemiya *et al.*, 2013). Both phot1 and phot2 phosphorylate BLUS1 in a blue light dependent manner, eventually leading to the activation of PP1 (Figure 1.9; Takemiya *et al.* 2013). This phosphorylation step, in addition to the kinase activity of BLUS1 itself, is required for blue light induced stomatal opening, but how the activation of phot1 and BLUS1 kinase activity causes activation of PP1 and later AHA1 phosphorylation remains unclear (Takemiya *et al.* 2013; Inoue and Kinoshita, 2017). Recently, a second kinase, BLUE LIGHT DEPENDENT H<sup>+</sup>-ATPASE PHOSPHORYLATION (BHP1), was found to physically interact with BLUS1, possibly in a phot1/BLUS1/BHP1 complex, and to also be important for AHA1 phosphorylation (Figure 1.9; Hayashi *et al.*, 2017). Substrates of BLUS1 and BHP1 have not yet been identified, and neither has the kinase responsible for AHA1 phosphorylation, which seems to act downstream of phot1, BLUS1, and BHP1. In a separate pathway, phot1 appears to phosphorylate CONVERGENCE OF BLUE LIGHT AND CO<sub>2</sub> 1 (CBC1), a kinase that along with CBC2 inhibits the S-type anion channels SLOW ANION CHANNEL ASSOCIATED 1 (SLAC1) and SLAC1 HOMOLOGUE 3 (SLAH3; Hiyama *et al.*, 2017). SLAC1 and SLAH3 both inhibit the membrane hyperpolarization that leads to stomatal opening, making CBC1 and CBC2 positive regulators of stomatal opening (Figure 1.9; Hiyama *et al.* 2017). Aside from protein phosphorylation, a screen looking for suppressors of phot1 activity for stomatal opening made the surprising connection that *early flowering 3 (elf3)* mutants had constitutively open stomata through overexpression of the florigen *FT* in guard cells (Kinoshita *et al.*, 2011). However, as these changes produce constitutively open stomata in a *phot1phot2* mutant background, it appears that this modulation of stomatal opening through increases in *FT* expression in guard cells is likely to be due to transcriptional changes associated with the circadian clock and may be independent of phot1 activity (Ando *et al.*, 2013; Inoue and Kinoshita, 2017). Continued investigation of stomatal opening can aid in the understanding of the differences between phot1 activity in guard cells for this response and its activity for other responses. Furthermore, solidifying the mechanisms of stomatal opening requires more substrates for all the kinases implicated in this process to be found, as well as generation of more information about how all of the kinases are organized into the signal cascade that eventually leads to stomatal opening.

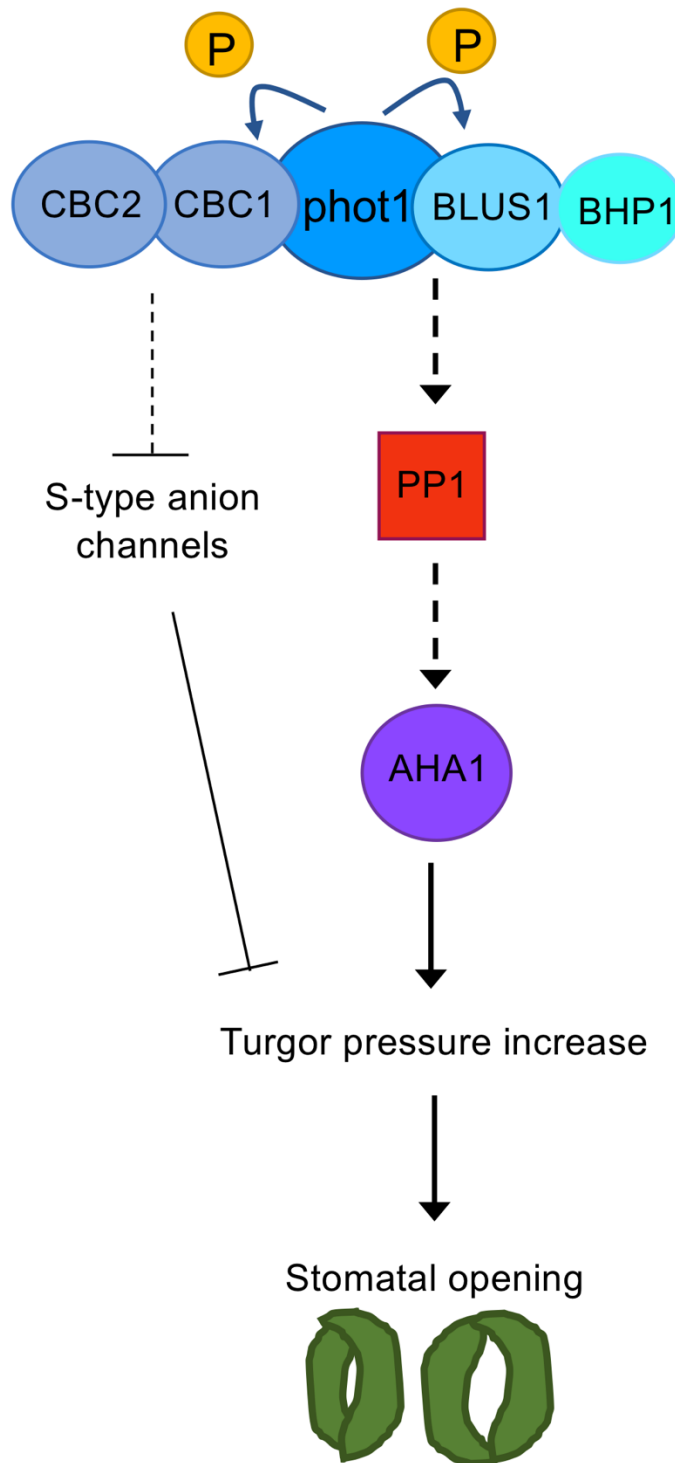


**Figure 1.9: Phot signal pathway for stomatal opening.** Light-activated phot1 phosphorylates BLUS1, which is required for the downstream activation of PP1, and later that of AHA1, which leads to the increase in turgor pressure that causes stomatal opening (indicated by broken lines to indicate uncertainty as to how these activation steps occur). The kinase BHP1 is also somehow involved in this process and physically interacts with BLUS1. Phot1 also phosphorylates CBC1, which along with CBC2, inhibits the activity of S-type anion channels for antagonizing the membrane hyperpolarization that leads to stomatal opening.

## 1.3 Modulating photoreceptor sensitivity

### 1.3.1 Photoreceptor overexpression

In addition to yielding information about photoreceptor function, early overexpression studies of phy and cry photoreceptors indicated that overexpression enhanced the light sensitivity of these photoreceptors by increasing the pool of protein available to produce signal. These studies demonstrated that *PHYA* (Boylan and Quail, 1991) and *PHYB* (Wagner, Tepperman and Quail, 1991) overexpression in *Arabidopsis* led to shorter hypocotyls than wild-type plants that was attributed to increased phy activity. The same decrease in hypocotyl length was later shown for *CRY1* and *CRY2* overexpression (Lin *et al.*, 1998) as well as for *UVR8* (Favory *et al.*, 2009). Constitutive overexpression of full-length photoreceptors has not yet been accomplished, leaving the role of photoreceptors with increased sensitivity due to overexpression uncertain. However, it was found that overexpression of the phot2 kinase domain in a wild-type genetic background led to constitutively open stomata, reduced phototropism, and small, compact plants (Kong *et al.*, 2007). By contrast, expression of full-length phot2 on a guard-cell-specific promoter increased phot2 levels in guard cells relative to wild-type plants but did not produce a noticeable effect on stomatal aperture (Wang *et al.*, 2014). Though the effects of photoreceptor overexpression are not clear in the published literature, for phy, cry, and UVR8, photoreceptor overexpression yields clear increases in sensitivity to light.

Expanding the investigations of photoreceptor overexpression to crop plants revealed the potential of increasing photoreceptor sensitivity. *PHY* overexpression was found to increase yields in both potato (Thiele *et al.*, 1999) and rice (Garg *et al.*, 2006). In potato, these yield improvements were attributed to altered palisade mesophyll cell structure and increased rates of photosynthesis (Thiele *et al.*, 1999; Boccalandro *et al.*, 2003). Overexpression of the native *CRY2* in tomato did not appear to enhance yield, but these transgenic tomatoes did accumulate more anthocyanins and carotenoids than wild-type plants, including substantial increases in fruit lycopene content (Giliberto *et al.*, 2005). The accumulation of these pigments is horticulturally desirable, since the consumption of these pigments as a part of human diets has been linked to positive health outcomes (Rao and Rao, 2007). Furthermore, all of these photoreceptor overexpression studies in crops noted decreased plant height and shorter internodes, likely through increased repression of SAS resulting from the increased sensitivity. This reduced plant height can protect against lodging in cereal crops, where this unintended bending of the stem can cause serious yield loss (Garg *et al.*, 2006; Ganesan *et*

*al.*, 2017). Further investigation of the benefits of this more compact plant architecture in potato revealed that *PHYB* overexpressing lines out-performed wild type for both carbon assimilation and yield when grown in high-density plantings, showing that photoreceptor engineering can also reduce the space required to reach desired yield levels (Boccalandro *et al.*, 2003). Taken together, these studies plainly indicate that manipulation of cry and phy sensitivity through overexpression has positive effects on yield and other horticulturally desirable traits.

### 1.3.2 Constitutively active photoreceptor variants

Maximum activity can be yielded through the generation of constitutively active variants of plant photoreceptors. However, as these variants tend to lead to constitutively photomorphogenic (COP) phenotypes, in which plants inappropriately de-etiolate and develop in darkness as though they had been exposed to light, constitutive activation demonstrates the limits of increasing photoreceptor activity. In *phys*, this development in darkness can be seen in the constitutively active phyB-Y276H (YHB) allele (Su and Lagarias, 2007). The same can be observed in some cry1 and cry2 mutants of the tryptophan triad (Li *et al.*, 2011; Gao *et al.*, 2015), as well as transgenic plants expressing the CCT domain of either cry on its own due to loss of light regulation conferred by the PHR (Yang *et al.*, 2000). Similarly, UVR8-W285A mutants are constitutively active and also exhibit this COP phenotype (Heijde and Ulm, 2013). For all of the photoreceptors that mediate photomorphogenesis in plants, constitutive activation is deleterious to the development of seedlings by leading to this COP phenotype. In the case of plants expressing the cry1 CCT, constitutive activation also leads to early flowering (Yang *et al.*, 2000), demonstrating that these alleles can also affect other aspects of plant development.

Constitutively active alleles of phot1, such as phot1-I608E and phot1-R472H, which disrupt the alpha helices accompanying LOV2, eliminating light-regulation of the kinase domain, have also been identified. Unlike the other photoreceptors discussed here, though these alleles can be characterized *in vitro* for their “always on” autophosphorylation activity (Jones *et al.*, 2007; Kaiserli *et al.*, 2009; Petersen *et al.*, 2017), it has been difficult to assess their activity *in planta*. Though *PHOT1* transcript expression in these mutants appears to be similar to that of wild type, the phot1 protein of these constitutively active alleles seems to be destabilized, leading to poor protein expression *in planta* (Kaiserli *et al.*, 2009; Petersen *et al.*, 2017). Furthermore, phot1-R472H does not seem to be constitutively active for phot1-mediated responses, with this mutant requiring high-intensity light to drive both petiole

positioning and phototropism, though the decreased sensitivity relative to wild type is difficult to separate from low protein expression (Petersen *et al.*, 2017). It is possible that there is a mechanism in place to limit the level of phot1 activation and signal transduction by targeting it for degradation. In contrast to the other photoreceptors, which showed clear phenotypes related to constitutive activation, the impact constitutively active phot1 has on physiology is not yet well-understood.

Application of constitutively active photoreceptor alleles to crop plants has not been extensively undertaken, likely because phenotypes like COP would be undesirable in agricultural settings. When YHB was expressed in tomato plants, it was found that the COP phenotype leads to vivipary, or germination of seeds while still in the fruit and attached to the parent plant, an unattractive trait for fruit that is to be freshly consumed (Ganesan *et al.*, 2017). Though sensitivity is increased, expressing constitutively active photoreceptors in crop plants is not a viable approach to increase growth or yields, demonstrating that the expression of very active photoreceptors, while conferring certain benefits, still requires a measured approach.

### 1.3.3 Targeting photoreceptor sensitivity through photocycles

Modifying photoreceptor photocycles by limiting dark reversion represents an alternative approach to increase photoreceptor sensitivity to positively impact plant growth and development. Photoreceptors exist in a photoequilibrium such that, under most light conditions, the pool of protein is balanced between active and inactive receptors due to thermal reversion (Rockwell, Su and Lagarias, 2006; Christie *et al.*, 2015). Controlling photocycles by limiting this reversion process has the potential to enhance sensitivity by increasing the amount of active protein available to signal. While the underlying mechanism of the cry photocycle is still subject to debate, dark reversion of phy has long been understood to modulate the activity of these photoreceptors. EMS mutant screens identified phyB alleles with either enhanced or reduced activity that possessed either slow (*phyB-401*; Kretsch, Poppe and Schäfer, 2000) or fast (*phyB-101*; Elich and Chory, 1997) rates of  $P_{FR}$  to  $P_R$  reversion, respectively. Rationally designed mutations have also been successful in tuning the phyB photocycle, with mutants exhibiting slow dark reversion, such as phyB-Y361F, demonstrating increased activity for inhibition of hypocotyl elongation, shorter overall petiole lengths, and reduced hyponasty (Zhang, Stankey and Vierstra, 2013). In addition to thermal reversion of the phy lit state, the protein PERIODIC CONTROL OF HYPOCOTYL 1 (PCH1) was recently found to physically interact with phyB in order to

slow its dark reversion and positively regulate photobody formation and duration (Huang *et al.*, 2016; Enderle *et al.*, 2017). As expected considering its impact on the phyB photocycle, the presence of PCH1 increases phyB activity for inhibition of hypocotyl elongation (Huang *et al.*, 2016; Enderle *et al.*, 2017). Though the activity of phyB is enhanced by these photocycle modifications, increased phyB activity by slowing dark reversion has not yet been linked to changes in biomass accumulation or crop yield, which represents the next logical step for these studies.

The discovery of LOV domain photosensory modules sparked interest in optogenetics, which is the artificial control of cellular phenomena by light (Pudasaini, El-Arab and Zoltowski, 2015). Because the use of LOV domains as optogenetic tools necessitated careful control of their period of activation through the photocycle, LOV domain photocycles have been very thoroughly characterized, with many studies identifying fast and slow photocycling LOV domain variants (Christie *et al.*, 2007; Zoltowski, Vaccaro and Crane, 2009; Kawano *et al.*, 2013). Physiological characterization of the role these photocycles play in light-driven responses in their native systems, however, is relatively sparse. As a part of the characterization of LOV domain photocycles, the photocycle of the fungal photoreceptor VVD was tuned over four orders of magnitude (Zoltowski, Vaccaro and Crane, 2009). To address the significance of the VVD photocycle *Neurospora crassa*, Dasgupta *et al.* (2015) used the mutations identified by Zoltowski, Vaccaro and Crane (2009) to see whether VVD activity was changed by these variants. VVD negatively regulates the transcriptional activity of the White Collar Complex (WCC) in response to blue light. VVD variants with a fast photocycle reduced its activity by decreasing its affinity for the WCC (Dasgupta *et al.*, 2015). While the fast photocycling VVD variants had clear defects in function that were attributed to the photocycle, no differences in VVD activity could be observed in the slow photocycle mutants (Dasgupta *et al.*, 2015). The lack of functional significance observed for a VVD slow photocycle *in vivo* could be due to the fact that wild-type VVD already has a very slow photocycle (Zoltowski, Vaccaro and Crane, 2009). The slow VVD photocycle probably biases the pool of VVD in the cell entirely towards the lit state under most light conditions such that slowing the photocycle further does not have a noticeable effect (Zoltowski, Vaccaro and Crane, 2009; Dasgupta *et al.*, 2015).

In plants, examination of the LOV photocycle in *ztl* has shown that the photocycle is important in its specialized role as a component of the circadian clock. Mathematical models suggested that the length of the *ztl* photocycle enables it to sense the fluence rate of blue light, facilitating its perception of the onset of dusk and dawn (Pudasaini and Zoltowski,

2013). Indeed, it was later found that when the *ztl* photocycle was slowed *in vivo*, *ztl*-mediated turnover of PRR5 and TOC1 was enhanced, leading to a rapid dampening of circadian rhythmicity when the slow photocycle mutants were removed from 12 hour dark/light cycles and placed in constant light conditions (Pudasaini *et al.*, 2017). In the case of both *ztl* and VVD, the LOV domain photocycle seems to be exquisitely adapted to suit the role of each photoreceptor, though any potential to positively impact development has not yet been exploited. Since modifications to plant photoreceptor photocycles can enhance activity without producing COP or other undesirable phenotypes as well as offer a more finessed approach than protein overexpression, targeting photoreceptor sensitivity through managing dark reversion has the potential to be an ideal approach to increase plant growth.

## 1.4 Project aims

As described, modulating photoreceptor sensitivity has substantial effects on plant growth, and in some cases can increase crop yield. Because the phot photoreceptors are so intimately linked to photosynthetic potential in plants, modulating their sensitivity is particularly attractive. However, little work has been done thus far to address the factors affecting phot sensitivity *in planta* or to establish whether increasing phot sensitivity can actually positively affect plant growth and development. To this end, two approaches were taken to further our understanding of phot1 sensitivity and signaling. Because phot1 is more sensitive than phot2 and is more highly expressed in light-limiting conditions, the studies here focused on phot1 sensitivity specifically.

In the first approach, the phot1 photocycle was modified through targeted mutagenesis in an attempt to increase its sensitivity. Unlike the LOV photocycle observed for VVD (Zoltowski, Vaccaro and Crane, 2009), the phot1 photocycle is relatively fast (Christie *et al.*, 2002; Kasahara, Swartz, Olney, *et al.*, 2002; Kaiserli *et al.*, 2009). It was hypothesized that slowing dark reversion in the LOV2 domain would allow the kinase portion of the protein to signal for a greater period of time, increasing its activity. Slow photocycling variants of phot1 were first to be generated *in vitro*, following which whether those photocycle variants did in fact show increased light sensitivity or better plant growth would be investigated *in planta*. Unlike the observations recently made for the role of the *ztl* LOV domain photocycle in *Arabidopsis*, the physiological role of the phot photocycle is still not understood and it was expected that the phot1 photocycle mutants generated for this study may provide some details on this as well as increase phot1 sensitivity.

In the second tactic, a genetic screen was performed to identify suppressors of phot1 activity to determine whether other proteins act on phot1 to modify its sensitivity. This screen was performed on a transgenic line expressing a truncated version of phot1 that lacks sensitivity to low fluence rates of blue light in order to identify any individuals that exhibited increased sensitivity. Furthermore, though phot-mediated physiological responses have been well-characterized, information on its signaling partners and substrates of its phosphorylation activity are still lacking. It was also anticipated that the suppressor screen could aid in the identification of some of these signaling components, providing information both on phot1 sensitivity and the mechanisms of its action.

## Chapter 2 Materials and Methods

### 2.1 Materials used in this study

All chemical reagents were obtained from either Sigma-Aldrich, VWR International, or Thermo-Fisher unless otherwise noted in the text.

Restriction enzymes, polymerases, and other enzymes such as ligases were all obtained from either New England Biolabs or Promega as recorded for each method.

All western blotting equipment was from Bio-Rad. DNA gel electrophoresis equipment was from VWR International. Light intensity was measured using a LI-250A light meter with a LI-190R photosynthetically active radiation (PAR) sensor (LI-Cor). Micropipette tips were TipOne tips from Star Lab. Whatman paper was obtained from VWR International. Square and round petri dishes were from Thermo-Fisher.

### 2.2 DNA isolation

#### 2.2.1 Plasmid DNA isolation

To isolate plasmid DNA from transformed *Escherichia coli* (*E. coli*) cells, 5 ml of Luria Broth (1% (w/v) tryptone, 0.5% (w/v) yeast extract, 170 mM sodium chloride) containing the appropriate selective antibiotic was inoculated with a single *E. coli* colony. The culture was then incubated overnight at 37°C with shaking. The next morning, the culture was centrifuged at 4000 RPM for 10 minutes at room temperature to pellet the *E. coli* cells. The medium was decanted, and the pellet was resuspended in 250 µl Buffer P1 from the QIAprep Spin Miniprep Kit (Qiagen) as described in the manufacturer's protocol. The manufacturer's protocol was then followed for the rest of the preparation, with the exception that the plasmid was eluted from the column using 30 µl buffer EB rather than 50. The DNA content of the sample was then quantified using an Implen nanophotometer.

#### 2.2.2 Genomic DNA isolation from *Arabidopsis*

##### 2.2.2.1 Rapid genomic DNA isolation for PCR

Two leaves were excised from each *Arabidopsis* rosette of interest and flash frozen in liquid nitrogen. The leaves were finely ground in a microcentrifuge tube using a chilled micropestle (Sigma-Aldrich) followed by further grinding in 300 µl of DNA Extraction Buffer (200 mM

Tris-HCl pH 8, 250 mM sodium chloride, 25 mM EDTA, 0.5% (v/v) SDS). Next, 150  $\mu$ l 3 M sodium acetate, pH 5.2 was added and the mixture was vortexed. The tubes were then incubated at  $-20^{\circ}\text{C}$  for 10 minutes. The samples were centrifuged for 5 minutes at maximum speed to pellet the plant material, and the supernatant was transferred to a new microcentrifuge tube. An equal volume of isopropanol was added to the supernatant with gentle mixing following which the tubes were incubated at room temperature for 5 minutes to precipitate the DNA. After precipitation, the DNA was pelleted by centrifuging at maximum speed for 5 minutes. The pellet was washed with 70% ethanol and centrifuged again as described above. The ethanol was decanted, and the pellet was aspirated and allowed to dry for 5 minutes prior to resuspension in 30-60  $\mu$ l deionized water containing 0.1 mg/ml RNase A (Qiagen). The DNA content of each sample was then quantified using an Implen nanophotometer. This protocol was adapted from both Cenis (1992) and Edwards, Johnstone and Thompson, (1991).

#### **2.2.2.2 Spin column isolation of genomic DNA**

DNA samples that were subjected to deep genomic sequencing were prepared using the DNeasy Plant Mini Kit (Qiagen). Around 100  $F_2$  seedlings from a cross between the mutant of interest and its LOV2Kinase parent that were exhibiting the raised petiole phenotype were flash frozen in liquid nitrogen. The tissue was finely ground in a mortar and pestle cooled with liquid nitrogen. One hundred milligrams of powdered tissue from each set was then used for genomic DNA isolation using the manufacturer's protocol. The DNA content of the sample was then quantified using an Implen nanophotometer.

### **2.3 DNA cloning and manipulation**

#### **2.3.1 DNA agarose gel electrophoresis**

Resolution of DNA samples using gel electrophoresis was used to estimate the size, relative concentration, and purity of DNA fragments of interest. The agarose gel consisted of 0.8% (w/v) UltraPure Agarose (Invitrogen) melted into TAE Buffer (Tris-Acetate-EDTA; 40 mM Tris, 20 mM acetic acid, 1 mM EDTA) supplemented with a 1:12,500 dilution of Sybr Safe (Invotrogen) as a DNA stain. Purple loading dye (New England Biolabs) was diluted 6 times into the DNA samples to be separated on the gel. The gel was placed into an electrophoresis tank filled with TAE buffer and the dye-DNA mixture was loaded into the wells of the gel. The GeneRuler 1 kb DNA ladder (Thermo-Fisher) was added to the gel alongside the DNA samples as a standard for DNA fragment size and relative quantity. Electrophoresis was

typically conducted at 100V for 35 minutes. The DNA samples were visualized using the UV fluorescence setting of the Fusion Fx imager (Vilber).

### 2.3.2 Gel purification

When necessary, DNA fragments were excised from agarose gels following separation by electrophoresis and purified using the QIAquick Gel Extraction Kit (Qiagen) according to the manufacturer's protocol.

### 2.3.3 Primer design

In general, primers for PCR were designed directly from the sequence of the DNA template. For genomic DNA, primers were designed using the Primer3 software (<http://primer3.ut.ee/>). For Gibson Assembly, NEBuilder (<https://nebuilder.neb.com/>) was used to design the primers and create the cloning strategy. Gibson Assembly primers were made to anneal to the insert of interest and have a 20 base pair overhang that was specific to the vector and integrate restriction sites or ATG start codons where necessary. Mutagenic primers were designed to change the fewest number of base pairs possible while considering *Arabidopsis* codon usage and were generated using the Agilent QuikChange Primer Design tool (<http://www.genomics.agilent.com/primerDesignProgram.jsp>). A list of mutagenic primers used in this study is provided in in Table 2.1, qPCR primers in Table 2.2, cloning primers in Table 2.3, and genomic DNA primers for amplifying *Arabidopsis* genes for sequencing in Table 2.4.

### 2.3.4 Polymerase chain reaction (PCR)

PCR was performed on a G-Storm GS04822 thermal cycler using Phusion high-fidelity polymerase from New England Biolabs. PCR was performed in 50 µl reactions consisting of 1x Phusion High-Fidelity Buffer, 200 µM dNTPs, 0.5 µM forward primer, 0.5 µM reverse primer, ~30-50 ng of DNA template, and 1 unit of Phusion DNA polymerase.

A typical PCR program for Phusion polymerase was conducted as follows: initial denaturation at 98°C for 1 minute and 30 seconds, followed by 32 cycles of: denaturing at 98°C for 20 seconds, annealing at 55°C for 30 seconds, and extending at 72°C for 30 seconds per kilobase pair of expected amplicon size, ending with a final extension at 72°C for 10 minutes. The annealing temperature was 55°C unless further optimization was required.

#### **2.3.4.1 Colony PCR**

When *E. coli* colonies were obtained from a cloning strategy, the colonies were screened by PCR prior to sequencing plasmid DNA. PCR reactions were prepared in a 10 µl volume using the 2x GoTaq Master Mix (Promega) and 1 µM each of forward and reverse primers that could amplify the entire length of the cloned DNA insert. A pipette tip was dabbed into the center of the colony to be tested and then mixed into the prepared PCR reaction. As a negative control, a pipette tip was placed onto a part of the plate without colonies and mixed into a separate reaction. The PCR was carried out as recommended by Promega, with the modification that the initial denaturation at 94°C was extended to 5 minutes to lyse the cells. Successful amplification was confirmed by DNA agarose gel electrophoresis (see section 2.3.1).

#### **2.3.4.2 Site-directed mutagenic PCR**

Mutagenic PCR was conducted using KOD Hotstart Polymerase (Merck) according to the standard KOD 50 µl reaction using mutagenic primers designed as described above (see section 2.3.3). The manufacturer's protocol was used for the reaction, with a 55°C annealing temperature and extending for 30 seconds per kb of the entire plasmid template size for 28 cycles. Following the PCR, the product was digested with 1 unit of DpnI (Promega) for 1 hour at 37°C to eliminate any wild-type template DNA before transforming the mutated plasmid into XL10Gold *E. coli* cells (Agilent Technologies; see section 2.9.2). Successful mutagenesis was confirmed by sequencing the plasmid insert (see section 2.3.8).

Primer name	Sequence (5' to 3')
C234A F	CAAAGAAGTCGTCGGCAGAAACGCCCGATTTTTACAAGGAT
C234A R	ATCCTTGTA AAAATCGGGCGTTTCTGCCGACGACTTCTTTG
N476L F	CACTCGAACGTATCGAGAAGCTTTTCGTCATCACTGATCCTA
N476L R	TAGGATCAGTGATGACGAAAAGCTTCTCGATACGTTTCGAGTG
V478I F	CGTATCGAGAAGAATTTTCATCATCACTGATCCTAGGC
V478I R	GCCTAGGATCAGTGATGATGAAATTCTTCTCGATACG
T520R F	GTTTCTACAAGGTCCAGAGAGAGATCTAACCACAGTGAAGAA
T520R R	TCCTCCACTGTGGTTAGATCTCTCTCTGGACCTTGTAGAAAC
T524I F	GTCCAGAGACTGATCTAACCATTGTGAAGAAGATTTCGAAATGCT
T524I R	AGCATTTTCAATCTTCTTCAATGGTTAGATCAGTCTCTGGAC
N511S F	TAGCCGTGAAGAAATTTCTTGAAGAAGTTGCAGGTTTCTAC
N511S R	GTAGAAACCTGCAACTTCTTCCAAGAATTTCTTACGGCTA
W553L F	TACACCAAGAGCGGAAAGAAGTTCCTTAACATTTTCCACTTGCAACCTATG
W553L R	CATAGGTTGCAAGTGAAAATGTTAAGGAACTTCTTCCGCTCTTGGTGTA
H557A F	CGGAAAGAAGTTCTGGAACATTTTCCGCTTGCAACCTATGCGTG
H557A R	CACGCATAGGTTGCAAGGCGAAAATGTTCCAGAACTTCTTCCG
L558I F	AAGTTCTGGAACATTTTCCACATTCAACCTATGCGTGATCAGAAG
L558I R	CTTCTGATCACGCATAGGTTGAATGTGGAAAATGTTCCAGAACTT
Q575L F	CAATACTTTATTGGAGTTCTTCTAGACGGGAGCAAGCACG
Q575L R	CGTGCTTGCTCCCGTCTAGAAGAACTCCAATAAAGTATTG
H581A F	GCGAACTGGTTCTACGGCCTTGCTCCCGTCTAGT
H581A R	ACTAGACGGGAGCAAGGCCGTAGAACCAGTTCCG
R586L F	CAAGCACGTAGAACCAGTTCTTAATGTCATTGAAGAAACCGC
R586L R	GCGGTTTCTTCAATGACATTAAGAAGTGGTTCTACGTGCTTG

**Table 2.1: Mutagenic primers for PCR.** Mutagenic primers were designed as described in 2.3.3.

### 2.3.4.3 Inverse PCR

The insertion of 9 amino acids that is present in the Zeitlupe (ztl) family LOV domains, but not in phot LOV domains was introduced to LOV2 in the phot1 LOV1+LOV2 construct between phot1 residues E519 and T520. The forward primer was designed to anneal to the template from the codon encoding T520 downstream for 24 bases, with a 5' overhang of the 27 bases that code for the ztl insertion. The reverse primer had no overhang and was designed to reverse-complement the template upstream from the E519 residue for 24 bases. Phusion PCR was conducted using these primers, and the product was incubated with 1 unit of T4 kinase (Invitrogen) at 37°C for 15 minutes to prepare the PCR product for ligation by adding phosphates to the ztl overhang. The plasmid DNA was recircularized by ligation and transformed into *E. coli*, as described in 2.3.6 and 2.9.2, respectively.

#### 2.3.4.4 Reverse transcription PCR (RT PCR)

RT PCR was conducted to synthesize cDNA from RNA using the Superscript IV kit (Invitrogen) according to the manufacturer's protocol. One microgram of DNase treated RNA was used as the template and random hexamers were used as primers.

#### 2.3.4.5 Quantitative PCR (qPCR)

Quantitative PCR was performed using the StepOnePlus Real-Time PCR System (Applied Biosystems) using a SybrGreen Mastermix (Agilent Technologies). ROX dye that was diluted 1:50 was used as a control for loading. For qPCR analysis on plant tissues, *IRON-SULFUR CLUSTERASE (ISU1)* was used as an internal control. Each DNA and primer combination was tested in triplicate for each experiment to ensure reproducibility. Transcript levels were quantified using the relative standard curve method.

Primer name	Sequence (5' to 3')
qPHOT1-F	ATGCCAACATGACACCAGAG
qPHOT1-R	CCATGGTGGTGAATCTTTCC
qISU1-F	GCCATCGCTTCTTCATCTGTTGC
qISU1-R	TGGGAGAGAAAGATGCTTTGCG
IE1 F	CCCGTAACGGACCTCGTACTT
IE1 R	TTATCGAGATTTATTTGCATACAACAAG

**Table 2.2: qPCR primers used in this study.** The phot1 and ISU1 primers were derived from Petersen *et al.* (2017) and were used to quantify phot1 transcript expression. The IE1 F and R primers were used to analyse baculovirus titer (see section 2.13.2) as described in in Lo and Chao, (2004).

#### 2.3.5 DNA digestion

DNA was digested with restriction enzymes to both linearize vectors for cloning and to indirectly confirm the identity of the insert in a plasmid following cloning. Restriction enzymes were obtained from New England Biolabs unless otherwise noted. The digestion reaction was assembled as follows: 1 unit of restriction enzyme was added per microgram of DNA to be digested, 1X CutSmart Buffer, DNA template, and deionized water to the final volume. To prevent non-specific activity, the final volume was always determined such that the restriction enzyme did not make up more than 10% of the total reaction volume. After the reaction was prepared, it was incubated at 37°C for at least 1 hour. Reactions using SmaI (Promega) were incubated at 25°C. The digest pattern was visualized using DNA agarose gel electrophoresis (see section 2.3.1) and, if necessary, the fragments of interest corresponding to the appropriate size were excised and gel purified as described in 2.3.2.

### 2.3.6 DNA ligation

Ligations were performed using T4 DNA ligase (New England Biolabs). For cloning, the digested insert DNA and vector backbone were combined in a 3:1 insert to vector ratio (by moles of DNA). The DNA fragments to be ligated were then added to a reaction including 1X Ligase Buffer, 1 unit of T4 DNA ligase, and deionized water to 20  $\mu$ l. The reaction was allowed to proceed at room temperature for 2 hours before transformation into *E. coli* (see section 2.9.2). For recircularization of T4 Kinase treated inverse PCR products (section 2.3.4.3), the plasmid was ligated back together as above, taking care that its concentration was <10 ng/ $\mu$ l to promote circularization over concatenation.

### 2.3.7 Cloning techniques

Several different cloning techniques were used to generate the plasmid constructs used in this study. A list of expression constructs used in this study is given in Table 2.3.

Vector and construct name	Expression system	Tag	Protein encoded (native protein residues)	Source or cloning primers used (5' to 3')
LOV1+LOV2 pCal-n-EK	<i>E. coli</i>	CBP N-term	LOV1+LOV2 (180-638)	Kaiserli <i>et al.</i> (2009)
LOV1+LOV2 -ztli pCal-n-EK	<i>E. coli</i>	CBP N-term	LOV1+LOV2 (180-638)	F: CCGTTTGCTAAAAGAAGGCATC CATTAACTGATCTAACCACAGT GAAGAAG R: CTCTGGACCTGTAGAAACCTG
LOV1+LOV2 -fkf1i pCal-n-EK	<i>E. coli</i>	CBP N-term	LOV1+LOV2 (180-638)	F: CCGTTTGCTAAAAGAAGGCATC CATTAACTGATCTAACCACAGT GAAGAAG R: same as ztli
LOV1+LOV2 -ztli-C234A pCal-n-EK	<i>E. coli</i>	CBP N-term	LOV1+LOV2 (180-638)	C234A mutagenic primers
LOV1+LOV2 -N476L pCal-n-EK	<i>E. coli</i>	CBP N-term	LOV1+LOV2 (180-638)	N476L mutagenic primers
LOV1+LOV2 -V478I pCal-n-EK	<i>E. coli</i>	CBP N-term	LOV1+LOV2 (180-638)	V478I mutagenic primers
LOV1+LOV2 -V478L pCal-n-EK	<i>E. coli</i>	CBP N-term	LOV1+LOV2 (180-638)	Generated by Dr. Jan Petersen
LOV1+LOV2 -T520R pCal-n-EK	<i>E. coli</i>	CBP N-term	LOV1+LOV2 (180-638)	T520R mutagenic primers
LOV1+LOV2 -T524I	<i>E. coli</i>	CBP N-term	LOV1+LOV2 (180-638)	T524I mutagenic primers

pCal-n-EK			(180-638)	
LOV1+LOV2 -N511S pCal-n-EK	<i>E. coli</i>	CBP N-term	LOV1+LOV2 -N511S (180-638)	N511S mutagenic primers
LOV1+LOV2 -H557A pCal-n-EK	<i>E. coli</i>	CBP N-term	LOV1+LOV2 -H557A (180-638)	H557A mutagenic primers
LOV1+LOV2 -L558I pCal-n-EK	<i>E. coli</i>	CBP N-term	LOV1+LOV2 -L558I (180-638)	L558I mutagenic primers
LOV1+LOV2 - N476LV525 R pCal-n-EK	<i>E. coli</i>	CBP N-term	LOV1+LOV2 - N476LV525 R (180-638)	N476L mutagenic primers on LOV1+LOV1-V525R pCal-n-EK from Dr. Jan Petersen
LOV1+LOV2 -N476LL558I pCal-n-EK	<i>E. coli</i>	CBP N-term	LOV1+LOV2 -N476LL558I (180-638)	N476L mutagenic primers on LOV1+LOV1-L558I pCal-n-EK
LOV1+LOV2 - H557AH581 A pCal-n-EK	<i>E. coli</i>	CBP N-term	LOV1+LOV2 - H557AH581 A (180-638)	H581A mutagenic primers on LOV1+LOV1-H557A pCal-n-EK
WT LOV2 pGB1-6His	<i>E. coli</i>	6xHis N-term	WT LOV2 (452-615)	F: GCCGACCCATGGATAGTGTGG ATGATAAAGTGAGAC R: GCCGACGCGGCCGCTCAAAGT TCTCGAACCGCTTCATCG
LOV2-V478L pGB1-6His	<i>E. coli</i>	6xHis N-term	LOV2-V478L (452-615)	Same as for WT LOV2
WT phot1 pAcHLT-a	Sf9 cells	6xHis N-term	WT phot1 (1-996)	Christie <i>et al.</i> (1998)
phot1-V478I pAcHLT-a	Sf9 cells	6xHis N-term	phot1-V478I (1-996)	V478I mutagenic primers
phot1-N476L pAcHLT-a	Sf9 cells	6xHis N-term	phot1-N476L (1-996)	N476L mutagenic primers
phot1-L558I pAcHLT-a	Sf9 cells	6xHis N-term	phot1-L558I (1-996)	L558I mutagenic primers
WT phot1::phot1- GFP pEZR(K)-LN	<i>Arabidopsis</i>	GFP C-term	WT phot1- GFP (1-996)	Sullivan <i>et al.</i> (2016)
WT phot1::phot1- N476L-GFP pEZR(K)-LN	<i>Arabidopsis</i>	GFP C-term	phot1- N476L-GFP (1-996)	F: AAGATCTAAAAGATGCGTTGTG GACGTTTCAACAAACGTTTGTG R: AGCGGCAGCGGCAGCAGCCG GATCCGCAAAAACATTTGTTT CAGATC
WT phot1::phot1- V478I-GFP pEZR(K)-LN	<i>Arabidopsis</i>	GFP C-term	phot1-V478I- GFP (1-996)	Same as for phot1-N476L-GFP
WT phot1::phot1- W553L-GFP pEZR(K)-LN	<i>Arabidopsis</i>	GFP C-term	phot1- W553L-GFP (1-996)	Same as for phot1-N476L-GFP
WT phot1::phot1- L558I-GFP pEZR(K)-LN	<i>Arabidopsis</i>	GFP C-term	phot1-L558I- GFP (1-996)	Same as for phot1-N476L-GFP

WT phot1::phot1- R586L-GFP pEZR(K)-LN	<i>Arabidopsis</i>	GFP C-term	phot1- R586L-GFP (1-996)	Same as for phot1-N476L-GFP
WT phot1 pSPYNE	<i>Nicotiana benthamiana</i>	YFP <sub>N</sub> , c-myc C-term	WT phot1- YFP <sub>N</sub> (1-996)	Kaiserli <i>et al.</i> (2009)
WT phot1 pSPYCE	<i>Nicotiana benthamiana</i>	YFP <sub>C</sub> , HA C-term	WT phot1- YFP <sub>C</sub> (1-996)	Kaiserli <i>et al.</i> (2009)
phot1-V478I pSPYNE	<i>Nicotiana benthamiana</i>	YFP <sub>N</sub> , c-myc C-term	phot1-V478I- YFP <sub>N</sub> (1-996)	F: GGCGCGCCACTAGTGGATCCA TGGAACCAACAGAAAAAC R: AGCGGCAGCGGCAGCAGCCG GATCCGCAAAAACATTTGTTTG CAGATC
phot1-V478I pSPYCE	<i>Nicotiana benthamiana</i>	YFP <sub>C</sub> , HA C-term	phot1-V478I- YFP <sub>C</sub> (1-996)	F: same as for phot1-V478I pSPYNE F primer  R: CGTATGGGTACATCCCGGAA AACATTTGTTTG CAGATC
phot1-V478L pSPYNE	<i>Nicotiana benthamiana</i>	YFP <sub>N</sub> , c-myc C-term	phot1- V478L- YFP <sub>N</sub> (1-996)	Same as for phot1-V478I pSPYNE
phot1-V478L pSPYCE	<i>Nicotiana benthamiana</i>	YFP <sub>C</sub> , HA C-term	phot1- V478L- YFP <sub>C</sub> (1-996)	Same as for phot1-V478I pSPYCE
phot1-Q575L pSPYNE	<i>Nicotiana benthamiana</i>	YFP <sub>C</sub> , c-myc C-term	phot1- Q575L- YFP <sub>N</sub> (1-996)	Same as for phot1-V478I pSPYNE
phot1-Q575L pSPYCE	<i>Nicotiana benthamiana</i>	YFP <sub>C</sub> , HA C-term	phot1- Q575L- YFP <sub>C</sub> (1-996)	Same as for phot1-V478I pSPYCE
LOV1+LOV2 pSPYNE	<i>Nicotiana benthamiana</i>	YFP <sub>N</sub> , c-myc C-term	LOV1+LOV2 - YFP <sub>N</sub> (180-628)	F: GGCCTGGCGCGCCACTAGTGG ATCCATGGGGATTCCAAGAGTA TCGGAAG R: ATCAACTTTTGCTCCATCCCGG GGTTTGCCATAAATCCTCTG
LOV1+LOV2 pSPYCE	<i>Nicotiana benthamiana</i>	YFP <sub>C</sub> , HA C-term	LOV1+LOV2 - YFP <sub>C</sub> (180-628)	F: same as for LOV1+LOV2 pSPYNE F primer  R: ATCAACTTTTGCTCCATCCCGG GGTTTGCCATAAATCCTCTG
phot1 kinase domain pSPYNE	<i>Nicotiana benthamiana</i>	YFP <sub>N</sub> , c-myc C-term	kinase-YFP <sub>N</sub> (663-996)	F: GGCCTGGCGCGCCACTAGTGG ATCCATGTTCAAACCGGTGAAA CCTTTG R: same as for phot1-V478I pSPYNE
phot1 kinase domain pSPYCE	<i>Nicotiana benthamiana</i>	YFP <sub>C</sub> , HA C-term	kinase-YFP <sub>C</sub> (663-996)	F: same as for kinase-pSPYNE F primer  R: same as for phot1-V478I pSPYCE

LOV2Kinase pSPYNE	<i>Nicotiana benthamiana</i>	YFP <sub>N</sub> , c-myc C-term	LOV2Kinase - YFP <sub>N</sub> (448-996)	F: GGCGCGCCACTAGTGGATCCA TGAGACCTGAGAGTGTGGATG R: same as for phot1-V478l pSPYNE
LOV2Kinase pSPYCE	<i>Nicotiana benthamiana</i>	YFP <sub>C</sub> , HA C-term	LOV2Kinase - YFP <sub>C</sub> (448-996)	F: same as for LOV2Kinase pSPYNE R: same as for phot1-V478l pSPYCE

**Table 2.3: Expression constructs and the associated cloning primers or sources.** Plasmid constructs were either obtained from colleagues and published manuscripts or generated using one of the cloning processes described below. “N-” or “C-term” denotes an N- or C-terminal tag. YFP<sub>N</sub> and YFP<sub>C</sub> indicate the tag is either the N-terminal or C-terminal half of YFP, respectively.

### 2.3.7.1 Traditional cloning

The *Arabidopsis* phot1 LOV2 construct (amino acids 452-615) used for biophysical analysis was cloned into the pGB1-6His expression vector using traditional cloning. The vector backbone was linearized by digestion with NcoI and NotI restriction enzymes (see 2.3.5) and the digested vector backbone was gel purified. The LOV2 domain was amplified by PCR with the At LOV2 forward and reverse primers (Table 2.3), which had overhangs that contained NcoI and NotI restriction sites. The PCR product was then digested with NcoI and NotI. The digested LOV2 insert and vector were ligated as described and transformed into DH5 $\alpha$  competent *E. coli* cells (see section 2.9.2). The colonies obtained following antibiotic selection on plates were subjected to colony PCR to verify successful cloning (section 2.3.4.1) and three PCR positive colonies were sequenced for further confirmation (section 2.3.8).

### 2.3.7.2 Gibson Assembly

The DNA insert to be cloned was amplified using PCR with Gibson Assembly primers, and the vector of interest was linearized by digest (see 2.3.5). For *in planta* expression of phot1 variants, pEZR(K)-LN (Sullivan *et al.*, 2016) was digested with SalI and BamHI. The pSPYNE and pSPYCE vectors for BiFC assays (Walter *et al.*, 2004) were linearized with SmaI and BamHI (Promega). Following these steps, both the PCR product and the vector backbone were gel purified (section 2.3.2). The insert and vector were then combined in a 3:1 ratio (by moles of DNA) and an equal volume of 2X Gibson Assembly Mastermix (New England Biolabs) was added. The Gibson Assembly reaction was then incubated at 50°C for 15-30 minutes. Two microliters of the Gibson Assembly product were transformed into 5-alpha competent *E. coli* cells (New England Biolabs; see 2.9.2 for the transformation

protocol). The colonies obtained following antibiotic selection on plates were subjected to colony PCR (section 2.3.4.1) and three PCR positive colonies were sequenced for further confirmation (section 2.3.8).

### 2.3.7.3 TOPO cloning of *Arabidopsis* genomic DNA

*Arabidopsis* genomic DNA was obtained as described (2.2.2.1). The genomic DNA of interest was amplified by PCR and the PCR product was separated by agarose gel electrophoresis and gel purified (a list of genomic DNA primers is given in table 2.4; see sections 2.3.1 and 2.3.2). Because the Phusion polymerase creates blunt-ended PCR products, adenine overhangs were added by incubating 4 µl purified PCR product with 5 µl 2x GoTaq Mastermix (Promega) and 1 µl of 10 mM dATP (Promega) at 72°C for 10 minutes. The A-overhang product was then immediately combined with the pCR4TOPO vector (Invitrogen) in a 3:1 PCR product to vector ratio (by moles of DNA), 1 µl of the provided salt solution, and deionized water to a final volume of approximately 5 µl. The TOPO reaction was incubated at room temperature for 15-30 minutes before 1 µl of the reaction was transformed into DH5α competent *E. coli* cells (homemade; see 2.9.2). The colonies obtained were subjected to colony PCR, following which 3 PCR-positive colonies were sequenced.

Primer name	Sequence (5' to 3')
PhyB-1 F	TCTCCCCATTTTCTTCTTCCTCA
PhyB-1 R	CCAGTCAAGTCCCTCACACT
PhyB-2 F	CTGGTGCTGTTCAATCGCA
PhyB-2 R	ATTTCCGCAGTTTCCCATGG
PhyB-3 F	GAATGCATCCTCGTTTCGTCC
PhyB-3 R	GGCTCGGGATTTGCAAGAAA
PhyB-6 F	CATAATGCGATTGGTGGCCA
PhyB-6 R	TCTAGGCCTATGGATGTGTCT
PhyB-7 F	ACATTTTATTGTTCCCGCTGT
PhyB-7 R	CGGAGTTGTCAATTTACACAGC
LOV2Kinase genotype F	CCTGAGAGTGTGGATGAT
LOV2Kinase genotype R	TCAAAAACATTTGTTTGCAG

**Table 2.4: Genomic DNA primers.** Genomic DNA primers were designed as described in 2.3.3. The LOV2Kinase genotyping primers were derived from Thompson (2008).

### **2.3.8 DNA sequencing**

In general, DNA was sequenced by GATC Biotechnology (Konstanz, Germany) using Sanger Sequencing with an ABI 3730xl DNA Analyzer system. Next generation deep sequencing of EMS mutants was performed using the Illumina NextSeq 500 platform by Glasgow Polyomics.

## **2.4 RNA isolation**

Three-day-old etiolated seedlings were harvested under a dim red safe light and flash frozen in liquid nitrogen. The frozen tissue was disrupted in a microcentrifuge tube with a chilled micropestle. Total RNA was extracted using the RNeasy Plant Mini Kit (Qiagen) following the manufacturer's protocol. The RNA was then DNase treated using the TURBO DNA-free kit (Invitrogen) following the manufacturer's protocol. RNA content was quantified using an Implen nanophotometer.

## **2.5 Isolation of whole protein extracts**

Unless otherwise noted, protein extraction was performed in 2x SDS Buffer (120 mM Tris-pH 6.8, 20% glycerol, 4% SDS, 5% 2-Mercaptoethanol, 0.001% w/w bromophenol blue). This buffer was also used as a loading dye for SDS-PAGE, and to terminate reactions by adding an equal volume of 2x SDS buffer.

### **2.5.1 Isolation of whole protein extracts from *Arabidopsis* seedlings**

Following experimental treatments, approximately 50 seedlings were harvested under a dim red safe light, placed in a microcentrifuge tube and ground with a micropestle in 100 µl of 2x SDS Buffer and boiled for 5 minutes at 90°C. The extracts were then centrifuged for 5 minutes at maximum speed before recovering the supernatant for immediate analysis using SDS-PAGE or storage at -20°C for later use.

### **2.5.2 Isolation of whole protein extracts from mature plants**

For adult *Arabidopsis* plants, leaf tissue was harvested and frozen in liquid nitrogen to maximize tissue disruption. The frozen tissue was ground with a chilled micropestle, following which 200 µl 2x SDS Buffer supplemented with a cComplete mini EDTA-free protease inhibitor tablet (Roche) was added per 100 mg tissue. The tissue was further ground

in the buffer before boiling for 5 minutes at 90°C and centrifuging at maximum speed for 5 minutes to recover the supernatant. If necessary, the adult plants were placed in darkness overnight prior to protein isolation to maximize the accumulation of phot1 protein. For protein extraction from *Nicotiana benthamiana* used for BiFC analysis, three discs excised from the leaf with the lid of a microcentrifuge tube were harvested for each pair of expressed proteins and harvested in 150 µl 2x SDS buffer as described above.

### **2.5.3 Isolation of soluble protein extracts from Sf9 insect cells**

Under a dim red safe light, 3 ml of adherent insect cell culture was resuspended in its media and gently pelleted by centrifuging at 1000 RPM for 1 minute in a test tube. From the supernatant, 2.5 ml was discarded, and the pellet was resuspended again in the remaining media and transferred to a microcentrifuge tube. The tube was centrifuged again for 1000 RPM for 1 minute. The supernatant was then fully removed, and the pellet was resuspended in 100 µl 1x Phosphorylation Buffer (see section 2.14) and sonicated with 5 brief bursts. After sonication, the extracts were centrifuged at full speed for 3 minutes, following which the soluble fraction was recovered. Protein content was assessed by Bradford Assay.

## **2.6 Determination of protein content**

### **2.6.1 Bradford assay**

Bradford reagent (Bio-Rad) was diluted 1:5 in deionized water and filtered through Whatman paper. A standard curve was constructed by mixing 0, 5, 10, 15, and 20 µg bovine serum albumin (BSA; Promega) with the diluted Bradford reagent and measuring the  $A_{595}$  of each protein mixture. The absorbance versus concentration data points were fitted using a linear regression. One microliter of a protein sample of unknown concentration was added to 999 µl of the prepared Bradford reagent and vortexed. The  $A_{595}$  of the sample was then measured, and the linear regression was used to estimate its concentration. If the absorbance was greater than 1.0, the sample was diluted, and the concentration was estimated again.

### **2.6.2 Absorbance at 450 nanometers**

Protein content for phot1 LOV1+LOV2 and LOV2 proteins calculated from their absorbance at 450 nm using Beer's law (Absorbance = molecular absorptivity\*pathlength\*molarity) unless otherwise noted. The molecular absorptivity of LOV domains was taken as 12,500 M<sup>-1</sup> cm<sup>-1</sup> (Losi *et al.*, 2002). The pathlength of the Quartz SUPRASIL Micro cuvette (Perkin-

Elmer) used was 0.5 cm. For phot1 LOV1+LOV2, the concentration was divided by two after the calculation was made to account for the two LOV domains in the protein.

## **2.7 Protein electrophoresis and Western Blotting**

### **2.7.1 SDS-Polyacrylamide gel electrophoresis (SDS-PAGE)**

Protein extracts in SDS buffer were resolved using SDS-PAGE as developed by Laemmli (1970). In general, polyacrylamide gels were cast with a 7.5% (v/v) polyacrylamide (40% Acrylamide/Bis Solution 37.5:1; Bio-Rad) resolving gel and a 10% polyacrylamide stacking gel. Electrophoretic mobility shift experiments with phot1-GFP were resolved using a 6.5% polyacrylamide resolving gel. Prior to electrophoresis, the protein extracts were boiled for 5 minutes at 90°C to denature the proteins. The protein extracts were then loaded onto the gel along with the PageRuler Prestained Protein Ladder (Thermo-Fisher) standard to aid in estimation of protein size and migration. Electrophoresis was conducted at 200V for 45 minutes, or until the desired migration was achieved, as estimated by the progress of the protein ladder in the gel.

### **2.7.2 Coomassie staining and gel drying**

Coomassie staining solution was prepared by mixing 0.1% (w/v) Coomassie Brilliant Blue R-250 (Bio-Rad) dye into a 10% (v/v) acetic acid, 50% (v/v) methanol solution until solubilized. The stain was then filtered through Whatman paper. Following SDS-PAGE, the polyacrylamide gel was incubated in the staining solution for 15 minutes with agitation. The stain was then discarded, and the gel was destained with agitation in a 7% (v/v) acetic acid, 12% (v/v) methanol solution with a small piece of paper towel to absorb excess dye for at least 2 hours, up to overnight, to sufficiently reduce the amount of background dye. If necessary, the stained gel was dried by placing it onto a piece of Whatman paper and drying it in a gel dryer (Scie-Plas GD4534) at 80°C for 1 hour with vacuum applied.

### **2.7.3 Western blotting**

Following SDS-PAGE, proteins in the polyacrylamide gel were immobilized onto a nitrocellulose membrane (Thermo-Fisher) by electro-transfer in Transfer Buffer (25 mM Tris, 190 mM glycine, 20% (v/v) methanol) at 100V for 1 hour. To confirm successful transfer and equal protein loading, the membrane was stained in Ponceau Solution (0.1% (w/v) Ponceau S, 1% (v/v) acetic acid) for 5 minutes and rinsed with deionized water to

remove background staining. The membrane was then blocked in Tris-Buffered Salts with Triton (TBS-T; 25 mM Tris-HCl, 137 mM sodium chloride, 2.7 mM potassium chloride, 0.1% (v/v) Triton X-100) containing 5% dissolved milk powder (Marvel) for 1 hour at room temperature with agitation. Following blocking, the membrane was incubated with the primary antibody at the appropriate dilution (see table 2.4) in the Milk-TBS-T buffer overnight at 4°C. The next day, the membrane was washed three times with the Milk-TBS-T buffer, incubating 5 minutes at room temperature for each wash. The appropriate HRP-conjugated secondary antibody was diluted in the Milk-TBS-T buffer and added to the membrane to incubate for 1 hour at room temperature with agitation. To prepare to detect the proteins of interest, the membrane was then washed 5 times in TBS-TT buffer (25 mM Tris-HCl, 137 mM sodium chloride, 2.7 mM potassium chloride, 0.2% (v/v) Triton X-100, 0.05% (v/v) Tween-20), incubating for 5 minutes with agitation for each rinse. Immediately prior to visualization, the solutions in the Pierce ECL Western Blotting Substrate (Thermo-Fisher) were combined according to the manufacturer's protocol and incubated on the membrane for 5 minutes. The immuno-detected proteins were then visualized by exposing Medical X-Ray Film (Carestream) to the membrane. Table 2.5 details all antibodies used in this study and their working dilutions.

<b>Primary antibody</b>	<b>Primary antibody working concentration</b>	<b>Primary antibody source</b>	<b>Secondary antibody and its working concentration</b>
Anti-c-myc	1/1,000	Santa-Cruz (9E10)	Mouse; 1/1,000
Anti-HA	1/1,000	Roche (3F10)	Rat; 1/1,000
Anti-phot1 C-terminal	1/10,000	Cho <i>et al.</i> (2007)	Rabbit 1/15,000
Anti-phyA	1/2,000	Agrisera (AS07220)	Rabbit; 1/5,000
Anti-phyB	1/5,000	Shinomura <i>et al.</i> , 1996	Mouse; 1/10,000
Anti-NPH3	1/10,000	Peptide antibody from Dr. Noriyuki Suetsugu	Rabbit; 1/15,000
Anti-UGPase	1/10,000	Agrisera (AS05086)	Rabbit; 1/15,000

**Table 2.5: Antibodies used in this study.** For each primary antibody used, the source, appropriate dilution, and secondary antibody with its dilution is listed.

## 2.8 Sequence alignment

Orthologous and homologous DNA and protein sequences were aligned using Clustal Omega (<https://www.ebi.ac.uk/Tools/msa/clustalo/>). Sanger sequencing results were checked for mutations by submitting them to NCBI Blast (<https://blast.ncbi.nlm.nih.gov/Blast.cgi>). NCBI Blast was also used to identify sequences similar to the gene or protein of interest.

## 2.9 Bacterial transformation and growth

### 2.9.1 Generation of chemically competent *E. coli*

One hundred milliliters of PSI broth (0.5% (w/v) yeast extract, 2% (w/v) tryptone, 42 mM magnesium sulfate, pH 7.6) was inoculated with 1 ml of an overnight culture of DH5 $\alpha$  *E. coli* cells from a single colony and grown at 37°C with shaking to an OD<sub>600</sub> of 0.5. The culture was then cooled on ice for 15 minutes. The culture was pelleted by centrifugation at 3500 RPM for 5 minutes at 4°C. The supernatant was decanted, and the cells were resuspended in 0.4x volume of TfbI Buffer (30 mM potassium acetate, 100 mM rubidium chloride, 10 mM calcium chloride, 50 mM manganese chloride, 15% (v/v) glycerol, pH 5.8 with acetic acid). The cells were then chilled on ice for 15 minutes. The centrifugation step was repeated, and the supernatant was decanted. The cells were then resuspended in 0.04x original volume of TfbII Buffer (10 mM MOPS, 75 mM calcium chloride, 10 mM rubidium chloride, 15% (v/v) glycerol, pH 6.5 with sodium hydroxide) and chilled again on ice for 15 minutes. The competent cells were then aliquoted into microcentrifuge tubes in 50  $\mu$ l volumes, flash frozen in liquid nitrogen, and stored at -80°C.

### 2.9.2 Transformation of chemically competent *E. coli*

Chemically competent cells were thawed on ice. Between 5-20 ng of the plasmid DNA to be transformed into the cells was added per 50  $\mu$ l of competent *E. coli* cells and incubated on ice for 30 minutes. The cells were then heat shocked at 42°C for 30 seconds and immediately placed on ice for 2 minutes. To recover the heat shocked cells, 450  $\mu$ l of LB was added to the cells, which were then incubated at 37°C with shaking for 1 hour. Following the recovery step, the cells were spread onto an LB agar (Luria broth with 0.8% agar) plates containing the appropriate selective antibiotic and placed in a 37°C incubator overnight to obtain colonies.

### **2.9.3 Generation of electrocompetent *Agrobacterium tumefaciens* cells**

Five hundred milliliters of LB media supplemented with 50 µg/ml gentamycin sulfate (Melford) was inoculated with 10 ml of an overnight culture of GV3101 *Agrobacterium tumefaciens* cells. The culture was then grown at 28°C with shaking until it reached an OD<sub>600</sub> of 0.5-1. The culture was then chilled on ice for 15 minutes. The culture was pelleted by centrifugation at 4000 RPM for 15 minutes at 4°C. The supernatant was decanted, and the pellet was resuspended in 500 ml of cold deionized water, followed by a repeat of the centrifugation step. The supernatant was decanted once more, and the pellet was resuspended in 10 ml of cold 10% (v/v) glycerol, and the centrifugation step was repeated. The supernatant was gently removed from the loose pellet, which was then resuspended in 2-3 ml of the cold 10% glycerol solution. The cells were then aliquoted in 50 µl volumes, flash frozen in liquid nitrogen, and stored at -80°C.

### **2.9.4 Transformation of *Agrobacterium* by electroporation**

Fifty microliters of electrocompetent *Agrobacterium* cells were thawed on ice, combined with 20-40 ng of plasmid DNA and placed in a cold 0.1 cm electroporation cuvette (Bio-Rad). The cells were then electroporated in a Bio-Rad MicroPulser using the *Agrobacterium* setting. Immediately following electroporation, 1 ml of ice-cold LB was added to the cuvette and the cells were then removed to a microcentrifuge tube. The cells were incubated at 28°C with shaking for 2-3 hours to recover. One hundred microliters of the cells were then spread onto an LB agar plate supplemented with 50 µg/ml gentamycin in addition to the selective antibiotic appropriate for the transformed plasmid. The plate was incubated at 28°C for 3 days to obtain colonies.

## **2.10 Heterologous expression and purification of proteins in *E. coli***

### **2.10.1 Heterologous protein expression in *E. coli***

The plasmid construct of interest was first transformed into Rosetta (DE3) pLysS competent cells (Novagen; as in section 2.9.2). A single colony was selected for a 100 ml overnight culture of LB containing 20 µg/ml of chloramphenicol (Duchefa) and the appropriate concentration of selective antibiotic for the transformed plasmid. The next day, 1 L of LB with 20 µg/ml of chloramphenicol and the correct dilution of the other selective antibiotic

was inoculated with 20 ml of the overnight culture. The large culture was then incubated at 37°C with shaking until an OD<sub>600</sub> of 0.6 was reached. The temperature was then lowered to 24°C and the culture was incubated for 30 minutes to allow the temperature of the culture to equilibrate. The culture was then induced by adding isopropyl β-D-1-thiogalactopyranoside (IPTG) to a final concentration of 0.5 mM and the incubation at 24°C with shaking was continued overnight. Phot1 LOV1+LOV2 proteins were expressed exactly as above; phot1 LOV2 proteins were expressed as above with the exceptions that the temperature was instead lowered to 18°C and a final concentration of 0.2 mM IPTG induced the culture.

Proteins were harvested from the *E. coli* cells by centrifuging the culture at 4000 RPM for 20 minutes at 4°C. The supernatant was decanted, saving 30 ml from the supernatant to resuspend the pellet. The centrifugation step was repeated, following which the supernatant was totally discarded. For cells that expressed the LOV1+LOV2 protein, the pellet was then resuspended in 10 ml of Breaking Buffer (50 mM Tris-HCl pH 8.0, 500 mM sodium chloride, 10 mM imidazole, 10% glycerol, 0.2% Triton-X100). For the single LOV2 protein, the pellet was resuspended in Buffer A (Halavaty and Moffat, 2013; 20 mM Tris-HCl pH 7.4, 20 mM sodium chloride). Both sets of cells were flash frozen in liquid nitrogen to encourage lysis by freeze/thawing. The resuspended pellet was then stored at -80°C or used immediately for purification.

### **2.10.2 Affinity chromatography purification of proteins**

Phot1 LOV1+LOV2 proteins were expressed using the pCal-n-EK vector, which encodes a protein with an N-terminal calmodulin binding protein (CBP) tag, and purified using the Affinity Protein Expression and Purification System (Stratagene), which uses the affinity of the CBP tag for calmodulin resin in the presence of calcium to purify tagged proteins. LOV1+LOV2 consists of the portion of phot1 from amino acids 180 to 628 and was cloned into the pCal-n-EK vector as described in Kaiserli *et al.* (2009). For biophysical study, the single LOV2 domain was cloned into the pGB1-6His expression vector with an N-terminal 6xHis tag as described in section 2.3.7.1. LOV2 with the 6xHis tag was purified using the affinity of the 6xHis tag for Ni-NTA resin (Bio-rad) as described by Halavaty and Moffat (2013). Mutant variants of both constructs were generated by site-directed mutagenesis as described in section 2.3.4.2. All purification steps were conducted at room temperature.

Prior to purification of phot1 LOV1+LOV2 proteins, the cells that were harvested from *E. coli* culture as described in section 2.9.1 were thawed on ice. One volume of Calcium

Chloride Buffer (50 mM Tris-HCl pH 7.6, 1 mM magnesium acetate, 1 mM imidazole, 2 mM calcium chloride, 150 mM sodium chloride, 5% glycerol) was added to the thawed cells, which were then sonicated on ice using a Sanyo Soniprep 150 to ensure that the cell walls were thoroughly disrupted. The cell debris was then pelleted by centrifugation at 30,000 RPM for 30 minutes at 4°C. The supernatant containing the soluble fraction was recovered and used to purify the protein of interest.

To prepare the calmodulin affinity column, 3 ml of calmodulin affinity resin was added to an empty column. The column was equilibrated with 5 column-volumes of Calcium Chloride Buffer. The soluble protein fraction from the previous step was then added to the column and allowed to flow through. The bound protein was then washed with 10 column-volumes of Calcium Chloride Buffer. The bound protein was eluted with approximately 10 ml of Elution Buffer (50 mM Tris-HCl pH 7.6, 2 mM EGTA, 1 M sodium chloride, 5% glycerol). The eluted protein was collected in 0.5 ml fractions and protein content was assessed.

The 6xHis tagged LOV2 protein was purified similarly. The cell pellet resuspended in Buffer A was sonicated and then centrifuged to recover the soluble fraction as described. The column was prepared with Ni-NTA resin (Bio-Rad) as described and equilibrated with Buffer A, following which the soluble fraction was added. The column was washed with Buffer A supplemented with 20 mM imidazole and the protein was eluted using Buffer A supplemented with 250 mM imidazole and the eluted fractions were collected as above.

If necessary, the eluted LOV1+LOV2 fractions were pooled and concentrated using Amicon Ultra centrifugation filter devices (Millipore). For phot1 LOV2 proteins, the filter devices were used to eliminate imidazole by concentrating the protein to 0.5 ml and then topping up the volume to 4 ml with Buffer A without imidazole twice. The purity and integrity of purified proteins was assessed by a Coomassie-stained SDS-PAGE gel.

### **2.10.3 TEV cleavage of the 6xHis tag from LOV2**

Tobacco etch virus (TEV) protease was used to cleave the 6xHis tag from the purified phot1 LOV2 protein. One milligram of homemade TEV (supplied by the Zoltowski lab, Southern Methodist University) was added per 30 mg of protein and incubated overnight at 4°C. To remove the cleaved tag from the sample, the protein was passed once more through the Ni-NTA column, which bound the tag and uncleaved protein, but not cleaved LOV2.

### **2.10.4 Size exclusion chromatography**

As the final purification step of LOV2 protein for crystallography and NMR analysis, the cleaved LOV2 protein was subjected to size exclusion chromatography (SEC) using a Superdex s200 column (GE Healthcare). Fractions 8, 9, and 10 were collected for downstream use.

### **2.11 NMR spectroscopy**

To generate  $^{15}\text{N}$ -labelled protein, BL21(DE3) cells (Novagen) transformed with the pGB1-6His-LOV2 construct were grown to an  $\text{OD}_{600}$  of 0.6 in M9 medium (48 mM disodium phosphate, 22 mM monopotassium phosphate, 8.6 mM sodium chloride, 19 mM  $^{15}\text{N}$ -enriched ammonium chloride, 0.76  $\mu\text{M}$  calcium chloride, 10  $\mu\text{M}$  magnesium sulfate, 1  $\mu\text{g}/\text{ml}$  thiamine, 1  $\mu\text{g}/\text{ml}$  biotin, 0.3% glucose) as described in section 2.10.1. The culture was induced with 0.2 mM IPTG and grown overnight as described in 2.10.1. The LOV2 protein was prepared for NMR as described above in sections 2.10.1-2.10.4.

The purified protein was dialyzed overnight in a 3 ml Slide-A-Lyzer Dialysis Cassette with a 10 kDa molecular weight cut-off (Thermo-Fisher) to exchange the buffer from Buffer A to Phosphate Buffer (6 mM disodium phosphate, 44 mM monosodium phosphate, 100 mM sodium chloride, pH 6). In preparation for recording the NMR spectra, the protein was diluted to a concentration of 125  $\mu\text{M}$  and deuterated water ( $\text{D}_2\text{O}$ ) was added to a final concentration of 10% (v/v).

The heteronuclear single quantum correlation (HSQC) 2D experiment was performed in an 800 MHz NMR spectrometer (Agilent DD2). Spectra were taken in both the dark state and following a saturating illumination of the protein with a 450 nm laser for approximately 30 seconds.

### **2.12 UV-Vis spectroscopy**

UV-Vis spectroscopy was conducted using a Shimadzu Multispec 1501 photodiode array spectrophotometer. The scan speed was 0.1 seconds, and the light sources were 20W halogen and deuterium lamps. The slit width was 1 nm. Each measurement was taken at room temperature.

### 2.12.1 Generation of dark absorption spectra

Measurements of the absorbance of LOV1+LOV2 proteins in their dark-adapted state were generated by measuring the absorbance of fully dark-adapted protein samples from 320-520 nm in 1 nm increments in a UV-Vis spectrophotometer (Shimadzu Multispec 1501) using the Calmodulin Elution Buffer as a reference.

### 2.12.2 Generation of light-minus-dark absorption spectra

For this experiment, the fully dark-adapted LOV1+LOV2 protein of interest was used as the reference. The sample was then exposed to a saturating camera flash (Cannon EOS flash gun) of white light, immediately followed by a measurement of the loss of absorbance of the protein from 320-520 nm in 1 nm increments. The sample absorbance was then measured at the same range of wavelengths at regular intervals (most often 30 seconds) until the protein absorbance returned to its baseline dark state.

### 2.12.3 Calculation of percent photoproduct remaining

Photoproduct formation was inferred from absorbance at 450 nm. The absorbance lost at 450 nm immediately after the camera flash (see section 2.12.2) was taken to represent complete (100%) photoproduct formation. Over the course of subsequent scans the absorbance recovered to the dark state, and the percent photoproduct remaining was calculated at each time point as a percentage of the first absorbance reading  $((A_{ti} / A_{flash}) * 100)$ . The percent photoproduct remaining versus time data was then fitted to a double exponential curve using the Curve Fitting Tool from Matlab. The fast and slow half-lifetimes of recovery were calculated as  $t_{1/2 \text{ fast}} = \ln(2)/b$  and  $t_{1/2 \text{ slow}} = \ln(2)/d$  where  $b$  and  $d$  are constants from the double exponential curve (general formula:  $y = ae^{bx} + ce^{dx}$ ). Where the percent photoproduct remaining data is shown in a figure, the data is displayed as individual points connected by the fitted curve calculated by Matlab.

## 2.13 Culture and transfection of Sf9 insect cells

### 2.13.1 Culture of Sf9 cells

*Spodoptera frugiperda* cells (Sf9; Invitrogen) were grown in adherent culture in 75 cm<sup>2</sup> cell culture flasks (Corning) in 12 ml TC-100 Insect Medium (Gibco) supplemented with fetal bovine serum (FBS; Gibco) to a final concentration of 10% (v/v) at 28°C. The cells were subcultured by resuspending the cells in their media with a glass pipette and seeding half of

the total volume of cells into a new 75 cm<sup>2</sup> flask as they began to approach 90% confluence, approximately every 3 days.

### 2.13.2 Transfection of Sf9 cells to express phot1

Sf9 cells were used to express full-length phot1 for *in vitro* autophosphorylation assays. The baculovirus expression vector pAcHLT-A encoding phot1 was generated by Christie *et al.* (1998), and its variants used for this study were created using site-directed mutagenesis (see section 2.2.4.2).

Cells were prepared for transfection by seeding 1 well in a 6 well culture cluster plate (Corning) to ~50% confluence (1 ml 90% confluent cells + 1 ml of TC-100) and allowing the cells to settle for 1 hour. To exchange the serum-supplemented media for serum-free media, the cells were rinsed twice with 2 ml serum-free TC-100 before finally adding a final 2 ml of the serum-free medium to the cells as the medium for the transfection. A transfection mix was prepared by combining 100 µl serum-free TC-100, 100 ng flashBAC viral DNA, 500 ng of the pACHLT-A transfer plasmid containing the construct of interest, and 1.2 µl of baculoFECTIN II using the reagents and protocol from the flashBAC ultra kit (Oxford Expression Technologies). The transfection mix was then incubated at room temperature for 15 minutes. The mix was added dropwise to the prepared cells while gently shifting the plate to ensure even distribution. The cells were then placed in the 28°C incubator overnight. The following morning, 1 ml of serum-containing TC-100 media was added to the cells, which were then returned to 28°C. Five days following the transfection, the entire contents of the well, which is the A-stock of the virus, was removed to a 15 ml falcon tube (Corning) and stored at 4°C for future use.

The virus A-stock was then amplified to increase virus titer by adding 100 µl of the A-stock to 50% confluent cells in a 25 cm<sup>2</sup> flask (Corning) and incubating at 28°C. Five to 10 days later, the contents of the flask, which will make up the virus B-stock, were removed to a 15 ml falcon tube, centrifuged at 2500 RPM for 5 minutes to pellet cell debris, and placed into a fresh 15 ml falcon tube and stored at 4°C for future use. The virus B-stock was generally used for transfecting cells to experimentally express phot1. If necessary, the viral titer of multiple stocks was estimated by qPCR of the baculovirus IE-1 gene (section 2.3.4.5; according to the Oxford Protein Production Facilities protocol (<https://www.oppf.rc-harwell.ac.uk/OPPF/protocols/sop/OPPF->

UK%20SOP%20Insect%20Expression%2020161006.pdf); adapted from Lo and Chao,

2004) to ensure even expression. If the titer of the B-stock was determined to be very low, a C-stock was amplified from the B-stock as described above.

To express full-length phot1 in insect cells for autophosphorylation assays, 100  $\mu\text{l}$  of the virus stock of interest was added to 50% confluent cells in a 25  $\text{cm}^2$  flask supplemented with 60  $\mu\text{l}$  of 1 mM riboflavin. The flask was then wrapped in foil to protect the expressed phot1 protein from the light and incubated at 28°C for 3 days. Soluble protein extracts were harvested under a dim red safe light as described in 2.5.3.

## 2.14 Autophosphorylation assays

Autophosphorylation assays were conducted at room temperature on protein extracts from Sf9 cells expressing the phot1 variant of interest (see sections 2.13.2 and 2.5.3). A working stock of radiolabeled ATP was prepared by diluting  $\gamma$ - $^{32}\text{P}$  adenosine triphosphate ( $^{32}\text{P}$ -ATP; Perkin-Elmer) 5 times in 10  $\mu\text{M}$  unlabeled MgATP for a final activity of 0.074 MBq  $\mu\text{l}^{-1}$ . Under a dim red safe light, 1  $\mu\text{l}$  of the diluted, radiolabeled ATP was added to 10  $\mu\text{g}$  of the protein extracts and the final volume was brought to 10  $\mu\text{l}$  with Phosphorylation Buffer (37.5 mM Tris-HCl pH 7.5, 5.3 mM magnesium sulfate, 150 mM sodium chloride, 1 mM EGTA, 1 mM DTT, 1 mM PMSF, supplemented with a cOmplete mini EDTA-free protease inhibitor tablet). For the dark control samples, the reaction mix was incubated in darkness for 2 minutes following the addition of the  $^{32}\text{P}$ -ATP before the reaction was terminated by adding an equal volume of 2xSDS buffer and boiling at 95°C for 2 minutes. For the light-treated samples, the reaction mix was exposed to white light for 10 seconds for a total fluence of 30,000  $\mu\text{mol m}^{-2}$  and the reaction was allowed to continue for a total period of 2 minutes before the reaction was terminated as above.

To visualize the autophosphorylation activity, the reactions were resolved by SDS-PAGE (see section 2.7.1). The gel was then Coomassie-stained and dried (see section 2.7.2). Medical X-Ray film (Carestream) was exposed to the dried gel overnight before developing the next morning to generate the autoradiogram. To confirm equal phot1 expression in the insect cell extracts between samples, a western blot was performed on 10  $\mu\text{g}$  of the extracts using the phot1 antibody (see sections 2.7.1 and 2.7.3).

## 2.15 *Arabidopsis* growth

### 2.15.1 Plant materials

The *Arabidopsis thaliana* ecotype Colombia (Col-0) was used in this study and the wild-type control plants and phototropin mutants were Col-0 plants in the trichome deficient *glabrous* (*gll*) mutant background. Mutants of *phot1* (*phot1-5*) and *phot2* (*phot2-1*) and the *phot1phot2* double mutant have been characterized (Liscum and Briggs, 1995; Jarillo *et al.*, 2001; Kagawa *et al.*, 2001; Sakai *et al.*, 2001). The phytochrome mutants *phyA-211* and *phyB-9* were originally characterized in Nagatani *et al.* (1993) and Reed *et al.* (1993), respectively. Transgenic lines used in this study that were previously characterized includes *PHOT1::phot1-GFP* (Sullivan *et al.*, 2016) and *35S::LOV2Kinase* (Sullivan *et al.*, 2008).

### 2.15.2 *Arabidopsis* growth conditions

In general, *Arabidopsis* seeds were sown onto soil and stratified for 2 days in darkness at 4°C before being placed in a Fitotron growth chamber (Weiss Technik) fitted with LEDs emitting white light (Philips). The plants were grown in the chamber under white light at a fluence rate of 100  $\mu\text{mol m}^{-2} \text{s}^{-1}$  with 16/8 hour light/dark cycles at a temperature of 22°C during the day and 18°C during the night.

For experiments involving seedlings, surface-sterilized seeds were sown onto half-strength Murashige and Skoog medium (MS; Murashige and Skoog, 1962) plates containing 0.8% agar and stratified for 2 days as above before placement in the experimental light condition of interest. If etiolated seedlings were required, they were given a 6 hour pulse of white light to induce germination before they were covered in aluminium foil and placed in darkness for 72 hours from the onset of the germinating light pulse.

### 2.15.3 Surface sterilization of seeds

Seeds were sterilized by incubation in a solution of 0.05% Tween-20 and 20% sodium hypochlorite solution (available chlorine 4.00-4.99%) for 10 minutes with agitation. The seeds were then rinsed with sterile water 3 times before finally resuspending the seeds in 1 ml of sterile water for sowing the seeds on half-strength MS media plates.

## 2.15.4 Isolation of microsomal membranes from *Arabidopsis*

In preparation for the isolation, approximately 100 µl-worth of dry seeds in a microcentrifuge tube were surface sterilized and sown on half-strength MS agar plates and etiolated as described in 2.15.2 and 2.15.3. Three-day-old etiolated seedlings were ground in 3 ml of Microsome Extraction Buffer (50 mM Tris-HCl pH 7.5, 300 mM sucrose, 150 mM sodium chloride, 10 mM potassium acetate, 5 mM EDTA, 1 mM PMSF, with a cOmplete mini EDTA-free protease inhibitor tablet) under a dim red safe light with a mortar and pestle on ice. The ground seedlings in buffer were then centrifuged in a Sorvall Discovery M120SE ultracentrifuge at 10,000  $xg$  for 10 minutes. The supernatant was recovered the pellet and then centrifuged again as above. The supernatant was recovered from the pellet once more and then centrifuged at 100,000  $xg$  for 1 hour and 15 minutes. The supernatant was discarded, and the pellet was resuspended in 100 µl of Microsome Extraction Buffer. Protein content was determined by Bradford Assay. Autophosphorylation assays were performed using 10 µg of protein as described in 2.14, with the alteration that 1 µl 10% Triton X-100 was added and the reaction was warmed in the hands for 1 minute prior to the addition of  $^{32}P$ -ATP.

## 2.16 Generation of transgenic *Arabidopsis*

### 2.16.1 *Arabidopsis* transformation by floral dip

For floral dipping, the plasmid construct of interest was first transformed into *Agrobacterium* cells by electroporation as described in 2.9.4. The *PHOT1::phot1-GFP-pEZR(K)-LN* constructs coding for the mutants of *phot1* to be studied *in planta* were generated by Gibson Assembly as described in 2.3.7.2.

All constructs were transformed into the *phot1phot2* mutant, which were densely sown on soil in a 10 cm pot, stratified and grown as described in 2.15.2. When the plants were flowering, all of the siliques present were trimmed to reduce the background of non-transformed seeds.

On the day before the floral dip, a single *Agrobacterium* colony transformed with the pEZR(K)-LN construct of interest was inoculated into a 50 ml overnight culture of YEBS media (1 g/L yeast extract, 5 g/L beef extract, 5 g/L sucrose, 5 g/L peptone, 0.5 g/L magnesium sulfate, pH 7) supplemented with 50 µg/ml gentamycin and 50 µg/ml kanamycin (Melford) and grown at 28°C with shaking. The next morning, 500 ml of YEBS media was inoculated with the entire overnight culture and grown at 28°C with shaking until very dense

(toward the finish of the working day). The culture was then combined with 500 ml of 5% (w/v) sucrose and 200  $\mu$ l Silwet L-77 (Loveland Industries). The inflorescences of the *phot1phot2* mutant plants were then dipped into the mixture and swirled for 10 seconds. Excess mixture was allowed to drip off the inflorescences and then the pot was placed in a tray on its side, which was then wrapped in an autoclave bag to increase humidity and left overnight. The mixture was saved and stored at 4°C. The next morning, the autoclave bags were removed, and the pots were returned to an upright position. Four days after the first dip, the plants were dipped again as above in order to transform any recently-emerged flowers. This protocol is adapted from Davis *et al.*, 2009.

### 2.16.2 Selection of transformants

Transformants generated by floral dip were screened for both resistance to kanamycin, which is encoded by the pEZR(K)-LN vector, and phototropic response on sand (Silicon Dioxide; Davis *et al.* 2009). The sand (approximately 15 ml) was added to a 10 cm square plate and moistened with quarter-strength MS media containing 100  $\mu$ g/ml kanamycin. The seeds were then sown directly onto the sand and stratified at 4°C for 2 days before receiving a 6 hour germinating pulse of white light and etiolating as described (2.14.2). The 3-day-old etiolated seedlings were then given a phototropic stimulus of blue light at 0.5  $\mu$ mol m<sup>-2</sup> s<sup>-1</sup> for 8 hours from the side. Phototropically responsive individuals were noted. Following the phototropic stimulus, the plants were placed in white light overnight to fully deetiolate. Kanamycin-resistant seedlings were able to de-etiolate normally. Individuals that were both phototropically responsive and kanamycin resistant were selected to be carried on to the next generation and transferred to soil.

The first round of selection on the T<sub>1</sub> individuals was performed directly on seeds obtained from floral dip. Lines from the T<sub>2</sub> generation were chosen for a segregation ratio of approximately 3:1 of kanamycin resistance and phototropic curvature to non-resistant, non-phototropic plants in order to try to obtain single-insertion site transgenic lines. In the T<sub>3</sub> generation, 100% of the plants were expected to be kanamycin resistant and phototropically responsive. Following selection, the T<sub>3</sub> individuals to use for *in planta* physiological analysis was determined by the similarity of protein levels of the phot1-GFP variants to wild-type phot1 in *gll* and wild-type phot1-GFP in the *phot1phot2* double mutant background (Sullivan *et al.*, 2016). Three independent transgenic lines were chosen for further analysis for each phot1 mutant generated.

## 2.17 Screen for suppressors of LOV2Kinase

The suppressor screen was designed using the transgenic line LOV2Kinase (L2K; Sullivan *et al.*, 2008). LOV2Kinase is a truncated version of *phot1* expressed on the *35S* promoter in the *phot1phot2* double mutant background that is fully functional at high light intensities but does not complement *phot1* responses under low light. L2K transgenic seeds were treated with ethane methylsulfonate (EMS) to introduce random point mutations. Those seeds were then self-fertilized for two generations to create a large pool of T<sub>3</sub> seeds that were homozygous for the introduced mutations. The author is grateful to Bobby Brown, who performed this work. The seeds were then sowed onto a thin layer of soil and stratified as described in 2.15.2. They were then grown under a fluence rate of 50  $\mu\text{molm}^{-2}\text{s}^{-1}$  of white light for 1 week to establish the seedlings before the light intensity was lowered to 10  $\mu\text{mol m}^{-2} \text{s}^{-1}$ . One week later, the seedlings were visually examined for individuals with raised petioles. From ~75,000-80,000 seedlings screened, many were isolated that appeared to have raised petioles. The selected individuals were then rescreened and individuals with significantly higher petiole angles relative to L2K were used for further analysis. Petiole angles were quantified as described in section 2.18.4. The selected lines were then back-crossed against L2K and self-fertilized for 2 generations. The F<sub>2</sub> seeds segregated at a ~3:1 ratio, indicating recessive inheritance. The F<sub>2</sub> seeds with raised petioles were harvested for deep sequencing (see sections 2.3.8 and 2.2.2.2)

## 2.18 Physiological evaluation of *Arabidopsis*

### 2.18.1 Phototropism

End point phototropism was conducted on 3-day-old etiolated seedlings, which were grown vertically on half-strength MS agar square plates as described (2.15.2). The plated seedlings were exposed to a unilateral blue light stimulus of 0.5  $\mu\text{mol m}^{-2} \text{s}^{-1}$  (or the noted fluence rate) for 24 hours. At the end of the experiment, the plates were scanned and the angle of phototropic curvature for each seedling was quantified using ImageJ (National Institutes of Health).

Kinetic measurements of phototropism were conducted over 4 hours with a Retiga 6000 (QImaging) camera that captured images of the seedlings at 5-minute intervals over the course of the experiment using the Q-Capture Pro7 software (QImaging). These experiments were conducted on free-standing 3-day-old etiolated seedlings, which were prepared by sowing seeds on sand moistened with quarter-strength MS media in plastic entomology

boxes (Sullivan *et al.* 2016; Watkins and Doncaster). Stratification and etiolation were performed as described (2.15.2). For experiments involving de-etiolated seedlings, the seedlings were etiolated for 2 days following the germinating light pulse, then given an 8 hour pulse of white light to deetiolate the seedlings, followed by a 16 hour dark incubation before the onset of the experiment. Unless otherwise noted, the phototropic stimulus used for these experiments was  $0.5 \mu\text{mol m}^{-2} \text{s}^{-1}$  of blue light. The imaging software was used to generate a stack of images of the seedlings bending every 10 minutes. The curvature of each seedling in the experiment was measured every 10 minutes from the stack of images using ImageJ (National Institutes of Health).

### **2.18.2 Leaf flattening**

Leaf flattening experiments were performed as described (Takemiya *et al.*, 2005). Twelve fully expanded leaves were excised from 4-week-old plants of each genotype to be analyzed. The leaves were placed on white paper with their adaxial surfaces facing upward and imaged. Each leaf was then carefully flattened onto the paper using clear tape and the flattened leaf was imaged. The leaf area of each leaf before and after flattening was measured using ImageJ (National Institutes of Health). The leaf flattening index was calculated as the ratio of the leaf area before flattening to the area following flattening. A perfectly flat leaf would have a leaf flattening index of 1.

### **2.18.3 Chloroplast accumulation**

Chloroplast accumulation was examined using the slit-assay as developed by Suetsugu *et al.* (2005). Ten leaves from 4-week-old plants were taken from each genotype of interest and placed on 0.8% agar plates. The leaves were covered with a piece of foil that had a 2 mm slit in the middle such that the only part of the leaf that was exposed to the light was the part directly under the slit. The plates were then treated with blue light at a fluence rate of  $2 \mu\text{mol m}^{-2} \text{s}^{-1}$  for 2 hours to induce chloroplast accumulation in the lit portion of the leaves. The plates were then placed on a light box and photographed with a long exposure. Using the blue channel of each image on ImageJ, the integrated density of the covered portion of the leaf as well as the density of the illuminated section was measured. The pixels were denser where chloroplasts had accumulated than where they remained dispersed throughout the cells. The ratio of density of the lit portion to the shaded portion was calculated. Plants that were unable to perform chloroplast accumulation had a ratio near one, whereas wild-type plants had a ratio closer to 2.

#### **2.18.4 Petiole positioning**

For petiole positioning experiments, seeds were sown in pots, prepared as described (2.15.2), and grown under  $80 \mu\text{mol m}^{-2} \text{s}^{-1}$  of white light for one week before the light was lowered to  $10 \mu\text{mol m}^{-2} \text{s}^{-1}$  of white light for another week. When the plants were 2 weeks old, the plants were gently transferred to 0.8% agar plates, taking care to not disturb their architecture, so that the angle of the petioles of the first pair of true leaves relative to the horizontal could be imaged and measured using ImageJ. If necessary, one of the cotyledons was removed using a razor blade so that the plants would lie flat on the agar surface.

#### **2.18.5 Fresh and dry weight determination**

Fresh and dry weight was measured from the rosette of 4-week-old plants. A razor blade was used to remove the rosette from its roots and the rosette was weighed immediately to determine fresh weight. For dry weight, the rosette was then wrapped in a piece of foil of known weight and placed in a Unitemp drying oven (LTE Scientific) at  $65^{\circ}\text{C}$  for 4 weeks to thoroughly dry. The dry weight was then calculated from the weight of the plant in the foil packet minus the weight of the foil.

#### **2.18.6 Hypocotyl elongation**

Seeds from the genotypes of interest were sown on vertical half-strength MS agar plates and stratified as described (2.15.2). The plates were transferred directly from stratification to the light conditions to be studied, which was typically  $1 \mu\text{mol m}^{-2} \text{s}^{-1}$  of red, blue, or far-red light administered with LEDs (Philips; red: 650-670 nm, blue: 455-485 nm, far-red: 725-750 nm). If seedlings were to be grown in darkness or far-red light, they were given a 6-8 hour pulse of white light to induce germination before being placed in those conditions. The seedlings were imaged by scanning 4 days after the onset of treatment. Hypocotyl lengths were measured with the ImageJ software.

#### **2.18.7 Phot1 modulation of gravity sensing**

The gravitropic response of the EMS mutants was tested using the method developed by Lariguet and Fankhauser, 2004. Seeds from the genotypes of interest were sown on vertical half-strength MS agar plates as described (2.15.2). Immediately following stratification, the plates were transferred to blue light at a fluence rate of either  $1 \mu\text{mol m}^{-2} \text{s}^{-1}$  (for the low-blue response) or  $20 \mu\text{mol m}^{-2} \text{s}^{-1}$  (for the high-blue response) for 4 days. The plates were then

imaged and the degrees deviation from vertical of each seedling was measured using the ImageJ software.

## 2.19 Use of BiFC to probe phot1 dimerization

Phot1 dimerization using bimolecular fluorescence complementation (BiFC) was previously reported using the phot1-pSPYNE (bearing phot1 tagged with the N-terminal half of YFP) and phot1-pSPYCE (C-terminal half of YFP tagged) vectors (Walter *et al.*, 2004; Kaiserli *et al.*, 2009). To test the dimerization of mutants and truncations of phot1, the requisite pSPYNE and pSPYCE vectors were generated for each mutant of interest by Gibson Assembly (described in section 2.3.7.2) and transformed into *Agrobacterium* by electroporation (see section 2.9.4).

Overnight cultures were made by inoculating 5 ml of LB supplemented with 50 µg/ml gentamycin and 50 µg/ml kanamycin with a single *Agrobacterium* colony bearing the construct of interest (each protein to be tested for dimerization required overnights to be made of both the pSPYNE and pSPYCE versions of the construct) and grown overnight at 28°C with shaking. The next morning, the overnight cultures were pelleted by centrifugation at 4000 RPM for 10 minutes at room temperature. The supernatant was decanted and replaced with 5 ml of MES Buffer (10 mM MES, 10 mM magnesium chloride, pH 5.6 with potassium hydroxide). The OD<sub>600</sub> of each culture was measured. For each combination of interest, such as phot1-pSPYNE and phot1-pSPYCE, the cultures in MES buffer were mixed at a ratio of OD<sub>600</sub> 0.5:0.5 and supplemented with p19 (Lindbo, 2007) at a final OD<sub>600</sub> of 0.1. The volume of the mixtures was made up to 3 ml with MES buffer and the cultures were incubated at room temperature between 45 minutes and 2 hours to acclimate.

The abaxial side of *Nicotiana benthamiana* (tobacco) leaves were inoculated with the combined cultures using a 1 ml syringe and the site of inoculation was noted using a permanent marker. Three days post inoculation, a microcentrifuge tube lid was used to make discs from the leaves to be used for confocal microscopy. A Leica SP8 confocal microscope set on the 20x objective was used for imaging the plasma membranes of the tobacco epidermal pavement cells. YFP fluorescence was excited using a 552 nm excitation wavelength and emission was collected using wavelengths between 555 and 625 nm. As negative controls, both the phot1 variant of interest combined with the empty vector containing the opposite half of YFP as well as the empty pSPYNE and pSPYCE vectors

combined together were used. Images were analyzed using ImageJ. To confirm protein expression, a western blot was performed on the tobacco discs as described in 2.5.2.

## Chapter 3 Modifying the Phot1 Photocycle *in vitro*

### 3.1 Introduction

Light sensing in LOV domain photoreceptors is characterized by the formation of a covalent photoadduct between a conserved cysteine within the domain and the C(4a) carbon of the flavin chromophore (Salomon *et al.*, 2000). Over a period of time ranging from seconds to many hours, depending on the photoreceptor, the photoadduct decays and the photoreceptor returns to its dark state, completing the photocycle (Salomon *et al.*, 2000; mechanism reviewed in Briggs, 2007). Remarkably, this mechanism is very well conserved in diverse LOV domains found in organisms as varied as bacteria, fungi, and plants (Glantz *et al.*, 2016; Briggs, 2007). Relative to other LOV-based blue light photoreceptors, the photoadduct of phototropin LOV domains is fairly short-lived, with the photocycle completing within approximately 15 minutes (Kaiserli *et al.*, 2009).

The photocycle of LOV domains has been extensively characterized. Modulating the period of LOV domain activity is considered a key feature of their usefulness as light sensors for optogenetic tools, many of which use blue light perception in LOV domains to artificially control events at a molecular or cellular level (Pudasaini, El-Arab and Zoltowski, 2015). Since LOV domains are well-conserved, the information uncovered for optogenetic devices as well as from naturally occurring LOV-based photoreceptors should be broadly applicable to engineering the photocycle of LOV domains generally. However, little work has been done to investigate whether the photocycle can be manipulated to change the threshold of sensitivity of native photoreceptors *in vivo*. The goal of the work presented in this chapter was to use established literature on LOV domain photocycles in order to manipulate the slowness of the *Arabidopsis* phot1 photocycle to increase the length of time over which the photoadduct is stable. The resulting larger pool of activated phot1 within the cell at a given time should transduce more signal, increasing overall sensitivity for phot1-mediated responses.

Our system for studying the *Arabidopsis* phot1 photocycle *in vitro* is LOV1+LOV2, a truncation of phot1 that only contains the light-perceiving domains. This truncated protein is amenable to heterologous expression in *E. coli* and has a similar photocycle to the full-length protein (Kasahara *et al.*, 2002). While the photocycle has traditionally been studied using single LOV domains, LOV1 as well as LOV2 contributes to the overall photocycle (Christie *et al.*, 2002; Kasahara *et al.*, 2002; Kaiserli *et al.*, 2009), therefore both LOV

domains were retained in order to simulate the *in vivo* photocycle as accurately as possible. Though both LOV domains are present in our system, only LOV2 was modified with photocycle mutations as the LOV2 domain is the primary light sensor in phot1 and is solely responsible for the conformational changes that activate the kinase domain upon light perception (Harper *et al.*, 2004; Sullivan *et al.*, 2008; Kaiserli *et al.*, 2009). In this study, photocycle modifying mutations based on the literature were introduced into LOV2 within the *Arabidopsis* phot1 LOV1+LOV2 protein to investigate whether the photocycle can be substantially altered in order to later investigate its effects on sensitivity *in vivo*.

## 3.2 Results

### 3.2.1 Characterization of the wild-type LOV1+LOV2 photocycle

The photochemistry of the LOV1+LOV2 protein has been thoroughly described (Christie *et al.*, 2002; Kasahara, Swartz, Olney, *et al.*, 2002; Guo *et al.*, 2005; Kaiserli *et al.*, 2009); the LOV1+LOV2 construct for this study derives from Kaiserli *et al.* (2009). In order to ground the mutagenesis study presented in this chapter, the photocycle and dark absorbance of wild-type LOV1+LOV2 were re-examined. The LOV1+LOV2 protein was tagged at its N-terminus with a calmodulin binding peptide tag (CBP; see schematic in Figure 3.1A) and expressed heterologously in *E. coli*. Purification by affinity chromatography using a calmodulin affinity resin yielded a 54 kDa protein (Figure 3.1B). In the dark state, LOV1+LOV2 absorbs maximally at 448 nm, as previously reported (Figure 3.1C; Kasahara *et al.*, 2002).

The photocycle of wild-type LOV1+LOV2 was probed using UV-Vis spectroscopy to generate light-minus-dark difference spectra. LOV1+LOV2 shows a large loss of absorbance following a saturating flash of white light and fully recovers back to the dark baseline over time (Figure 3.1D). Using the light-minus-dark spectra, photoadduct formation was inferred through LOV1+LOV2 absorbance at 450 nm, which is lost upon light exposure, and increases with time as a greater proportion of the pool of LOV1+LOV2 proteins return to the dark state. Though wild-type LOV1+LOV2 absorbs maximally at 448 nm, there are subtle variations in maximum absorbance between variants of LOV1+LOV2. For consistency, 450 nm was the wavelength used for dark recovery analysis. A dark recovery kinetics curve was generated from the absorbance at 450 nm over the course of the experiment and fitted to a double exponential curve (Figure 3.1E). The half-lifetimes of recovery were 51 and 484 seconds, with the protein sample fully re-acclimated to the dark

state around 15 minutes following light exposure, reflecting the recovery of LOV1+LOV2 that was previously reported (Kaiserli *et al.*, 2009).

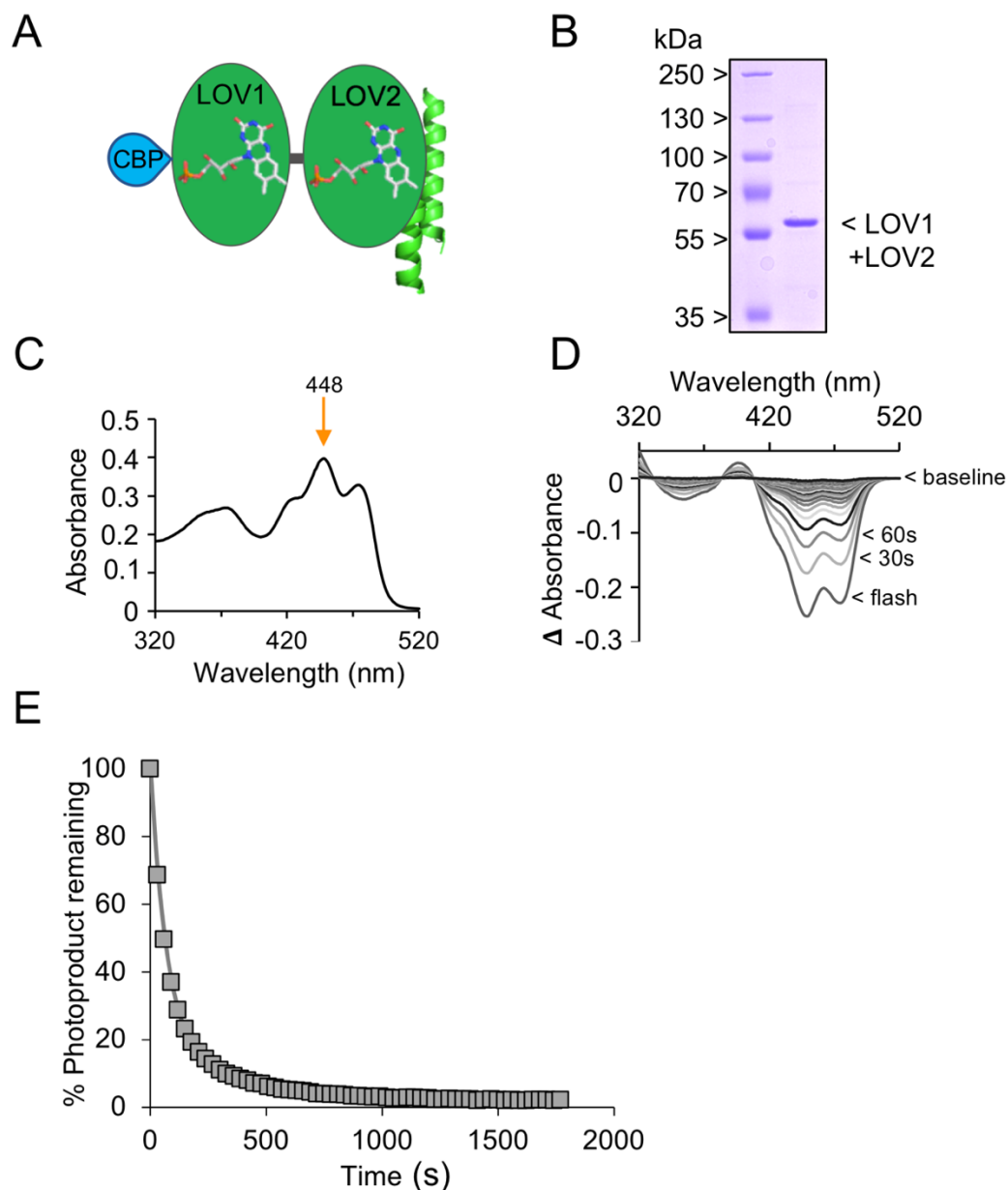


**Figure 3.1: Photochemistry of wild-type LOV1+LOV2.** **A.** Illustration of the LOV1+LOV2 fusion protein. LOV1+LOV2 is a truncation of phot1 (amino acids 180-628) consisting of the photosensory domains LOV1 and LOV2, including the A'α and Jα helices (in bright green) and is N-terminally tagged with calmodulin binding peptide (CBP). **B.** Coomassie stained SDS-PAGE of 10 μg of LOV1+LOV2 heterologously expressed and purified from *E. coli*. **C.** Dark absorption spectrum of LOV1+LOV2, with its  $A_{max}$  at 448 nm indicated. The concentration of LOV1+LOV2 was approximately 1.8 mg/ml, as determined by  $A_{450}$ . **D.** Light-minus-dark difference spectra of LOV1+LOV2. With a baseline of LOV1+LOV2 in the dark, absorbance was tracked immediately following a bright flash of white light and subsequently every 30 seconds until the dark state was recovered. The spectra after the flash and 30 and 60 seconds later are indicated for clarity. **E.** Dark recovery kinetics of LOV1+LOV2. Recovery is shown as percent photoproduct remaining. The absorbance at 450 nm immediately following the light pulse was taken as 100% photoproduct formation, and the percent photoproduct at subsequent time points is expressed as a percentage of the absorbance at that time point relative to the first measurement. The curve shown is the percent photoproduct data (gray squares) fitted to a double-exponential decay (gray line). Wild-type LOV1+LOV2 recovers with half-lifetimes of 51 and 484 seconds. These experiments were performed as a control alongside each mutant in this chapter.

### 3.2.2 Addition of the Zeitzlupe-family FAD loop to LOV1+LOV2

Though members of the Zeitzlupe (*ztl*) family of photoreceptors, which perceive blue light through a single LOV domain, bind FMN as their chromophore, these photoreceptors possess an extended loop of nine additional amino acids in their LOV domains between helices E and F that is typically characteristic of LOV domains that bind the larger FAD chromophore, but not those that bind FMN (Figure 3.2A and B; (Imaizumi *et al.*, 2003; Zoltowski *et al.*, 2007). *Ztl*-family LOV domains exhibit very slow photocycles—this is particularly true of Flavin-binding, kelch repeat, f-box 1 (*fkf1*), which recovers with a time constant of 62 hours (Zikihara *et al.*, 2006). It was later found that though the FAD loop insertion does not accommodate an FAD chromophore in these LOV domains, it does contribute to the remarkably slow photocycle of *fkf1* (Nakasone *et al.*, 2010). Due to the relatively high conservation of amino acid identity in the region around the insertion site between *phot1* LOV2 and the *fkf1* and *ztl* LOV domains (Figure 3.2A), the nine amino acid insertions from *fkf1* and *ztl* were added to LOV2 in the LOV1+LOV2 protein with the hypothesis that it could slow the LOV1+LOV2 photocycle.

The purified insertion proteins LOV1+LOV2-*ztl*-i and LOV1+LOV2-*fkf1*-i (referred to hereafter as *ztl*-i and *fkf1*-i, respectively) were analyzed photochemically. The insertion proteins exhibited an upward mobility shift when subjected to SDS-PAGE, consistent with the slight increase in size due to the nine amino acid insertion (Figure 3.2C). The dark absorbance of *ztl*-i and *fkf1*-i revealed two minor peaks in the UV-A portion of the absorbance spectrum not present in wild-type LOV1+LOV2 or the LOV domains of *ztl* or *fkf1* (Figure 3.2C; Pudasaini and Zoltowski, 2013; Imaizumi *et al.*, 2003). Initially there was a concern that the presence of the insertion could reduce occupancy of the FMN chromophore within LOV2. When 2.5 mg/ml of each protein was used to generate the dark absorbance spectra (determined by Bradford assay), the proteins yielded similar absorbances at 450 nm ( $A_{450}$  was 0.125 for wild-type, for 0.123 *ztl*-i, and 0.103 for *fkf1*-i) even though the concentration of the insertion proteins appeared to be somewhat lower on the Coomassie-stained SDS-PAGE gel (Figure 3.2C). If LOV2 were unable to bind FMN, the absorbance would have been approximately half that of wild-type LOV1+LOV2 because only LOV1 would contain the chromophore. Though there were some differences in absorbance properties relative to wild type, the presence of the *ztl*-family FAD loop insertion in LOV1+LOV2 did not seem to compromise the integrity of the protein.

**A**

Phot1 LOV2	NCRFLQGPET-----DLTTVKKIRNAID-	533
Fkfl1 LOV	NCRFLQYRDP <b>RAQRRHPL</b> VDPVVVSEIRRCLEE	122
Ztl1 LOV	NCRFLQCRGP <b>FAKRRHPL</b> VDSMVVSEIRKCID	113
	*****	* .*. :*. :*. :*

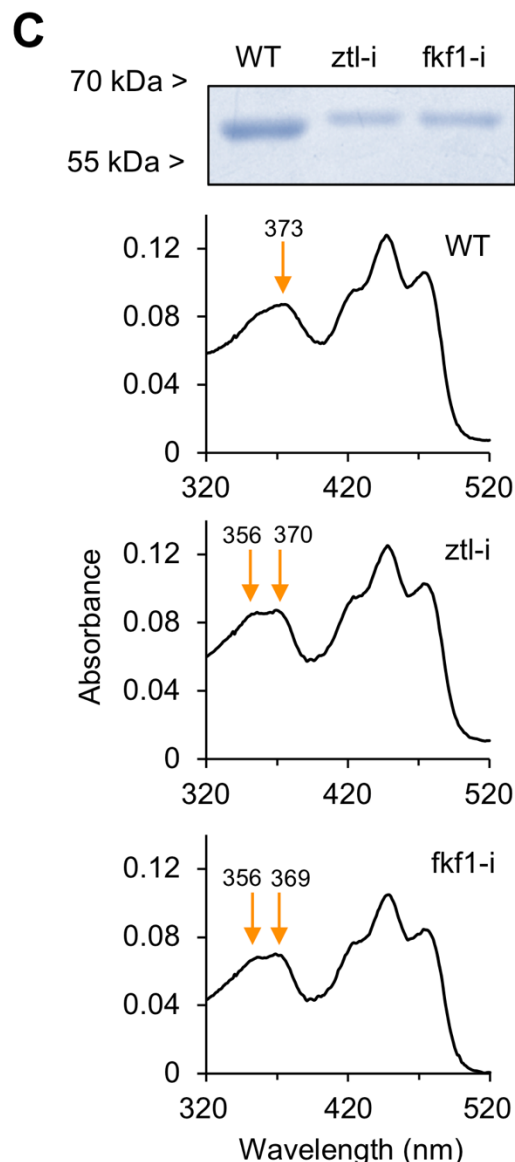
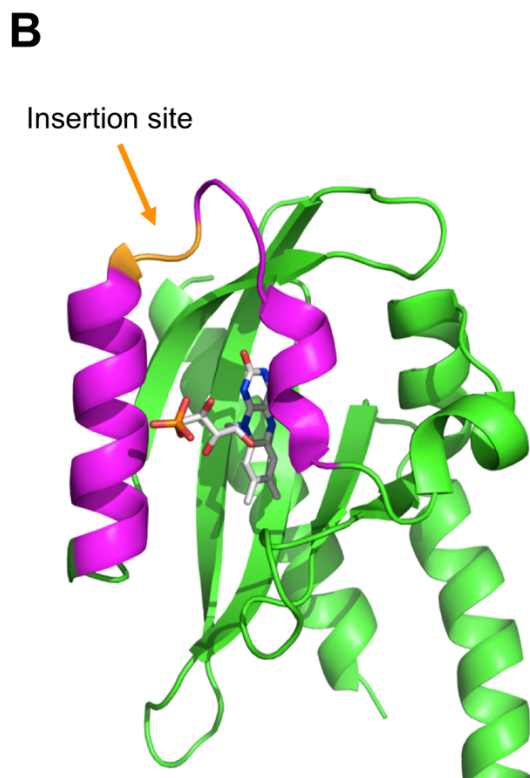


**Figure 3.2: Addition of the nine amino acid ztl family FAD loop insertion to LOV2 in LOV1+LOV2.** **A.** Clustalw alignment of the region of fkfl1 and ztl LOV domains and phot1 LOV2 around the site of the nine amino acid FAD loop present in the ztl family LOV domains but not in phot1 LOV2. Asterisks indicate the same amino acid, colons a high degree of similarity, and periods a small degree of similarity. Numbering is from the full-length amino acid sequence of the indicated protein. **B.** Phot1 LOV2 crystal structure from Halavaty and Moffat (2013). The two amino acids between which the insertion was added are highlighted in orange. The portion of phot1 LOV2 included in the alignment in 3.2A is magenta. **C.** Dark absorption spectrum of the LOV1+LOV2 insertion mutants at a concentration of 2.5 mg/ml. For the coomassie stained SDS-PAGE, 5  $\mu$ g of each protein was used. Protein content was determined by Bradford assay due to initial uncertainty regarding FMN binding in these proteins. Arrows and numbers indicate the location of the fine absorption peaks in the UV-A portion of the spectrum (in nanometers). The dark absorbance spectrum was of ztl-i was examined with three independent replicates, a representative experiment is shown; that of fkf1-i was examined once.

Due to the similarity of the nine amino insertions in *ztl* and *fkf1* (Figure 3.2A), and their similar dark absorbances, only *ztl-i* was utilized for further analysis. When the light-minus-dark difference spectra of *ztl-i* was compared to wild type, it was revealed that the *ztl-i* protein exhibited an unexpectedly fast photocycle, recovering fully in approximately two minutes, while the wild-type protein took approximately 13 minutes (Figure 3.3A; dark recovery kinetics not shown). It was also noted that the *ztl-i* protein was unable to photobleach as strongly as wild type even though the protein content was 1.8 mg/ml by  $A_{450}$  for both samples (Figure 3.3A).

The presence of the two minor peaks in the UV-A region of the dark absorbance spectrum of these proteins, coupled with the small loss of absorbance in response to light treatment and fast photocycle are characteristic of LOV1+LOV2 variants that lack a functional LOV2 domain (Christie *et al.*, 2002; Kaiserli *et al.*, 2009). To test whether LOV2 activity was abolished in *ztl-i*, LOV1 was mutated to possess the C234A mutation, which abrogates light sensing in LOV1 by preventing the covalent photoadduct from forming in that domain, leaving LOV2 as the only possible light sensor (Christie *et al.*, 2002). *Ztl-i-C234A* showed a dark absorbance spectrum that was similar to *ztl-i* and *fkf1-i*, but with further exaggerated peaks in the UV-A portion of the spectrum (Figure 3.3B). When the light-minus-dark difference spectra were examined, it was clear that *ztl-i-C234A* was unable to respond to light treatment with a loss of absorbance (Figure 3.3C), demonstrating that LOV1 was the only functional light sensor in *ztl-i*. The addition of the *ztl*-family FAD loop insertion to LOV2 in LOV1+LOV2 therefore produces a fast photocycling variant by eliminating light sensing in LOV2, but not by impairing flavin binding.

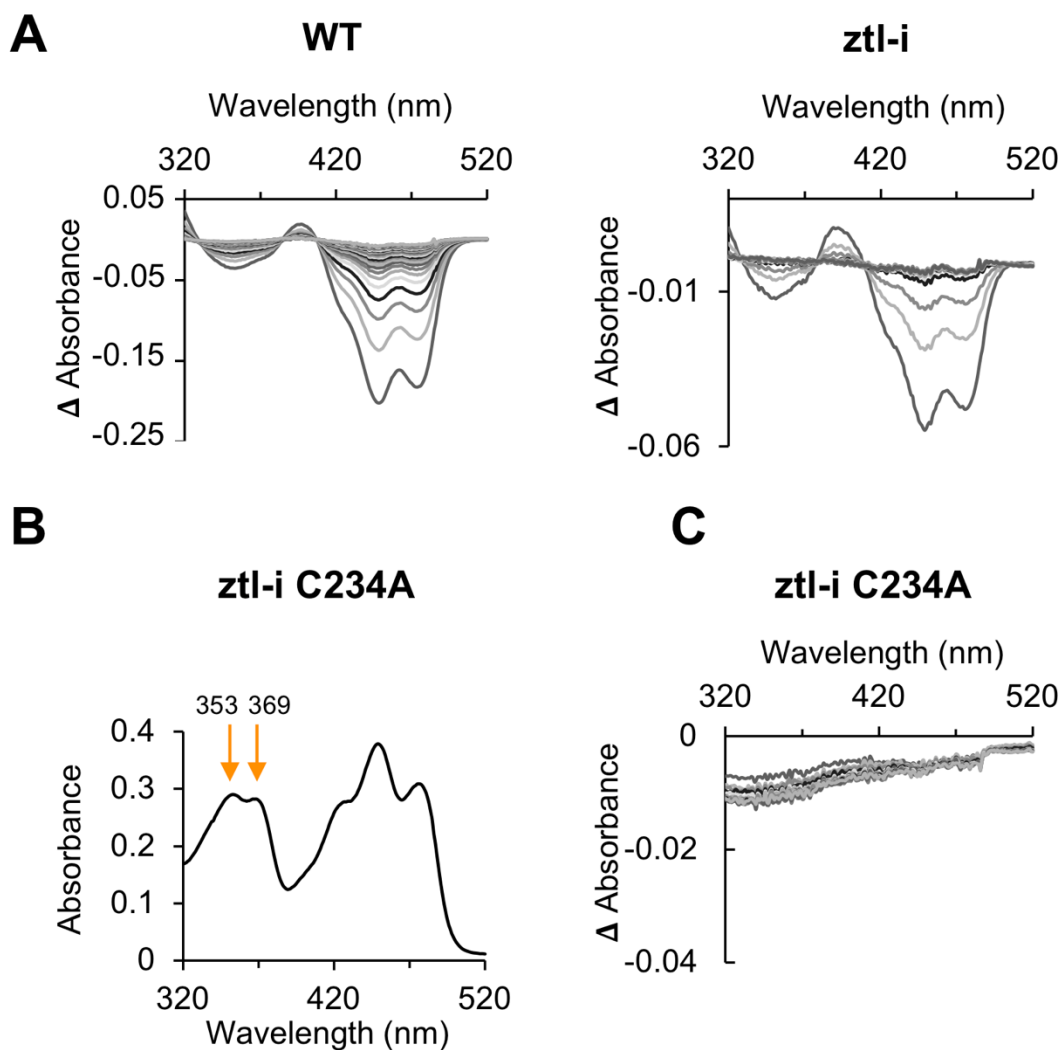


**Figure 3.3: Photoreactivity of ztl-i.** **A.** Light-minus-dark difference spectra of wild-type LOV1+LOV2 and ztl-i. Measurements were made immediately following a flash of light and subsequently every 30 seconds as described in Figure 3.1. Note the difference in the magnitude of absorbance loss between wild-type and ztl-i. Protein content was 1.8 mg/ml for both proteins, as determined by  $A_{450}$ . **B.** Dark absorption spectrum of LOV1+LOV2-ztl-i harboring the C234A mutation. The fine peaks in the UV-A spectrum are noted. **C.** Light-minus-dark difference spectra of LOV1+LOV2 ztl-i C234A. Measurements were taken immediately following the light pulse and every 15 seconds afterward as above. The light-minus dark difference spectra of ztl-i was performed with three independent replicates; ztl-i-C234A was examined using two technical replicates of the same sample.

### 3.2.3 Mutagenesis of LOV1+LOV2 based on a naturally occurring slow photocycling LOV domain

Though LOV-based photoreceptors are divergent in function, sequence conservation between LOV domains is high, most likely due to the preservation of the light-sensing mechanism (Glantz *et al.*, 2016). Given this conservation, it was hypothesized that residues known to contribute to slow photocycles in other LOV domains could also slow the photocycle of LOV1+LOV2. The *Pseudomonas putida* Sensory Box 1 (SB1) LOV domain was reported to have two unique arginine residues, R61 and R66, that contribute to an

unusually slow photocycle with half-lifetimes of 78 and 1750 minutes (Jentzsch *et al.*, 2009; Circolone *et al.*, 2012). The phot1 residue T520 (depicted in Figure 3.4D), which occupies the same position as the SB1 LOV R61, was therefore mutated to arginine to generate LOV1+LOV2-T520R to investigate whether this substitution would generate a slow-cycling LOV1+LOV2 protein.

The LOV1+LOV2-T520R protein exhibited a similar dark absorbance spectrum to wild-type LOV1+LOV2 in the blue region but showed high absorbance in the UV-A, indicating aggregation in the sample, which perhaps resulted from reduced protein stability (Figure 3.4A; compare Figure 3.1C). When the light-minus-dark difference spectra were investigated, the protein did not photobleach well in response to illumination (Figure 3.4B; compare to loss of absorbance in wild-type in Figure 3.1D, which shows around a 4-fold stronger absorbance loss). Despite the apparent lower stability and smaller response to light, the light-minus-dark spectra could be analyzed, and a dark recovery kinetics curve was generated (Figure 3.4C), revealing a photocycle that was highly similar to that of wild type. It is worth noting that the other arginine mutation, V525R, which contains the substitution corresponding to SB1 LOV R66, was examined in LOV1+LOV2 by Dr. Jan Petersen. In contrast to LOV1+LOV2-T520R, V525R exhibited a very slow photocycle, with half-lifetimes of 217 and 2310 seconds (data not shown).

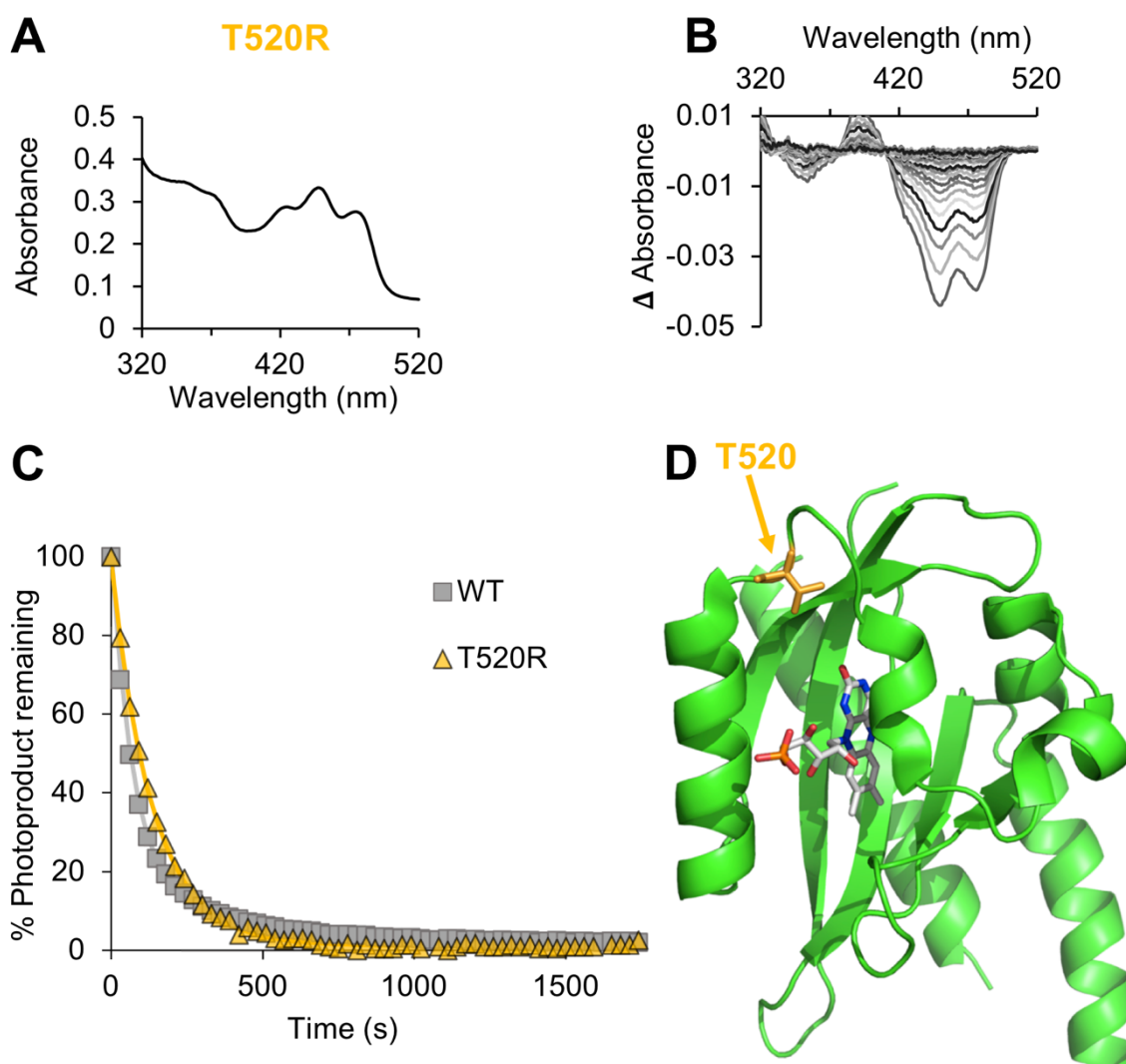


**Figure 3.4: Photochemistry of T520R, a substitution based on a slow-recovering LOV domain.** **A.** Dark absorption spectrum of LOV1+LOV2-T520R. **B.** Light-minus-dark difference spectra of LOV1+LOV2-T520R. Absorbance was tracked immediately following a bright pulse of white light and subsequently every 30 seconds as described in Figure 3.1. **C.** Dark recovery kinetics of LOV1+LOV2-T520R. Percent photoproduct is used to demonstrate recovery kinetics as shown in Figure 3.1. The half-lifetimes of recovery were 93 and 2130 seconds. These experiments were performed three times independently; a representative experiment is shown. **D.** LOV2 crystal structure from Halavaty and Moffat (2013) depicting the position of T520.

### 3.2.4 Photocycle mutations within the flavin binding pocket of LOV2

Amino acid substitutions facing the flavin chromophore of LOV domains have been reported to dramatically alter photocycles (Christie *et al.*, 2007; Yamamoto *et al.*, 2008; Zoltowski, Vaccaro and Crane, 2009; Kawano *et al.*, 2013). Generally, there are two mechanisms by which the photocycle can be modulated by these substitutions. The first is by introducing substitutions that can sterically stabilize the photoadduct forming cysteine (C512 in phot1 LOV2) in either the light-signaling conformation or the inactive dark state conformation, shifting the equilibrium of the photocycle (Zoltowski, Vaccaro and Crane, 2009). The second

is by changing the electronic density of residues surrounding the *re*-face of the flavin (opposite from the *si*-face, where photoadduct formation occurs) by substituting either with aliphatic or electron-dense residues (Yamamoto *et al.* 2008; Zoltowski, Vaccaro and Crane, 2009; reviewed briefly in Pudasaini *et al.* 2015). The LOV1+LOV2 photocycle was probed with substitutions that originated in both approaches.

To generate a fast photocycling mutant, the substitution N511S was made in our LOV1+LOV2 system. The N511S substitution was found in a random mutagenesis screen to hasten photocycle kinetics of *Avena sativa* phot1 LOV2 (*Arabidopsis* phot1 amino acid numbering; Christie *et al.*, 2007). The N511 residue is directly adjacent to C512, which forms the LOV2 covalent photoadduct, and may produce a fast photocycle by putting a more strongly polar serine side chain next to the cysteine (position of N511 shown in Figure 3.5D). Results from a single experiment show that the dark absorbance spectrum of LOV1+LOV2-N511S was typical of a functional LOV1+LOV2 protein (Figure 3.5A). The light-minus-dark difference spectra and dark recovery kinetics revealed that LOV1+LOV2-N511S is also a fast-cycling mutant in our system (Figure 5B and C). Consistent with its fast photocycle, the protein does not photobleach well, as previously reported for a similar variant (N511D) at the same residue (Figure 3.5B; Christie *et al.*, 2007; Salomon *et al.*, 2000). It is also worth noting that the percent photoproduct begins to rebound towards the end of the measurements (Figure 5D); this may be due to LOV1+LOV2-N511S completely recovering to its dark state relatively quickly and subsequently becoming re-activated by the light used to scan the protein to generate the spectra.

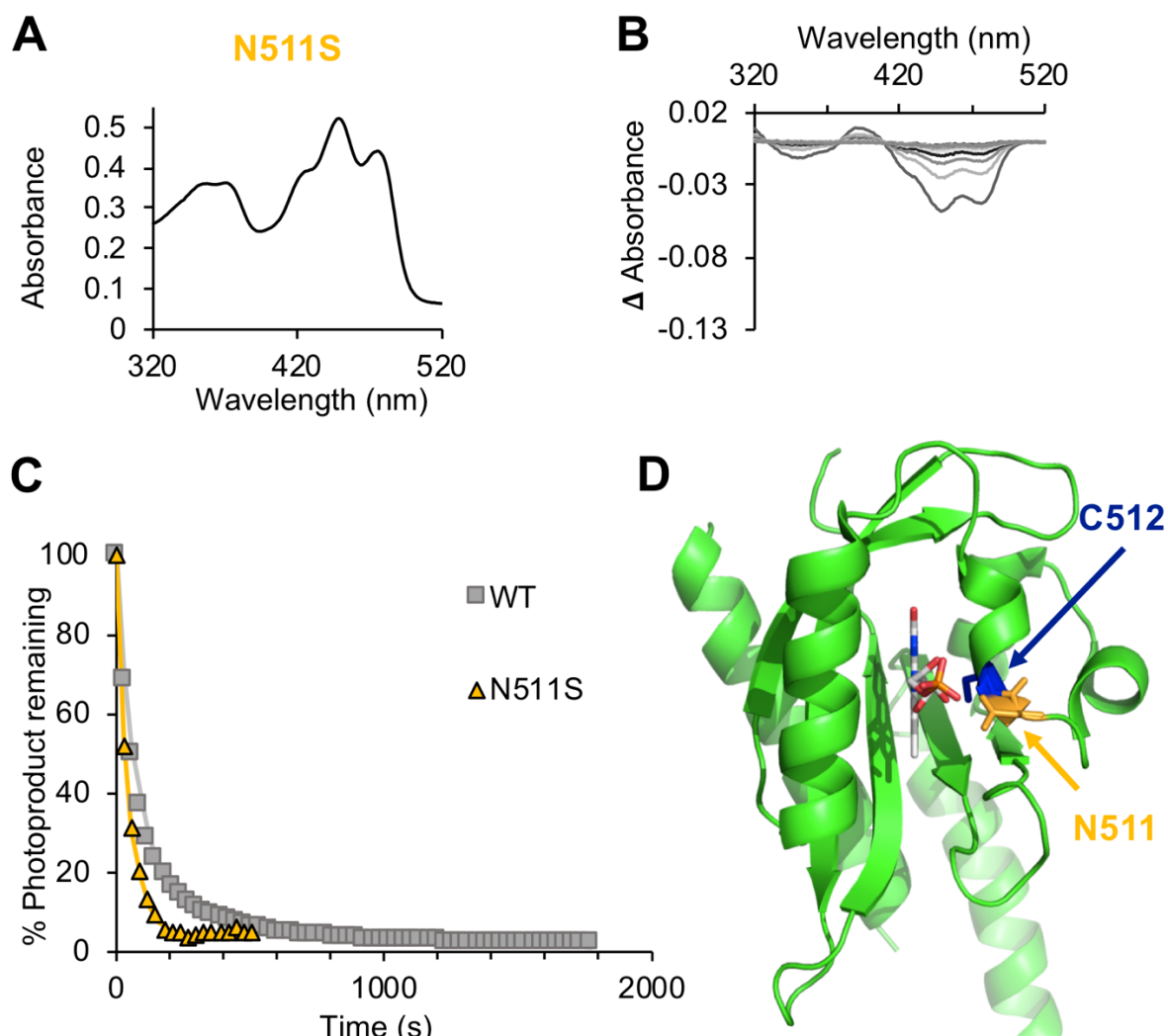


**Figure 3.5: Photochemistry of substitutions facing FMN: N511S.** **A.** Dark absorption spectrum of LOV1+LOV2-N511S. **B.** Light-minus-dark difference spectra of LOV1+LOV2-N511S. Absorbance was measured immediately following a bright pulse of white light and subsequently every 30 seconds as described in Figure 3.1. **C.** Dark recovery kinetics of LOV1+LOV2-N511S. Percent photoproduct is used to demonstrate recovery kinetics as shown in Figure 3.1. The half-lifetimes of recovery are 32 and 2562 seconds. LOV1+LOV2-N511S was investigated one time, this experiment is shown. **D.** LOV2 crystal structure from Halavaty and Moffat (2013) depicting the positions of N511 and the photoactive C512.

Two other mutations, V478L and V478I, were introduced to LOV1+LOV2 that were also hypothesized to modulate the photocycle through steric interaction with C512. The equivalent residue to phot1 V478 in the fungal photoreceptor VVD is I74, which is reported to make van der Waals contact with the photoactive cysteine (Zoltowski, Vaccaro and Crane, 2009). Kawano *et al.* (2013) uncovered the slow-cycling V478L variant through a random mutagenesis screen for photocycle mutants of *Avena sativa* phot1 LOV2. The substitution I74V generates a fast photocycle in VVD, which normally is very slow photocycling (Zoltowski, Vaccaro and Crane, 2009). Since the wild-type residue at the same position in phot1 LOV2 is a valine to begin with, we rationalized that the substitution of V478 to the isoleucine found in wild-type VVD (LOV1+LOV2-V478I) may also produce a slow

photocycle in LOV1+LOV2. We therefore generated two substitutions at V478, LOV1+LOV2-V478I and -V478L (the V478L variant was generated and characterized by Dr. Jan Petersen). The dark absorbance spectra of LOV1+LOV2-V478L and -V478I were similar to each other and to wild-type LOV1+LOV2 (Figure 3.6A; compare Figure 3.1C). Likewise, the light-minus-dark difference spectra of V478I and V478L were similar (Figure 3.6B). When the dark recovery kinetics were investigated, it was clear that both V478I and V478L possessed substantially slower photocycles than wild-type LOV1+LOV2, with V478I being slightly faster to recover than its V478L counterpart (Figure 3.6C). The half-lifetimes of recovery were 147 and 1688 seconds for V478I and 176 and 1658 seconds for V478L; wild-type LOV1+LOV2 recovers with half-lifetimes of 51 and 484 seconds.

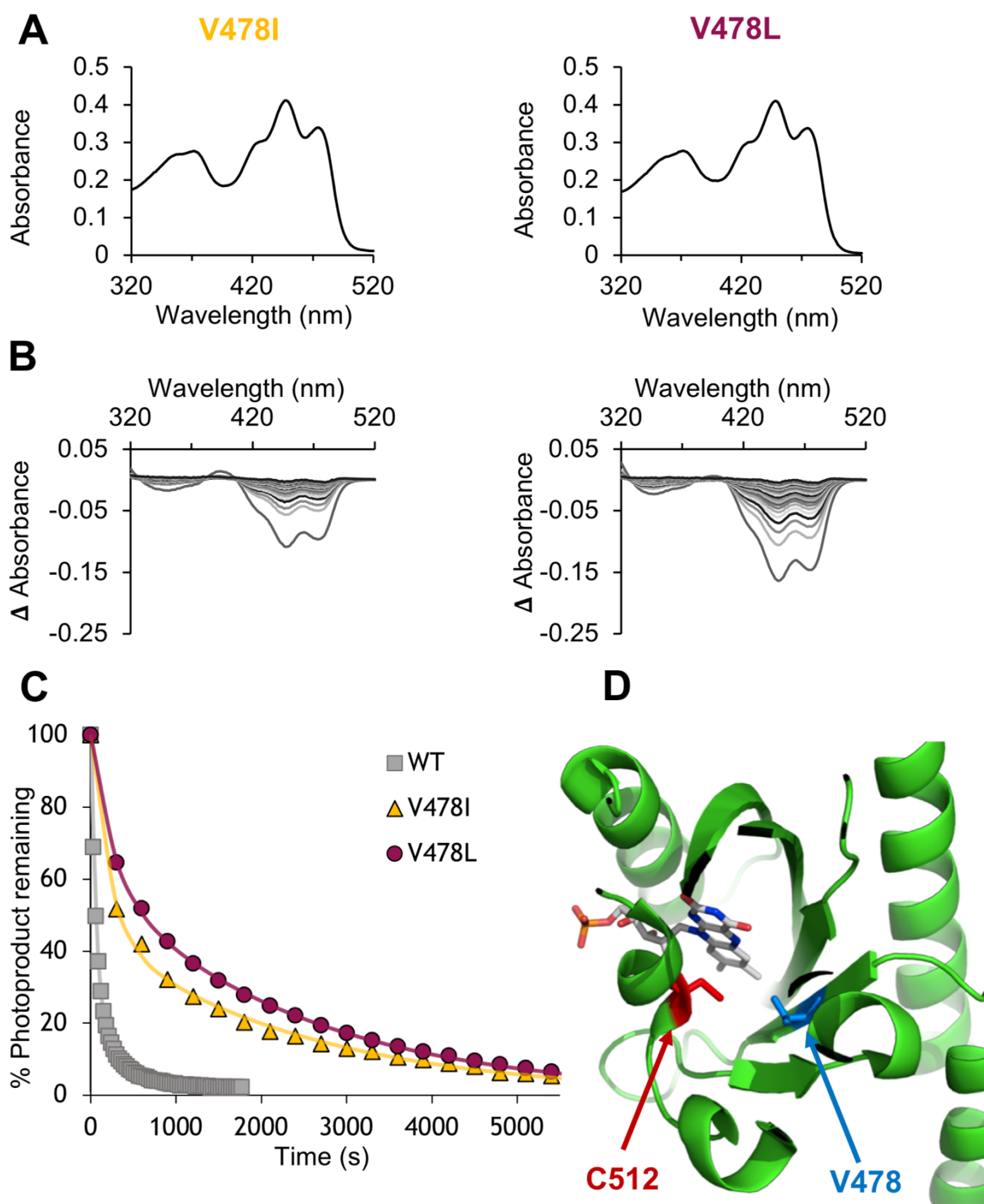


**Figure 3.6: Photochemistry of V478 substitutions facing FMN.** **A.** Dark absorption spectrum of LOV1+LOV2-V478I and -V478L. **B.** Light-minus-dark difference spectra of LOV1+LOV2-V478I and -V478L. Absorbance was measured immediately following a bright pulse of white light and subsequently every 300 seconds as described in Figure 3.1. **C.** Dark recovery kinetics of LOV1+LOV2-V478I and -V478L. Percent photoproduct is used to demonstrate recovery kinetics as shown in Figure 3.1. The half-lifetimes of recovery are 147 and 1688 seconds for V478I and 176 and 1658 seconds for V478L. These experiments were performed three times independently; a representative experiment is shown. **D.** LOV2 crystal structure from Halavaty and Moffat (2013) depicting the position of C512 and V478.

Utilizing the second strategy to modulate photocycle kinetics, LOV1+LOV2-L558I was generated on the basis of a substitution to the same position in VVD that changed the sidechain interacting with the flavin *re*-face in VVD (M165I), leading to a slow photocycle

(Zoltowski, Vaccaro and Crane, 2009). The L558I substitution did not perturb the dark absorbance of LOV1+LOV2 and appeared similar to wild-type (Figure 3.7A; compare Figure 3.1C). Analysis of the light-minus-dark difference spectra and dark recovery kinetics showed that LOV1+LOV2-L558I was a moderately slow photocycler relative to wild-type, with half-lifetimes of 67 and 687 seconds (Figure 3.7 B and C).

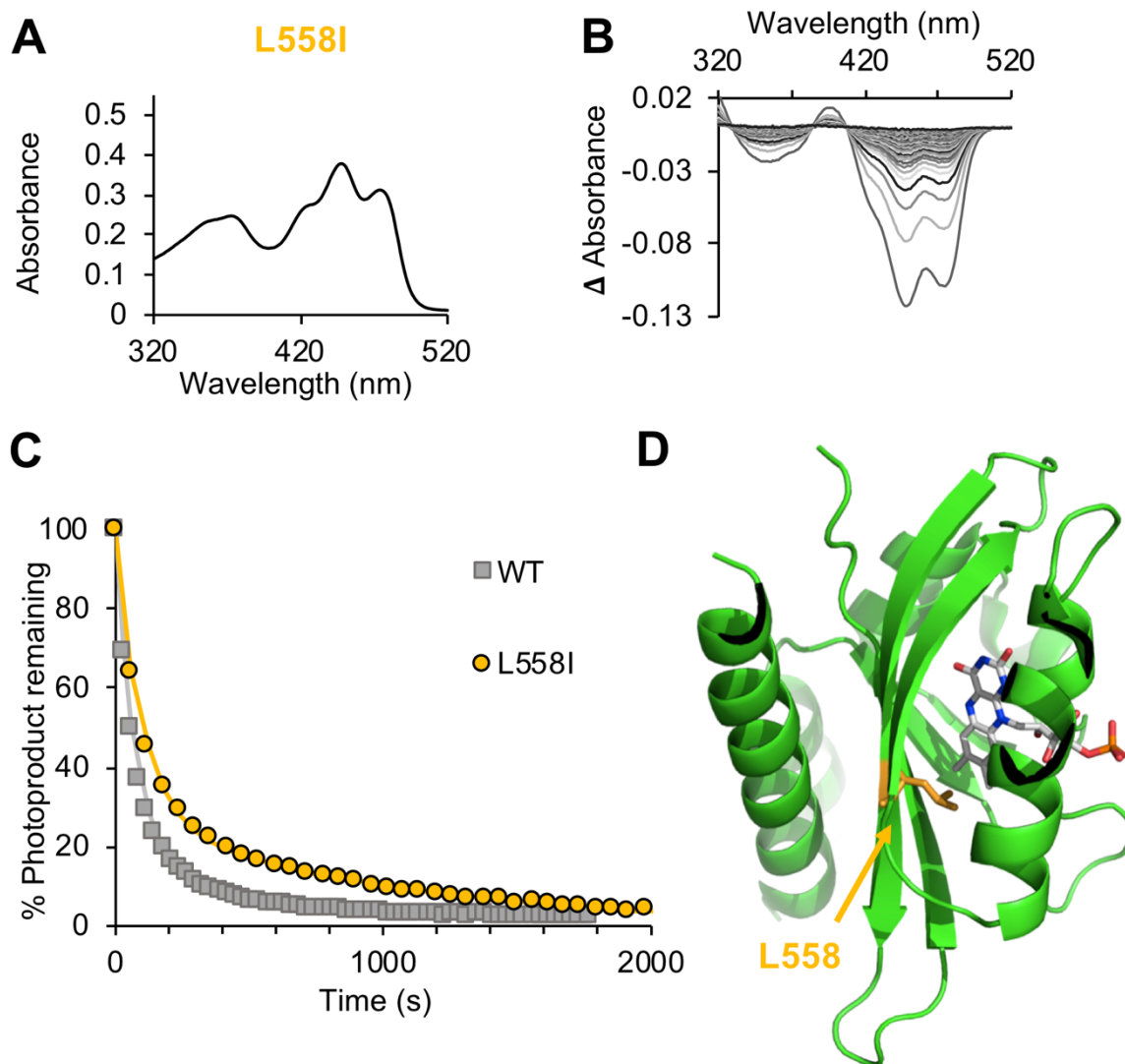


**Figure 3.7: Photochemistry of substitutions facing FMN: L558I.** **A.** Dark absorption spectrum of LOV1+LOV2-L558I. **B.** Light-minus-dark difference spectra of LOV1+LOV2-L558I. Absorbance was measured immediately following a bright pulse of white light and subsequently 60 seconds as described in Figure 3.1. **C.** Dark recovery kinetics of LOV1+LOV2-L558I. Percent photoproduct is used to demonstrate recovery kinetics as shown in Figure 3.1. The half-lifetimes of recovery are 67 and 687 seconds for L558I. The experiments were performed three times independently; a representative experiment is shown. **D.** LOV2 crystal structure from Halavaty and Moffat (2013) depicting the position of L558.

Creating substitutions within the flavin binding pocket was a successful approach that yielded four photocycle mutants. A fast photocycle mutant was generated from the N511S

substitution. Of the slow photocycling variants in the LOV2 flavin binding pocket, V478L was the slowest, followed closely by V478I, and finally the moderately slow variant L558I.

### 3.2.5 Substitutions on the LOV2 surface

The next set of photocycle mutations generated to test in LOV1+LOV2 were located on the surface of LOV2 rather than within the flavin binding pocket. Base-catalysis has been proposed as the mechanism by which the covalent photoadduct decays to the dark state, either through extended hydrogen bonding networks within and around LOV2 or through, and possibly in cooperation with, solvent access into the LOV domain (Swartz *et al.*, 2001; Alexandre *et al.*, 2007). Given the potential for slowing dark reversion presented by altering the base-catalysis mechanism, substitutions on the LOV2 surface that could alter this mechanism in LOV1+LOV2 were sought.

Zayner and Sosnick (2014) found that in *Avena sativa* phot1 LOV2, the substitution N476L (*Arabidopsis* phot1 amino acid numbering) substantially slowed the photocycle and proposed that the more hydrophobic leucine residue inhibited solvent entry into the flavin-binding pocket, slowing the decay of the photoadduct. The LOV1+LOV2-N476L variant was therefore tested as a potential slow photocycle mutant in our system. To produce a surface substitution that may lead to a fast photocycle, we generated LOV1+LOV2-T524I. It was hypothesized based on the slowness of the photocycle of LOV1+LOV2-V525R (see section 3.2.3), that at the next residue over, T524, by replacing the slightly polar threonine with the hydrophobic residue isoleucine (T524I), we could potentially hasten the photocycle. Both LOV1+LOV2-N476L and LOV1+LOV2-T524I showed typical dark absorbance spectra (Figure 3.8A). When the light-minus-dark difference spectra were probed, both mutants photobleached similarly and, unexpectedly, both N476L and T524I variants appeared to have slower photocycles than wild type (Figure 3.8B). Indeed, the dark recovery kinetics indicated quite slow half-lifetimes of recovery of 298 and 2242 seconds for N476L, and a more moderately slow recovery of 139 and 1728 seconds for T524I (Figure 3.8C).

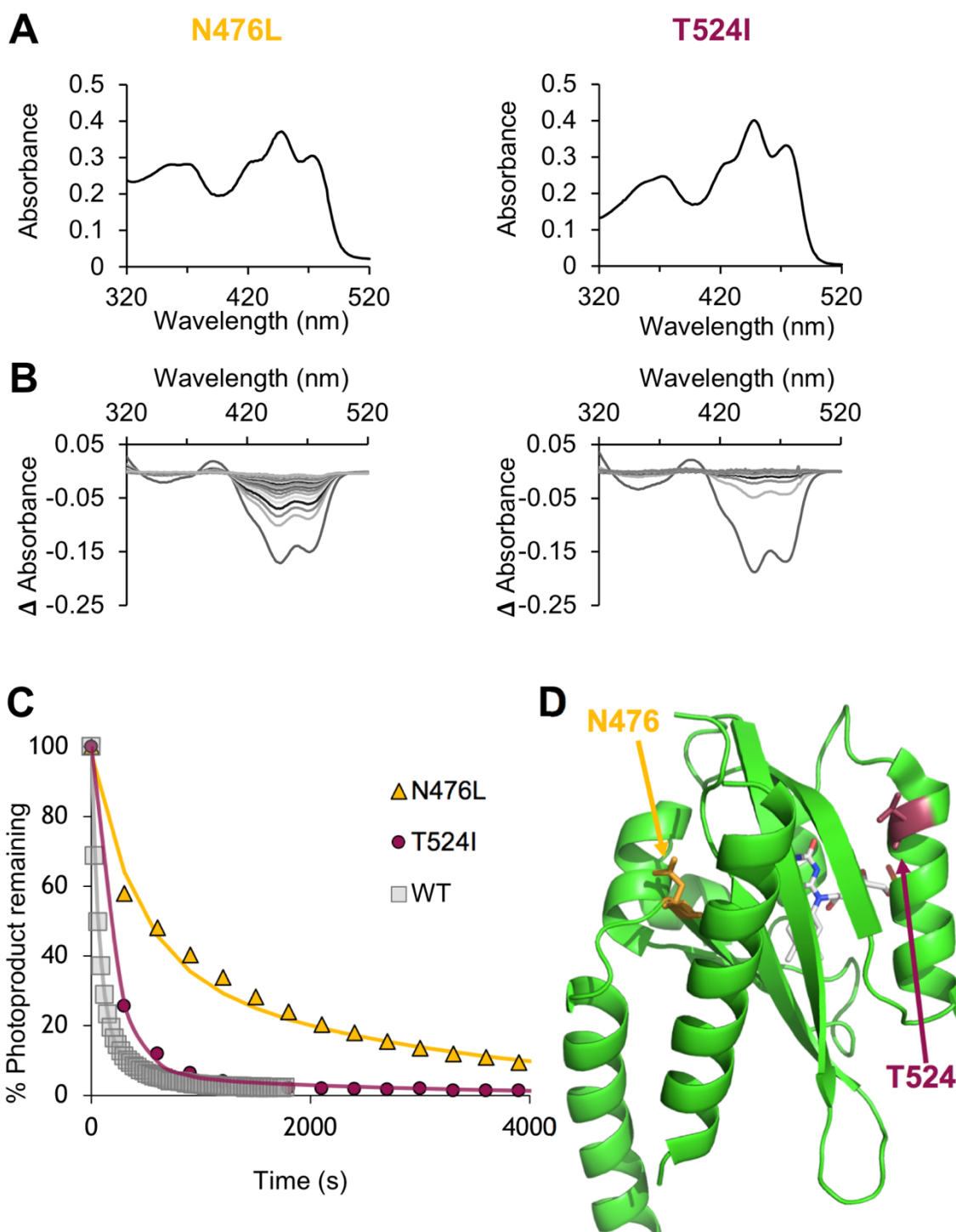


**Figure 3.8: Photochemistry of amino acid substitutions on the LOV2 surface** **A.** Dark absorption spectrum of LOV1+LOV2-N476L, and -T524I. **B.** Light-minus-dark difference spectra of LOV1+LOV2-N476L, and -T524I. Absorbance was measured immediately following a bright pulse of white light and subsequently every 300 seconds as described in Figure 3.1. **C.** Dark recovery kinetics of LOV1+LOV2-N476L, and -T524I. Percent photoproduct is used to demonstrate recovery kinetics as shown in Figure 3.1. The half-lifetimes of recovery are 298 and 2242 seconds for N476L, 139 and 1728 seconds for T524I. The N476L experiments were performed three times independently, while T524I was examined once; a representative experiment is shown. **D.** LOV2 crystal structure from Halavaty and Moffat (2013) depicting the position of N476 and T524.

Aside from solvent entry into the LOV domain to speed recovery, Alexandre *et al.* (2007) proposed that two histidines on the surface of *Avena sativa* phot1 LOV2, H557 and H581 (*Arabidopsis* phot1 amino acid numbering), were acting to hasten base-catalyzed adduct decay by coordinating a hydrogen bonding network between the solvent, flavin-binding pocket, and surface of the protein. This hypothesis was not directly tested by mutagenesis in that study, but it seemed that mutating these histidines could slow the photocycle, so LOV1+LOV2 was mutated to harbor the single histidine mutation H557A and both histidine mutations together, H557A H581A. Both LOV1+LOV2-H557A and LOV1+LOV2-H557A H581A exhibited typical dark absorbance spectra and light-minus-dark difference spectra (Figure 3.9A and B). The dark recovery kinetics revealed that LOV1+LOV2-H557A had a photocycle nearly identical to that of wild type (Figure 3.9C). Unexpectedly, the protein bearing both histidine mutations, LOV1+LOV2-H557A H581A, recovered with photocycle kinetics that were faster than wild type (Figure 3.9C). Based on these observations, it does not seem that the LOV2 surface histidines coordinate hydrogen bonding in a fashion that accelerates photoadduct scission within the LOV1+LOV2 protein.

By targeting surface sites within LOV2 that were implicated the literature as being involved in the photocycle, three substitutions were found to modify dark recovery kinetics: LOV1+LOV2-N476L is a slow-cycling variant, LOV1+LOV2-T524I is a moderately slow-cycling variant, and LOV1+LOV2H557A H581A is a fast-cycling variant.

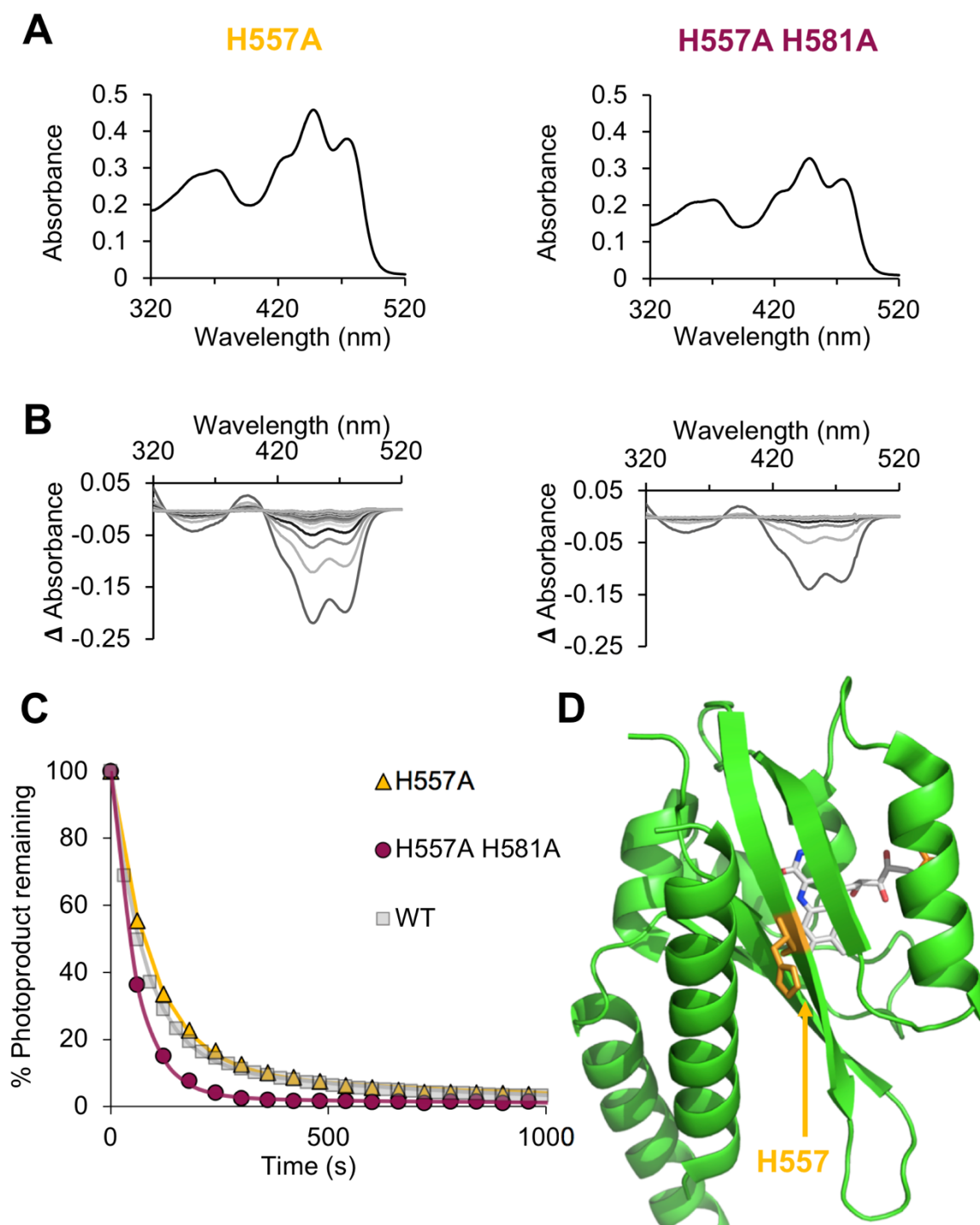


**Figure 3.9: Photochemistry of histidine substitutions on the LOV2 surface** **A.** Dark absorption spectrum of LOV1+LOV2-H557A, and -H557A H581A. **B.** Light-minus-dark difference spectra of LOV1+LOV2-H557A, and -H557A H581A. Absorbance was measured immediately following a bright pulse of white light and subsequently every 60 seconds as described in Figure 3.1. **C.** Dark recovery kinetics of LOV1+LOV2-H557A, and -H557A H581A. Percent photoproduct is used to demonstrate recovery kinetics as shown in Figure 3.1. The half-lifetimes of recovery are 64 and 667 seconds for H557A, and 40 and 742 seconds for H557A H581A. These experiments were performed a single time. **D.** LOV2 crystal structure from Halavaty and Moffat (2013) depicting the position of H557. H581 was not included in the structure.

### 3.2.6 Combination of slow photocycle mutations in LOV1+LOV2

Having produced a range of slow photocycle mutations, some of the slowest mutants generated in this study were combined in an attempt to further slow the photocycle. As such, the photochemistry of the combinations LOV1+LOV2-N476L V525R and LOV1+LOV2-N476L L558I was investigated (results from the single mutations are given in sections 3.2.3 (V525R), 3.2.4 (L558I) and 3.2.5 (N476L)). Both combinations showed typical dark absorbance spectra, which was an encouraging sign that the combinations did not significantly alter the integrity of LOV1+LOV2 (Figure 3.10A). When the light-minus-dark difference spectra and dark recovery kinetics were examined, both combinations exhibited slow photocycles (Figure 3.10 B and C). The N476L V525R combination showed an unusual dark recovery with half-lifetimes of 30 and 1196 seconds. The fast component of the recovery of N476L V525R was faster than wild type (which has half-lifetimes of 51 and 484 seconds), but the slow recovery was substantially slower than that of wild type, with a half-lifetime of 1196 seconds. Measurements of N476L V525R protein fully recovering to the dark state were not possible, as it tended to substantially aggregate over the course of the experiment. On the other hand, the N476L L558I combination did fully recover and was particularly slow, with half-lifetimes of recovery of 118 and 1758 seconds, making it the slowest photocycling variant examined here.

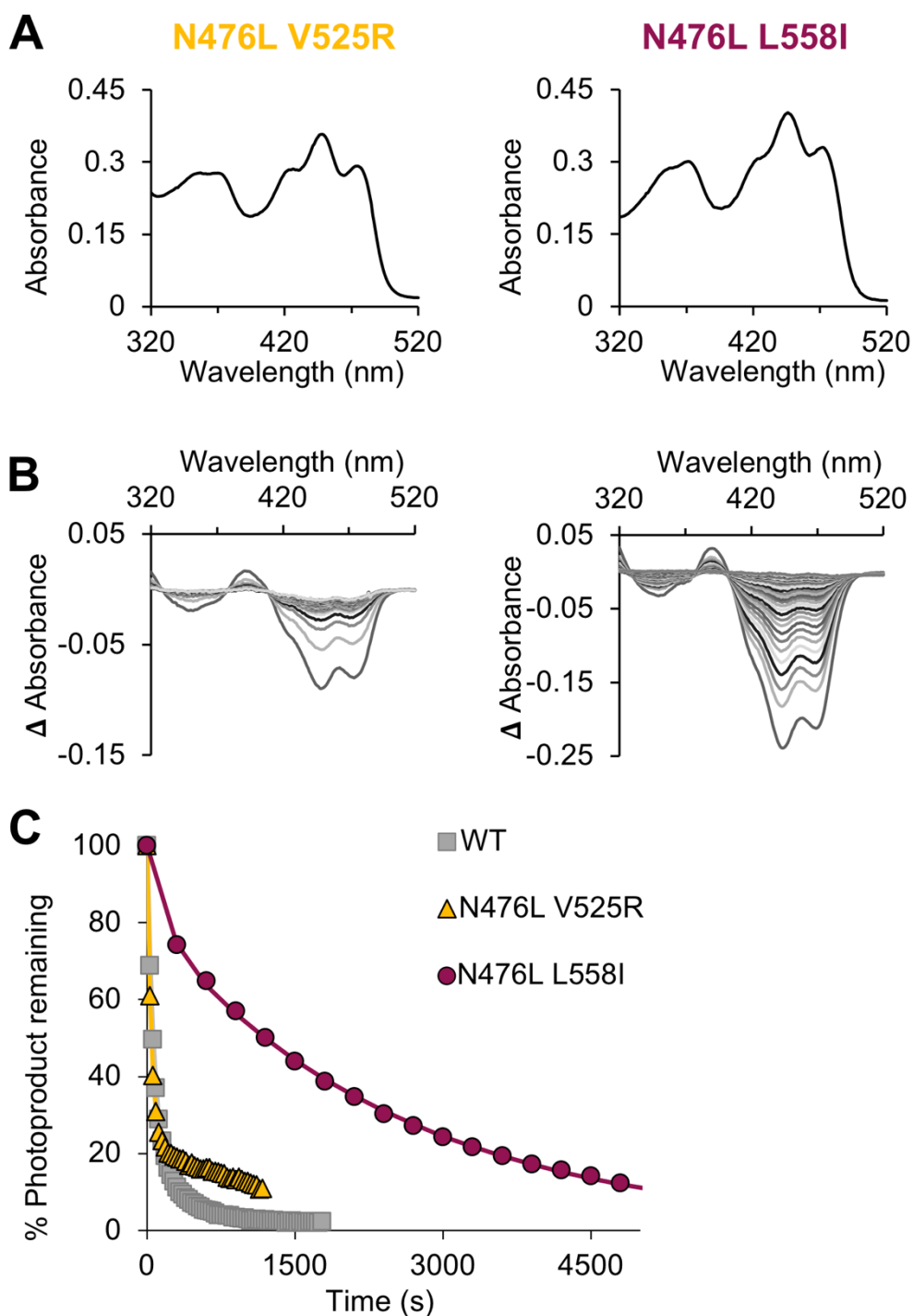


**Figure 3.10: Photochemistry of combinatorial substitutions.** **A.** Dark absorption spectrum of LOV1+LOV2-N476L V525R and -N476L L558I. **B.** Light-minus-dark difference spectra of LOV1+LOV2-N476L V525R and -N476L L558I. Absorbance was measured immediately following a bright pulse of white light and subsequently every 30 (N476L V525R) or 300 seconds (N476L L558I) as described in Figure 3.1. **C.** Dark recovery kinetics of LOV1+LOV2-N476L V525R and -N476L L558I. Percent photoproduct is used to demonstrate recovery kinetics as shown in Figure 3.1. The half-lifetimes of recovery are 30 and 1196 seconds for N476L V525R and 118 and 1758 seconds for N476L L558I. These experiments were each performed using two technical replicates of the same protein preparation; representative technical replicates are shown.

### 3.2.7 Photocycle mutants selected for further study

In total, 14 variants of LOV1+LOV2 were characterized for their photochemistry, including wild type. Table 3.1 shows the recovery half-lifetimes of all the substitutions examined in this study. Note that the half-lifetimes do not always correspond well with the recovery relative to wild type when compared to the dark recovery kinetics curves (see discussion in 3.3.2). The variants N476L, V478I, and L558I were selected for further study on the basis of the range of photocycles they produce, in addition to the varying mechanisms proposed for the manner in which they modify the photocycle. For a direct comparison of dark recovery kinetics of these mutants, see Figure 3.11. The variants V478L and V525R were also examined further but are not the focus of this study (work conducted by Dr. Stuart Sullivan). Though LOV1+LOV2-N476L L558I possessed the slowest photocycle tested here, this combinatorial mutant was not further characterized because its photocycle was similar in magnitude to the V525R variant (data not shown). Additionally, it was decided to not investigate the fast photocycle mutations N511S and H557A H581A further since a fast photocycle has been shown to reduce the activity of VVD *in vivo* (Dasgupta *et al.*, 2015) and the goal of this work was to seek a gain in sensitivity. As such, the single photocycle mutants N476L, V478I, and L558I were carried on for further examination.

Variant	$t_{1/2 \text{ fast}}$ (s)	$t_{1/2 \text{ slow}}$ (s)
Wild-type	51	484
N476L	298	2242
V478I	147	1688
V478L	176	1658
N511S	32	2562
T520R	92	2130
T524I	139	1728
H557A	64	667
L558I	67	687
N476L V525R	30	1196
N476L L558I	118	1758
H557A H581A	40	742

**Table 3.1: Dark recovery half-lifetimes for all photocycle mutants in this study.** Mutants that were chosen for further analysis *in vitro* and *in planta* are colored. Since each mutant exhibited a double exponential recovery pattern, both the fast ( $t_{1/2 \text{ fast}}$ ) and slow ( $t_{1/2 \text{ slow}}$ ) half-lifetimes of recovery are given.

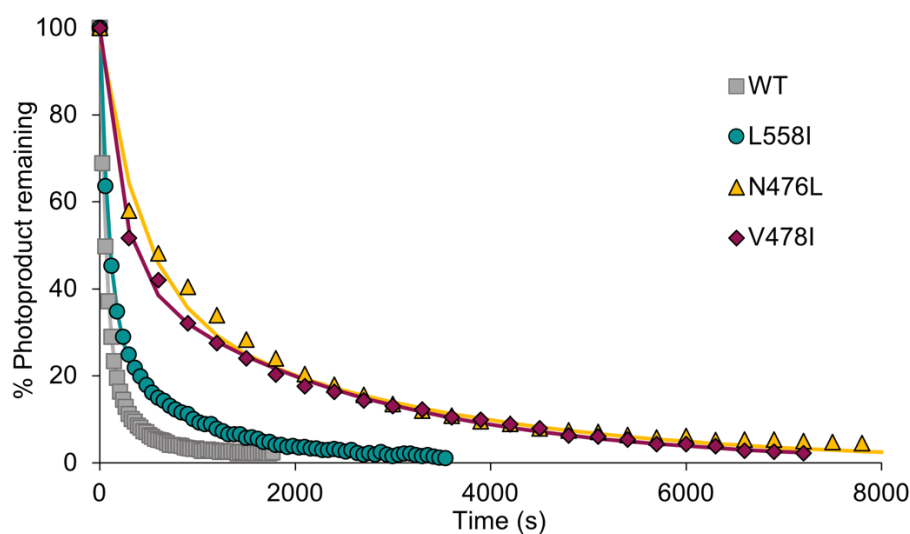


**Figure 3.11: Dark recovery kinetics of photocycle mutants selected for further study.** Percent photoproduct remaining is used to demonstrate recovery kinetics as shown in Figure 3.1.

### 3.2.8 *In vitro* autophosphorylation assays indicate that the photocycle mutants exhibit light-dependent kinase activity

Though the photocycle mutants selected for further study did not seem to impinge on function and stability in the LOV1+LOV2 protein, it was important to assess functionality of full-length phot1 bearing these mutations before moving on to *in planta* analysis. Phot1 autophosphorylates upon light perception *in vitro* and *in vivo* (Christie *et al.*, 1998; Inoue *et al.*, 2008A). To examine the functionality of the photocycle mutants, this autophosphorylation response was tested in the photocycle mutants *in vitro* to ensure that the substitutions did not prevent light sensing in LOV2 from being transferred to activation of the kinase domain. Full-length wild-type phot1 and variants of phot1 bearing the N476L, V478I, or L558I mutations were introduced into the phot1-pAcHLT-a construct in order to generate recombinant baculovirus bearing these phot1 variants. Full-length phot1 was then heterologously expressed in Sf9 insect cells through baculovirus-mediated transfection. The autophosphorylation assays were performed on soluble protein extracts from the insect cells in the dark or with a light treatment. The photocycle mutants all exhibit light-dependent autophosphorylation (Figure 3.11). With this information in hand, the phot1-N476L, V478I, and L558I variants were carried forward for *in planta* analysis, which will be presented in the next chapter.

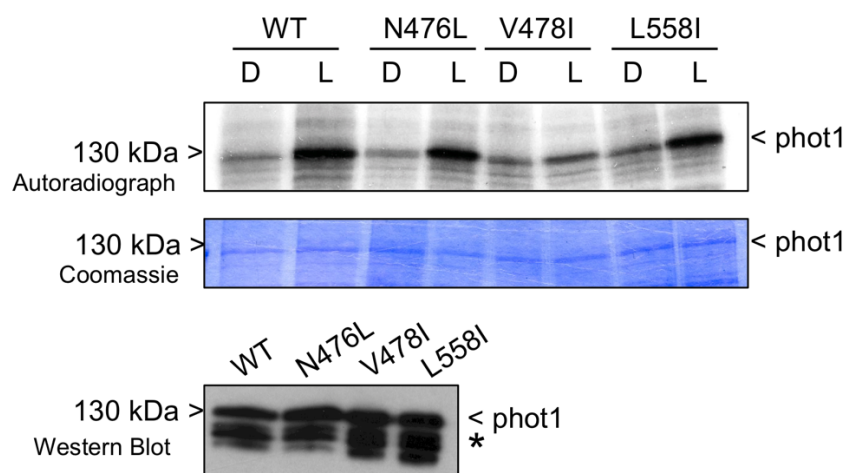


**Figure 3.12: Autophosphorylation activity of the photocycle mutants *in vitro*.** Wild-type and mutant versions of full-length phot1 were heterologously expressed in Sf9 insect cells. Ten micrograms of soluble protein extracts from the insect cells were exposed to  $\gamma^{32}\text{P}$ -ATP either in the dark (D) or with a 10 second pulse of white light (L). The western blot shows the equivalent amount of protein extract, which was maintained in darkness, separated on a second SDS-PAGE gel and probed with an anti-phot1 antibody to show protein expression; asterisk on the western blot indicates phot1 degradation products. A representative experiment from three independent repeats is shown.

### 3.3 Discussion

Several different approaches were employed to rationally modify the LOV1+LOV2 photocycle, which introduced 13 different variants into the LOV2 domain within LOV1+LOV2. Of the insertions and point mutations investigated in this study, three slow photocycle mutants, N476L, V478I, and L558I, with differing slow recovery rates and proposed mechanisms behind their observed slowness were selected for further analysis. When the photocycle mutations were introduced into full-length phot1, each demonstrated light-dependent kinase activity *in vitro*, providing a foundation for further studies that were undertaken *in planta*.

#### 3.3.1 The *ztl*-family FAD loop insertion abolishes photoreactivity in LOV2

The first approach to slowing the LOV1+LOV2 photocycle was to introduce the FAD loop insertion of *ztl* and *fkf1* into LOV2. When the *ztl*-insertion mutant *ztl-i* was chosen for further characterization, it was found that the nine amino acid addition appeared to compromise light sensing without attenuating flavin binding within LOV2. In *fkf1*, this loop region was reported not only to contribute to the photocycle, but also to a large conformational change between the dark and lit states (Nakasone *et al.*, 2010). It may be the case that this conformational change is crucial to signal transduction in *ztl*-family LOV

domains but is deleterious to light sensing in phot1 LOV2. It is difficult to say how the insertion could impede light sensing in ztl-i without probing the protein structurally, but it is tempting to speculate that increasing the length of the loop between the E and F helices introduces too much flexibility into the beta sheet core of LOV2, increasing the distance between the photoactive C512 and the C4a of FMN and preventing efficient photoadduct formation. An alternative hypothesis to explain these findings could be that the introduction of the amino acid insertion markedly hastened the photocycle of ztl-i to the extent that when the photocycle of ztl-i-C234A was examined, the photocycle was too fast to be accurately measured by the spectrophotometer. In either case, these studies indicate that this insertional mutagenesis approach is not feasible for generating slow photocycle mutants of LOV1+LOV2.

### **3.3.2 The LOV1+LOV2 photocycle can be effectively altered with point mutations**

The point mutations in this study varied the length of the LOV1+LOV2 photocycle over two orders of magnitude and generated both fast and slow photocycling variants. These changes in N476L, V478I, and L558I were hoped to be substantial enough to observe the effect of the phot1 photocycle *in vivo*. This degree of tuning is still not to the same extent as photocycle mutations in other LOV-based photoreceptors, such as VVD, which was modified to exhibit fast and slow photocycles over five orders of magnitude by Zoltowski, Vaccaro and Crane (2009). Even in random mutagenesis screens examining a large number of variants of the single *Avena sativa* phot1 LOV2 domain, the photocycle was not varied over more than two orders of magnitude (Christie *et al.*, 2007; Kawano *et al.*, 2013). Future screens could perhaps benefit from attempting site-saturation mutagenesis on residues known to modulate the photocycle, such as V478, to try to expand the range of the phot1 photocycle. Though the LOV1+LOV2 photocycle can be modified within these bounds, there may be yet-unknown characteristics intrinsic specifically to phot1 LOV domains that prevent the generation of slow photocycle mutants that recover with a degree of slowness comparable to VVD or fkl1.

Supporting the idea that phot1 LOV domains have individual characteristics limiting the photocycle, it is also clear that substitutions or natural variants that cause slowness in other LOV domains do not necessarily translate to a slow photocycle in LOV1+LOV2. Of the two arginine residues that engender an extremely slow dark recovery in *P. putida* SB1-LOV, LOV1+LOV2-T525R lead to a slow photocycle but not -T520R. Furthermore, even though

the T525R variant is one of the slowest recovering LOV1+LOV2 proteins tested in our system, its slow half-lifetime of recovery of 2310 seconds is not nearly as slow as the SB1-LOV protein from which the mutation originates, which has a slow half-lifetime of 105,000 seconds (Circolone *et al.*, 2012). Similarly, the L558I substitution did not slow the photocycle as much as the equivalent substitution M165I in VVD (VVD numbering), though this may be due to the difference in character between the original residues, which in VVD is an electron-rich methionine, while in phot1 LOV2 it is an aliphatic leucine (Zoltowski, Vaccaro and Crane, 2009). If the approach of using information on the photocycle in other LOV-based photoreceptors to engineer LOV1+LOV2 is used further to uncover more photocycle variants, many more modifications will need to be tested, since these mutations do not necessarily have predictable effects.

It may be possible that some of the barriers to translating variants from other LOV domains into our system could arise from the fact that the LOV1+LOV2 photocycle that we measure is the sum of two photocycles: that of LOV1, and that of LOV2. Limiting the study by only introducing photocycle variants within LOV2 has the potential disadvantage that the presence of LOV1 could dampen the measurement of any effects brought about by altering LOV2. It also is conceivable that larger effects could be observed if both LOV1 and LOV2 were tuned concurrently. Though it is not clear how LOV1 and LOV2 interact with each other in the LOV1+LOV2 protein, or, indeed, in full-length phot1, it has been established that the presence of photoactive LOV1 is sufficient to slow the photocycle relative to LOV1+LOV2-C234A, in which LOV1 cannot respond to light, and to LOV2 on its own (Christie *et al.*, 2002; Kasierli *et al.*, 2009). However, since mutations in this study that were based directly on substitutions in single *Avena sativa* phot1 LOV2 domains (N511S, V478L, N476L) had predictable effects on LOV1+LOV2 that were comparable in magnitude to the single *Avena sativa* LOV2 domain, it seems most likely that whatever is limiting the tuning of the LOV1+LOV2 photocycle, it arises from intrinsic differences between phototropin LOV domains and other LOV-based photoreceptors and not the presence of LOV1 in the LOV1+LOV2 construct.

Another layer of complexity in interpreting the results is that it can also be difficult to compare half-lifetimes of recovery between photocycle variants. In the established literature, sometimes LOV domains show kinetics of recovery with two half-lifetimes and other times with just one (Guo *et al.*, 2005). Even with constructs containing single LOV domains, the SB1-LOV protein has two half-lifetimes of recovery (Circolone *et al.*, 2012), while VVD tends to recover with just one (Zoltowski, Vaccaro and Crane, 2009). This can make it

difficult to directly compare recoveries, particularly between studies. Within this study, the slow half-lifetime component of recovery was sometimes misleading. The N511S fast photocycle variant has a slow half-lifetime of 2562 seconds while wild-type has a slow half-lifetime of 484 seconds even though it is clear when the dark recovery kinetics curves are compared that N511S is in fact much faster to recover (Figure 3.5C). In this case, it is because the fast photocycle causes LOV1+LOV2-N511S to recover quickly and then become re-activated by the light from the spectrophotometer, causing the protein to begin to lose absorbance again. An artificially long slow half-lifetime may also be observed if the protein is not fully dark-adapted when it is used to create the baseline for the light-minus-dark difference spectra, causing the appearance mathematically that the protein has yet to fully recover to the baseline, when in fact the protein has fully recovered, but the baseline itself does not match the fully recovered state. Some care is required when analyzing these results, and it is perhaps best to compare dark recovery curves between two variants rather than their half-lifetimes to examine their photocycles.

### **3.3.3 Surface substitutions slow the photocycle as much as substitutions within the FMN binding pocket**

Though rationally designed mutagenesis studies on LOV domains tend to target the flavin binding pocket (Zoltowski, Vaccaro and Crane, 2009; Raffelberg *et al.*, 2011), it is clear that substitutions on the surface of the LOV domains can also substantially modify the photocycle (Zayner and Sosnick, 2014). In this study, the slow-cycling LOV1+LOV2 surface variant N476L had a slow photocycle comparable to that of V478I and V478L, which are located within the flavin binding pocket. Additionally, the V525R substitution also sits well outside the flavin binding pocket and was one of the slowest LOV1+LOV2 variants identified thus far. These surface residues do interact with FMN (N476 possibly through a hydrogen bonding network and SB-1 LOV R66 through a salt bridge with the FMN phosphates) but are less likely to interrupt signal transduction or light perception in the way that residues in the flavin binding pocket have a higher propensity to do (Nash *et al.*, 2008; Yamamoto *et al.*, 2008). Still, some care should be taken when introducing surface substitutions, as T520R, a mutation similar to T525R, seems to cause instability in LOV1+LOV2 (Figure 3.4A). Given the similarity of recovery between slow-cycling substitutions to the LOV2 surface and those within the flavin binding pocket and the reduced chance for unexpected signalling effects, further mutagenesis studies may benefit from focusing on substitutions that can be made outside the flavin binding pocket.

### 3.3.4 The photocycle mutants in full-length phot1 are functional *in vitro*

When wild-type phot1 and the photocycle variants were expressed in insect cells, kinase assays showed that all of the photocycle mutants had autophosphorylation activity, providing some assurance that the mutations introduced into LOV2 did not lead to any issues in light-dependent activation. Though it appears in the autophosphorylation assay in Figure 3.11 as though the phot1-V478I variant shows reduced activity compared to wild type and the other mutants, independent repeats of this experiment show activity levels of V478I that is comparable to wild-type (Appendix Figure 3.1). This result enabled the photocycle mutants to be studied *in planta* without the fear that the mutations fundamentally altered the integrity or light sensing of full-length phot1.

With the N476L, V478I, and L558I mutants characterized thoroughly for their photocycle and autophosphorylation activity *in vitro*, steps to analyze the functionality and sensitivity of full-length phot1 harboring the photocycle mutations *in planta* were initiated. The next chapter details those characterizations as well as possible roles of LOV domain structure in the function of full-length phot1.

## Chapter 4 Investigating the Phot1 Photocycle *in planta*

### 4.1 Introduction

How photoreceptor photocycles influence signaling output is generally not well understood, though the knowledge base is beginning to expand. As previously mentioned, PHOTOPERIODIC CONTROL OF HYPOCOTYL 1 (PCH1) was found to influence the photocycle of the red light photoreceptor phytochrome B (phyB) by physically prolonging its light signaling state, positively modulating phyB activity for hypocotyl elongation (Huang *et al.*, 2016; Enderle *et al.*, 2017). Though other phenotypes were not explored, the extended photocycle due to interaction with PCH1 most likely would have a similar effect on other phyB-mediated responses since its light activation is upstream of signaling. Interest in the interplay between light and temperature sensing in photoreceptors has also increased the focus on photoreceptor photocycles, with evidence showing that the photocycle of phyB and the *Marchantia* phototropin, and by extension the activity of those photoreceptors, is substantially influenced by ambient temperatures (Jung *et al.*, 2016; Legris *et al.*, 2016; Fujii *et al.*, 2017). Still, deeper investigations into the impact these photocycles have on plant physiology broadly are required. In the case of *Arabidopsis* phot1, if a role for the photocycle can be assigned, there is potential for altering plant development by increasing phot1 sensitivity through its photocycle.

How the phot1 photocycle effects plant physiology has yet to be explored. The single *Marchantia* phot can mediate a blue light dependent cold-avoidance response in chloroplasts (Fujii *et al.*, 2017). When a fast photocycle mutation (V478T; *Arabidopsis* phot1 amino acid numbering) was introduced into the *Marchantia* phot, this response was eliminated, which was attributed to the faster dark reversion of the mutant (Fujii *et al.*, 2017). Unfortunately, only one photocycle mutant was examined and there are conflicting reports as to whether *Arabidopsis* phot1s perform the cold avoidance response (Łabuz, Hermanowicz and Gabryś, 2015; Fujii *et al.*, 2017). To address the knowledge gap regarding the phot1 photocycle, the candidate slow photocycle mutations N476L, V478I, and L558I were investigated *in planta*. The work presented here is particularly interested in whether slowing the phot1 photocycle enlarges the pool of photoactivated phot1 under a given light condition, leading to enhanced sensitivity for phot1-mediated responses. Learning more about how the phot1 photocycle influences its downstream responses is not only useful from an engineering perspective but also could provide more information on the mechanism of phot1 signaling generally.

## 4.2 Results

### 4.2.1 Expression of photocycle mutants of *phot1* *in planta*

To express *phot1* bearing the photocycle mutations N476L, V478I, and L558I in *Arabidopsis*, *phot1phot2* double mutant plants were transformed to encode each photocycle variant of *phot1* tagged C-terminally with GFP with expression driven by the native *PHOT1* promoter (Figure 4.1A; Sullivan *et al.* 2016). When the T<sub>3</sub> transformants were confirmed as homozygous for the introduced transgene using the segregation pattern of resistance to kanamycin as a readout, *phot1*-GFP protein expression in the transgenic lines was compared to the established wild-type *phot1*-GFP line (Figure 4.1B; Sullivan *et al.*, 2016). On the basis of similarity of *phot1* expression between wild-type *phot1*-GFP and the photocycle mutant lines, *phot1*-N476L 1-5-8, *phot1*-N476L 2-7-12, *phot1*-V478I 1-4-10, *phot1*-V478I 2-4-9, *phot1*-L558I 1-10-5, and *phot1*-L558I 2-3-8 (which will be referred to afterward by the first number in the set of three, such as N476L-1 and N476L-2) were selected for biochemical and physiological characterization (Figure 4.1B).

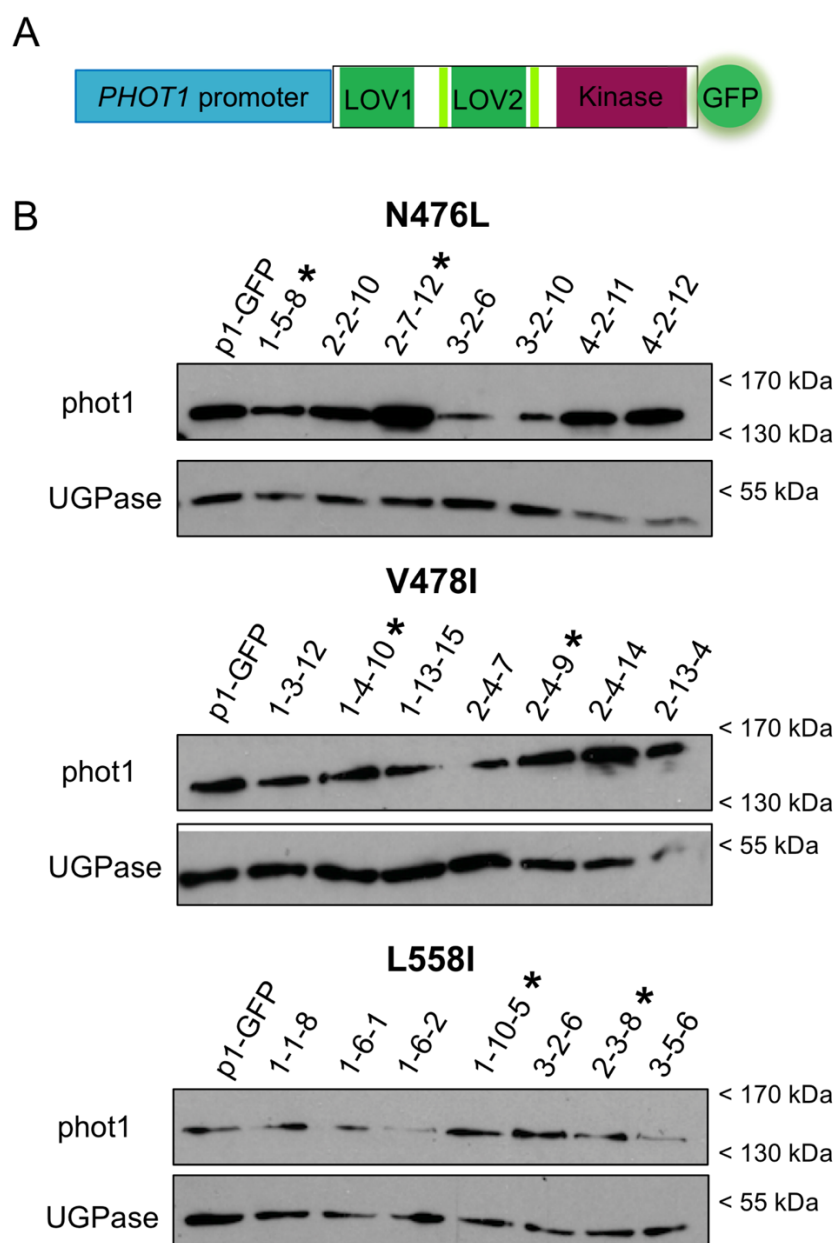


**Figure 4.1: Phot1 expression construct and phot1 protein expression in T<sub>3</sub> transgenic lines.**  
**A.** Schematic of the phot1 expression construct. Phot1 was expressed in *Arabidopsis* by *Agrobacterium*-mediated transformation with the pEZR(K)-LN expression construct, which codes for a T-DNA insertion of full-length phot1 C-terminally tagged with GFP and expressed on its native promoter. **B.** Phot1 protein levels in etiolated seedlings of the T<sub>3</sub> transgenic lines that were identified as homozygous for the indicated mutant version of phot1. Phot1-GFP (p1-GFP; Sullivan *et al.* 2016) is included as a reference. The western blot was performed twice with the phot1 antibody that recognizes its C-terminus, using the UGPase antibody as a loading control. Representative images are shown. Asterisks indicate lines selected for biochemical and physiological analysis of phot1-mediated responses.

#### 4.2.2 The phot1 photocycle mutants are biochemically active

Phot1 autophosphorylates extensively upon activation by blue light, leading to an upward electrophoretic mobility shift when subjected to SDS-PAGE (Liscum and Briggs, 1995; Christie *et al.*, 1998). This autophosphorylation response is required for the downstream activity of phot1 (Inoue *et al.*, 2008A). As a preliminary assessment of the activity of the

photocycle mutants, this mobility shift upon light treatment was investigated in the transgenic lines expressing the photocycle variants of *phot1*. Consistent with the autophosphorylation activity of the photocycle mutants observed when these *phot1* variants were expressed in insect cell extracts *in vitro* (Figure 3.11), all of the mutants showed an upward electrophoretic mobility shift after exposure to blue light that was indicative of light-induced autophosphorylation activity *in planta* (Figure 4.2).

Similarly, the *phot1*-interacting partner NON-PHOTOTROPIC HYPOCOTYL 3 (NPH3) is dephosphorylated in a *phot1*-dependent manner following blue light treatment, leading to increased electrophoretic mobility (Pedmale and Liscum, 2007). Since NPH3 is required for the transduction of many *phot1*-mediated responses, such as phototropism (Motchoulski and Liscum, 1999) and leaf flatness and positioning (Inoue *et al.*, 2008B), NPH3 dephosphorylation is a good hallmark of *phot1* activity. Electrophoretic mobility shifts indicated that NPH3 was dephosphorylated upon blue light treatment in each of the photocycle mutants (Figure 4.2). *Phot1* activation by phosphorylation, and subsequent NPH3 dephosphorylation were both intact in the photocycle mutants, demonstrating that the primary steps of signal transduction required for *phot1*-mediated responses were unimpaired.

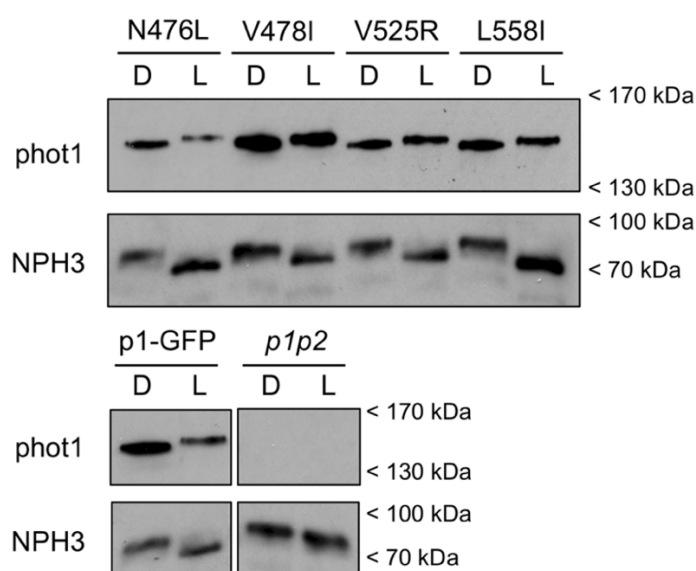


**Figure 4.2: Electrophoretic mobility shifts of *phot1*-GFP and NPH3 in the photocycle mutants.**

Western blots of *phot1* and NPH3 mobility shifts showing protein phosphorylation (*phot1*) and dephosphorylation (NPH3). Protein extracts were either harvested from 3-day-old etiolated seedlings either in the dark (D) or following an overhead irradiation with blue light at a fluence rate of  $20 \mu\text{mol m}^{-2} \text{s}^{-1}$  for 15 minutes (L). A representative line from each photocycle mutant is shown (N476L-2; V478I-2; V525R-3; L558I-2). V525R is a photocycle mutant generated by Dr. Stuart Sullivan and will not be further analyzed here. *Phot1*-GFP (p1-GFP) and the *phot1phot2* double mutant (*p1p2*) were probed separately due to space limitations on the gel. The UGPase loading control was run off during electrophoresis and could not be assessed. A representative experiment from three independent repeats is shown.

### 4.2.3 The photocycle mutants complement phot1-mediated responses *in planta*

When the whole-plant phenotypes of the transgenic photocycle mutant lines were investigated, there seemed to be some differences between the phot1-GFP line and the photocycle mutants in terms of leaf expansion (Figure 4.3). Phot1 has a strong effect on leaf architecture by controlling leaf expansion and flatness (Sakamoto and Briggs, 2002; Takemiya *et al.*, 2005). The leaf flattening index of mature leaves from the photocycle mutants was therefore quantified (Figure 4.3). Leaves were excised from the photocycle mutants after four weeks of growth in  $100 \mu\text{mol m}^{-2} \text{s}^{-1}$  white light in long days. The leaf flattening index quantifies leaf flatness by comparing the ratio of the area of each leaf immediately after it was excised to the area of the leaf after it was completely flattened onto a piece of paper. While none of the mutants showed the severely curled phenotype of *phot1phot2* double mutants, the phot1-N476L mutant lines in particular did not fully complement phot1-mediated leaf flattening. There was variation between the two phot1-V478I lines in terms of the degree of flatness, but at least V478I-2 was capable of complementing leaf flattening to a degree comparable to phot1-GFP. The phot1-L558I lines consistently had the flattest leaves of the photocycle mutants with a leaf flattening index of around 0.8, complementing at a level that was just below that of phot1-GFP, which had a leaf flattening index of 0.86. Since the mutants all expressed the phot1-GFP protein to a degree similar to the wild-type phot1-GFP transgenic line (at least as etiolated seedlings; Figure 4.1), these differences were not likely to be due to variation in protein expression. Despite these relatively minor differences in leaf flattening in the photocycle mutants, overall, the lines complemented the phot1 leaf flattening response.

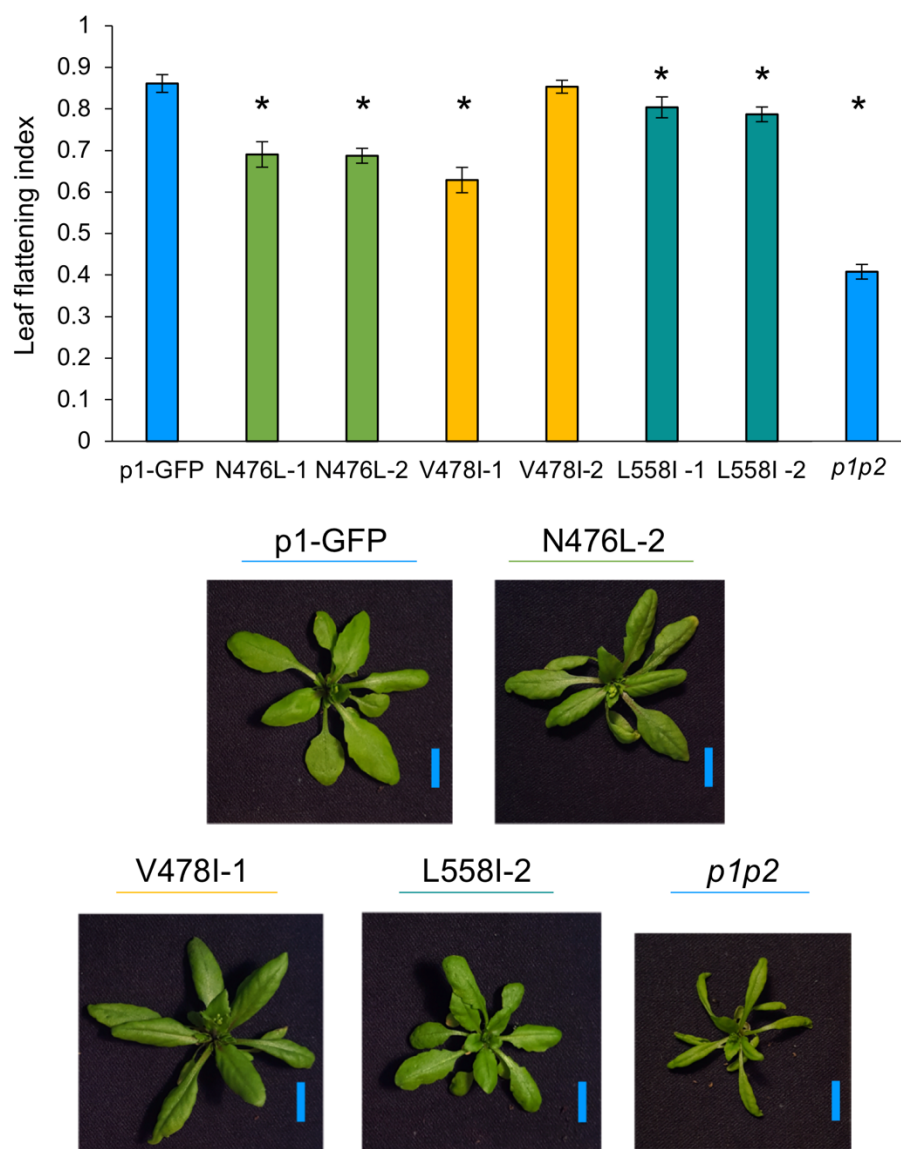


**Figure 4.3: Leaf flattening of the photocycle mutants.** Leaf flattening experiments were conducted on four-week-old *phot1*-GFP (*p1*-GFP), the slow photocycle mutant lines, and the *phot1phot2* (*p1p2*) double mutant plants grown in long days under  $100 \mu\text{mol m}^{-2} \text{s}^{-1}$  white light. Twelve fully expanded leaves from different plants were measured for each genotype. Asterisks indicate a significant difference from *phot1*-GFP (Student's *t*-test;  $p < 0.05$ ); error bars are standard error of the mean. The results of one representative experiment of three independent replicates is shown. Representative images for each photocycle mutation at four weeks are shown; the scale bar is 1 cm.

Noting the differences in the level of complementation for leaf flattening, other *phot1*-mediated responses were characterized. Chloroplast accumulation within the leaf is an important *phot1* response to maximize light capture and efficient chloroplast positioning is hypothesized to be related to photosynthetic output (Suetsugu and Wada, 2012). The responsiveness of the photocycle mutants for chloroplast accumulation in leaves from four-week-old *phot1* mutants was therefore probed. Leaves from four-week-old plants were irradiated with low-intensity blue light to induce chloroplast accumulation, the extent of

which was quantified in leaves from each photocycle mutant line. All of the photocycle mutants could complement chloroplast accumulation: the V478I lines and L558I-1 were indistinguishable from phot1-GFP in their responsiveness, while the N476L lines showed the weakest chloroplast positioning of the photocycle mutants (Figure 4.4). As for the leaf flattening response, the photocycle mutants showed a small degree of variation in the level of complementation for chloroplast accumulation but overall showed no major defects in functionality.

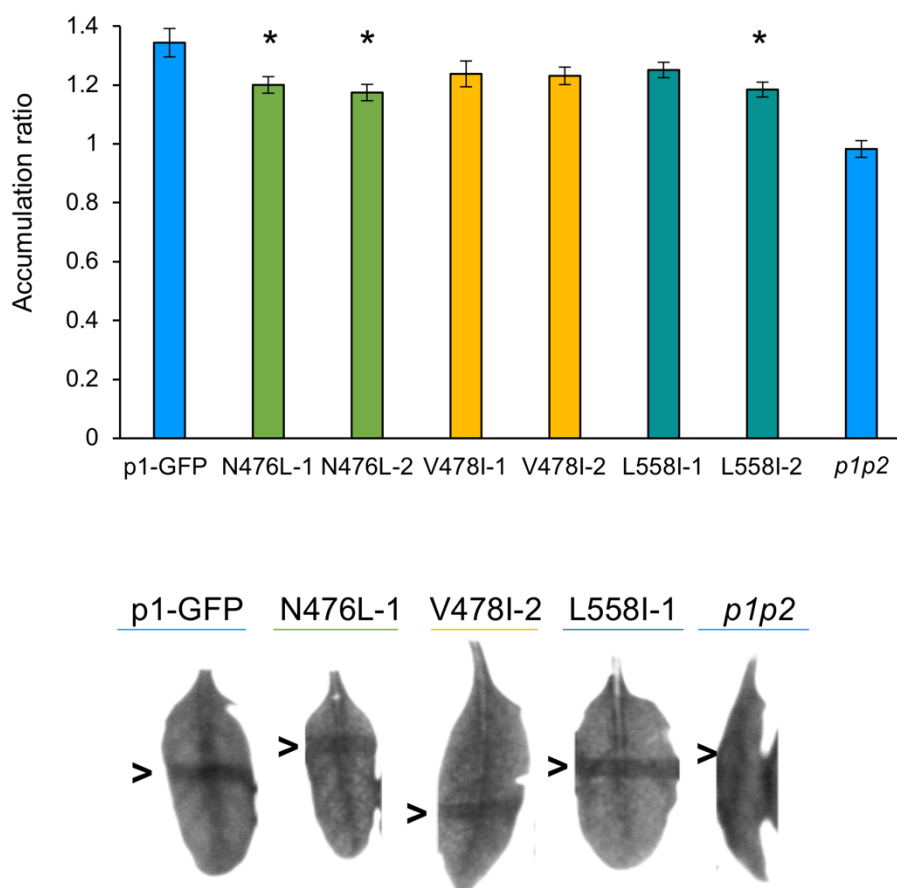


**Figure 4.4: Chloroplast accumulation of the photocycle mutants.** Chloroplast accumulation was tested on leaves excised from four-week-old phot1-GFP (p1-GFP), the slow photocycle mutant lines, and the *phot1phot2* (*p1p2*) double mutants that were placed on agar plates. The entire leaf was protected from light exposure except for a small slit that was irradiated with blue light at a fluence rate of  $2 \mu\text{mol m}^{-2} \text{s}^{-1}$  to induce chloroplast accumulation. Asterisks indicate a significant difference from phot1-GFP (Student's t-test;  $p < 0.05$ ). The experiment was repeated three times independently; one representative experiment is shown, with between nine and 16 fully expanded leaves from different plants tested for each line. Representative images of chloroplast accumulation in each photocycle mutant is shown.

Petiole positioning under low light is another phot1 response thought to optimize light capture (Inoue *et al.*, 2008B) and was therefore compared between wild-type phot1-GFP and the photocycle mutants. This experiment was conducted by examining the petiole angle of the first pair of true leaves of two-week-old seedlings grown under low-intensity white light to induce the inclination of the petioles. With the exception of the N476L-1 line, all of the

photocycle mutants complemented petiole positioning at a level that was at or above that of *phot1*-GFP, with no significant difference observed between them (Figure 4.5).

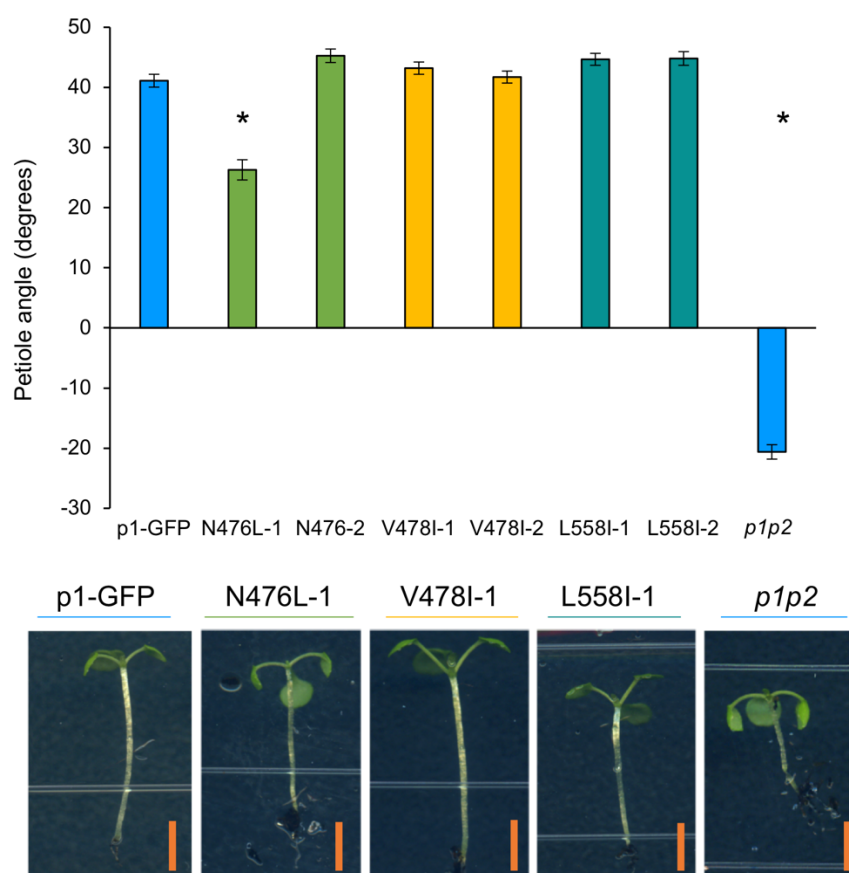


**Figure 4.5: Petiole positioning of photocycle mutants.** Seeds from the photocycle mutants, *phot1*-GFP (*p1*-GFP), and the *phot1phot2* (*p1p2*) double mutant were sown onto soil and grown for one week under  $80 \mu\text{mol m}^{-2} \text{s}^{-1}$  white light, after which the fluence rate was lowered to  $10 \mu\text{mol m}^{-2} \text{s}^{-1}$  white light for another week. The two-week-old seedlings were then imaged to quantify seedling angle. Results shown are the mean of 63-72 seedlings from each line over three experiments. Asterisks indicate a significant difference from *phot1*-GFP (Student's t-test;  $p < 0.05$ ). Error bars are the standard error of the mean. Representative images are shown; scale bar is 2.5 mm.

Finally, the phototropic response of the photocycle mutants was studied in three-day-old etiolated seedlings. Phototropism under low blue light ( $0.5 \mu\text{mol m}^{-2} \text{s}^{-1}$ ) requires a higher degree of *phot1* sensitivity than the other physiological tests presented here. As a result, the functionality differences between wild-type *phot1*-GFP and the photocycle mutants were more pronounced (Figure 4.6). The phototropic curvature of the slow photocycle mutants in response to  $0.5 \mu\text{mol m}^{-2} \text{s}^{-1}$  blue light seemed to exaggerate the trend of *phot1*-N476L showing the lowest degree of complementation of the photocycle mutants for *phot1*-mediated responses, *phot1*-L558I performing the strongest of the set, and *phot1*-V478I functioning to a degree between L558I and N476L (Figure 4.5). The photocycle mutants could all respond to the phototropic stimulus, but even the L558I lines, which exhibited the

strongest response, showed just over half the extent of phototropic curvature of wild-type *phot1*-GFP. Though the photocycle mutants could respond to the unilateral light stimulus with clear curvature, the extent of the response of each mutant was well below that of the *phot1*-GFP line.

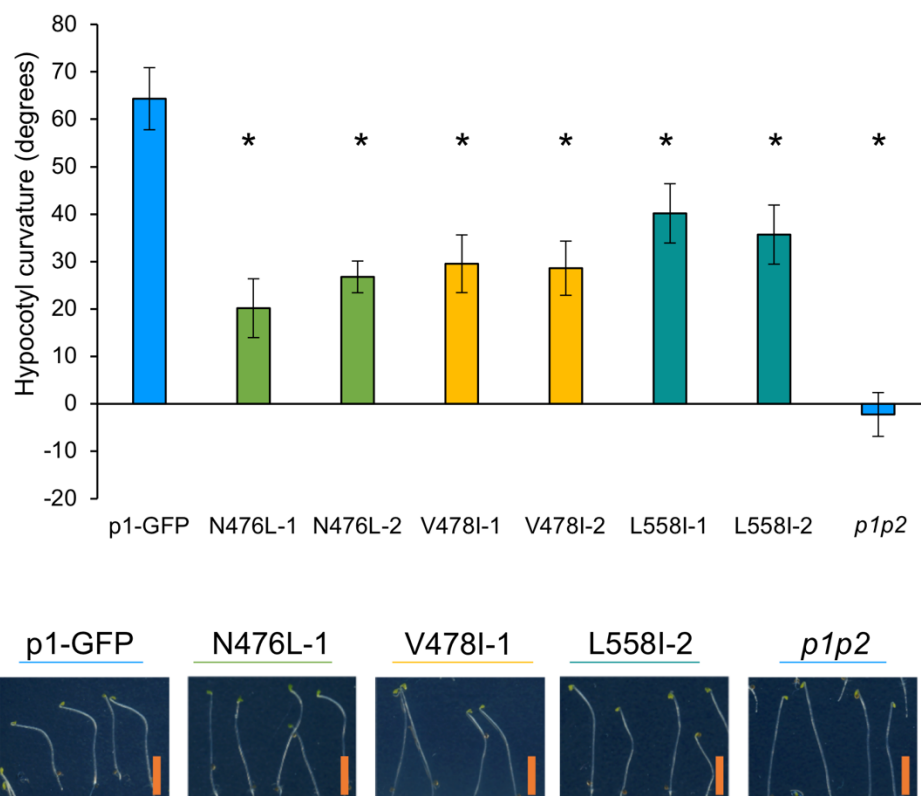


**Figure 4.6: Phototropism of the photocycle mutants.** Three-day-old etiolated photocycle mutant, wild-type *phot1*-GFP, and *phot1phot2* (*p1p2*) double mutant seedlings grown on half-strength MS agar plates were treated with a unilateral blue light stimulus of  $0.5 \mu\text{mol m}^{-2} \text{s}^{-1}$  for 24 hours. Results show one representative experiment from two independent repeats using 20-25 seedlings per genotype. Asterisks indicate a significant difference from *phot1*-GFP (Student's t-test;  $p < 0.05$ ). Error bars are standard error of the mean. Representative images are shown; the scale bar is 2.5 mm.

In sum, the slow photocycle mutants generated here all complement *phot1*-mediated responses to varying degrees. For long-term experiments at saturating light intensities, such as leaf flattening, any differences between wild-type *phot1*-GFP and the photocycle mutants were noticeable but relatively minor. When the light intensity is lowered, and the experiment is conducted over a relatively short time span, such as for phototropism, the differences in functionality were further exaggerated. From the data, it seemed that *phot1*-L558I is the most functional of the photocycle mutants for the *phot1*-mediated responses studied here, with the most robust leaf flattening (Figure 4.3) and curvature for phototropism (Figure 4.6) of the photocycle mutant lines. Whether the overall complementation of the V478I lines was significantly different from L558I was not assessed—an Analysis of Variance (ANOVA)

test could be used to compare whether this is the case—though the extent of its complementation seemed to be consistently lower than those observed for L558I. By contrast, the N476L lines exhibited complementation at levels well above that of the *phot1phot2* double mutant but seemed to consistently underperform the other photocycle mutant lines for the physiological responses tested here.

#### **4.2.4 NPH3 phosphorylation status confirms the slow photocycle of *phot1-V478I* and *-L558I***

Once it was verified that the photocycle mutants exhibited functionality *in planta* as well as *in vitro*, whether the slow photocycles of these mutants were upheld *in planta* was investigated. The phosphorylation status of NPH3 was used as a proxy for *phot1* activation. As previously demonstrated, in both wild-type *phot1*-GFP and the photocycle mutants, NPH3 is dephosphorylated upon light exposure in a manner dependent upon *phot1* activation, as monitored by electrophoretic mobility shift (Figure 4.2). When the seedlings are returned to darkness following the light treatment, NPH3 becomes re-phosphorylated over time, with the pool of NPH3 apparently completely in its phosphorylated state after around two hours in darkness in the *phot1*-GFP background, reflecting the period of *phot1* activation (Figure 4.7A and B).

The phosphorylation status of NPH3 in the *phot1*-N476L lines over the time course closely reflected that of wild-type *phot*-GFP line (Figure 4.7). Conversely, *phot1*-L558I and *-V478I* both exhibited slower rates of NPH3 re-phosphorylation following a return to darkness after the light treatment. The L558I lines showed the phosphorylated state of NPH3 appearing after one hour of dark incubation but maintained a pool of dephosphorylated NPH3 for four hours following the light treatment (Figure 4.7). The V478I lines appeared to exhibit an even slower recovery of the phosphorylated state of NPH3, with the phosphorylated band of NPH3 only becoming apparent four hours following light treatment (Figure 4.7). Though the *phot1*-N476L photocycle does not seem to be slower than *phot*-GFP *in planta* as inferred from NPH3 phosphorylation status, the dark recovery of phosphorylated NPH3 in *phot1*-L558I and *-V478I* appears to reflect the photocycles observed *in vitro*, with the L558I being moderately slow to recover to the dark state and V478I being quite slow to recover.

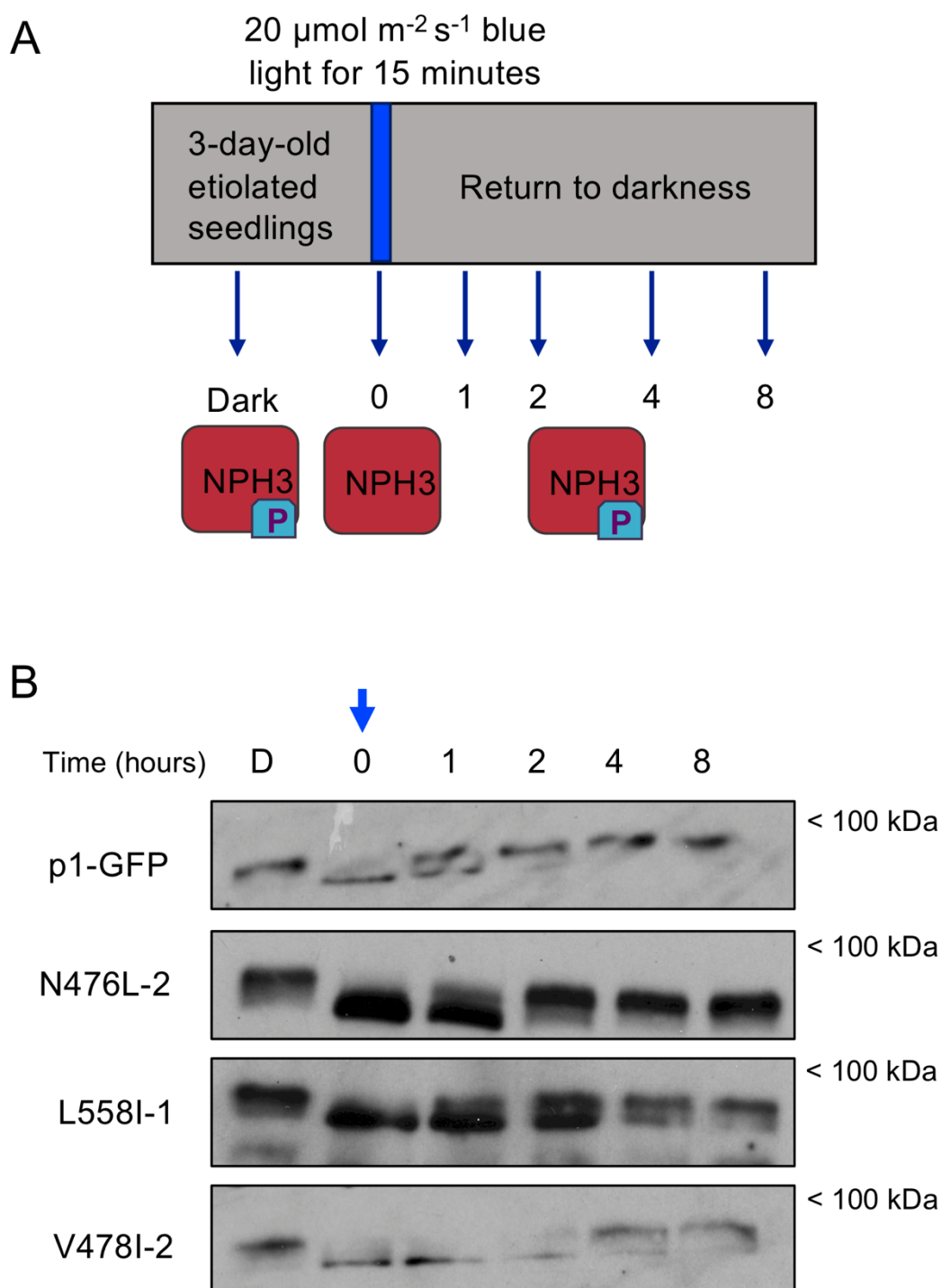


**Figure 4.7: NPH3 phosphorylation status is altered in the photocycle mutants.** **A.** Schematic depicting how the experiment was performed. Protein extracts were either harvested from three-day-old etiolated seedlings of phot1-GFP (p1-GFP) or the photocycle mutant transgenic lines in the dark (D) or immediately following an overhead irradiation of blue light at 20  $\mu\text{mol m}^{-2} \text{s}^{-1}$  for 15 minutes. The seedlings were then returned to darkness and protein extracts were harvested 1, 2, 4, or 8 hours following the irradiation. **B.** Western blots of NPH3 mobility shifts showing NPH3 phosphorylation status over time. The blue arrow indicates the timepoint immediately following the blue light treatment. The UGPase control was run off during electrophoresis to obtain clear bandshifts of NPH3 and could not be assessed. Representative blots from three independent experiments are shown; each photocycle mutant transgenic line was tested.

#### 4.2.5 Phototropism of the photocycle mutant lines across multiple fluence rates does not indicate increased sensitivity

Once it was established that the phot1-L558I and -V478I lines showed altered NPH3 phosphorylation kinetics *in vivo* that may correspond to a slowed phot1 photocycle, whether there was any gain in sensitivity for the phototropic response of these two lines when exposed to very low intensity blue light was explored. Since the N476L line showed NPH3 phosphorylation over time similar to that of the phot1-GFP control (Figure 4.7), it was not used for this analysis. Although the L558I and V478I photocycle mutants showed reduced phototropic curvature relative to the phot1-GFP line at  $0.5 \mu\text{mol m}^{-2} \text{s}^{-1}$  (Figure 4.6), it was hypothesized that the responsiveness of the photocycle mutants may be increased relative to phot1-GFP when treated with lower intensity light. However, it was found that when the blue light intensity used for phototropism was decreased 10-fold from the first set of experiments, to  $0.05 \mu\text{mol m}^{-2} \text{s}^{-1}$  of blue light, hypocotyl curvature remained weaker in the L558I and V478I lines than in phot1-GFP (Figure 4.8). Furthermore, when phototropism was explored at a higher fluence rate of  $5 \mu\text{mol m}^{-2} \text{s}^{-1}$ , the degree of phototropic curvature increased in the L558I and V478I lines, with the two L558I lines responding to a degree that was similar to phot1-GFP at this fluence rate (Figure 4.8). Unexpectedly, rather than observing increased light sensitivity for phototropism in these two slow photocycle mutant lines, the extent of the response increased as the fluence rate increased as did the functionality of the lines relative to phot1-GFP. This evidence suggests that the L558I and V478I photocycle mutants are impaired for phototropism compared to wild-type phot1-GFP at low light intensities.

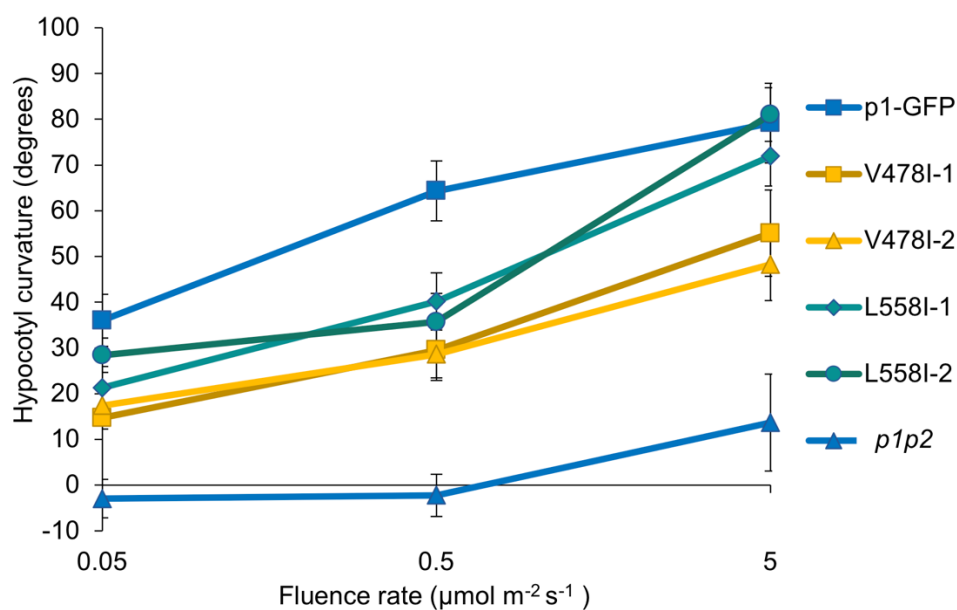


**Figure 4.8: Phototropism of the photocycle mutants across varying fluence rates.** Phototropism was conducted on three-day-old etiolated seedlings of the photocycle mutants, *phot1*-GFP (*p1*-GFP) and the *phot1phot2* (*p1p2*) double mutant as described in Figure 4.6 using the indicated fluence rate of blue light as the stimulus. Results show one representative experiment from three independent repeats using 20-30 seedlings per genotype. Error bars are standard error of the mean.

#### 4.2.6 The *phot1*-L558I photocycle mutants do not accumulate more biomass than *phot1*-GFP under low light

Since *phot1* responses are closely tied to photosynthetic competence by optimizing light capture and carbon dioxide uptake through stomata (Spalding and Folta, 2005; Christie *et al.*, 2015; Inoue and Kinoshita, 2017), whether a slow *phot1* photocycle increased biomass accumulation under light-limiting conditions was tested. The *phot1*-L558I lines were used for this experiment, since L558I both showed slowed recovery of phosphorylated NPH3 following light treatment relative to *phot1*-GFP (Figure 4.7) and appeared to be the most functional of the slow photocycle mutants for the *phot1* responses examined here (as in Figures 4.3 and 4.8). This experiment was conducted on plants grown under a light regime consisting of  $25 \mu\text{mol m}^{-2} \text{s}^{-1}$  red light and  $0.1 \mu\text{mol m}^{-2} \text{s}^{-1}$  blue light in long days. The fresh weight of each line was measured at the end of four weeks of growth. The L558I lines had fresh weights of around 10-12 mg, which was not significantly different from the weight of *phot1*-GFP at around 10 mg (Figure 4.9; Student's *t*-test,  $p > 0.05$ ). Consistent with the other physiological experiments presented in this chapter, the data suggests that the slow photocycle of *phot1*-L558I does not confer an advantage over *phot1*-GFP for biomass accumulation, even under growth conditions consisting of low-intensity light.

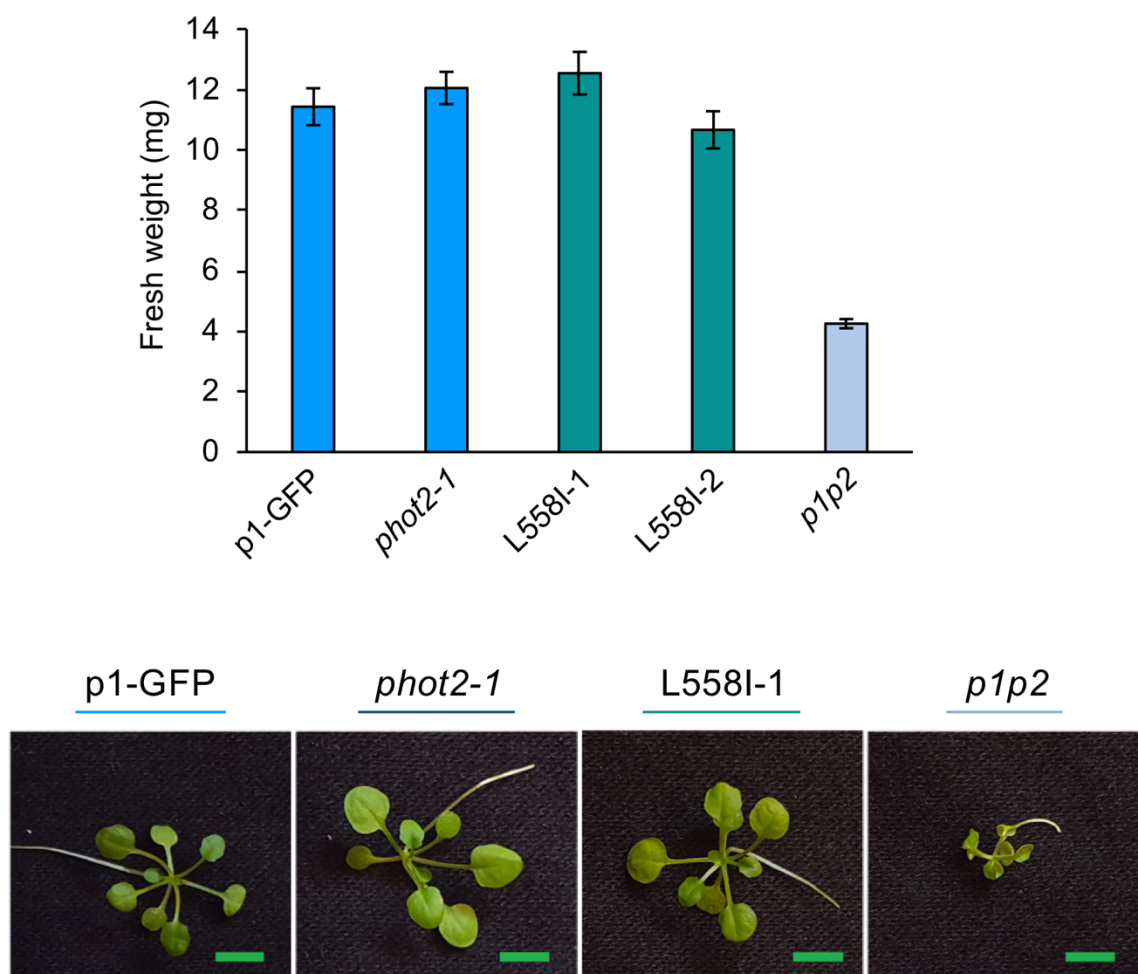


**Figure 4.9: There is no gain in fresh weight accumulation in the L558I slow photocycle mutant under low light relative to phot1-GFP.** The two phot1-L558I slow photocycle mutant lines, along with phot1-GFP (p1-GFP), the *phot2-1* single mutant, and the *phot1phot2* (*p1p2*) double mutant were grown for four weeks under  $25 \mu\text{mol m}^{-2} \text{s}^{-1}$  red light and  $0.1 \mu\text{mol m}^{-2} \text{s}^{-1}$  blue light in long days for four weeks prior to weighing each plant. Data shown are the results of one experiment from two independent repeats measuring 20 plants from each genotype. Error bars are standard error of the mean. Representative images are shown; scale bar is 5 mm.

#### 4.2.7 Structural probe of low functionality in variants of V478

It was demonstrated in the previous chapter that two variants at the V478 position in LOV1+LOV2, V478I and V478L, showed similar photocycles *in vitro*, with the V478L variant showing slightly slower dark recovery kinetics than V478I (Figure 3.6). The phot1-V478L transgenic *Arabidopsis* lines were generated and characterized by Dr. Stuart Sullivan. It was found that NPH3 does not return to its dark phosphorylated state in the phot1-V478L background during the eight-hour time course used for these experiments, possibly reflecting a strikingly slower photocycle than that of phot1-V478I (Figure 4.10A). In spite of phot1 autophosphorylation and NPH3 dephosphorylation appearing normal following light treatment in the phot1-V478L lines (Stuart Sullivan and John M. Christie, data not shown),

the whole-plant phenotype of the transgenic lines indicated that phot1-V478L did not complement leaf flattening and appeared similar to the *phot1phot2* double mutant (Figure 4.10B). Phot1-V478L also could not complement phototropism (Figure 4.10C). These results were unexpected, both because phot1 autophosphorylation and NPH3 dephosphorylation were similar to wild-type phot1-GFP following a light treatment and since the impact of substituting a valine at residue 478 with either leucine or isoleucine was not predicted to be strong, considering the similarity of these three aliphatic amino acids.

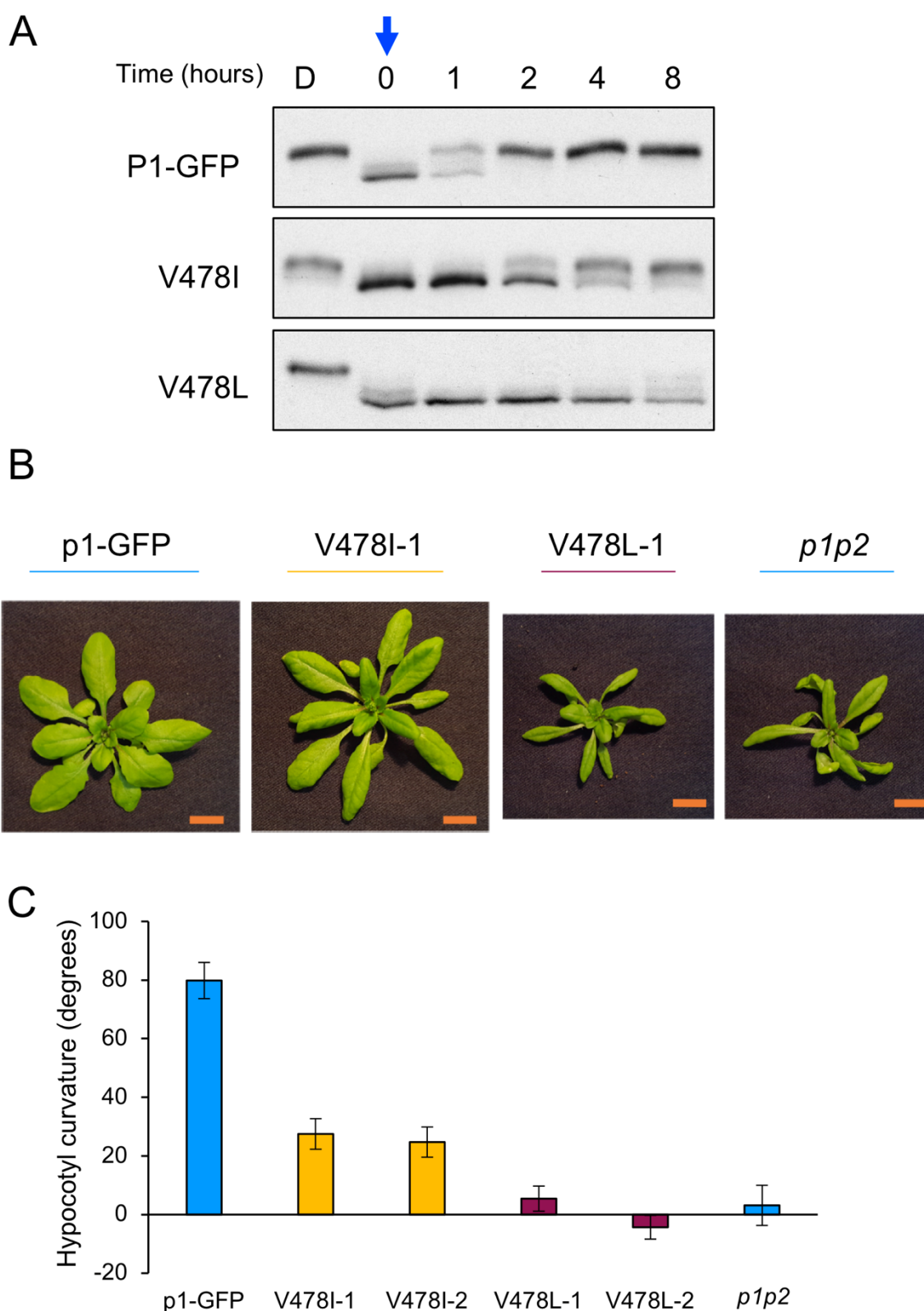


**Figure 4.10: Comparison of V478I and V478L functionality *in planta*.** **A.** NPH3 phosphorylation status following blue light treatment and incubation in the dark of *phot1*-GFP (*p1*-GFP) and the V478I and V478L photocycle mutant lines. This experiment was conducted by Dr. Stuart Sullivan (unpublished data) as described in Figure 4.7. The UGPase loading control was run off during electrophoresis and could not be assessed. **B.** Rosette phenotypes of *p1*-GFP, V478I, V478L, and the *phot1phot2* (*p1p2*) double mutant at 4 weeks. Scale bar is 1 cm. **C.** Phototropism of *p1*-GFP, V478I, V478L and *p1p2* seedlings exposed to  $0.5 \mu\text{mol m}^{-2} \text{s}^{-1}$  unilateral blue light. Phototropism was conducted as described in Figure 4.6. Results of one experiment from three independent repeats are shown.

To probe the underlying causes of the observed differences in functionality due to substitutions at V478, structural studies of the single wild-type LOV2 domain and LOV2-V478L (amino acids 452-615, encompassing the LOV2 domain and the J $\alpha$  and A' $\alpha$  helices and deriving from the construct used by Halavaty and Moffat, 2013) were undertaken using an x-ray crystallography approach. While wild-type LOV2 crystals could be obtained, crystals of LOV2-V478L were neither obtained using the previously reported crystallization conditions for *Arabidopsis* phot1 LOV2 (Halavaty and Moffat, 2013), nor using broad crystallization screens (data not shown).

An alternative approach was adopted to generate structural information.  $^{15}\text{N}$ -labelled LOV2-V478L was therefore investigated by NMR in a 2D HSQC (two-dimensional heteronuclear single quantum coherence) experiment. NMR spectra were generated both in the dark and following a saturating light treatment. Comparison between the two spectra for LOV2-V478L revealed that the protein appeared to be somewhat disordered in its dark state and relatively more ordered in the light, as inferred from the size and sharpness of the contours in the spectra, where larger peaks indicate lower-quality reads resulting from disorder (Figure 4.11A). Because the light signaling state of LOV2 is characterized by unfolding of the J $\alpha$  and A' $\alpha$  helices (Harper, Christie and Gardner, 2004; Zayner, Antoniou and Sosnick, 2012), leading to increased disorder following light treatment, this result was unexpected. Though the relatively low resolution of the NMR spectra made it difficult to assign the peaks to individual amino acids, a large chemical shift was observed for W553 in the LOV2-V478L lit-state spectra that was not present in wild-type LOV2 (Figure 4.11A; comparison of W553 conformations in wild-type LOV2 and LOV2-V478L in Appendix Figure 4.1). The degree of disorder in the dark state made clear the reason that it was difficult to generate crystals of LOV2-V478L, but overall the results from the NMR experiment were puzzling.

It was then hypothesized that the disorder of LOV2-V478L in the dark may be due to some degree of inappropriate oligomerization. LOV domains have been widely reported to be monomeric in the dark and to dimerize upon light perception as a precursor to signal transduction in their native systems (Möglich and Moffat, 2007; Zoltowski and Crane, 2008; Heintz and Schlichting, 2016). When LOV2-V478L was subjected to size-exclusion chromatography (SEC), there was a broader elution peak in the dark state, signaling a mixture of monomeric and dimeric LOV2, than in the lit state which had a single, narrow peak corresponding to a dimer, providing some explanation for the disorder observed in the dark state NMR spectra (Figure 4.11B). Based on this structural analysis of LOV2-V478L,

it seemed that the observed defects in functionality *in planta* could potentially be due to an altered dimerization pattern.

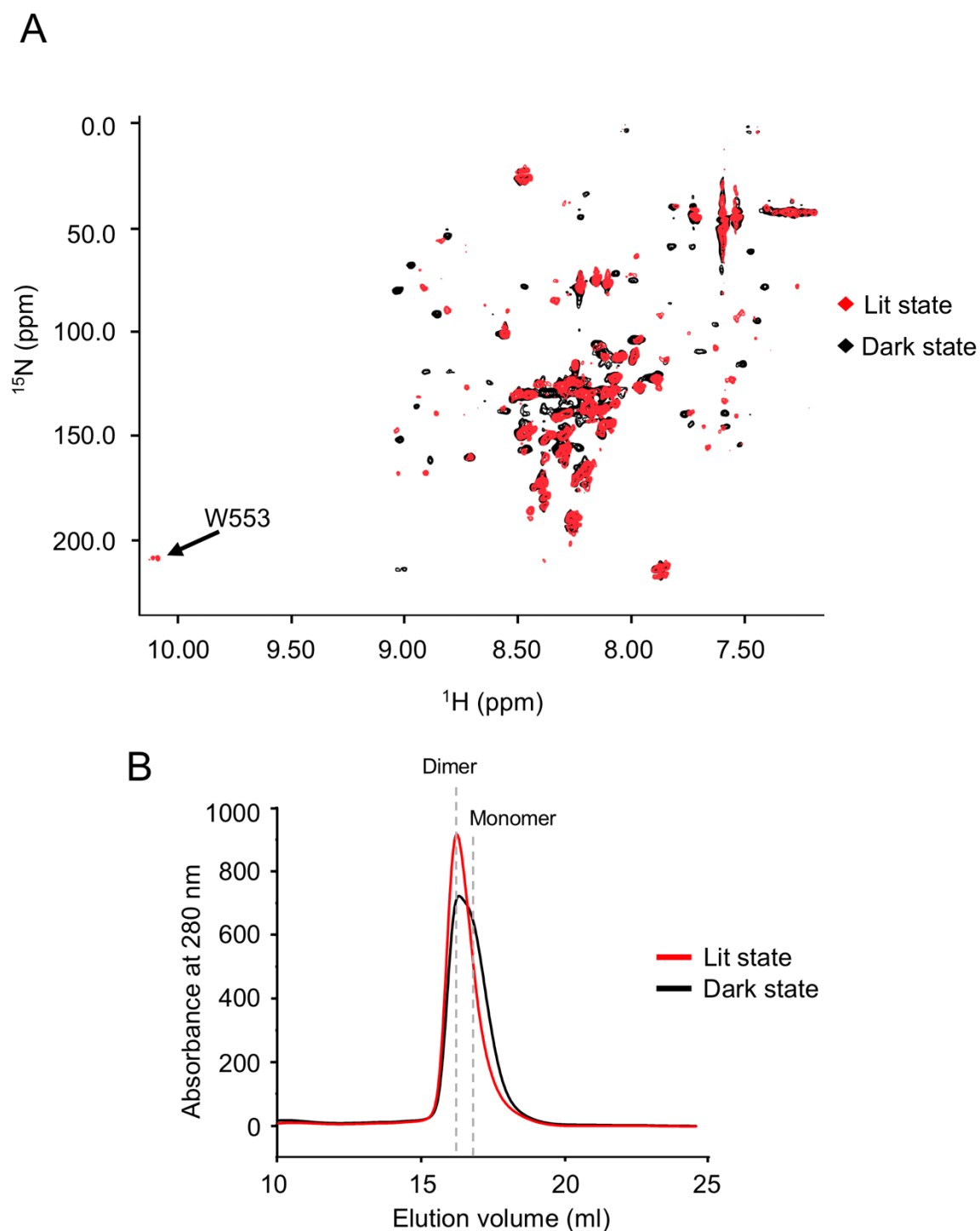


**Figure 4.11: NMR and size exclusion chromatography analysis of LOV2-V478L.** **A.** NMR spectra of LOV2-V478L in the dark (black contours) and following a saturating light treatment (red contours). The position of the peak corresponding to W553 in the light is indicated. **B.** Size exclusion chromatography of LOV2-V478L in the dark (black line) and following a saturating light treatment (red line). The elution volumes corresponding to the dimer and monomer forms of LOV2 are indicated with light gray broken lines.

#### **4.2.8 Dimerization is not perturbed in phot1-V478I or -V478L in the light *in planta***

To further explore the altered dimer status observed in the isolated LOV2-V478L domain, the dimerization of the V478 variants of full-length phot1 *in vivo* was explored. Light-dependent dimerization of phot1 at the plasma membrane has been reported using Bimolecular Fluorescence Complementation (BiFC; Kaiserli *et al.*, 2009; Xue *et al.*, 2018). A similar BiFC approach was therefore adopted here to probe whether phot1-V478L or -V478I showed altered dimerization patterns. Wild-type *Arabidopsis* phot1 and the V478I and V478L variants were tagged with either the N-terminal or C-terminal half of the Yellow Fluorescent Protein (YFP; Walter *et al.*, 2004; tags are referred to as YFP<sub>N</sub> and YFP<sub>C</sub>, respectively). Both versions of each protein were transiently co-expressed in tobacco (*Nicotiana benthamiana*) epidermal cells to test their dimerization through the reconstitution of YFP fluorescence. Phot1-V478I and phot1-V478L expressed at levels similar to the wild-type protein and show dimerization similar to that of wild-type phot1 in epidermal cells of light-grown tobacco plants (Figure 4.12).

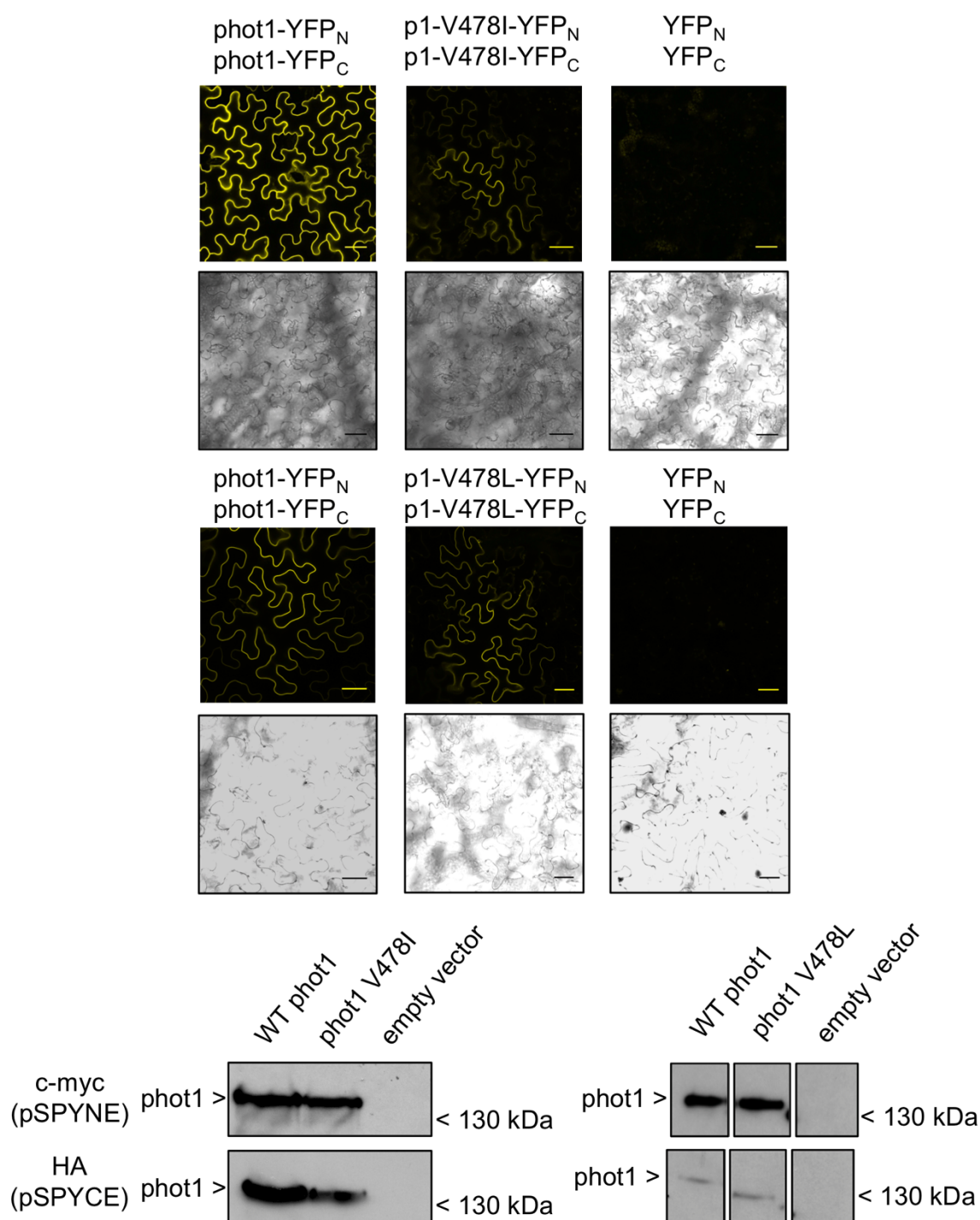


**Figure 4.12: Phot1-V478I and -V478L can dimerize.** BiFC was used to test the dimerization of phot1-V478I and -V478L, which are not fully functional for phot1-mediated responses. The pSPYNE (YFP<sub>N</sub>-tagged) and pSPYCE (YFP<sub>C</sub>-tagged) phot1 constructs of interest were transformed into *Agrobacterium*. The *Agrobacterium* cultures of both constructs were co-inoculated into the intracellular space of light grown tobacco (*Nicotiana benthamiana*) leaves. Three days post inoculation, the epidermal pavement cells of the tobacco leaves expressing each construct combination of interest were probed with confocal microscopy to test dimerization using reconstituted YFP signal as a proxy. All manipulations were carried out in the light. The scale bar is 50  $\mu$ m. One experiment is shown for phot1-V478I and separate one for phot1-V478L out of three independent experiments for each. Western blots using c-myc antibodies for the pSPYNE constructs and HA for the pSPYCE constructs were performed on the tobacco tissue expressing each combination to verify expression.

#### 4.2.9 Determining the region of phot1 dimerization

Though the above studies were based on the assumption that disruptions to LOV2 are sufficient to disrupt dimerization in the full-length protein, which domain or domains are responsible for full-length phot1 dimerization has not been thoroughly investigated. Because LOV domains are a branch of the larger PAS (Per, Arnt, Sim) domain superfamily (Christie *et al.*, 2015; Vogt and Schippers, 2015), which often control protein/protein interactions or dimerization following a stimulus (Vogt and Schoppers, 2015), it seemed most likely that either cooperation between LOV1 and LOV2 or one of the LOV domains individually controls dimerization. Supporting this hypothesis, based on analysis of single LOV domains *in vitro*, previous reports have speculated that LOV1 is the site of phototropin dimerization (Salomon, Lempert and Rüdiger, 2004; Nakasako *et al.*, 2008; Katsura *et al.*, 2009).

LOV2kinase (L2K) is a truncation of phot1 that lacks LOV1 and the linker region between LOV1 and LOV2, leaving only LOV2 and the kinase domain (amino acids 448 to 996; Sullivan *et al.*, 2008). When L2K is expressed in *Arabidopsis* in the *phot1phot2* double mutant background, it is insensitive to low fluence rates of blue light, and only complements phot1-mediated responses under moderate and high intensity light (Sullivan *et al.*, 2008). Given the evidence that LOV1 could be facilitating dimerization, whether the absence of LOV1 in L2K inhibited its dimerization, and by extension if any alteration in dimerization could be linked to its lowered sensitivity, was probed by BiFC. It was found that L2K produced a dimerization signal at the plasma membrane, though the signal was not as strong as that of wild-type phot1 even though the expression of the two proteins appeared to be similar (Figure 4.13; the bright foci of YFP signal in the L2K micrograph are unlikely to be dimerization signal). This evidence indicates that the presence of LOV1 is not required for dimerization in our BiFC system, though its presence may enhance the degree of dimerization.

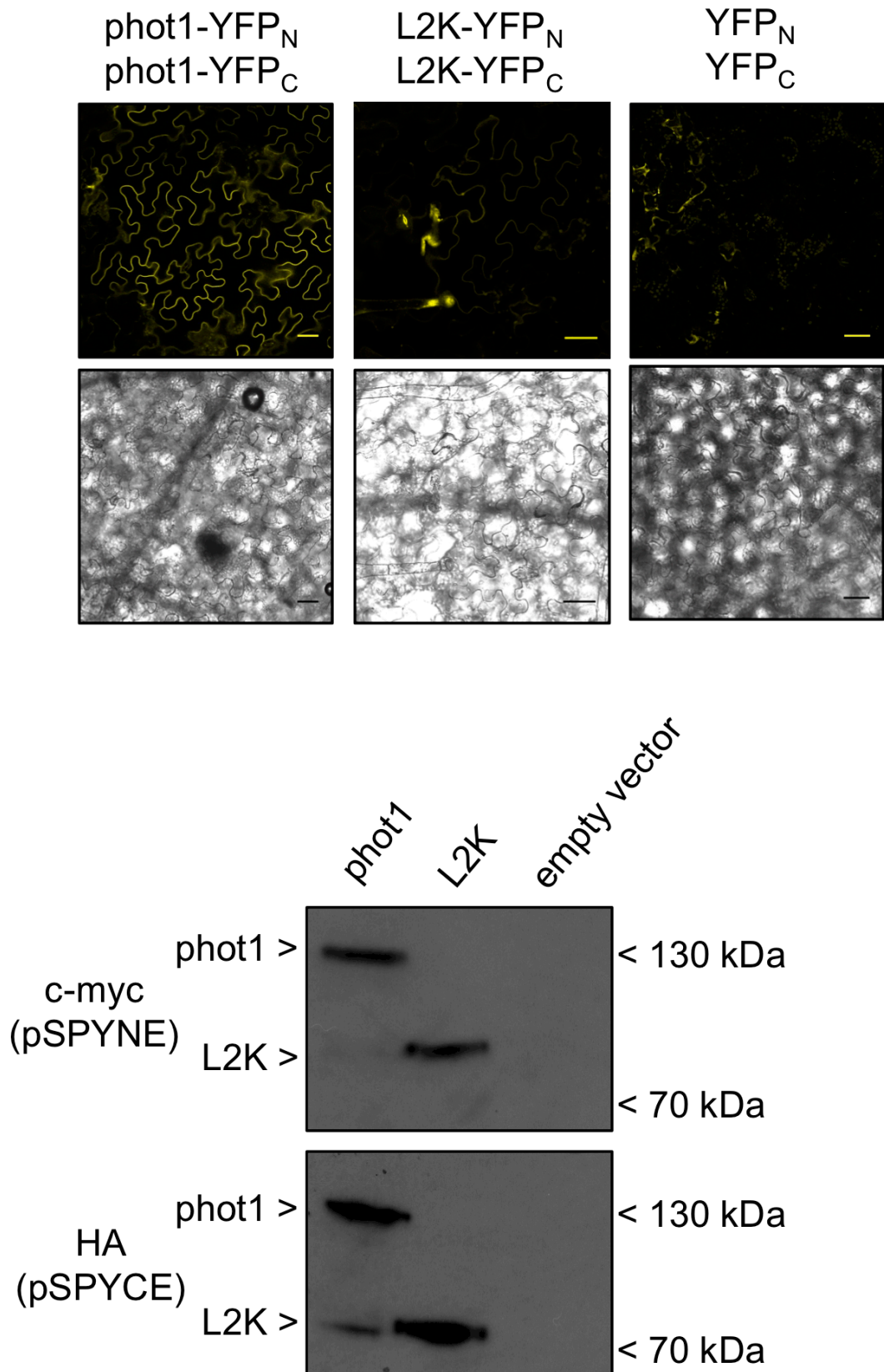


**Figure 4.13: The truncated phot1 protein LOV2Kinase can dimerize.** BiFC was used as described in Figure 4.12 to test the dimerization of LOV2Kinase, a truncated version of phot1 that lacks LOV1 and the linker region between LOV1 and LOV2. Fluorescent and bright field images from one experiment from three independent repeats are shown. The scale bar is 50  $\mu$ m. A western blot was performed on the tobacco tissue expressing each combination to verify expression.

To further explore phot1 dimerization, whether individual portions of phot1 could dimerize on their own *in vivo* was explored. To this end, phot1 was divided into two parts: the photosensory core of LOV1+LOV2 (amino acids 180-628) and the single kinase domain (amino acids 663-996). Neither LOV1+LOV2 nor the kinase domain expressed singly were able to recapitulate YFP fluorescence at a level that was above the background of the empty vector control (Figure 4.14). This lack of signal did not seem to be due to poor expression or protein stability since LOV1+LOV2 and the kinase domain were able to interact with each other (Figure 4.14). Taken together, the data suggests that in our BiFC system, LOV1 is dispensable for phot1 dimerization, but that both LOV2 and the kinase domain must be present to form a substantial dimer *in vivo*.

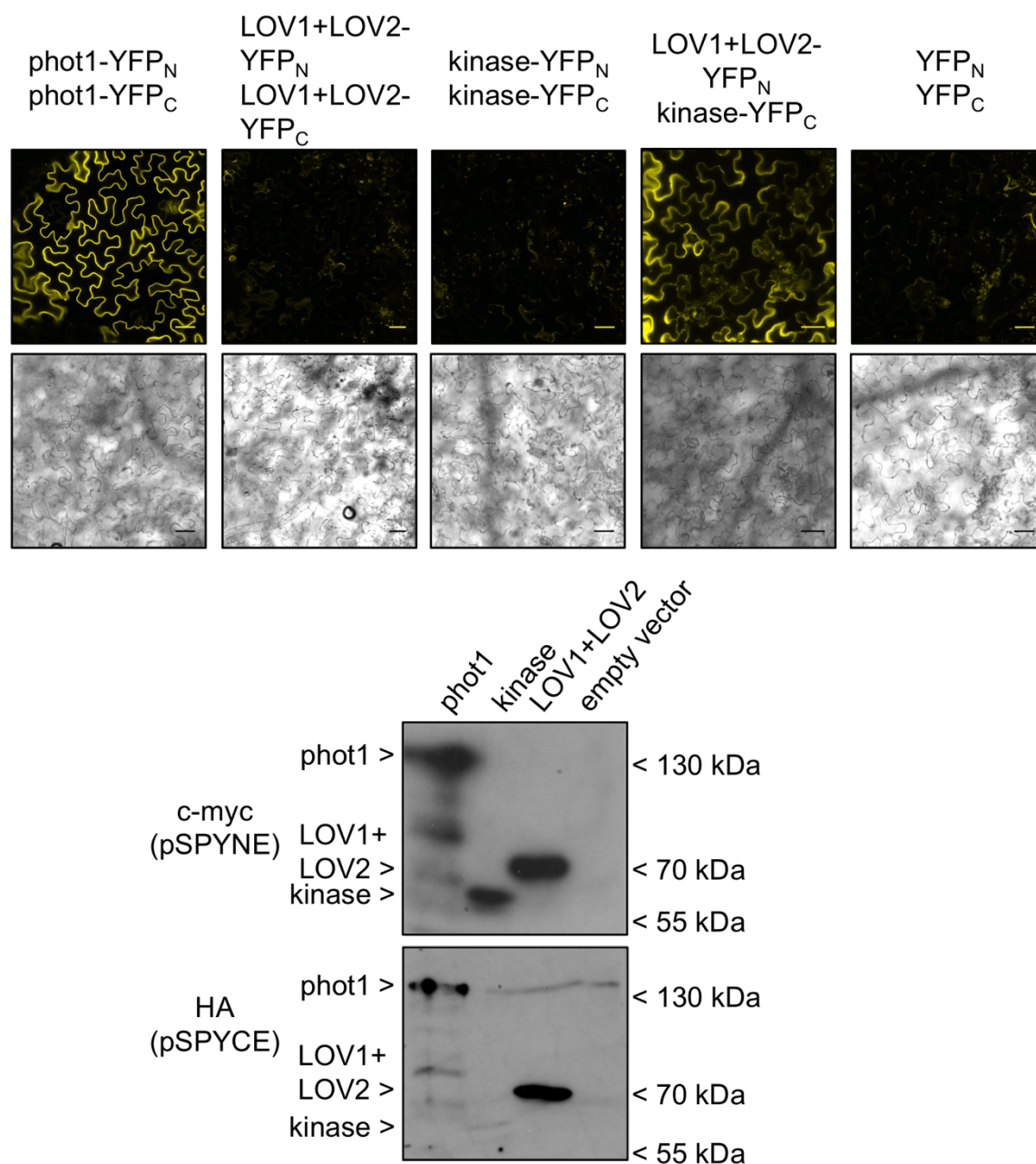


**Figure 4.14: Dimerization pattern of LOV1+LOV2 and the phot1 kinase domain.** BiFC was used as described in Figure 4.12 to test the dimerization of the phot1 truncations encompassing either LOV1 and LOV2 (LOV1+LOV2) or the kinase domain. Fluorescent and bright field images from one representative experiment from three independent repeats are shown. The scale bar is 50  $\mu\text{m}$ . A western blot was performed on the tobacco tissue expressing each combination to verify expression.

### 4.3 Discussion

The studies undertaken in this chapter investigate phot1 sensitivity *in vivo* through the photocycle mutants and also take a structure/function approach to further understanding of phot1 light perception and signaling. Any increased sensitivity or plant growth as a result of the introduced slow photocycle mutations has not yet been observed. In addition to probing

the role of the phot1 photocycle *in planta*, these studies were fruitful in providing a foundation for further work in understanding how the V478 residue is important for phot1 activity as well as for how phot1 dimerization may relate to its function.

#### **4.3.1 The photocycles of V478I and L558I are slow *in planta* as well as *in vitro***

Of the three candidate slow photocycle mutants investigated here, two, phot1-V478I and phot1-L558I, seem to maintain a slow photocycle *in planta* using recovery of the phosphorylated form of NPH3 as a readout for photocycle kinetics (Figure 4.7B). The phot1-N476L mutant did not appear to have a different recovery of the phosphorylated state of NPH3 from that of wild-type phot1-GFP (Figure 4.7B). Interestingly, of the two other slow photocycle mutants chosen for *in planta* investigation, phot1-V478L and phot1-V525R, which were generated by Dr. Stuart Sullivan, only V478L appeared to have a slow photocycle as measured through NPH3 phosphorylation status (Figure 4.10; V525R data not shown). Though not all of the mutants that were slow *in vitro* proved to be slow photocycle mutants *in vivo* as explored through NPH3 phosphorylation status, the mutants that did translate the slow photocycle to phot1-GFP showed recovery kinetics that correlated with those observed in LOV1+LOV2. Phot1-L558I is moderately slow to recover to the dark state *in vitro* and *in vivo*, and the recovery of phot1-V478I was quite slow *in vivo*, as it was *in vitro*, though still faster than that of phot1-V478L, which appears to have the slowest recovery of the phosphorylated form of NPH3 observed here (Figures 4.7B and 4.10; *in vitro* recoveries in Figure 3.11).

It is not clear why the phot1-N476L and -V525R photocycles, as measured by the recovery of NPH3 to its phosphorylated state, were not slow *in vivo*. Since N476L and V525R showed some of the slowest photocycles measured *in vitro*, it does not seem likely that the photocycle was not slow enough to observe an effect on NPH3 phosphorylation status *in vivo*. It is possible that the factors determining the photocycle may be somewhat different between LOV1+LOV2 *in vitro* and full-length phot1 *in vivo*. In the case of N476L, which was hypothesized to slow the photocycle by limiting solvent access to the FMN binding pocket (see section 3.2.5), perhaps solvent access to LOV2 is more limited in full-length phot1 than in the LOV1+LOV2 protein, rendering the hypothesized altered solvent access not a significant determining factor of the photocycle *in vivo*.

### 4.3.2 The photocycle mutants are functional to varying degrees

None of the candidate slow photocycle mutants were able to fully complement all of the phot1-mediated responses tested here to the same extent as wild-type phot1-GFP. For chloroplast positioning (Figure 4.4) and petiole positioning (Figure 4.5), the differences between the photocycle mutants and wild type were slight. The degree of leaf flattening was lower in the photocycle mutants than in wild type, but the lower level of complementation did not produce a major defect (Figure 4.3). By contrast, differences in functionality for phototropism at low fluence rates, which requires exquisite phot1 sensitivity, were stark (Figures 4.6 and 4.8). For future analysis, changing the use of statistics from using student's t-tests to ANOVAs would enable a more rigorous comparison between mutant lines and reduce the likelihood of encountering false-positives when examining whether differences in complementation were statistically significant. Aside from the statistical analysis, there are two possibilities that could account for the lack of complete complementation in the mutants generated in this study: the first is that the slow photocycle itself is leading to reduced responsiveness, and the second is that the introduced mutations are leading to general signaling defects.

Of the slow photocycle mutants presented here, the level of functionality may be inversely correlated with the extent to which photocycle was slowed. Phot1-V478L, which shows the slowest photocycle *in vivo*, is unable to complement phot1-mediated responses (Figure 4.10). The next slowest, phot1-V478I, is functional but its complementation is fairly weak (Figure 4.10). The most functional photocycle mutant for phot1-mediated responses, phot1-L558I, has a moderately slow photocycle as measured by NPH3 phosphorylation status and is the fastest to recover of the three photocycle mutants (Figures 4.6 and 4.7). Additionally, because these mutants all demonstrate phot1 autophosphorylation and NPH3 dephosphorylation (Figure 4.2), the initial biochemical steps for signaling appear to be fully intact, although NPH3 does not recover its phosphorylated state in the phot1-V478L background over the period of the time course (Figure 4.8). It was initially speculated that the observed defects could be due to enhanced sensitivity conferred by the photocycle, with the optimal responsiveness occurring at a very low fluence rate. This is not the case, as our investigation of phototropism over two orders of magnitude of light intensity indicates that at least with continuous illumination for 24 hours, the functionality of the photocycle mutants relative to wild-type phot1-GFP increases with increasing fluence rate (Figure 4.8). The evidence indicates that the photocycle mutants are less sensitive than wild type in a

manner that may be tied to the slowness of the photocycle of each mutant, requiring higher light intensities to drive complementation.

There could be suppressors of phot1 that tightly regulate its activity, preventing the kinase domain from producing too much signal, which could potentially be deleterious to normal plant development. It could be that the photocycle mutations do increase phot1 activity, but these possible suppressors act on the slow-cycling phot1 to inhibit its activity, leading to no apparent increase in sensitivity. Indeed, constitutively active variants of phot1 neither exhibit constitutive signaling nor express wild-type levels of phot1 protein *in planta*, though this could also arise from instability inherent to those proteins (Kaiserli *et al.*, 2009; Petersen *et al.*, 2017). However, when the stability of phot1-V478L, the slowest-recovering photocycle mutant, was investigated, the protein accumulated in the dark and was turned over in response to an intense treatment of blue light in a manner similar to that of wild-type phot1-GFP (Appendix Figure 4.2). If a mechanism negatively regulating the activity of the photocycle mutants is the reason that they are not more sensitive than wild-type phot1 *in planta*, it is not clear what factors would correlate functionality with the photocycle.

Phot1-N476L, which appears not to be a slow photocycle mutant by the rate of the recovery of the phosphorylated form of NPH3 following a light treatment and return to darkness (Figure 4.7), is also not fully functional for phot1-mediated responses, raising the possibility that the observed defects in complementation in this study may not be related to the photocycle but to general signaling defects produced by mutating phot1 LOV2. Furthermore, the structural observations presented in this chapter may imply that V478L is non-functional due to perturbations in its dark state, which is not likely to be related to its photocycle. When amino acid sequence identity of phot1 LOV2 is compared across a broad range of plant species, from basal plants to monocot and dicot crops, the amino acid sequence of LOV2 shows almost no variation (Appendix Figure 4.3). The identities of N476, V478, and L558 are invariant across all of the species investigated here, and V478 and L558 are also conserved between *Arabidopsis* phot1 LOV2 and the *Arabidopsis* zeitlupe LOV domain. The conservation of LOV2, and of these residues in particular, implies that a strong selective pressure may have maintained this degree of homology, perhaps because even minor substitutions to LOV2 tend to cause functional defects. This hypothesis is not mutually exclusive with the idea that the slow photocycle itself is deleterious to functionality, but since nearly all the residues of LOV2 are well-conserved, it seems more likely that the answer may lie in signal transduction generally.

It is worth noting that when the photocycle was slowed in the *Arabidopsis zeitlupe* (*ztl*) LOV domain using the substitution V48I, which is equivalent to V478I in *phot1* LOV2, concurrent functionality issues in full-length *ztl* also arose (Pudasaini *et al.*, 2017). This valine may be important for proper function in both LOV domains. In the case of *ztl* signaling, the defects arising from V48I substitution seemed not to be related to the photocycle, since the slow photocycle mutant G80R, which exhibited a photocycle that was slower than wild-type *ztl* but faster than V48I, appeared to be fully functional (Pudasaini *et al.*, 2017). Though it cannot be assumed that because slowing the *ztl* photocycle does not directly correlate with functional activity in that photoreceptor, that the same must be true for *phot1*, it does suggest the possibility that the signal defects are not related to the photocycle. However, it remains difficult to draw definitive conclusions as to what causes the variations in functionality in the set of mutants generated in this study.

### **4.3.3 The chemical shift of W553 in LOV2-V478L upon light exposure does not appear to underpin the low functionality of phot1-V478L**

In addition to the altered dimerization pattern of LOV2-V478L revealed by structural investigation, an unusually large chemical shift of W553 between LOV2-V478L and wild-type LOV2 was observed in the NMR spectra (Appendix Figure 4.1). The peaks for W553 were able to be assigned because W553 is the only tryptophan present in LOV2 (Appendix Figure 3). To test the significance of this altered conformation of W553 in LOV2-V478L, transgenic plants were generated to express *phot1*-GFP harboring the W553L substitution using resistance to kanamycin as the selectable marker. When T<sub>1</sub> individuals were screened for phototropism and kanamycin resistance, all of the kanamycin resistant individuals were responsive to the phototropic stimulus (Appendix Figure 4.4). When the phototropic individuals were rescued and grown to maturity, it was also evident that the *phot1*-W553L mutants could complement leaf flattening (Appendix Figure 4.4). The chemical shift of W553 may be significant in terms of the structural perturbations witnessed in LOV2-V478L, but the W553 residue does not appear to be required for *phot1* activity because it did not phenocopy the non-functional *phot1*-V478L transgenic line (Figure 4.11; Appendix Figure 4.1).

### **4.3.4 Dimerization of phot1**

The preliminary structural studies on the dimerization of LOV2-V478L *in vitro* indicated that LOV2-V478L was a dimer following light treatment but also exhibited unusual dimer

formation in the dark (Figure 4.11B). Consistent with those results, full-length phot1-V478L expressed in tobacco epidermal cells was able to dimerize normally in light-grown plants in our BiFC system (Figure 4.12). An investigation into whether phot1-V478L was present as a dimer in dark-adapted plants was also undertaken, but the results were unreliable due to high background signal and because dimerization in the dark was sometimes observed in the wild-type phot1 controls (data not shown). This is an important experiment and should be optimized in order to uncover whether dimer formation in the dark occurs in phot1-V478L *in planta*, and by extension, if that is causing its lack of function for phot1 responses.

Previous studies on assigning the site of phot1 dimerization have focused on single LOV domains examined *in vitro*, with most studies concluding that LOV1 primarily mediates dimerization (Salomon *et al.*, 2004; Nakasako *et al.*, 2008; Katsura *et al.*, 2009; Halavaty and Moffat, 2013). Matching that framework, a truncated phot1 protein encompassing LOV2 and the kinase domain that is similar to the L2K protein studied here (amino acids 449 to 996; the construct used here encompasses amino acids 448-996) was reported to be a monomer *in vitro* when probed with small angle x-ray scattering (SAXS; Okajima, Matsuoka and Tokutomi, 2011). No studies thoroughly examining the dimerization of full-length phot1 *in vitro* have been performed to our knowledge, likely due to difficulty producing large quantities of phot1 heterologously. Additionally, to draw conclusions about biological significance of phot1 dimerization, *in vivo* investigation was required. To resolve some of these outstanding questions, this study explored the dimerization of truncations of phot1 by transient expression in tobacco epidermal cells.

According to the work presented here, both LOV2 and the kinase domain must be present for dimerization to occur (Figures 4.13 and 4.14); the presence of LOV1 was not necessary to produce a dimerization signal (Figure 4.13) and neither LOV1+LOV2 nor the kinase domain expressed on its own was able to dimerize (Figure 4.14). This data does not fit the hypothesis that LOV1 mediates phot1 dimerization or the finding that a protein encompassing the LOV2 and kinase domain of phot1 is a monomer (Okajima *et al.*, 2011). These discrepancies are probably due to differences between the dimerization pattern *in vitro*, which is often buffer- and concentration-dependent (Katsura *et al.*, 2009), and *in vivo* which, though expressed outside of *Arabidopsis*, provides a more realistic reflection of phot1 dimerization.

This work provides a foundation for further investigations into the biological significance of phot1 dimerization. For example, the lowered sensitivity observed in transgenic plants

expressing L2K (Sullivan *et al.*, 2008) does not appear to be due to stymied dimerization in the light (Figure 4.11). To draw firmer conclusions from these studies, it would be useful to quantify fluorescence, especially when the signal is apparent but begins approaching the level of background fluorescence. Fluorescence quantification would also give some indication of the strength of the interaction of the two proteins (for example, is it significant that the dimer signal from L2K consistently appears to be weaker than that of phot1?; Figure 4.13). Furthermore, finding a phot1 mutation (or mutations) that blocks dimerization entirely could provide insight into the mechanism as well as provide a useful negative control for these studies. Finally, conclusions drawn from BiFC studies can benefit from validation in other systems, such as yeast two-hybrid or co-IP experiments. These steps would add weight to the results and allow stronger conclusions to be drawn regarding their significance for phot1 function.

### 4.3.5 Phot1 sensitivity and the photocycle

Investigations into whether slowing the phot1 photocycle can provide an advantage over wild type for specific responses or light conditions are still underway. Petiole positioning may be a good response to study further, as it was for this response that the phot1-V478I and -L558I slow photocycle mutants most closely matched phot1-GFP in terms of the level of complementation (Figure 4.5). Perhaps lowering the fluence rate used for petiole positioning could tease out any possible increase in sensitivity of the photocycle mutants. However, phototropism in response to blue light over two orders of magnitude did not reveal any increased responsiveness (Figure 4.8) and that the L558I transgenic lines were not able to out compete phot1-GFP for biomass accumulation under very low intensity light ( $25 \mu\text{mol m}^{-2} \text{s}^{-1}$  red light,  $0.1 \mu\text{mol m}^{-2} \text{s}^{-1}$  blue light) in a long-term experiment (Figure 4.9). Though no difference in growth was detected using the fresh weight measurements, it would be informative to redo them to probe whether there are alterations in dry weight between wild-type phot1 and the L558I mutant, since phot1 activity is associated with stomatal opening and can effect plant water content through transpiration, and could mask whether phot1-L558I mutant plants do in fact accumulate more biomass (Kinoshita *et al.* 2001). Nevertheless, given the data presented in this chapter, it appears that lowering the fluence rate at which the light is administered is not sufficient for the slow photocycle mutants to have more efficient phot1 responses.

Encouragingly, evidence from our collaborators suggests that the slow photocycle of phot1-L558I leads to enhanced chloroplast accumulation relative to phot1-GFP in response to a 0.1

second pulse of blue light (Dr. Justyna Łabuz, Appendix Figure 4.5). It may be that in order to thoroughly study these mutants, light treatments need to be well below durations that saturate the activity of wild-type phot1. In light of the increased sensitivity for chloroplast accumulation in response to pulses, it may be that moving from continuous irradiation to light administered as pulses may be able to reveal differences in responsiveness between wild-type phot1-GFP and the slow photocycle mutants. Pulse-based first-positive phototropism, which measures the phototropic response of seedlings exposed to a brief pulse (~10 seconds) of low-intensity blue light (Christie and Murphy, 2013), may provide a better assessment of the photocycle than the 24-hour irradiations conducted here. Indeed, Steinitz and Poff (1986) found that first-positive phototropism was greatly enhanced when multiple pulses were given 20 minutes apart, an interval that is tantalizingly close to the observed length of the phot1 photocycle *in vitro* (Figure 3.1; Christie *et al.*, 2002; Kasahara *et al.*, 2002).

This chapter also provides a preliminary investigation into L2K, a truncated version of phot1 lacking the LOV1 domain. Our findings show that its dimerization is not likely to be the underlying cause of its poor sensitivity (Figure 4.11; Sullivan *et al.*, 2008). As discussed in the previous chapter, when LOV1 is disabled, a fast phot1 photocycle is observed (Christie *et al.*, 2002; Kaiserli *et al.*, 2009). L2K may therefore be a fast photocycle mutant, which could explain its lowered sensitivity relative to wild type. This makes L2K an interesting genetic background with which to further our understanding of phot1 sensitivity. In the next chapter, the sensitivity of L2K is explored further and the L2K transgenic line that was previously generated (Sullivan *et al.*, 2008) is used as the basis for a suppressor screen to discover possible suppressors of phot1 activity *in planta*.

## Chapter 5 Identification of Putative Suppressors of Phot1 activity

### 5.1 Introduction

Unlike the best understood photoreceptors, the red/far-red perceiving phytochromes and the blue light sensing cryptochromes, which generally modulate physiology in response to light through influencing transcription (Franklin and Quail, 2010; Wang *et al.*, 2018), phot1 is a kinase and signals in a fashion that is unique relative to those photoreceptors. Much information about phot1 signaling remains to be identified, including substrates of phot1 kinase activity. A handful of phosphorylation targets of phot1 have already been identified, including the auxin efflux transporter ATP-BINDING CASSETTE B19 (ABCB19) (Christie *et al.*, 2007), and the kinase BLUE LIGHT SIGNALLING 1 (BLUS1) (Takemiya *et al.*, 2013), which is involved in stomatal opening. Indeed, phot1-mediated stomatal opening is perhaps the best characterized of all its signalling pathways. In addition to phosphorylation substrates, a suppressor of phot1 activity for stomatal opening has also been identified: mutants of the evening complex component EARLY FLOWERING 3 (ELF3) were found to have constitutively open stomata through overexpression of FLOWERING LOCUS T (FT) in a *phot1phot2* double mutant background, which normally have closed stomata (Kinoshita *et al.*, 2011). Stomatal opening is, however, NPH3-independent (Inada *et al.*, 2004) and is therefore not likely to be representative of the signal transduction or suppression of phot1 activity for other responses. Furthermore, how phot1 signaling combines with the activity of other photoreceptors, such as the phytochromes and cryptochromes, to bring about the overall response to the light environment is not well understood. In order to garner more information about phot1 activity for NPH3-dependent responses, as well as photoreceptor signal integration, a screen for suppressors of phot1 activity for petiole positioning, an NPH3-dependent response wherein phot1 initiates petiole inclination under low light to optimize light capture, was designed.

Although altered petiole positioning is an easily identifiable consequence of light-limiting conditions, the pathways that underlie the response are complex and how they work together is poorly understood. The contribution of phot1 and phot2 to the control of petiole angle is well-established in young plants (around two weeks old; Inoue *et al.*, 2008B; de Carbonnel *et al.*, 2010), where the *phot1phot2* mutant has downward sloping, drooping petioles under all light intensities. However, most studies on petiole angles in *Arabidopsis* have focused on mature plants (three to four weeks old) in the context of the Shade Avoidance Syndrome

(SAS), a series of responses that plants undergo when shaded and photosynthetic potential is limited (Franklin, 2008). This SAS-induced petiole inclination, or hyponasty, is reported to be due to the lowered activity of phytochromes (Whitelam and Johnson, 1982; Faigon-Soverna *et al.*, 2006) and cryptochromes (Millenaar *et al.*, 2009; Keller *et al.*, 2011) in the shade. Adding additional complexity to this response, petiole angle is also partly controlled by circadian rhythms (Dowson-Day and Millar, 1999; Dornbusch *et al.*, 2012, 2014). Further information on signal integration for petiole positioning overall, and particularly how photos fit into the framework, remains to be uncovered (van Zanten *et al.*, 2010).

Phot1 is overall quite sensitive to low-intensity blue light; therefore, a genetic screen targeting individuals with enhanced responsiveness for petiole positioning due to a suppressor mutation required an allele of phot1 with lowered sensitivity. As such, the petiole positioning screen conducted here was performed using the LOV2Kinase (L2K) transgenic line. L2K is a truncated version of phot1 that lacks the LOV1 domain and the linker region between LOV1 and LOV2 and is expressed on the viral 35S promoter in a *phot1phot2* mutant background such that L2K is the only phot present in the plant (Sullivan *et al.*, 2008). It was found that this truncation of phot1 lead to an interesting conditional phenotype, in which L2K was unresponsive to low fluence rates of blue light, but exhibited increased responsiveness under higher light intensities, eventually reaching near-wild-type levels of complementation (Sullivan *et al.*, 2008). As such, L2K does not complement petiole positioning under  $10 \mu\text{mol m}^{-2} \text{s}^{-1}$  of white light but does when the fluence rate is raised to  $50 \mu\text{mol m}^{-2} \text{s}^{-1}$  (Sullivan *et al.*, 2008). In a population of ethyl methanesulfonate (EMS) mutagenized L2K plants, it was hypothesized that some individuals may have enhanced responsiveness for petiole positioning compared to the L2K parent due to either a mutation within L2K itself that increased its photosensitivity, such as a lesion altering its photocycle, or mutation in a suppressor of L2K activity, which would increase the signalling potential of L2K. Both possibilities would lead to increased petiole inclination under circumstances where L2K cannot ordinarily complement the response. The screen for mutants with enhanced petiole positioning was therefore conducted with the expectation that either type of mutation could increase our current understanding of phot1 function and signalling for NPH3-dependent responses.

## 5.2 Results

### 5.2.1 L2K requires intense light to drive phototropism

The initial characterization of the L2K transgenic line found that L2K was unable to complement phototropism when stimulated with low fluence rates of blue light (Sullivan *et al.* 2008). To examine the phototropic response of L2K in more detail, the kinetics and extent of phototropism in freestanding seedlings over a four-hour period was investigated. Following the previous findings, L2K was not able to appreciably respond to a phototropic stimulus of  $0.5 \mu\text{mol m}^{-2} \text{s}^{-1}$  blue light (Figure 5.1A). When the same experiment was performed with stronger blue light at a fluence rate of  $10 \mu\text{mol m}^{-2} \text{s}^{-1}$ , L2K did respond, though its final angle after four hours as well as the rate of its curvature was well below that of wild-type seedlings (Figure 5.1A). Following this characterization, whether L2K-mediated phototropism was enhanced by de-etiolation, the process of exposing the dark-grown, etiolated seedlings to a light treatment to instigate the development of photosynthetic competence, was tested. De-etiolation of seedlings prior to phototropic stimulus has long been known to enhance curvature (Hart and MacDonald, 1981; Hasegawa *et al.*, 1987), but it was not clear whether L2K would be able to produce this response. Although etiolated L2K seedlings do not respond to phototropic stimulus at  $10 \mu\text{mol m}^{-2} \text{s}^{-1}$  of blue light to the same degree as wild type, surprisingly de-etiolation prior to the onset of phototropism at  $10 \mu\text{mol m}^{-2} \text{s}^{-1}$  almost completely rescued responsiveness in the L2K transgenic line, which exhibited curvature similar to that of wild type de-etiolated seedlings (Figure 5.1B). The low degree of L2K responsiveness therefore appeared to be related to its reduced sensitivity and not to another intrinsic defect resulting from the truncation of full-length phot1.

The lowered sensitivity for phototropism in etiolated L2K seedlings raised the question of whether its altered responsiveness corresponded to changes in NPH3 dephosphorylation. The phosphorylation status of NPH3 in the L2K transgenic line following blue light treatment was therefore examined. It was found that unlike wild-type phot1, which brought about complete dephosphorylation of NPH3 following a 15 minute treatment with  $20 \mu\text{mol m}^{-2} \text{s}^{-1}$  of blue light, in the L2K background higher light was required to drive NPH3 dephosphorylation (Figure 5.2). A substantial pool of dephosphorylated NPH3 was not apparent until the intensity of the light treatment was raised to around  $75 \mu\text{mol m}^{-2} \text{s}^{-1}$ , and even after treatment with  $150 \mu\text{mol m}^{-2} \text{s}^{-1}$  of blue light, most of the pool of NPH3 remained in its phosphorylated state. The observed lack of complete NPH3 dephosphorylation seems to underlie the reduced sensitivity of L2K for phototropism.

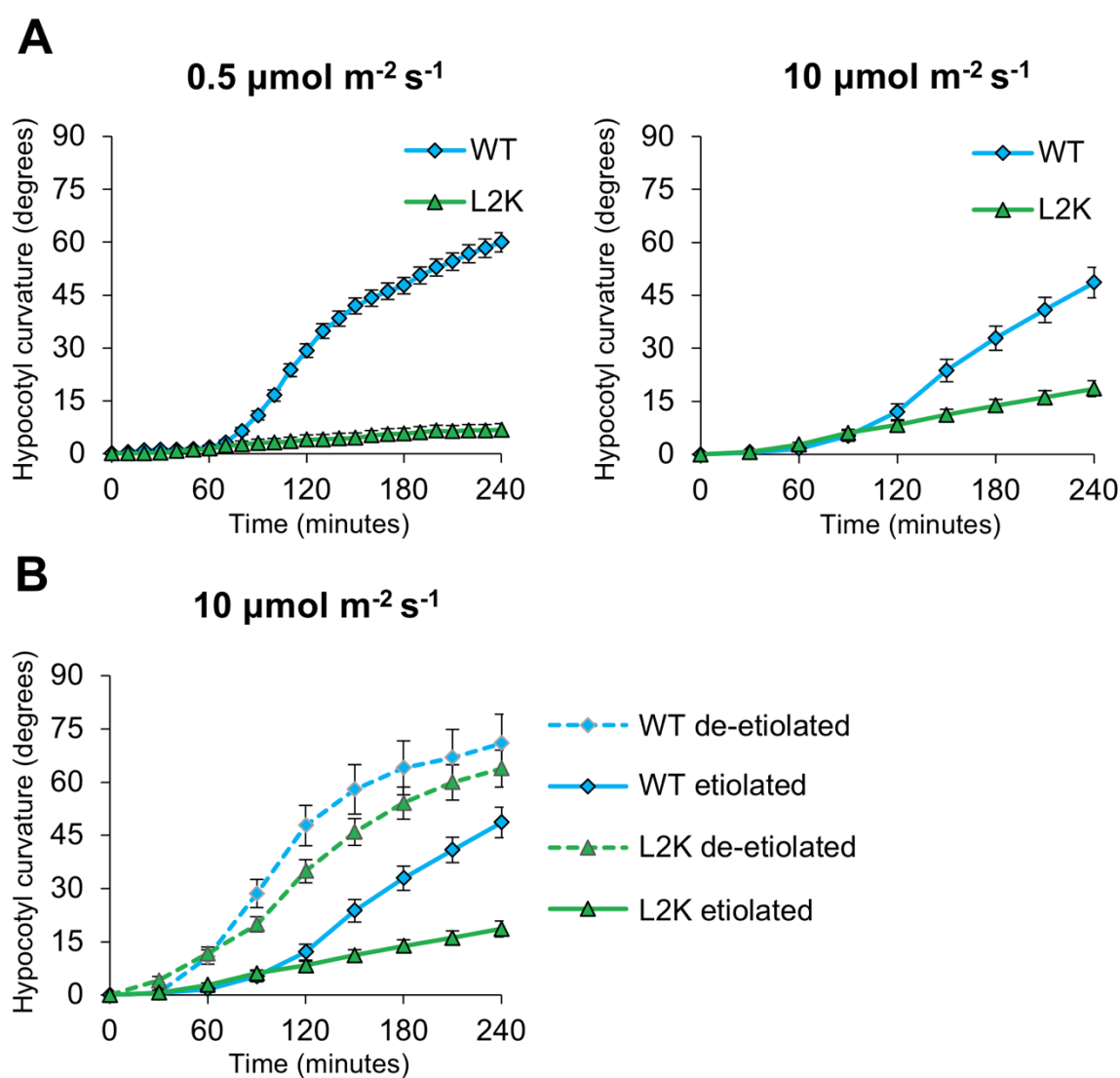


**Figure 5.1: Phototropic responses of the L2K transgenic line.** **A.** Phototropism of freestanding three-day-old etiolated seedlings exposed to unilateral blue light at fluence rates of  $0.5 \mu\text{mol m}^{-2} \text{s}^{-1}$  and  $10 \mu\text{mol m}^{-2} \text{s}^{-1}$  blue light. Hypocotyl curvature was measured every 10 minutes for the  $0.5 \mu\text{mol m}^{-2} \text{s}^{-1}$  data and every 30 minutes at  $10 \mu\text{mol m}^{-2} \text{s}^{-1}$ . The mean of 29-30 seedlings across three independent experiments is shown for both fluence rates. **B.** Phototropism of three-day-old seedlings that were either etiolated or de-etiolated by growing the seedlings in the dark for two days, placing them in the light for eight hours to de-etiolate, then placed in the dark again for 16 hours before performing the experiment. The mean of the angle of 30 seedlings across three independent experiments with measurements made every 30 minutes is shown. Error bars are standard error of the mean.

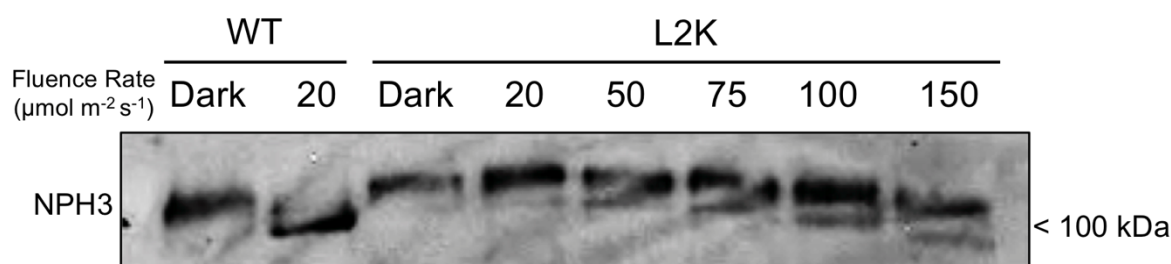


**Figure 5.2: L2K requires high intensity blue light to trigger NPH3 dephosphorylation.** Three-day-old etiolated seedlings were either left in darkness or treated with the indicated fluence rate of blue light ( $\mu\text{mol m}^{-2} \text{s}^{-1}$ ) for 15 minutes prior to isolation of total protein extracts and separation by SDS-PAGE. The UGPase loading control was run off and therefore could not be assessed. A representative blot from three independent repeats is shown.

### 5.2.2 An EMS screen for altered petiole identified three potential suppressor mutants of L2K

Since L2K does not respond to low light intensities but is capable of complementation under higher light conditions, L2K was selected as the basis of a screen for suppressors of phot1. EMS was used to introduce random point mutations into the genomes of a large batch of L2K transgenic seeds, which were then allowed to mature and self-pollinate (treatment and establishment of the segregating population was performed by Dr. Bobby Brown). The EMS-treated F<sub>2</sub> generation was screened for suppressor mutants by the identification of individuals within the population that possessed enhanced sensitivity under low-intensity light. To begin with, a screen was designed to find individuals in the population that could respond with phototropism to an 8-hour, unilateral  $0.5 \mu\text{mol m}^{-2} \text{s}^{-1}$  blue light treatment. This approach yielded many false positives, most likely due the randomized orientation of seedlings unable to respond to phototropic stimuli, resulting in individuals that appeared to respond but in fact were oriented randomly towards the light (data not shown).

To limit the isolation of false positives, a screen for petiole positioning was created. As described previously, L2K is unable to respond to low light conditions by inclining petiole angles in order to optimize light capture but exhibits petiole angles similar to those of wild type when the light intensity is raised (Sullivan *et al.*, 2008). To begin with, the mutagenized population of seeds was sown on soil, stratified for two days, and then placed under  $50 \mu\text{mol m}^{-2} \text{s}^{-1}$  of white light for one week in order to establish the seedlings. The following week, the fluence rate was lowered to  $10 \mu\text{mol m}^{-2} \text{s}^{-1}$ . When the seedlings were two weeks old, they were probed for individuals that had raised petioles in the first pair of true leaves. Around 75,000-80,000 EMS-mutagenized seedlings were screened in this manner. Twenty-seven individuals were selected from the screen based on visual assessment of enhanced

petiole angle. When the 27 individuals were screened a second time, petiole angles were quantified and three of the mutants, 24B, 24C, and 21D, were confirmed as having significantly more inclined petiole angles than L2K (Figure 5.3).

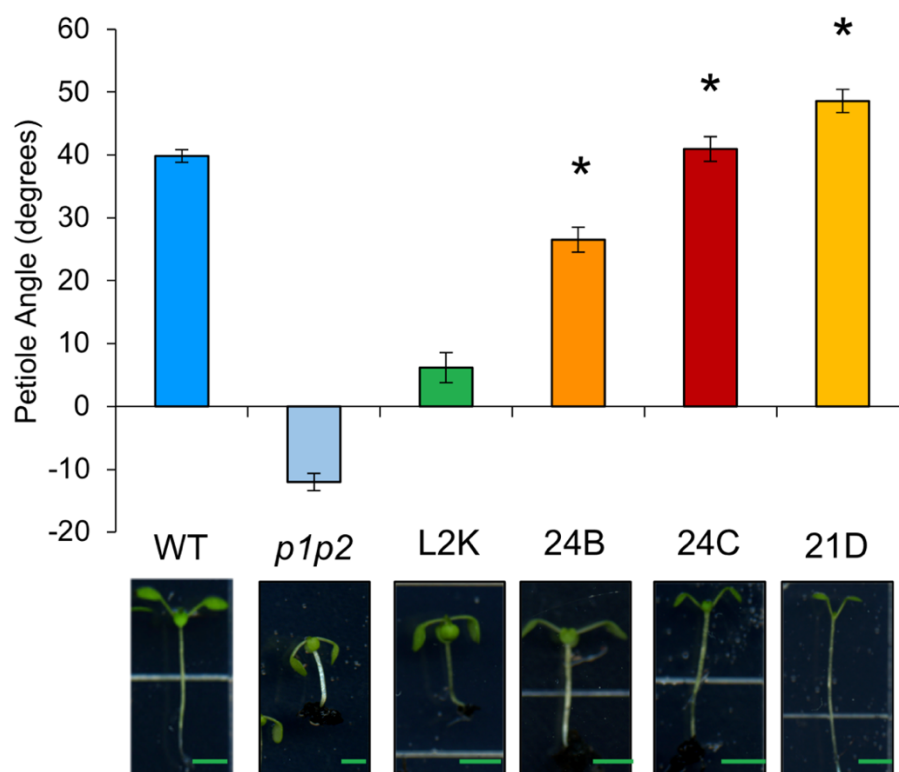


**Figure 5.3: Three EMS mutants of L2K have enhanced petiole positioning under low intensity light.** EMS-treated seeds from the L2K transgenic background, along with the L2K parental line, wild type (WT) and the *phot1phot2* (*p1p2*) double mutant, were sown onto soil and grown for one week in long days under  $50 \mu\text{mol m}^{-2} \text{s}^{-1}$  white light, after which the fluence rate was lowered to  $10 \mu\text{mol m}^{-2} \text{s}^{-1}$  white light for another week. The two-week-old seedlings with noticeably inclined petioles were imaged to quantify petiole angle. The 24B, 24C, and 21D mutants were found to have significantly higher petiole angles than L2K ( $p < 0.001$ , two-tailed student's t-test). Data shown is the mean of 55-90 petioles from three independent experiments; error bars are standard error of the mean. Scale bar is 2.5 mm.

In the following  $F_3$  generation, the three EMS lines with reproducibly enhanced petiole angles were confirmed as homozygous for their enhanced petiole positioning phenotype and as resistant to kanamycin, the selectable marker for the L2K transgene (data not shown). Once established as adult plants, genomic DNA was harvested from each line and the L2K transgene from each of the mutants was sequenced to determine whether the observed gain in sensitivity for petiole positioning could be attributed to a mutation within L2K that made it more responsive. However, no mutation was detected in the L2K transgene from any of the mutants, pointing to the possibility that these individuals could be mutants of suppressors of L2K activity (Figure 5.4).

```

phot1 PESVDDKVRQKEMRKGIDLATTLERIEKNFVIDPRLPDNPIIFASDSFLELTEYSREEI 507
L2K PESVDDKVRQKEMRKGIDLATTLERIEKNFVIDPRLPDNPIIFASDSFLELTEYSREEI 60
24B PESVDDKVRQKEMRKGIDLATTLERIEKNFVIDPRLPDNPIIFASDSFLELTEYSREEI 60
24C PESVDDKVRQKEMRKGIDLATTLERIEKNFVIDPRLPDNPIIFASDSFLELTEYSREEI 60
21D PESVDDKVRQKEMRKGIDLATTLERIEKNFVIDPRLPDNPIIFASDSFLELTEYSREEI 60
*****

phot1 LGRNCRFLQGPETDLTTVKKIRNAIDNQTEVTVQLINYTEKSGKFFWNIFHLQPMRDQKGE 567
L2K LGRNCRFLQGPETDLTTVKKIRNAIDNQTEVTVQLINYTEKSGKFFWNIFHLQPMRDQKGE 120
24B LGRNCRFLQGPETDLTTVKKIRNAIDNQTEVTVQLINYTEKSGKFFWNIFHLQPMRDQKGE 120
24C LGRNCRFLQGPETDLTTVKKIRNAIDNQTEVTVQLINYTEKSGKFFWNIFHLQPMRDQKGE 120
21D LGRNCRFLQGPETDLTTVKKIRNAIDNQTEVTVQLINYTEKSGKFFWNIFHLQPMRDQKGE 120
*****

phot1 VQYFIGVQLDGSKHVEPVRNVIETAVKEGEDLVKKTAVNIDEAVRELDPANMTPEDLWA 627
L2K VQYFIGVQLDGSKHVEPVRNVIETAVKEGEDLVKKTAVNIDEAVRELDPANMTPEDLWA 180
24B VQYFIGVQLDGSKHVEPVRNVIETAVKEGEDLVKKTAVNIDEAVRELDPANMTPEDLWA 180
24C VQYFIGVQLDGSKHVEPVRNVIETAVKEGEDLVKKTAVNIDEAVRELDPANMTPEDLWA 180
21D VQYFIGVQLDGSKHVEPVRNVIETAVKEGEDLVKKTAVNIDEAVRELDPANMTPEDLWA 180
*****

phot1 NHSKVVHCKPHRKDSPWIAIQKVLSEGEPIGLKHFKPVKPLGSGDTGSVHVELVGTDO 687
L2K NHSKVVHCKPHRKDSPWIAIQKVLSEGEPIGLKHFKPVKPLGSGDTGSVHVELVGTDO 240
24B NHSKVVHCKPHRKDSPWIAIQKVLSEGEPIGLKHFKPVKPLGSGDTGSVHVELVGTDO 240
24C NHSKVVHCKPHRKDSPWIAIQKVLSEGEPIGLKHFKPVKPLGSGDTGSVHVELVGTDO 240
21D NHSKVVHCKPHRKDSPWIAIQKVLSEGEPIGLKHFKPVKPLGSGDTGSVHVELVGTDO 240
*****

phot1 LFAMKAMDKAVMLNRNKVHRARAEREILDLLDHPFLPALYASFQTKTHICLITDYYPGGE 744
L2K LFAMKAMDKAVMLNRNKVHRARAEREILDLLDHPFLPALYASFQTKTHICLITDYYPGGE 300
24B LFAMKAMDKAVMLNRNKVHRARAEREILDLLDHPFLPALYASFQTKTHICLITDYYPGGE 300
24C LFAMKAMDKAVMLNRNKVHRARAEREILDLLDHPFLPALYASFQTKTHICLITDYYPGGE 300
21D LFAMKAMDKAVMLNRNKVHRARAEREILDLLDHPFLPALYASFQTKTHICLITDYYPGGE 300
*****

phot1 LFMLLDRQPRKVLKEDAVRFYAAQVVVALEYLHCQGIYRDLKPENVLIQNGDISLSDF 807
L2K LFMLLDRQPRKVLKEDAVRFYAAQVVVALEYLHCQGIYRDLKPENVLIQNGDISLSDF 360
24B LFMLLDRQPRKVLKEDAVRFYAAQVVVALEYLHCQGIYRDLKPENVLIQNGDISLSDF 360
24C LFMLLDRQPRKVLKEDAVRFYAAQVVVALEYLHCQGIYRDLKPENVLIQNGDISLSDF 360
21D LFMLLDRQPRKVLKEDAVRFYAAQVVVALEYLHCQGIYRDLKPENVLIQNGDISLSDF 360
*****

phot1 DLSCLTSCKPQLLIPSIDEKKKKKQKKSQQTPIFMAEPMRASNSFVGTTEEYIAPEIISGA 867
L2K DLSCLTSCKPQLLIPSIDEKKKKKQKKSQQTPIFMAEPMRASNSFVGTTEEYIAPEIISGA 420
24B DLSCLTSCKPQLLIPSIDEKKKKKQKKSQQTPIFMAEPMRASNSFVGTTEEYIAPEIISGA 420
24C DLSCLTSCKPQLLIPSIDEKKKKKQKKSQQTPIFMAEPMRASNSFVGTTEEYIAPEIISGA 420
21D DLSCLTSCKPQLLIPSIDEKKKKKQKKSQQTPIFMAEPMRASNSFVGTTEEYIAPEIISGA 420
*****

phot1 GHTSAVDWWALGILMYEMLYGYTPFRGKTRQKFTTNVLQKDLKFPASIPASLVQVKQLIFR 927
L2K GHTSAVDWWALGILMYEMLYGYTPFRGKTRQKFTTNVLQKDLKFPASIPASLVQVKQLIFR 480
24B GHTSAVDWWALGILMYEMLYGYTPFRGKTRQKFTTNVLQKDLKFPASIPASLVQVKQLIFR 480
24C GHTSAVDWWALGILMYEMLYGYTPFRGKTRQKFTTNVLQKDLKFPASIPASLVQVKQLIFR 480
21D GHTSAVDWWALGILMYEMLYGYTPFRGKTRQKFTTNVLQKDLKFPASIPASLVQVKQLIFR 480
*****

phot1 LLQRDPKKRLGCFEGANEVKQHSFFKGINWALIRCTNPPELETPIFSGEAENGEKVVDPE 987
L2K LLQRDPKKRLGCFEGANEVKQHSFFKGINWALIRCTNPPELETPIFSGEAENGEKVVDPE 540
24B LLQRDPKKRLGCFEGANEVKQHSFFKGINWALIRCTNPPELETPIFSGEAENGEKVVDPE 540
24C LLQRDPKKRLGCFEGANEVKQHSFFKGINWALIRCTNPPELETPIFSGEAENGEKVVDPE 540
21D LLQRDPKKRLGCFEGANEVKQHSFFKGINWALIRCTNPPELETPIFSGEAENGEKVVDPE 540
*****

phot1 LEDLQTNVF 996
L2K LEDLQTNVF 549
24B LEDLQTNVF 549
24C LEDLQTNVF 549
21D LEDLQTNVF 549
*****

```

**Figure 5.4: The L2K protein is wild-type in the 24B, 24C, and 21D mutants.** Clustalw alignment of the translated L2K DNA sequence is shown. Asterisks indicate identical amino acids. The L2K transgene of the unmutagenized L2K line (“L2K” sequence) and the three EMS mutants was amplified by PCR from genomic DNA and cloned. The L2K region of wild-type phot1 is shown as a reference. Amino acid numbering is that of either full-length phot1 (phot1) or that of L2K (L2K, 24B, 24C, 21D).

### 5.2.3 Rosette phenotypes and biomass accumulation of the EMS mutants

As mature plants, each of the EMS mutants isolated from the screen exhibited phenotypes that were quite distinct from the others (Figure 5.5A). The 24C and 21D mutants both possessed long petioles, a phenotype not exhibited by the 24B mutant, which had an overall appearance similar to that of the L2K parent. When viewed from the side, the 24C and 21D mutants had raised petioles even though they were grown under white light at a fluence rate of  $100 \mu\text{mol m}^{-2} \text{s}^{-1}$ , a fluence rate at which the petioles of the other lines were not raised (Appendix Figure 5.1). Although the 24C and 21D mutants had similar petiole phenotypes, the mutants could be distinguished from each other by their leaf size and morphology. The 24C mutant had flat leaves that were much smaller than wild type, whereas the 21D mutant had larger leaves than 24C which wrinkled at the tips (Figure 5.5A). Additionally, though it was not quantified, the 24C mutant appeared to be more vertically elongated than the other mutants from the screen, possibly due to longer internodes (Appendix Figure 5.1). These differing phenotypes suggested that the underlying mutations leading to altered petiole positioning in each of the three mutants could be independent.

The observed differences in size of the EMS mutants was quantified by measuring biomass accumulation after four weeks of growth. Their fresh weights correlated with their appearance, with the small-leafed 24C mutants having a weight even lower than that of the *phot1phot2* double mutant (Figure 5.5B). The 21D mutant was able to accumulate more biomass than *phot1phot2* and 24C but had only approximately half the fresh weight of L2K. The 24B mutant, which had an overall appearance indistinguishable from that of L2K, also had a similar fresh weight to its L2K parent. Due to the contribution of *phot1* to stomatal opening (Kinoshita *et al.*, 2001), dry weight was also quantified with the hypothesis that the increased sensitivity observed for petiole positioning may increase stomatal opening as well, leading stomata to be open a greater proportion of time than the L2K parent and causing increased water loss through transpiration. This seems not to be the case, however, because

dry weight amounted to approximately one-tenth of the fresh weight for each line tested, demonstrating that water loss was not increased in the EMS mutants (Figure 5.5B).

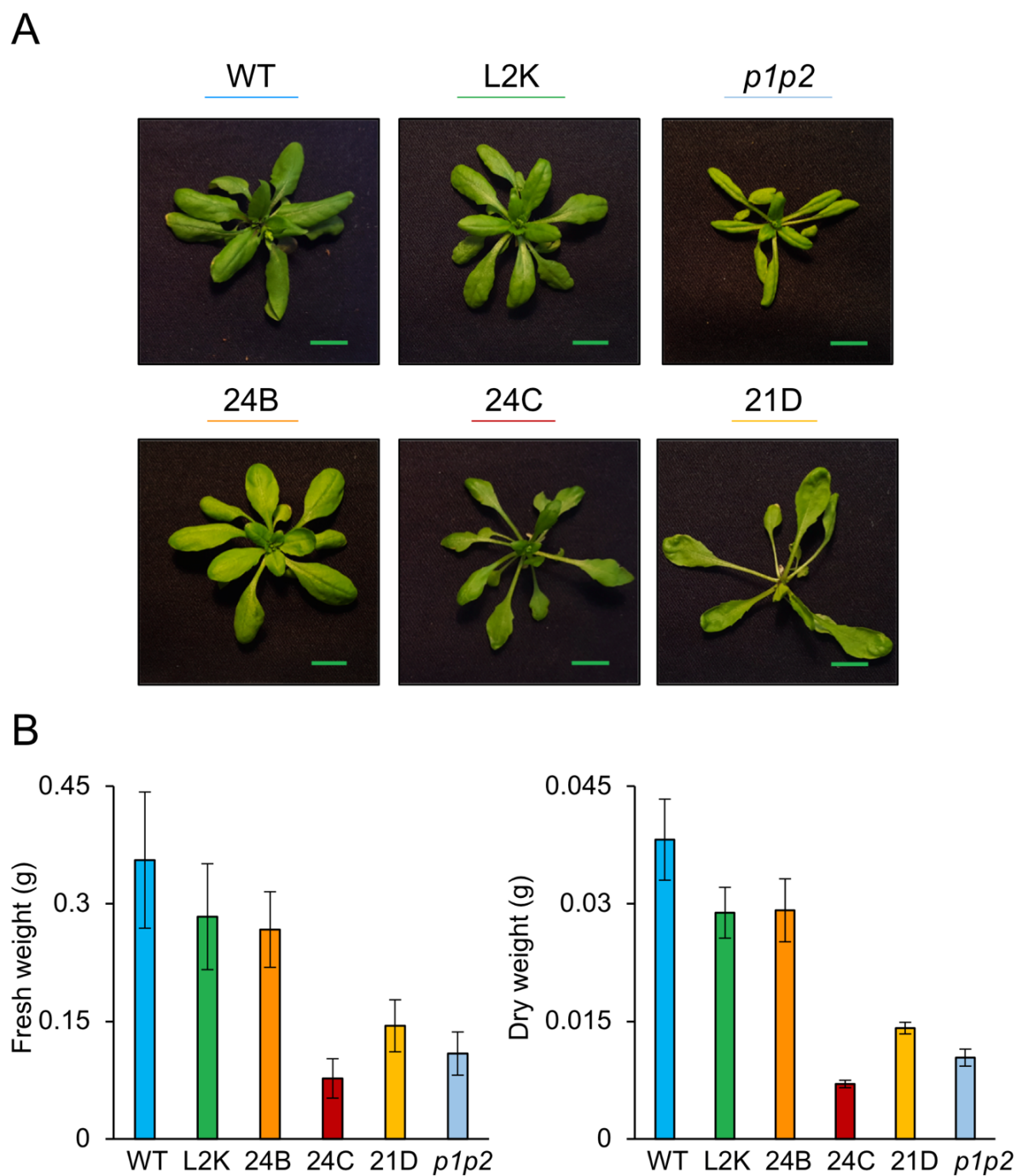


**Figure 5.5: Rosette phenotypes and fresh and dry weights of the EMS mutants.** **A.** Rosette phenotypes of the 24B, 24C, and 21D EMS mutants grown along with wild-type plants (WT), the L2K parental line, and the *phot1phot2* (*p1p2*) double mutant for four weeks under  $100 \mu\text{mol m}^{-2} \text{s}^{-1}$  white light in long day conditions. Representative images are shown; the scale bar is 1 cm. **B.** Fresh and dry weights of the EMS mutants at four weeks. The mean of two independent experiments is shown; the error bars are the standard error of the mean.

### 5.2.4 The 24B and 24C mutants have increased sensitivity for phototropism

To investigate whether the enhanced sensitivity for petiole positioning observed in the EMS mutants extended to other NPH3-dependent responses, the phototropic response of each of the mutants was probed. Initially, the mutants were tested with  $0.5 \mu\text{mol m}^{-2} \text{s}^{-1}$  blue light as the phototropic stimulus, a fluence rate to which wild-type seedlings respond very well but L2K seedlings do not (Figure 5.1A). The 24C mutant was able to perform phototropism at this fluence rate (Figure 5.6A). Interestingly, 24C seedlings showed an initial rate of response that was noticeably faster than that of wild type, though by the end of the four-hour experiment, its response began to level off, achieving a final angle of around 25 degrees, which was reduced from the final angle of wild type seedlings, at 60 degrees, but much stronger than that of the L2K parental line and the other EMS mutants, which only showed around 7 degrees of curvature (Figure 5.6A). When phototropism was conducted on the mutants using  $10 \mu\text{mol m}^{-2} \text{s}^{-1}$  blue light, an intensity to which L2K can respond, 24C and 24B were both able to produce more robust curvatures than the L2K parent, with each line reaching more than 40 degrees of curvature, while L2K had a mean final angle of 27 degrees (Figure 5.6A). Surprisingly, though 24B did not respond to the lower-intensity phototropic stimulus, the curvatures of the 24B and 24C mutants were indistinguishable from each other under the stronger light stimulus. For both mutants, the kinetics of the response to  $10 \mu\text{mol m}^{-2} \text{s}^{-1}$  blue light was faster than wild type at the onset of the experiment (Figure 5.6A). The 21D mutant behaved similarly to L2K under both light regimes, suggesting that its increased sensitivity may be specific to petiole positioning (Figure 5.6A).

It was then hypothesized that the increased sensitivity in the 24B and 24C mutants may result in increased NPH3 dephosphorylation in those mutants relative to the L2K transgenic line. Both the L2K and 21D lines did not show NPH3 dephosphorylation after treatment with  $20 \mu\text{mol m}^{-2} \text{s}^{-1}$  overhead blue light (Figure 5.6B). However, with the same treatment, NPH3 dephosphorylation was clearly visible in the 24B mutant and in the 24C mutant, NPH3 was completely dephosphorylated, with the phosphorylated state of NPH3 no longer detected by the antibody (Figure 5.6B). The increased pool of dephosphorylated NPH3 in the 24B and 24C mutants implies that the increased sensitivity in these mutants most likely extends to all of the NPH3-dependent phot1-mediated responses and not to just petiole positioning and phototropism.

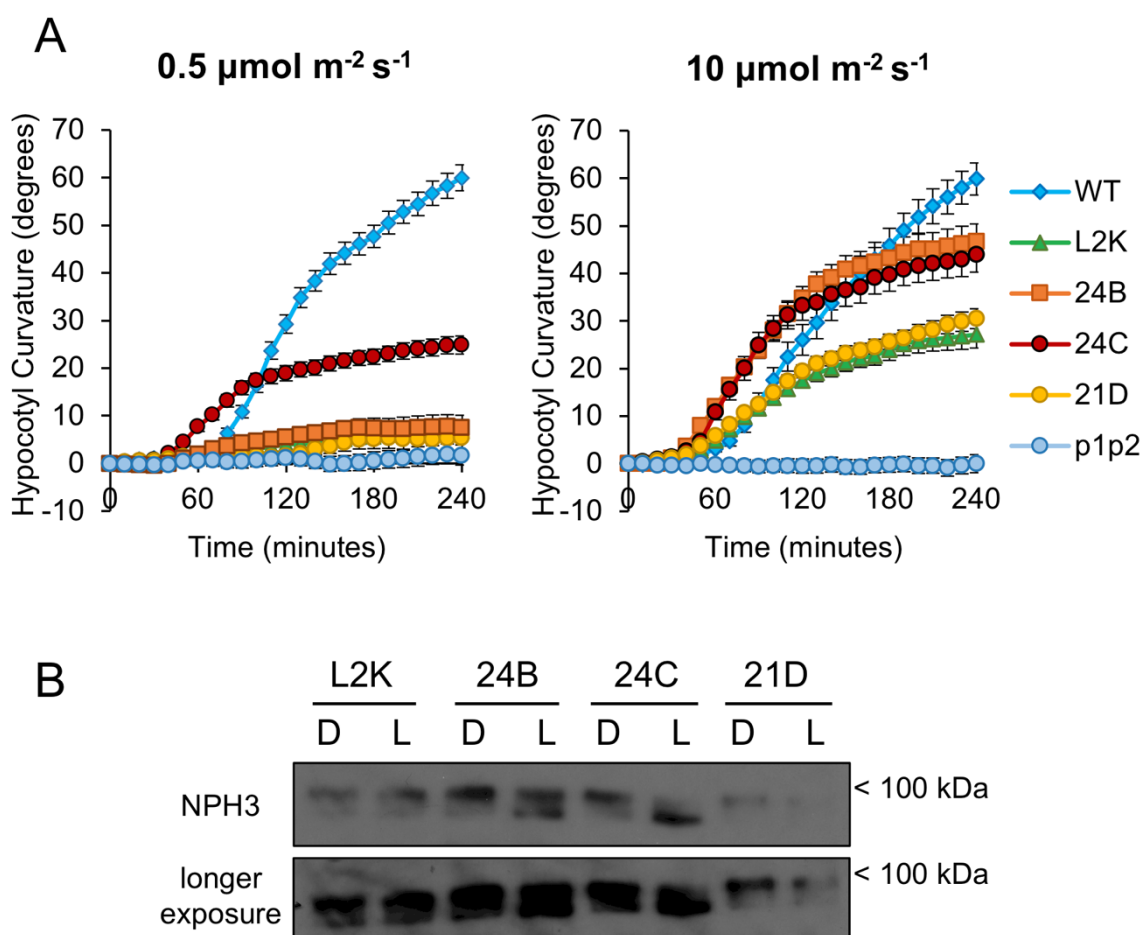


**Figure 5.6: The 24B and 24C mutants show increased sensitivity to blue light.** **A.** Phototropism of freestanding three-day-old etiolated seedlings at fluence rates of 0.5  $\mu\text{mol m}^{-2} \text{s}^{-1}$  and 10  $\mu\text{mol m}^{-2} \text{s}^{-1}$  blue light. Hypocotyl curvature was measured every 10 minutes. Data shown is the mean of around 30 seedlings of the wild type (WT), L2K parental line, 24B, 24C, 21D, and *phot1phot2* (*plp2*) genotypes from three independent experiments, except for the data for 24C and *plp2* at 10  $\mu\text{mol m}^{-2} \text{s}^{-1}$ , which is the mean of 20 seedlings from two experiments. Error bars are standard error of the mean. **B.** NPH3 dephosphorylation in the EMS mutants. Protein extracts were harvested either in the dark (D) or following blue light treatment at 20  $\mu\text{mol m}^{-2} \text{s}^{-1}$  for 15 minutes (L). Two exposures of the same western blot are shown for clarity. This experiment was performed three times independently; a representative blot is shown.

### 5.2.5 The 24C mutant is vertically oriented under low blue light

When seedlings are grown under monochromatic blue light from above, phot activity is responsible for maintaining vertical growth against the gravity vector (Lariguet and Fankhauser, 2004). Low, monochromatic blue light is perceived by the phytochrome A (phyA) photoreceptor as well as *phot1*; it was proposed that the activation of phyA leads to an inhibition of gravitropism, leaving *phot1* to maintain upward growth through phototropism (Lariguet and Fankhauser, 2004). PhyA is upstream of *phot1* in this pathway, since *phyA phot1* double mutants remain erect under monochromatic blue, whereas the single *phot1-5* mutants orient randomly (Lariguet and Fankhauser, 2004). Similarly, phyA positively enhances phototropism in seedlings given a red light treatment prior to phototropic

stimulus, also likely through inhibiting the gravitropic pathway (Briggs and Chon, 1966; Parks, Quail and Hangarter, 1996; Kim *et al.*, 2011; Kami *et al.*, 2012; Sullivan *et al.*, 2016).

Under low blue light, it was expected that L2K would be unable to properly orient itself against the gravity vector, but that perhaps the EMS mutants would be able to grow vertically due to their increased sensitivity to low-intensity light. To test this hypothesis, seedlings were grown under  $1 \mu\text{mol m}^{-2} \text{s}^{-1}$  overhead blue light for four days, at the end of which the deviation from vertical of each seedling was quantified. As anticipated, the fluence rate of blue light was too low for the L2K line or the *phot1-5* mutant to orient vertically (Figure 5.7). Proper orientation against the gravity vector was restored in the 24C mutant, while 24B and 21D remained randomized, demonstrating the increased sensitivity of the 24C mutant relative to L2K for this response (Figure 5.7). This closely reflects the phototropic responsiveness of the EMS mutants, where 24C was the most sensitive of the mutants to the unilateral  $0.5 \mu\text{mol m}^{-2} \text{s}^{-1}$  blue light stimulus. When the seedlings were grown under an increased light intensity of  $20 \mu\text{mol m}^{-2} \text{s}^{-1}$  blue light, the L2K line, *phot1-5*, and 24B were able to orient vertically (Appendix Figure 5.2). Curiously, the 21D mutant remained agravitropic under the higher light conditions (Appendix Figure 5.2).

If gravitropic growth is mediated by *phot1* under low blue light through the phototropism pathway, it seemed strange that the 21D mutant was unable to grow vertically under  $20 \mu\text{mol m}^{-2} \text{s}^{-1}$  blue light but could perform phototropism when stimulated with  $10 \mu\text{mol m}^{-2} \text{s}^{-1}$  blue light. Furthermore, phototropism is typically characterized by a response to a horizontal light stimulus, not to light coming from above the plant. To address these discrepancies, the orientation under low blue light of the *nph3-6* and *root phototropism 2 (rpt2-2)* mutants was probed. NPH3 and RPT2 are related proteins in the NRL (NPH3 and RPT2-like) family that are important for transducing many *phot1* responses (Christie *et al.*, 2017). As previously discussed, NPH3 is essential for phototropism, while RPT2 is also required except under fluence rates less than  $\sim 0.002 \mu\text{mol m}^{-2} \text{s}^{-1}$  (Haga *et al.*, 2015). Our findings indicated that neither RPT2 nor NPH3 was required for this orientation response, since the majority of seedlings were able to orient vertically, though randomization was somewhat increased in the two mutant backgrounds relative to wild-type seedlings (Appendix Figure 5.3). Since phototropism depends on the presence of NPH3, the vertical orientation of seedlings under low blue light cannot be operating through the phototropism pathway. The vertical orientation of seedlings under low blue light is *phot1*-dependent but not a true phototropic response, partly explaining the reason that the 21D mutant can complement high light

phototropism but not vertical orientation. In the EMS mutants studied here, vertical orientation is enhanced specifically in the 24C mutant, extending the increased sensitivity of 24C beyond phot1 responses dependent upon NPH3 for signal transduction.

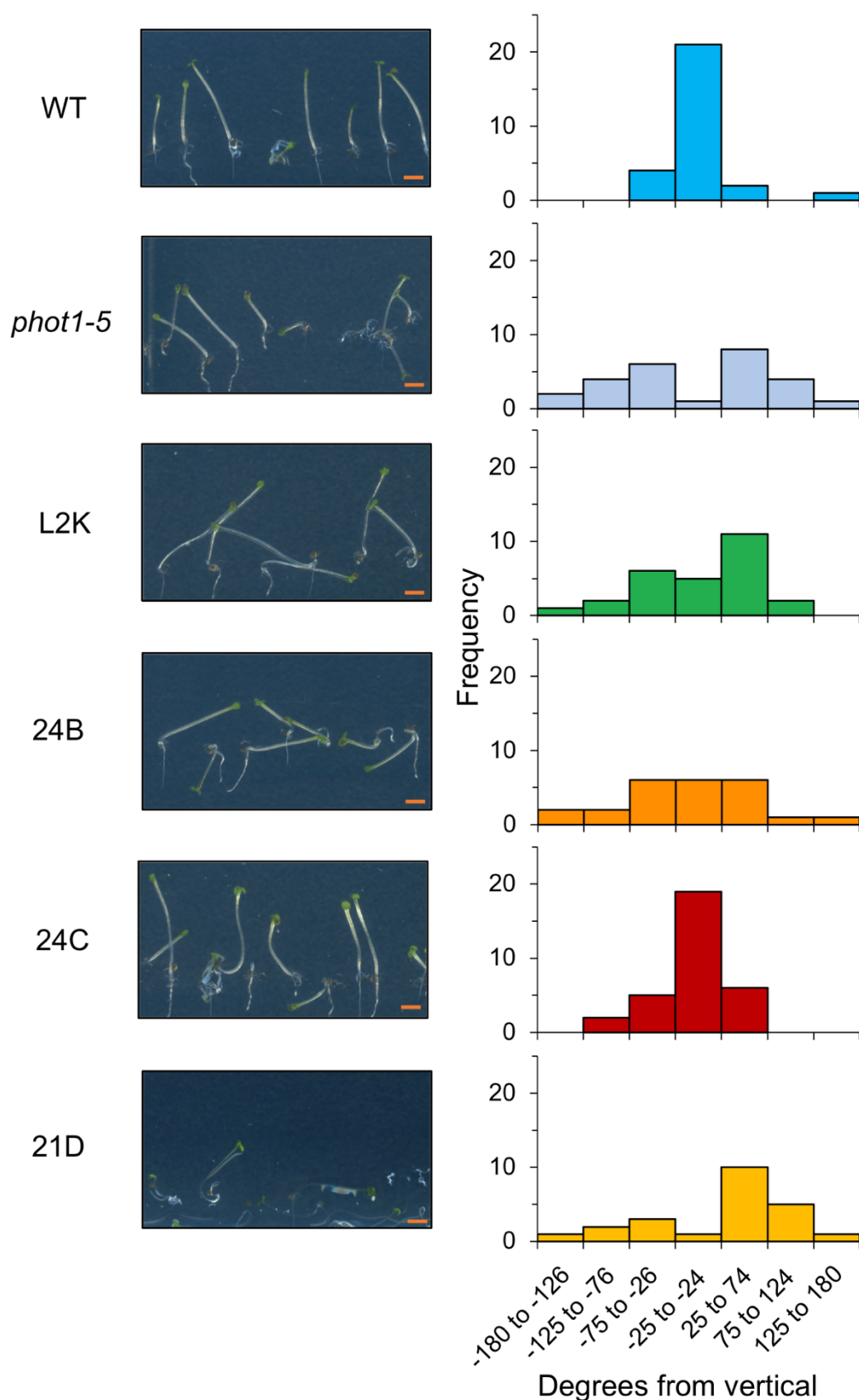


**Figure 5.7: Gravotropism is altered by differential sensitivity in the EMS mutants.** Wild-type (WT), L2K, *phot1-5*, and the 24B, 24C, and 21D EMS mutant seedlings were grown on vertical half-strength MS agar plates under  $1 \mu\text{mol m}^{-2} \text{s}^{-1}$  overhead blue light for four days and then imaged to quantify the angle of each seedling. The histograms show the distribution of seedling deviation from vertical for each genotype. One representative experiment is displayed from three independent repeats. Representative images are shown; scale bar is 2 mm.

## 5.2.6 The 24C mutant overexpresses the L2K protein

To further characterize the EMS mutants, the expression of the L2K protein in each mutant background in three-day-old etiolated seedlings was examined. While the 21D mutant displayed protein levels that approximated that of the L2K parent, the 24B mutant had slightly elevated expression and the 24C mutant had 14.6-fold higher protein levels than the L2K parent (Figure 5.8A). To date, full-length phot1 has not been constitutively overexpressed *in planta*, with 35S driven full-length phot1 possessing only moderately higher protein levels than L2K (Figure 5.8A). However, photoreceptor overexpression has been shown to enhance sensitivity in both phytochromes (Boylan and Quail, 1991; Wagner et al., 1991) and cryptochromes (Lin et al., 1998; Giliberto *et al.*, 2005). The enhanced sensitivity that the 24C mutant exhibited for petiole positioning (Figure 5.3), phototropism (Figure 5.6), and gravitropic orientation under low blue light (Figure 5.7) therefore seemed attributable to the overexpression of the L2K protein.

Following the characterization of protein levels in the EMS mutants, *L2K* transcript levels was compared between them by performing qPCR on cDNA synthesized from the mRNA of three-day-old etiolated seedlings to see whether the differences in protein expression for the 24C mutant could be attributed to corresponding alterations in transcript abundance. Primers specific to the 3' end of the phot1 gene were used so that the same set of primers could be used for L2K, which is truncated at the 5' end, and full-length phot1. As expected, the 21D mutant showed similar *L2K* transcript levels to its L2K parent, while the 24B mutant levels were just slightly elevated (Figure 5.8B). The 24C mutant showed the highest transcript levels of the lines tested, with approximately a four-fold increase in *L2K* transcript relative to the L2K transgenic line (Figure 5.8B). Although the L2K protein was overexpressed in the 24C background, it seemed that the increase in *L2K* transcript, while elevated relative to the other lines, was more modest than its high levels of L2K protein expression.

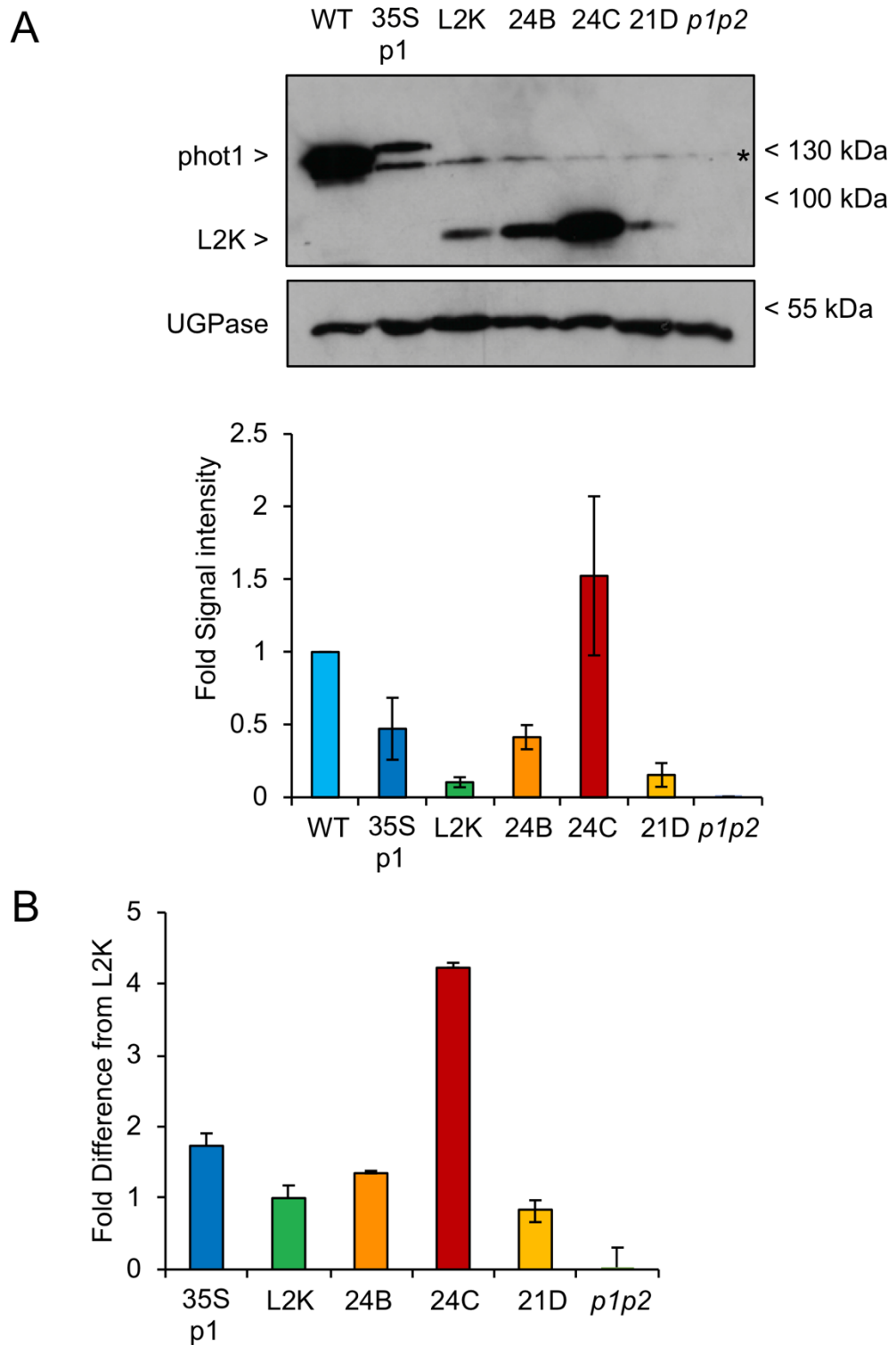


**Figure 5.8: The 24C mutant has increased L2K protein and transcript levels.** **A.** Abundance of L2K and phot1 protein in 3-day-old etiolated seedlings. “35S p1” is full-length phot1 expressed on the 35S promoter. Asterisk indicates a non-specific band. The blot was probed both with the C-terminal phot1 antibody and with UGPase as a loading control. The signal intensities of three biologically independent repeats were quantified using the ImageJ gel analyzer and normalized against UGPase to control for loading; the mean and standard error is shown. Protein levels were compared against full-length phot1 expression in wild-type plants; **B.** L2K and PHOT1 transcript levels in 3-day-old etiolated seedlings. The mean of two biologically independent qPCR experiments is shown. Transcript levels were compared using the standard curve method using *ISU1* as the housekeeping gene, and the transcript expression of each genotype was compared to that of the L2K transgenic line; error bars are standard error of the mean.

It was not clear whether the four-fold elevation in transcript levels observed for the 24C mutant was sufficient to lead to a nearly 15-fold increase in protein expression. It therefore seemed possible that the L2K protein accumulated to levels in the 24C background that could not be ascribed to the increase in *L2K* transcript alone. Phot1 protein is light-labile, with its abundance diminishing over time with prolonged irradiation with intense blue light (Sakamoto and Briggs, 2002; Sullivan *et al.*, 2010; Roberts *et al.*, 2011; Preuten *et al.*, 2015); L2K is also turned over similarly, though the kinetics of the response may be different (Figure 5.9). To test whether the accumulation of the L2K protein in the 24C background was due to increased stability, the 24C mutant was subjected to the same protein turnover experiment. Although the L2K protein expression in the 24C mutant in the dark is very high, it showed a protein turnover pattern similar to that of full-length phot1 (Figure 5.9). The mechanism through which the lesion(s) in the 24C background affect L2K protein expression therefore does not seem to be through the process that regulates phot1 protein levels over the course of a strong light treatment.

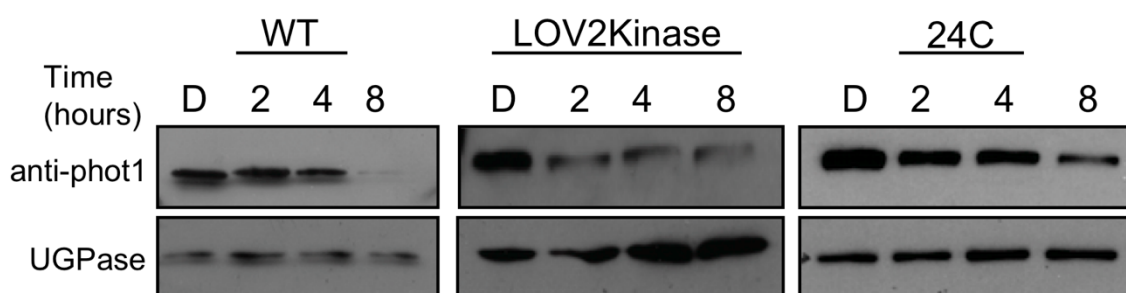


**Figure 5.9: Light-induced turnover of the L2K protein in the 24C mutant background is not altered.** Western blots of full-length phot1 and L2K protein levels over the course of blue light treatment probed with the C-terminal phot1 antibody and UGPase as a loading control. Protein extracts were either harvested from three-day-old etiolated seedlings in the dark (D) or after two, four, or eight hours of illumination with  $150 \mu\text{mol m}^{-2} \text{s}^{-1}$  of blue light from above. Representative results from three independent repeats are shown.

### 5.2.7 L2K is an active kinase in the 24C mutant background

Although L2K can complement phot1 responses, its kinase activity *in planta* has not yet been directly verified. The truncation of phot1 that engendered the L2K protein eliminated many phosphorylation sites that reside in the extreme N-terminus of the protein as well as linker region between LOV1 and LOV2, preventing a visible autophosphorylation-induced electrophoretic mobility shift of L2K upon light treatment (Sullivan *et al.*, 2008). Likewise, due to the relatively poor expression of L2K in etiolated seedlings (as in Figure 5.8B), its

autophosphorylation activity could not be detected when microsomal membrane extracts from etiolated seedlings were exposed to  $\gamma$ - $^{32}$ P-ATP as a phosphodonor (Sullivan *et al.*, 2008). In the 24C mutant, however, low expression of the L2K protein is not an issue (Figure 5.8B), making 24C a good background in which to verify the light-induced kinase activity of the L2K protein. As expected, in a preliminary study the L2K protein in the 24C mutant background showed light-induced autophosphorylation activity in microsomal membranes harvested from etiolated seedlings (Figure 5.10). The activity of wild-type L2K in this experiment could not be assessed due to a loading issue (Figure 5.10). The difference in the amount of  $\gamma$ - $^{32}$ P incorporation between the dark and light, though clear, appears to be smaller in magnitude in the 24C mutant than in full-length phot1, which is perhaps due to the missing phosphorylation sites in L2K, preventing the level of  $\gamma$ - $^{32}$ P incorporation observed in full-length phot1. Regardless, in the 24C mutant background the L2K protein exhibits clear light-induced autophosphorylation activity, demonstrating for the first time that L2K is an active kinase *in planta*.

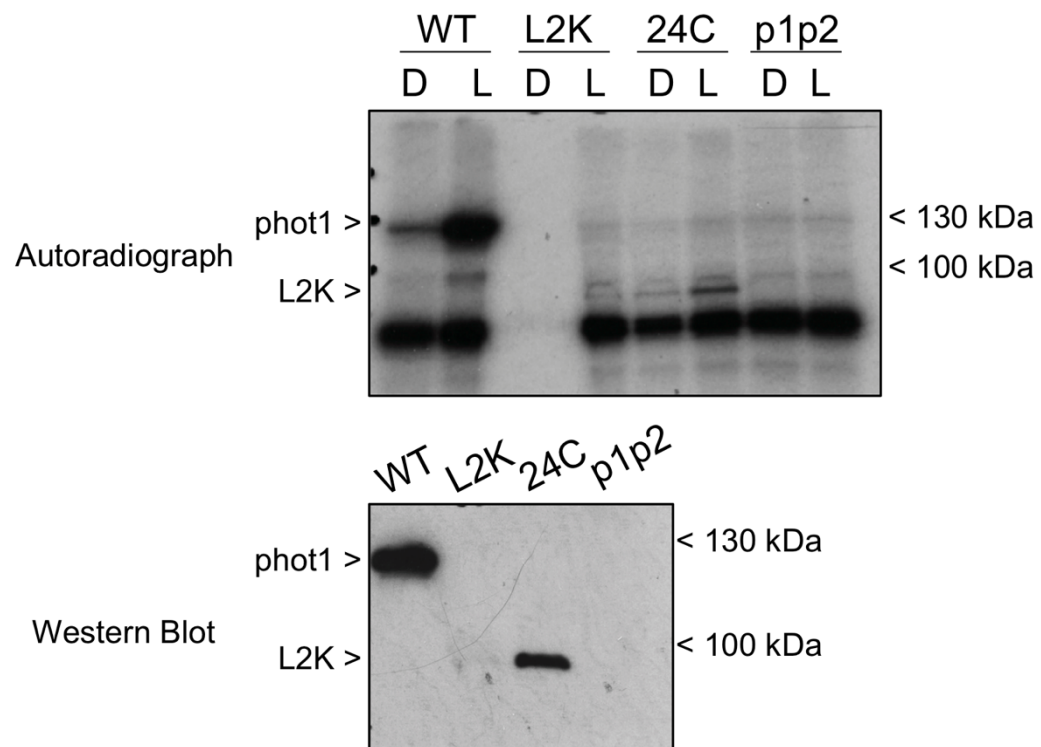


**Figure 5.10: The L2K protein 24C mutant background shows *in vitro* kinase activity.** Microsomal membranes were harvested from three-day-old etiolated seedlings. Ten micrograms of microsomal membrane extracts were exposed to  $\gamma$ - $^{32}$ P-ATP either in the dark (D) or with a 10 second pulse of white light (L). The western blot shows the equivalent amount of protein extract from the samples left in darkness separated on a second SDS-PAGE gel and probed with the C-terminal phot1 antibody to show protein expression. This experiment was performed one time.

### 5.2.8 The 24C and 21D mutants have a long hypocotyl phenotype specific to red light

During the course of the petiole positioning screen, it was observed that both the 24C and 21D mutants appeared to have longer hypocotyls than the other mutants in the EMS population (Figure 5.3). Additionally, both mutants showed longer petioles as mature plants than the other lines (Figure 5.5A). Both of these phenotypes can be associated with defects in red light signaling through the action of phytochrome photoreceptors (Nagatani *et al.*, 1991; Reed *et al.*, 1993). To test whether red light signaling is impaired in 24C and 21D, hypocotyl elongation assays were conducted in darkness and under monochromatic red, far-red, and blue light. Confirming the observations from the screen, the 24C and 21D mutants exhibited long hypocotyl phenotypes that were specific to red light, suggesting that in both lines, the underlying EMS-introduced mutations were likely linked to phytochrome signaling (Figure 5.11). Further narrowing the possibilities, the long hypocotyl phenotype was observed under red, but not far-red, light. This eliminated *PHYA* as a candidate gene since *phyA* is the only phytochrome responsible for inhibition of hypocotyl elongation in monochromatic far-red light (Nagatani, Reed and Chory, 1993; Parks and Quail, 1993; Whitelam *et al.*, 1993). Because *phyB* is the primary phytochrome acting in light-grown plants (Smith, 2000), it seemed probable that the 24C and 21D mutants were mutants either in *PHYB* itself or of a gene involved in the *phyB* signalling pathway.

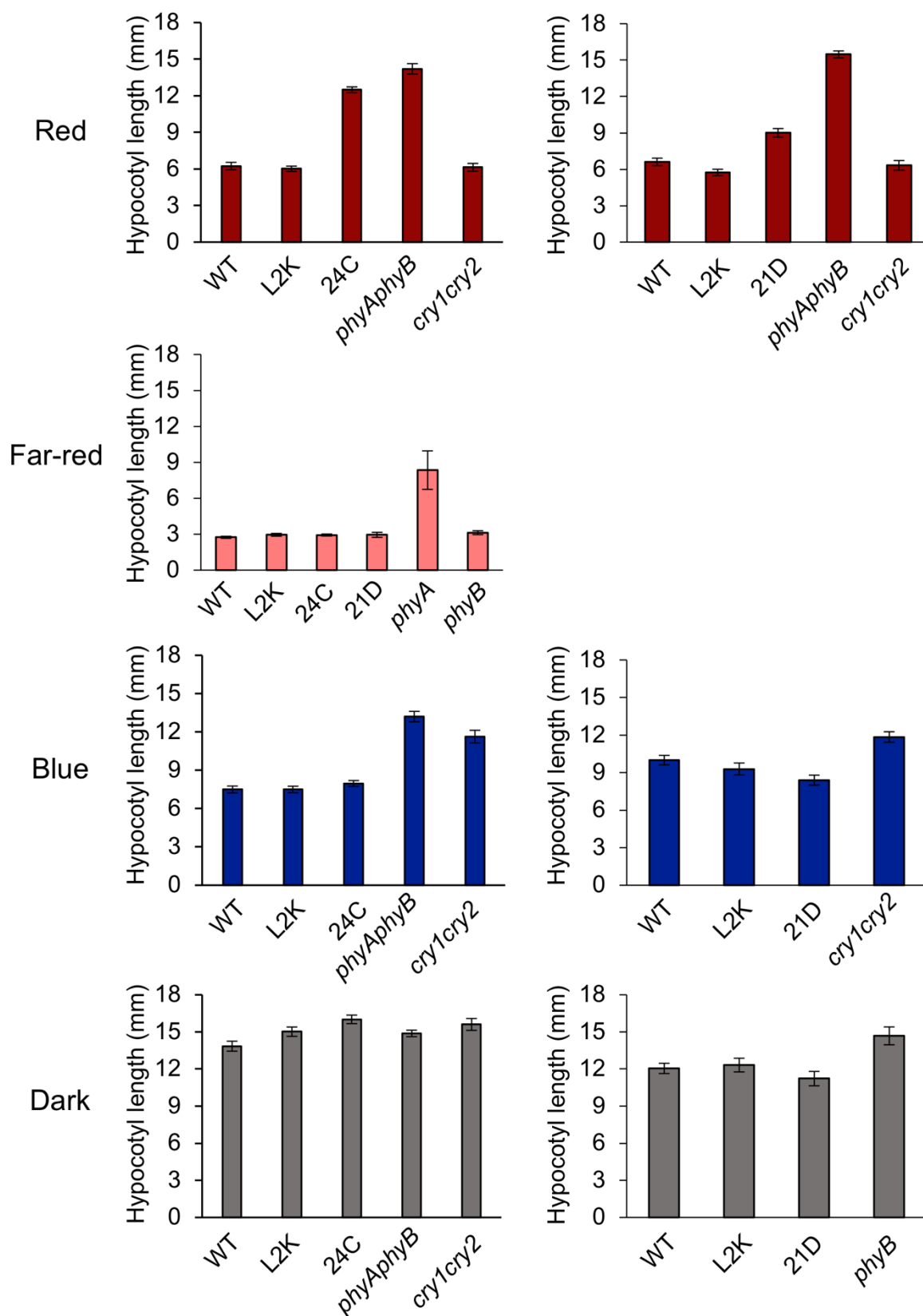


**Figure 5.11: The 24C and 21D mutants have long hypocotyls in red light.** Wild-type (WT), L2K, and the indicated mutant seedlings were grown vertically on half-strength MS agar plates under  $1 \mu\text{mol m}^{-2} \text{s}^{-1}$  of continuous red, blue, or far-red light or in darkness for four days and then imaged to quantify hypocotyl length for each genotype. The mean of one representative experiment using 20-40 seedlings out of three independent repeats is shown; error bars are standard error of the mean.

### 5.2.9 The 24C and 21D mutants both encode the same mutant allele of *PHYB*

The hypocotyl elongation results sparked a more detailed investigation, leading to examination of phyA and phyB protein expression in etiolated seedlings in the EMS mutants. PhyA levels were the same between the L2K line and all of the EMS mutants, but phyB was downregulated specifically in the 24C and 21D mutants, consistent with the hypocotyl elongation phenotypes of those mutants (Figure 5.12A). To uncover whether this downregulation was the result of mutation to *PHYB* itself, the entire *PHYB* gene was cloned from genomic DNA from L2K and the 24C and 21D mutants. The sequence data revealed that 24C and 21D, but not the L2K parent, encode the mutation W813R in the phyB PAS2 domain, which represents a novel allele of *PHYB* (Figure 5.12B). In the predicted structure of phyB PAS2, the W813 residue is expected to reside in the middle of a single, central beta strand within the domain (Figure 5.12C), a position at which placing a positively charged arginine residue is likely to be highly disruptive to the overall structure of the domain, possibly impacting phyB function as a whole. This W813R mutation therefore seemed to be the cause of the elongated hypocotyl, long petioles, and reduced phyB protein levels in the 24C and 21D EMS mutants.

When the 24C and 21D mutants were crossed against each other in an allelism test, the resulting progeny all showed the same exaggerated petiole angle and elongated hypocotyl phenotype as observed for each of the individual mutants, further confirming that the two mutants were allelic for the *PHYB* mutation (Appendix Figure 5.4). Furthermore, the 24C mutant was found to be allelic to the *phyB-9* null mutant (Appendix Figure 5.4). Given the different phenotypes of adult 24C and 21D plants (Figure 5.5A) as well as the clear differences in L2K protein expression between the two mutants (Figure 5.8B), it was very surprising that each showed an identical mutation within *PHYB*. Furthermore, though the two mutants were allelic for the petiole positioning response, the 24C mutant consistently exhibited a gain in sensitivity for phot1 responses that 21D did not (Figures 5.6 and 5.7). These observations suggested that the 24C mutant may have a second lesion besides the *PHYB* mutation that led to the increased sensitivity of L2K in the 24C background, while the 21D mutant may only have the phyB mutation underlying its enhanced petiole positioning.

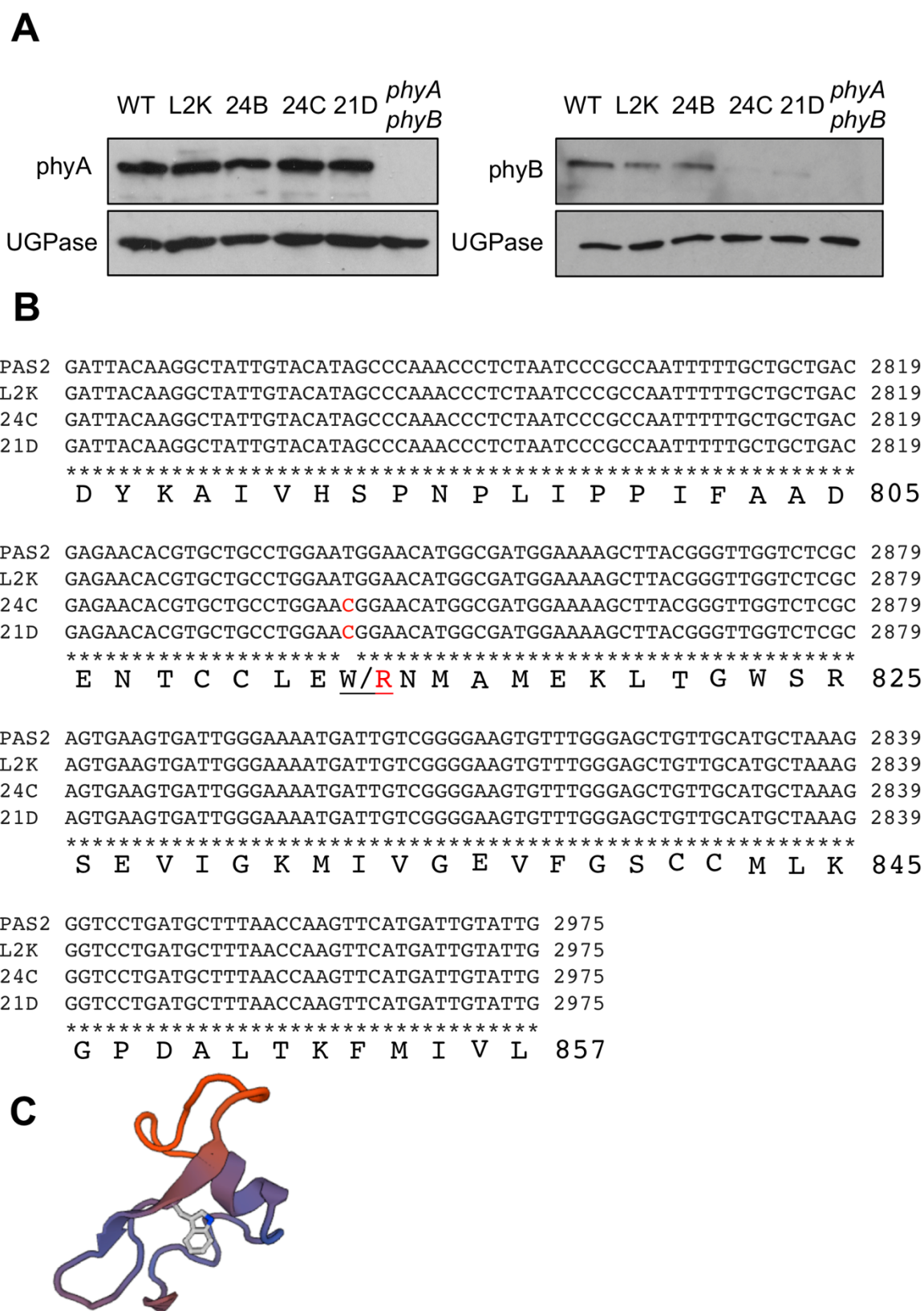


**Figure 5.12: *PHYB* is mutated in the 24C and 21D mutants.** **A.** Western blot analysis of phyA and B protein levels in three-day-old etiolated seedlings. UGPase is shown as a loading control. **B.** Clustalw alignment of the phyB PAS2 domain DNA sequence of wild-type phyB (PAS2), L2K, and the 24C and 21D mutants with the predicted amino acid sequence shown at bottom. Numbering is from *PHYB* genomic DNA and the full-length phyB amino acid sequence, respectively. Red letters indicate the mutated bases. **C.** The predicted SwissModel structure of the phyB PAS2 domain indicating the position of W813 in gray.

### 5.2.10 Inheritance of the suppressor phenotypes

If a second mutation was indeed present in the 24C background, leading to L2K overexpression and its gain in sensitivity, there was no immediately apparent candidate gene the second mutation could affect. The same was true of the 24B mutant, which aside from its increased sensitivity relative to the L2K parent for petiole positioning and phototropism, had no phenotype that could point to obvious suppressors. To isolate any single nucleotide polymorphisms (SNPs) that may account for the observed suppressor phenotypes, the mutant lines were prepared for deep genomic sequencing. Each of the EMS mutant lines was backcrossed against the L2K parent to eliminate some of the non-specific EMS-introduced SNPs. The parental L2K line was utilized for the crosses because crossing the mutants into a genetic background encoding full-length *phot1* could result in a loss of the suppressor phenotype, since the original petiole positioning screen depended on the lowered sensitivity of L2K.

In the first generation following the parental backcross, the vast majority of the seedlings had a L2K-like petiole positioning phenotype, suggesting a recessive inheritance pattern for each mutant (Table 5.1). The F<sub>1</sub> individuals were then allowed to self-pollinate, and in the following F<sub>2</sub> generation, the crosses between 24B and L2K as well as 21D and L2K exhibited segregation ratios of lowered petioles to raised petioles that were not significantly different from 3:1 by chi-square test ( $p > 0.05$ ), a segregation pattern typical of Mendelian segregation of a single recessive locus (Table 5.2).

Cross	Raised Petioles	Total Seedlings	Percent L2K-like
L2K	2	120	98.3333
24C and L2K	6	65	90.7692
21D and L2K	17	88	80.6818
24B and L2K	0	22	100

**Table 5.1 Petiole positioning in F<sub>1</sub> seedlings from the crosses between the L2K transgenic line and the EMS mutants.** Crosses were made in both directions, using both L2K and the EMS mutant of interest as the female parent at least once. The resulting seedlings were then scored for their petiole positioning phenotype as described in Figure 5.3. Data shown is pooled from crosses that were made in each direction. This experiment was performed twice.

	24B and L2K	24C and L2K	21D and L2K
Raised petioles	148	569	124
Total Seedlings	622	1753	436
%Raised	23.7942	32.4586	28.4404
Chi-square value	0.4202	51.6146	2.5719
Significantly different from 3:1	No; $p > 0.05$	Yes; $p < 0.001$	No; $p > 0.05$

**Table 5.2: Petiole positioning in F<sub>2</sub> seedlings from crosses between the L2K transgenic line and the EMS mutants.** Table indicates the petiole positioning phenotype of the generation following the F<sub>1</sub> individuals in Table 5.1. The segregation ratios were examined using a chi-square test with a Yates correction for experiments with one degree of freedom; the critical value for a significance level at  $p = 0.05$  is 3.84 and 10.83 for  $p = 0.001$ . The 24B and 21D crosses against L2K did not display a segregation pattern significantly different from the expected 3:1 ratio ( $p > 0.05$ ), while the 24C mutant crosses did ( $p < 0.001$ ). Segregation was analyzed once for the 24B and 21D crosses and twice for the 24C crosses.

The backcross of the 24C mutant against the L2K parent exhibited a segregation in the F<sub>2</sub> generation for petiole positioning that was significantly different from the 3:1 ratio of the other mutants ( $p < 0.05$ ; Table 5.2). The non-Mendelian inheritance of the raised petiole phenotype seemed consistent with the hypothesis that more than one mutation leads to the petiole positioning phenotype in the 24C mutant. Since the 24C mutant encodes a mutant *PHYB* allele, but also has increased sensitivity for phot1 responses due to L2K overexpression, it was hypothesized that in the segregating population of 24C crossed against L2K three distinct phenotypes should be observed: a L2K-like phenotype with a short hypocotyl and lowered petioles, a *PHYB*-like phenotype with a long hypocotyl and raised petioles, and a phenotype consisting of a short hypocotyl and raised petioles (called SR for Short and Raised) that is due to a gain in sensitivity conferred by L2K overexpression but not through mutation to *PHYB*. It was also predicted that any individuals that possessed both the *PHYB* mutation and the overexpressing mutation would be indistinguishable from the *PHYB* mutants, since both would exhibit raised petioles and long hypocotyls. Therefore, while Mendelian segregation of two independent loci typically yields a 9:3:3:1 segregation pattern, the phenotypes would be predicted to segregate in a 9:3:4 pattern of L2K-like: SR: *PHYB*-like due to the masking effect. The phenotypes of a large number of F<sub>2</sub> seedlings from crosses between 24C and L2K were scored to test whether the segregation pattern matched the predicted 9:3:4 ratio. A chi-square test led to a rejection of the hypothesis that the population was segregating in a 9:3:4 fashion; approximately 19% of all the individuals were expected to have the SR phenotype, but only around 5% were identified as SR (Table 5.3). The identification of SR individuals in the population was an encouraging sign that the *PHYB* mutation could be isolated from the SR causal mutation, though the two lesions did not appear to be segregating in a straightforward Mendelian manner.

	24C and L2K
L2K-like phenotype	708
<i>PHYB</i> -like phenotype	337
S&R phenotype	58
Total plants	1103
%S&R	5.2584
Chi-square value	46.0399
Significantly different from 9:3:4	Yes; $p < 0.001$

**Table 5.3: Segregation of petiole positioning and hypocotyl elongation in F<sub>2</sub> seedlings from crosses between the L2K transgenic line and 24C mutants.** Table results from the re-scoring of phenotypes in the 24C mutants of T<sub>2</sub> individuals in Table 2. “SR” is the “short and raised” phenotype, which is expected phenotype corresponding to mutants containing the SNP leading to L2K overexpression but not the *PHYB* mutation. The segregation ratios were tested using a chi-square test with two degrees of freedom; the critical value for  $p = 0.001$  for two degrees of freedom is 10.83. The segregation pattern was significantly different from the expected 9:3:4 ratio ( $p < 0.05$ ).

### 5.2.11 Genomic deep sequencing of 24B and 24C yields candidate suppressor SNPs

Once the 24B and 24C backcrosses against the L2K parent reached the F<sub>2</sub> generation, they were used for deep genomic sequencing in an attempt to identify EMS-introduced SNPs in the genome of each mutant that could be acting as suppressors. The 21D mutant was not selected for deep sequencing, since it showed a segregation pattern indicative of a single recessive mutation when backcrossed against L2K (Table 5.2) and that mutation was very likely to be the previously identified *PHYB* lesion (Figure 5.12B). The F<sub>2</sub> seedlings from the crosses between the 24B mutant and the L2K parent as well as those from the 24C mutant and L2K parent were screened again for their raised petiole phenotypes. For each set of crosses, around 100 seedlings with raised petioles were harvested. Additionally, 100 parental L2K seedlings were harvested. The tissue from the 100 seedlings was pooled within each background and genomic DNA was isolated from the pooled tissue of each set. The genomic DNA was subjected to next-generation deep genomic sequencing by Glasgow Polyomics using the Illumina NextSeq 500 platform. The L2K DNA had 66.9 million reads amounting to 74.33 times genomic coverage; 24B had 67.2 million reads with 74.67 times coverage; 24C had 63.5 million reads with 70.56 times coverage.

The L2K parent was used as the reference genome for the identification of SNPs in the 24B and 24C sequence data. A MiModD analysis of the reads was performed by Graham

Hamilton at Glasgow Polyomics to identify the presence of recessive SNPs (<https://celegans.de/mimodd/>). Based on the quality and quantity of reads identifying each SNP, as well as the SNP not being present in either L2K or in the other suppressor mutant, three candidate suppressor genes were identified for the 24B mutant (Table 5.4) and five genes for 24C (Table 5.5). The causal SNP for the *PHYB* W813R lesion was also identified in the 24C background sequencing data (data not shown). Work is currently underway to verify the presence of each of the candidate SNPs with traditional Sanger sequencing.

Gene	Type of mutation	Predicted protein features
<b>SPL14</b> AT1G20980	Splice donor variant	Zinc finger domain-containing protein
AT3G42560	Frameshift variant	Trans-membrane helix containing protein
<b>ABC12</b> ATMG00110	Upstream gene variant	ATP binding cassette protein

**Table 5.4: Candidate genes for suppressors in the 24B mutant.** SPL14 is SQUAMOSA PROMOTER BINDING-LIKE 14, a member of the Squamosa Promoter Binding-like (SPL) family. ABC12 is ATP BINDING CASSETTE 12.

Gene	Type of mutation	Predicted protein features
AT1G40104	Missense	No known domains or functions
AT2G08986	Missense	No known domains or functions
<b>Golgin</b> AT3G50430	Splice variant	Trans-membrane helix containing protein
AT1G40390	Upstream gene variant	DNase 1-like superfamily protein
AT1G43760	Downstream gene variant	Zinc finger domain-containing protein

**Table 5.5: Candidate genes for suppressors in the 24C mutant.**

## 5.3 Discussion

As previously established (Sullivan *et al.*, 2008) and re-affirmed here, L2K is not fully functional in response to low-intensity blue light. It is, however, capable of complementing *phot1* responses to a degree that is similar to wild type under some circumstances, as shown by its phototropic response following de-etiolation (Figure 5.1B). This conditional phenotype of the L2K transgenic line was a good basis for a genetic screen for suppressors of L2K activity; any EMS-mutated L2K seedlings that were able to respond to the low intensity light could have mutations in suppressors of L2K that ordinarily limit its signal output. The suppressor screen was successful, identifying three EMS mutants that exhibited enhanced petiole positioning relative to the L2K line under low light intensities: 24B, 24C, and 21D. The 24C and 21D mutants were identified as bearing a novel allele of the red light photoreceptor *phyB*. While the 21D mutant seems to only possess the *phyB* mutation to cause its raised petiole phenotype, there seemed to be a second mutation causing overexpression of L2K protein in the 24C mutant background. Possible suppressors acting in the 24B and 24C mutants have been shortlisted and are awaiting validation with Sanger sequencing and complementation studies. The identification of these putative suppressor mutations could aid in the fundamental understanding of *phot1* signalling and sensitivity *in planta* as well as benefit any strategy to engineer *phot1* activity by uncovering factors that negatively regulate *phot1* responses.

### 5.3.1 The isolated mutants may act as suppressors of *phot1* activity

It is difficult to say definitively from the current data whether the SNPs in each mutant background are acting as suppressors of L2K activity. The 24B and 24C mutants certainly show enhancements in sensitivity for multiple *phot1*-mediated responses in the L2K background, providing some evidence that the lesions in these two lines may influence *phot1* activity generally. The 24C lesion could be in a suppressor of *L2K* transcript or L2K protein levels, leading to the enhanced sensitivity of L2K in the 24C background. The 24B mutant does not show the same substantial differences in L2K expression observed in the 24C mutant (Figure 5.8), but still exhibits increased sensitivity, making it seem that 24B harbors a suppressor mutation involved in another pathway affecting *phot1* signaling. Though it cannot be determined definitively that these mutants are acting as suppressors of *phot1*, the increase in L2K activity for more than one *phot1*-mediated responses in the 24B and 24C mutant backgrounds suggests that this may be the case.

Nevertheless, it remained a possibility that the elevated *L2K* transcript observed in the 24C mutant background (Figure 5.8) was due to a mutation in the region around the *L2K* transgene insertion site that either increased *L2K* expression or affected the stability of the transcript. To address this question, following deep sequencing of the 24C mutant, the *L2K* transgene insertion site was mapped to chromosome 2 (work performed by Graham Hamilton, Glasgow Polyomics). When the region 5' and 3' to the insertion site was compared between the 24C mutant and *L2K*, it was found that there appeared to be no indication of strongly likely SNPs in the 24C mutant (Graham Hamilton; Appendix Figure 5.5). This evidence further strengthens the hypothesis that there is a suppressor SNP of *L2K* activity in the 24C mutant background that causes the increase in *L2K* transcript and *L2K* protein expression.

The 21D mutant, which has altered petiole positioning responses due to a *PHYB* mutation, may or may not be acting as a suppressor of *L2K* activity for petiole positioning. *PHYB* null mutants exhibit constitutively raised petioles due to the de-repression of SAS in the absence of phyB activity (Franklin, 2008). There is no evidence thus far that the SAS-induced hyponasty pathway involves phot1 or phot2; low blue light induced hyponasty is usually attributed to the activity of the blue light photoreceptor cryptochrome 1 (*cry1*; Millenaar *et al.*, 2009; Keller *et al.*, 2011). However, this hypothesis is not definitive. Keller *et al.* (2011) tested hyponasty in *phot1phot2* mutants and showed that phot1 and phot2 were not required, but the experiment was conducted under light that was filtered such that blue wavelengths were excluded, a condition under which there would be no predicted phot activity regardless of the mutant background or whether SAS was induced. In a separate study, Millenaar *et al.* (2009) found that hyponasty in *phot1phot2* mutants was not different from that of wild type under 20  $\mu\text{mol m}^{-2} \text{s}^{-1}$  white light. This initially seems puzzling, since investigation into phot1-dependent petiole positioning experiments are usually conducted under 10  $\mu\text{mol m}^{-2} \text{s}^{-1}$  white light, a similar light intensity, and generally leads to inclination of petioles in a phot-dependent manner. One key distinction is that Millenaar *et al.* (2009) conducted their study on plants with around 15 rosette leaves grown under short days, whereas most phot1 petiole positioning studies have focused on the first pair of true leaves in two-week-old seedlings grown under long days (Inoue *et al.*, 2008B; de Carbonnel *et al.*, 2010). It is possible that phot activity for petiole positioning could be dependent on developmental stage. If phot activity truly plays no role in SAS-induced hyponasty, then the *PHYB* mutation in the 21D background is likely not acting as a suppressor of *L2K* activity for petiole positioning, and its enhanced petiole positioning is solely through a deficiency in phyB

activity. Otherwise, the discovery of this *PHYB* allele in our screen could eventually reveal evidence of signal integration between *phot1* and *phyB* for petiole positioning. Further study should provide more information on what role, if any, *phyB* plays in phot-mediated petiole positioning.

Most importantly, whether any of these putative suppressor mutations have an appreciable effect when introduced into a background encoding full-length *phot1* remains to be seen. Unlike L2K, full-length *phot1* is a very light-sensitive protein, which could possibly make it difficult to detect the effect of the suppressor outside of the L2K background. Following complementation studies to validate the shortlisted candidates for 24B and 24C, what role the suppressors have in the activity of full-length *phot1* will be explored. If mutating the 24B and 24C suppressors does indeed enhance full-length *phot1* activity, this information could be useful from an engineering perspective to help increase the activity of *phot1* variants such as the photocycle mutants, which have lowered activity relative to *phot1*-GFP (for example, for phototropism; Figure 4.6). To address the question of whether *phyB* is a suppressor of *phot1* for petiole positioning, the role of phot activity in SAS-induced hyponasty should be explored. It would be of particular interest to observe petiole positioning of *phyBphot1phot2* mutants, since *phot1phot2* mutants exhibit curled, downward sloping petioles in young plants (Inoue *et al.*, 2008B), but *phyB* mutants exhibit raised petioles through SAS (Franklin, 2008), phenotypes that directly oppose each other. Additionally, whether there is a difference in petiole positioning between young and adult plants would be of interest. Specific experiments for the other putative suppressors will depend on the identity of the suppressors themselves but have an equal potential to aid in the understanding of *phot1* activity and how it integrates with plant physiology as a whole.

### 5.3.2 24C and 21D are *PHYB* mutants

Sequencing of the *PHYB* gene from the 24C and 21D mutants revealed that both lines encode a mutant allele of *PHYB* that harbors the substitution W813R within the PAS2 domain (Figure 5.11B). The W813 residue is predicted to be located in the center of the only projected beta strand within *phyB* PAS2 (Figure 5.11C). Although no structural information is available for either of the C-terminal *phyB* PAS domains, amino acids toward the middle of beta strands generally tend to be aromatic and hydrophobic (Bhattacharjee and Biswas, 2010), increasing the likelihood that the substitution of a central tryptophan for an arginine is structurally disruptive. It is probable that the W813R substitution is causing the red light signalling defects in the 24C and 21D mutants.

To our knowledge, this is the first report of an allele of *PHYB* containing the W813R substitution. However, the substitution E812K, just one residue upstream of W813, has been isolated from two independent EMS screens as a mutation that impairs phyB function (Wagner and Quail, 1995; Bradley *et al.*, 1996); the equivalent mutation in phyA, E377K, was identified similarly (Yanovsky *et al.*, 2002). As with the phyB-W813R allele identified here, the phyB-E812K mutants exhibit long hypocotyls and decreased phyB protein levels (Elich and Chory, 1997; Chen, Schwab and Chory, 2003). The recurrence of E812K and other mutations to phyB PAS2 in EMS screens as well as targeted structure/function studies have consistently pointed to this region as important for the modulation of phyB signalling (Wagner and Quail, 1995; Wagner *et al.*, 1996; Matsushita *et al.*, 2003). In particular, many mutations to this region, including phyB-E812K and phyA-E377K, cannot form nuclear bodies (Yanovsky *et al.*, 2002; Chen, Schwab and Chory, 2003; Matsushita, Mochizuki and Nagatani, 2003). The formation of phy nuclear bodies, which are foci where phy concentrate in the nucleus following light activation, seem to be related to phy activity, but their exact function in signalling is not understood and their formation is not required for a low level of phy activity to be observed (Chen, Schwab and Chory, 2003; Matsushita, Mochizuki and Nagatani, 2003; Chen, 2008; Perrella and Kaiserli, 2016). Indeed, though nuclear bodies are not formed by phyB-E812K, it is not a loss-of-function mutant and demonstrates residual phyB activity for hypocotyl elongation in spite of lowered protein levels (Wagner and Quail, 1995; Elich and Chory, 1997; Chen, Schwab and Chory, 2003). Study of the dark reversion following red light treatment of recombinant phyB-E812K expressed in yeast revealed that the photocycle of this mutant is much faster than that of wild-type phyB, which could explain its attenuated responsiveness (Elich and Chory, 1997). Supporting this hypothesis, photobody formation and duration in phyB does seem to be related to its photocycle (Ádám *et al.*, 2011; Van Buskirk *et al.*, 2014; Enderle *et al.*, 2017). A caveat to the hypothesis that phyB-E812K possesses a fast photocycle that impairs photobody formation is that it is impossible to distinguish in the current published data between a fast photocycle mutant and a mutant with impaired ability to form nuclear bodies due to structural perturbations. Because the E812K and W813R substitutions are adjacent, and both are substitutions to positively charged residues, it may be that the W813R allele from this screen has a similar impact on phyB function to the E812K substitution, providing a tempting framework for further study of the underlying cause of the phyB mutant phenotype observed in the 24C and 21D mutants.

It is not clear from the hypocotyl elongation studies presented here whether phyB-W813R is a loss-of-function mutant or simply substantially reduces phyB activity, as observed for

phyB-E812K (Figure 5.10). Similar to phyB-E812K, phyB-W813R has lowered phyB protein levels, but the protein is still detectable by western blot for both mutants, which perhaps increases the probability of the retention of some function (Elich and Chory, 1997; Chen, Schwab and Chory, 2003; Figure 5.11A). The hypocotyl elongation studies here used *phyAphyB* as a positive control for hypocotyl elongation in red light; if the response in the EMS mutants was compared to the single *phyB-9* null mutant, direct comparisons between the hypocotyl lengths could indicate whether phyB-W813R retains residual activity. Further complicating interpretation of hypocotyl elongation in these mutant lines, the 21D mutant had consistently poor germination rates across multiple seed batches, making the line appear to have shorter hypocotyls than 24C, which encodes the same mutation, due to delayed germination of some seeds in each experiment (Figure 5.11). It would perhaps be more informative to determine whether W813R causes a loss-of-function by investigating other aspects of phyB activity, such as whether the stability of PHYTOCHROME INTERACTING FACTOR (PIF) proteins, which are targeted for degradation by phyB activity (Al-Sady *et al.*, 2006; Shen *et al.*, 2007; Shen *et al.*, 2008), is similar to that of a loss-of-function mutant.

PhyB was previously reported as a suppressor of phot activity for responses other than petiole positioning, such as leaf flattening (Kozuka *et al.*, 2012), chloroplast avoidance (DeBlasio *et al.*, 2003; Luesse, Deblasio and Hangarter, 2010), and phototropism (Goyal *et al.*, 2016). In contrast, the 21D mutant, which is the only *PHYB* mutant from the screen that appears to be mutated only in *PHYB* and in no other genes according to the segregation of its raised petiole phenotype (Table 5.2), appears to have a gain in sensitivity for petiole positioning but no other phot1 response. In the case of suppression of chloroplast avoidance, phyB must be acting on phot2 specifically: only phot2 is responsible for mediating the chloroplast avoidance response (Jarillo *et al.*, 2001; Kagawa *et al.*, 2001); L2K, which is derived from phot1, would not be able to perform this response. Although Goyal *et al.* (2016) found that phyB suppresses phototropism in de-etiolated seedlings, in our hands and in most other studies, the presence of active phyA and phyB enhances phototropism (Janoudi *et al.*, 1997; Parks *et al.*, 1996; Kami *et al.*, 2012; Sullivan *et al.*, 2016). In our phototropism system, the 24C and 21D mutants would be expected to be inhibited in their phototropic response, but since L2K is already deficient in this regard (Sullivan *et al.*, 2008; Figure 5.1) it would be difficult to distinguish between poor phototropism due to the phyB lesion, and poor phototropism due to lowered L2K activity. Indeed, if phyB acts as suppressor of phot1 for some responses but is an enhancer of phototropism, this could be the reason that the 21D mutant does not show a phototropic response different from that of from that of the L2K

parent (Figure 5.6A). Reduced phototropism in *phyB* mutants could likewise explain the reason that the L2K-overexpressing 24C mutant exhibits phototropism at  $0.5 \mu\text{mol m}^{-2} \text{s}^{-1}$  unilateral blue light but does not respond as strongly as wild type seedlings (Figure 5.6).

As for leaf flattening, it is puzzling that the 21D mutants have wrinkled leaf tips (Figure 5.5A) but that mutation to *phyB* typically leads to flatter leaves (Kozuka *et al.*, 2012). One explanation is that the *phyB*-W813R allele does retain some residual activity and maintains its antagonism of phot activity for leaf flattening. Another possibility is that the phenotype could be due to another EMS-introduced lesion in the 21D background that is independent of the other phenotypes observed here. The 24C mutant, which possesses the same *phyB* mutation, has much flatter leaves than the 21D mutant (Figure 5.5A), though its increased activity due to overexpression of L2K confounds interpretation of *phyB* involvement in this case. It appears that the *phyB*-W813R allele identified in this screen may not fit neatly within the established framework of genetic interactions between *phyB* and *phot1*.

With further study, exactly how *phyB* and *phot1* interact to bring about the overall physiological responses to ambient light could be elucidated. It is possible that interaction could occur directly between the two photoreceptors; it was found in *Physcomitrella* that the native *phy4* and *photA1* photoreceptors as well as *Arabidopsis* *phyA* and *phot1* physically interact in a light-dependent manner (Jaedicke *et al.*, 2012). Additionally, *phyA* seems to regulate the internalization of *phot1* from the plasma membrane following treatment with both red and blue light (Han *et al.*, 2008), though *phot1* re-localization may not have functional significance (Preuten *et al.*, 2015; Liscum, 2016). The connection between *phyA* and *phot1* is strengthened by the association of both photoreceptors with members of the PHYTOCHROME KINASE SUBSTRATE (PKS) family, where PKS proteins seem to be involved in signal transduction following light perception for both *phyA* and *phot1* (Lariguet *et al.*, 2003; Schepens *et al.*, 2008; de Carbonnel *et al.*, 2010; Schumacher *et al.*, 2018). Though no similar signs of signal integration have been reported between *phyB* and *phot1*, any cooperation between *phyB* and *phot1* is more likely to be between signalling elements downstream of the activation of both photoreceptors than through physical interaction. As previously discussed (Section 5.3.1), whether *phot1* plays a role in SAS-induced hyponasty is a good place to start these investigations. Moreover, establishing whether the *PHYB* allele isolated from this screen, *phyB*-W813R, retains any *phyB* activity would further clarify the results presented in this study. Any explorations into *phyB* and *phot1* activity using the EMS mutants isolated in this study should focus on the 21D mutant rather than 24C, since 24C appears to overexpress L2K protein through an independent mechanism and has enhanced

phot1 responses. Alternatively, though it would not provide further information on the functionality of phyB-W813R, crossing the L2K line against the *phyB-9* null mutant would be an opportunity to explore how phyB acts on L2K without the possibility of the presence of confounding SNPs. These steps could lay the groundwork to understand more about how phot1 and phyB signalling integrate.

### 5.3.3 The 24C mutant overexpresses L2K protein

Because the 24C mutant overexpresses L2K protein while the 21D mutant, which shares the phyB-W813R mutation with 24C, does not, it was hypothesized that 24C possesses a second mutation that leads to increased L2K expression in the 24C background through a mechanism independent of the *PHYB* lesion. The overexpression of L2K in the 24C background is exciting, because all previous attempts to overexpress phot1 have not succeeded in our hands. Likewise, constitutively active variants of phot1 tend to have poor protein expression *in planta* in spite of transcript levels that are similar to wild type (Kaiserli *et al.*, 2009; Petersen *et al.*, 2017). These two points suggest that the activity of phot1 may be controlled through tight regulation of protein expression, and that 24C may possess a suppressor mutation that affects this potential regulatory mechanism. If a suppressor in the 24C background does act on phot1 protein levels, the fact that the 24C shows light lability similar to that of wild-type phot1 (Figure 5.9) would point to a complex mechanism with differential regulation of phot1 protein expression in the dark, where L2K protein is overexpressed in the 24C background, and in the light, where the L2K protein is turned over normally (Figure 5.10).

In fact, very little is understood about the mechanism of phot1 protein turnover following exposure to strong blue light. Although it was previously reported that NPH3 acts as an E3 ubiquitin ligase to target phot1 for degradation (Roberts *et al.*, 2011), in our experimental system, phot1 turnover was not altered in the *nph3-6* mutant background. (Appendix Figure 5.6). Concomitant treatment with red and blue light is also not able to alter the turnover pattern of phot1 (Appendix Figure 5.6). Furthermore, phot1 autophosphorylation following light treatment does not induce its turnover since the kinase-inactive variant *phot1-7* shows turnover following blue light treatment similar to that of wild-type phot1 (Sullivan *et al.*, 2010; Preuten *et al.*, 2015; Appendix figure 5.6). Since phot1 autophosphorylation activity itself does not lead to its turnover, whether other photoreceptors sense the light intensity and target phot1 for turnover was tested in the *phot2*, *cry1cry2*, and *phyAphyB* backgrounds. It was found that the light lability of phot1 was not altered by mutation to these photoreceptors

(Appendix Figure 5.6). Although the series of photoreceptor mutants tested here was not exhaustive—most notably the F-box-containing photoreceptors from the *ztl* family (Ito *et al.*, 2012) were not tested, it seems more likely that the conformational changes following light perception targets *phot1* for degradation, perhaps through exposing sites for ubiquitination or SUMOylation. This could be tested using mutants of *phot1* mutated in photoactive cysteines, thereby eliminating *phot1* light perception, to see whether these mutations stabilize *phot1* under intense blue light treatment.

Alternatively, if the 24C lesion is not in a suppressor of *phot1* protein levels but turns out to be a suppressor of *PHOT1* expression, this information will be useful for studying the effects of *phot1* on plant physiology by hinting at means by which *phot1* protein can be overexpressed. Indeed, the 24C mutant background already was useful in allowing the assessment of L2K autophosphorylation activity *in planta* (Figure 5.10). Studies on cryptochrome and phytochrome photoreceptors show that overexpression of these proteins confers enhanced sensitivity and ameliorates responses deleterious to biomass and crop yield such as SAS (Boylan and Quail, 1991; Wagner *et al.*, 1991; Lin *et al.*, 1995; Giliberto *et al.*, 2005). Interestingly, overexpression of *phyA* (Thiele *et al.*, 1999) and *phyB* (Garg *et al.*, 2005) in crop plants enhances yield without compromising the quality of the produce. The increase in sensitivity due to overexpression in other photoreceptors is similar to that observed for L2K in the 24C background, which is much more sensitive than its L2K parent for both phototropism (Figure 5.6) and orientation against the gravity vector (Figure 5.7).

On the other hand, it is likely that increased *phot1* activity could be deleterious to normal plant development. Since *phot1* activities related to plant orientation or movement, such as phototropism, depend on the formation of a gradient of activated *phot1* (Esmon *et al.*, 2006; Hohm *et al.*, 2014), the increased activity in constitutively active variants of *phot1*, which presumably would have either attenuated or no gradient formation, would be expected to ultimately inhibit *phot1* responses. Indeed, the constitutively active *phot1*-R472H variant, which possess a mutation that destabilizes the A' $\alpha$  helix associated with LOV2, requires higher light to drive *phot1* responses, though this could also be due to reduced protein expression in these mutants (Petersen *et al.*, 2017). Moreover, overexpression of the single kinase domain of either *phot2* (Kong *et al.*, 2007) or *phot1* (C.E. Thompson and J.M. Christie, unpublished data) on its own leads to a dwarf phenotype with leaves that appear to be smaller than those of wild-type plants. This phenotype is similar to that of the 24C mutant (Figure 5.5). If the overexpression of L2K in the 24C background can be conferred to full-length *phot1*, the effect of overexpressing *phot1* *in planta*, and whether it is detrimental or

improves productivity as for the overexpression of phytochromes, can be investigated more thoroughly.

### 5.3.4 The role of NPH3 in phot1 signal transduction

NPH3 is required for phot1 activity for responses hypothesized to require auxin redistribution such as phototropism (Motchoulski and Liscum, 1999), petiole positioning (Inoue *et al.*, 2008B; de Carbonnel *et al.*, 2010), and leaf flattening (Inoue *et al.*, 2008B; Kozuka *et al.*, 2012). The studies presented here suggest that NPH3 is not required for vertical orientation under low blue light (Appendix Figure 5.3), which is consistent with the hypothesis that NPH3 is somehow involved in the lateral redistribution of auxin for responses involved in directional growth (Haga *et al.*, 2005; Wan *et al.*, 2012). NPH3 function seems to involve a negative feedback loop with phot1, with NPH3 dephosphorylation following phot1 activation corresponding to the refractory period during which phototropic bending temporarily halts (Haga *et al.*, 2015), and also reportedly through initiating the turnover of phot1 following light activation (Roberts *et al.*, 2011). Although these observations suggest that NPH3 suppresses phot1 activity, neither NPH3 nor other members of the NRL family were expected to be pulled out of our screen, since mutation to NRL proteins involved in phot1 signaling tend to lead to loss of function for phot1 responses (Motchoulski and Liscum, 1999; Sakai *et al.*, 2000; Inoue *et al.*, 2008B; Suetsugu *et al.*, 2016; Christie *et al.*, 2018).

However, the involvement of NPH3 activity in phot1 signal transduction must be more complicated than that of a suppressor, since it not only modulates phot1 responses, but is required for many of them. Additionally, though dephosphorylated NPH3 is thought to correspond to its inactivation, preventing the transduction of phot1 responses (Haga *et al.*, 2015; Christie *et al.*, 2018), enhanced NPH3 dephosphorylation seems to correlate with improved L2K responsiveness in two of the EMS mutants (Figure 5.6). We have also not been able to confirm NPH3-driven phot1 turnover using our experimental system (Appendix Figure 5.6). The role that NPH3 activity plays in phot1 responses requires further evaluation. Indeed, how NPH3 is involved in phot1 signalling is likely to remain a bit of a mystery as long as the exact function of the protein is unknown. An investigation into the phosphorylation sites important for NPH3 activity and their precise role in phot1 signal transduction may be a good avenue of investigation to begin these studies.

### 5.3.5 Candidate suppressors in the 24B and 24C backgrounds

Although most of the candidate suppressors identified through deep sequencing of the 24B and 24C mutants lack an assigned function or domains that could hint at a specific role (Tables 5.5 and 5.6), the most promising candidate suppressor identified for the 24B mutant is SQUAMOSA PROMOTER-BINDING PROTEIN LIKE 14 (SPL14), which has been partially characterized in previous studies. SPL14 is a member of the SPL family of transcription factors, comprising of 16 members in *Arabidopsis*, which are defined by DNA-binding activity to the conserved sequence GTAC through a conserved SPB (Squamosa Promoter Binding) domain (Preston and Hileman, 2013). Intriguingly, some members of this family were shown to promote SAS through the PIF-mediated negative regulation of the microRNA *miR156*, which suppresses the expression of some SPL family members (Xie *et al.*, 2017). However, when the *SPL14* sequence was phylogenetically compared to other members of the SPL family from *Arabidopsis* as well as other species, *SPL14* clustered in Clade II of nine distinctive clades; members of this clade exhibited divergent functional roles, but all lacked the target sequence for *miR156* (Preston and Hileman, 2013).

A mutant resulting from T-DNA insertion in the 3' UTR of *SPL14* was isolated from a screen for mutants deficient in programmed cell death in response to treatment with the fungal toxin Fumonisin B1 (Stone *et al.*, 2005). Further investigation confirmed SPL14 localization to the nucleus and *in vitro* DNA binding assays showed that SPL14 can bind to the consensus sequence CCGATC(A/G) (Stone *et al.*, 2005; Liang, Nazareus and Stone, 2008). Although the authors of the initial screen reported longer petioles and a later flowering time in the *spl14* mutant, these observations were not quantified (Stone *et al.*, 2005), and there have been no further reports on the phenotypes of these mutants. The 24B mutant isolated in this study does not seem to exhibit either the long petiole or late flowering phenotypes (Figure 5.5A). Encouragingly, a SPL14 homologue from *Brassica* was identified as a quantitative trait locus involved in branch angle (Liu *et al.*, 2016), a phenotype that is similar to the enhanced petiole positioning by which 24B was identified in our screen.

It seems unlikely that SPL14 would act to influence petiole positioning in a manner independent of *phot1*, since the 24B mutant also has enhanced NPH3 dephosphorylation and sensitivity for phototropism relative to the L2K parent (Figure 5.6). Since SPL14 is a probable transcription factor (Liang, Nazareus and Stone, 2008), if it does act as a suppressor of *phot1* activity, its effect is likely to be indirect and possibly mediated through transcriptional regulation of other genes that interact more directly with *phot1*. The SNP in

*SPL14* identified using whole genomic sequencing needs to be verified using a traditional sequencing approach. If the presence of the mutation is validated, complementation studies using the 24B mutant and *spl14* T-DNA insertion lines can verify whether *SPL14* acts as a suppressor of *phot1* activity as well as identify a possible mechanism of suppression.

In addition to the identification of the *phyB*-W813R mutation, the top two suppressor candidates based on read quality and quantity for the 24C background from the deep sequencing data are AT1G40104 and AT2G08986. The sequences of both genes are highly repetitive and, surprisingly, bear a large degree of similarity to each other. Because slippage can be an issue in the sequencing of repetitive genes—repetition of DNA bases can make it difficult for the sequencing platform to distinguish both the identity and the number of the repeated bases—the SNPs identified in both genes could be artifacts of the sequencing process. The similarity of the two genes also made it extremely difficult to design primers that could differentiate between them to validate the presence of the SNPs (data not shown). Taken together, these issues seem to suggest that neither of these genes encodes a suppressor SNP and also that these genes, though they are annotated as protein-coding regions, may in fact be intergenic sequences or centromeric DNA. If that is the case, the probability that the deep sequencing of the 24C mutant yielded good suppressor candidates is diminished, though the other three candidates found in the deep sequencing data will also be validated and possibly used in complementation studies. If those candidates do not seem to be involved in *phot1* activity, the 24C mutant may require more backcrosses against the L2K parent to eliminate non-specific EMS-introduced SNPs to find better candidates from deep sequencing. Additionally, since the short and raised “SR” phenotype that seems to be related to the overexpression of L2K in the 24C mutant can be segregated away from the *phyB* lesion (Table 5.3), it would be most useful to try to perform further backcrosses specifically using individuals that have the SR phenotype. In the first deep sequencing run for the 24C mutant, seedlings were selected for sequencing only on the basis of their raised petiole phenotype: individuals that were singly mutated in *PHYB* would have been sequenced along with the SR mutants and may have reduced the likelihood of finding the SR-associated SNP. This is especially true since there was only a 5% occurrence of the SR phenotype in the F<sub>2</sub> segregating population arising from crosses between the 24C mutant and the L2K parent (Table 5.3). If the *phyB* lesion were removed from the 24C mutant background, it would be easier to identify good candidate SNPs for the SR phenotype.

Regardless of the identity of the EMS-introduced lesions in the three mutant lines uncovered from our screen, it was successful in identifying mutants with enhanced petiole positioning.

With more investigation, the possible suppressors identified here could further the understanding of phot1 signaling and its interaction partners. Nonetheless, this screen was not performed to saturation; between 75,000 and 80,000 individuals were screened here, but screens to saturation in *Arabidopsis* typically require >125,000 individuals (Jander *et al.*, 2003). Another indication of saturation in a genetic screen is the identification of multiple alleles of the same genes, which did not occur here. Furthermore, more mutants in genes involved in SAS-induced hyponasty, such as *CRY1* (Keller *et al.*, 2011) would have been expected to be isolated, but only the phyB-W813R variant was identified. Since the screen was successful in identifying at least one good candidate suppressor of phot1 activity in SPL14, it would be beneficial to continue the screen until it reaches saturation to ensure that as much information as possible was uncovered from the screen.

## Chapter 6 General Discussion

### 6.1 Introduction

The goal of the work presented here was to examine phot1 sensitivity *in planta* and determine whether the sensitivity of phot1 can be increased, leading to positive modulation of phot1 responses. Because phot-mediated responses optimize photosynthetic competence, it was hypothesized that enhanced phot1 sensitivity may increase plant growth. To approach this question, targeted mutations were introduced to influence the phot1 photocycle by slowing dark reversion, increasing the period over which signal is transduced by individual phot1 molecules as well as the size of the pool of phot1 that is light-activated and signaling at any given point following a light stimulus. Secondly, a genetic screen was employed to explore whether extrinsic factors contribute to phot1 sensitivity *in planta*. To perform this screen, seeds encoding a transgene for L2K, a less-sensitive version of phot1, were mutagenized and screened for individuals with increased sensitivity for the phot1-mediated petiole positioning response.

Examination of phot1 sensitivity was successful on both fronts. Phot1-L558I, a slow photocycle mutant *in vitro*, exhibited a slow photocycle *in planta* as assessed from NPH3 phosphorylation status which seemed to contribute to its increased sensitivity relative to wild type for chloroplast accumulation in response to brief pulses of blue light. The generation of slow phot1 photocycle mutants also led to the discovery that the V478 residue, located within the LOV2 light-sensing domain, seems to be important for signal transduction in phot1. Likewise, the mutants from the genetic screen appear to have isolated components of phot1 signaling that have not been previously identified. Three different mutants in the L2K transgenic background had increased sensitivity for the petiole positioning response, two of which also extended the increased sensitivity to other phot-mediated responses, such as phototropism, and seem to have done so through different mechanisms. Not only has phot1 sensitivity been increased in both of the investigations presented here but also, each approach has the potential to aid in the understanding of phot1 function and signaling in greater detail.

### 6.2 Phot sensitivity and the photocycle

When the slow photocycle mutations identified using the phot1 LOV1+LOV2 protein *in vitro* were integrated into full-length phot1 expressed *in vivo*, it was expected that the photocycle of each mutant would remain slower than that of wild type and that there would

be clear increases in sensitivity. Instead, of the three slow photocycle variants identified from our *in vitro* work, N476L, V478I, and L558I, only phot1-V478I and -L558I exhibited slow photocycles as inferred from the recovery of the phosphorylated state of NPH3 following illumination and a return to darkness (Figure 4.7). It was also observed that the phot1-V478I and -L558I variants were not as sensitive for phototropism as wild-type phot1-GFP in response to continuous light treatments, with stronger light intensities required to reach a level of complementation that was comparable to wild type (Figure 4.8). With deeper investigation, however, we found that chloroplast accumulation in response to a brief pulse of blue light was increased in the phot1-L558I slow photocycle mutant relative to phot1-GFP (work performed by Dr. Justyna Łabuz; Appendix Figure 4.5), demonstrating that when light treatments are administered as pulses the slow photocycle mutants are able to outperform wild type. As previously discussed (Section 4.3.5), this indicates that further evaluation of sensitivity in the slow photocycle mutants should be moved from continuous irradiations with blue light to pulse-based light treatments. It would also be worth further exploring the chloroplast accumulation response following pulses of blue light in the phot1-V478I slow photocycle mutant. Furthermore, given the clear indications of increased sensitivity for the slow photocycle mutant phot1-L558I for the chloroplast accumulation response when short pulses of blue light are administered, other responses, such as phototropism, should be investigated similarly in order to examine whether a comparable increase in sensitivity can be observed.

In addition to the slow-recovering mutants explored here, fast photocycle mutants of phot1 were generated in work by Drs. Stuart Sullivan and Jan Petersen. Though those investigations were outside the scope of this thesis, it is worth adding these mutants to a discussion of the role the phot1 photocycle plays in its function. The fast photocycle mutants phot1-V478T and -I489V were both fully functional and comparable to wild-type phot1-GFP for the leaf flattening response (Appendix Figure 6.1). The mutants showed a faster rate of recovery of the phosphorylated state of NPH3 following a light treatment and return to darkness than wild-type phot1-GFP, confirming a fast phot1 photocycle in these mutants (Appendix Figure 6.2A). In spite of this faster rate of recovery, the phototropic responsiveness of the fast photocycle mutants was almost the same as phot1-GFP across all of the fluence rates examined (Appendix Figure 6.2B). While the slow photocycle mutants had marked defects in phototropism, particularly when stimulated with low fluence rates, the fast mutants, which were expected to be less sensitive to light and therefore less responsive, did not appear to be different from wild-type phot1-GFP. This result was also surprising considering that one hypothesis for the lowered functionality of the slow

photocycle mutants was that introducing variants at highly conserved LOV2 residues caused defects in signaling that were independent of the photocycle (section 4.3.2). However, because the fast mutants, but not the slow ones, fully complemented phot1 responses, it may be that the reduced activity in the slow photocycle mutants may actually be related to slowing the photocycle itself.

To see whether the fast photocycle mutants behaved differently in response to pulses rather than continuous irradiation, as observed for the slow photocycle mutants, the fast mutants were probed by measuring chloroplast accumulation in response to pulsed blue light. These mutants were less responsive to the pulse than both the slow mutants and phot1-GFP, exhibiting reduced chloroplast accumulation (Dr. Justyna Łabuz; Appendix Figure 6.3). These results show that the phot1 photocycle is very important for sensitivity to brief illuminations with blue light. The role of the phot1 photocycle under constant light, however, remains unclear, with the slow mutants presenting some defects in responsiveness for leaf flattening and phototropism (Figures 4.3 and 4.6) while no discernible difference could be observed between the fast mutants and phot1-GFP for the same responses (Appendix Figures 6.1 and 6.2).

By contrast, investigations into the role of the LOV domain photocycle in the VVD photoreceptor in *Neurospora crassa* found that introducing a fast photocycle into VVD reduced VVD activity (Dasgupta *et al.*, 2015). In its lit state, VVD interacts with the White Collar Complex (WCC) to influence its transcriptional activity, but the fast photocycle mutants appeared to have reduced affinity for the WCC that was attributed to increased dark reversion (Dasgupta *et al.*, 2015). Meanwhile, the slow photocycle mutants of VVD seemed to have no effect on its activity (Dasgupta *et al.*, 2015). On the surface, our observations of the phot1 photocycle mutants under continuous light may not appear to correspond well with the biological role of the VVD photocycle in *Neurospora*. In our study, the fast phot1 photocycle mutants were completely functional while the slow mutants showed varying degrees of functional defects under continuous light. The reason for these disparities seems most likely to be due to the substantial differences between the original, wild-type photocycles of each photoreceptor. VVD has an extremely slow photocycle that remains in its activated state for a period of time that rivals the interval over which proteins remain stable ( $T_{1/2} \sim 2.5$  hours; Zoltowski, Vaccaro and Crane, 2009); wild-type phot1, on the other hand, has a fast photocycle for a LOV domain-containing photoreceptor ( $T_{1/2} \sim 8$  minutes; Christie *et al.*, 2002; Kasahara *et al.*, 2002). Therefore, making the slow photocycle of VVD even slower is not likely to have biologically relevant consequences (Dasgupta *et al.*, 2015),

while hastening the phot1 photocycle may not have strong effects on a signal transduction system already adapted to working with a fast phot1 recovery.

If it is the case that phot1 signaling pathways are well-adapted to the relatively fast photocycle of phot1, then increasing phot1 activity by slowing the photocycle may saturate the ability of its downstream signaling partners to produce signal, thereby limiting the functionality of the slow photocycle mutants. This may be especially true for directional phot1 responses, such as phototropism, which depend on the creation of a gradient of activated phot1 to guide growth (Solomon *et al.* 1997; Christie and Murphy, 2013). Gradient formation may be hindered by increased phot1 activity on both the lit and shaded sides of the plant in the slow photocycle mutants, limiting the ability of these mutants to respond to unilateral light with phototropic curvature. This may explain the reason that stronger light produces better phototropic responses in the slow photocycle mutants phot1-V478I and -L558I (Figure 4.8), the higher intensity may drive better gradient formation than low light in the slow photocycle mutants, increasing the magnitude of the response.

When the slow photocycle mutant phot1-V478L was found to be largely non-functional for phot-mediated responses, the equivalent mutation, V392L, was introduced into phot2-GFP with its expression driven by the phot1 promoter (*PHOT1::phot2-V392L-GFP*) in a *phot1phot2* mutant background to investigate whether phot2-V392L showed the same functional defects as phot1-V478L (work performed by Dr. Stuart Sullivan). Phot2-V392L showed enhanced NPH3 dephosphorylation compared to wild-type phot2-GFP, which cannot fully dephosphorylate NPH3, indicating increased sensitivity. However, unlike the phot1 slow photocycle mutants, in phot2-V392L, NPH3 returned to its phosphorylated state within one hour of returning the seedlings to darkness (Figure 6.1A). Similar to our findings for the phot1 slow photocycle mutants, phot2-V392L exhibited poor functionality for phototropism compared to wild-type phot2-GFP lines (Stuart Sullivan and John M. Christie, data not shown). Yet, in contrast to the phot1 slow photocycle mutants, it was also observed that phot2-V392L had increased sensitivity relative to phot2-GFP for petiole positioning in two-week-old seedlings grown under  $10 \mu\text{mol m}^{-2} \text{s}^{-1}$  white light (Stuart Sullivan and John M. Christie, data not shown). Following this result, it was found that phot2-V392L also exhibited increased activity for chloroplast avoidance compared to phot2-GFP in response to both pulsed and continuous blue light treatments (Dr. Justyna Labuz, data not shown). The phot2-V392L slow photocycle mutant therefore seemed to exhibit increased sensitivity under both pulsed and continuous light, which was not observed in the phot1 slow photocycle mutants.

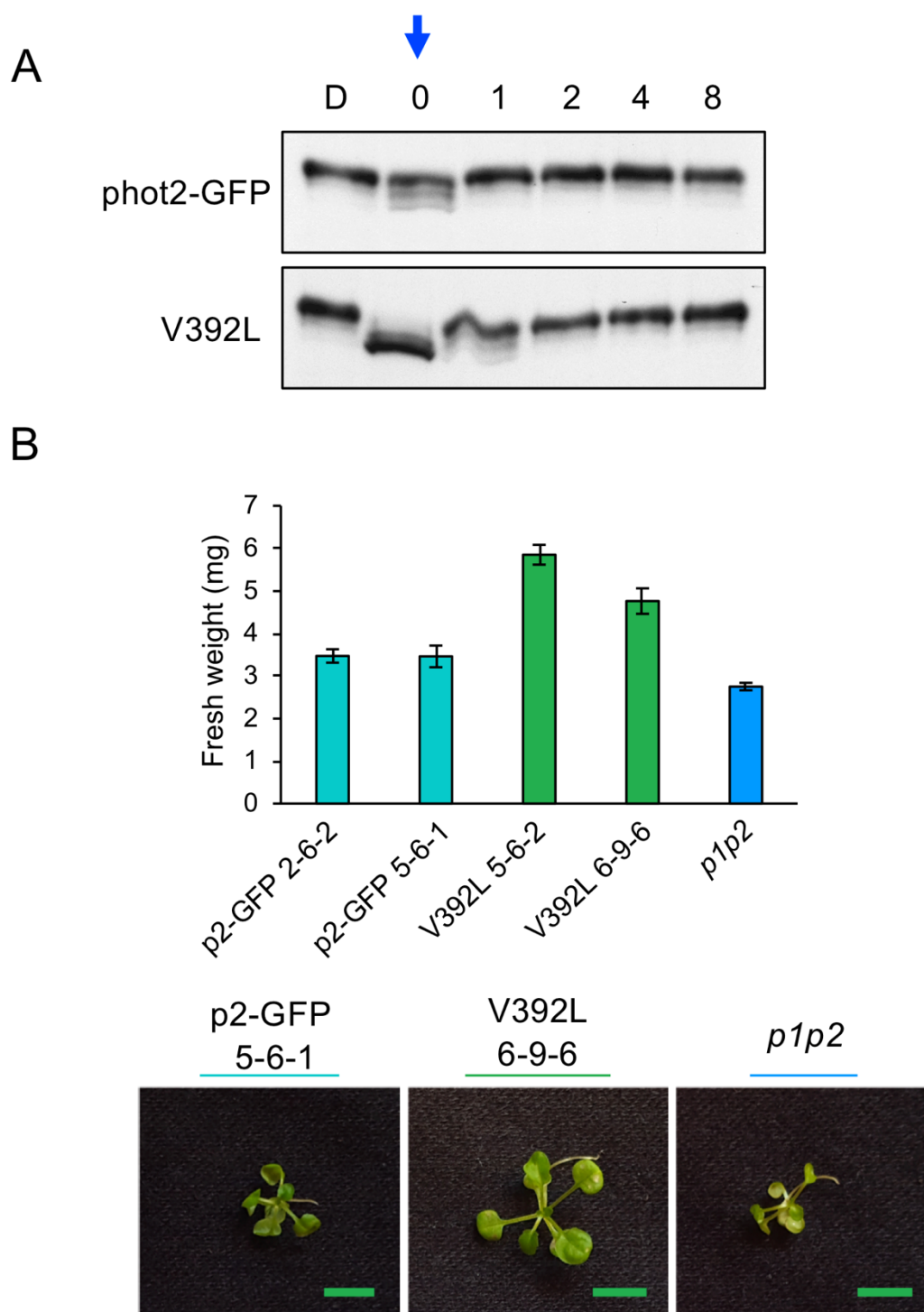


**Figure 6.1: NPH3 phosphorylation and fresh weight accumulation in the phot2-V392L transgenic lines.** **A.** NPH3 phosphorylation status of the phot2-GFP and phot2-V392L transgenic lines. Whole protein extracts were harvested from seedlings in the dark (D) and immediately following an overhead irradiation of blue light at  $20 \mu\text{mol m}^{-2} \text{s}^{-1}$  for 15 minutes (0; blue arrow). The seedlings were then returned to darkness and protein extracts were harvested 1, 2, 4, or 8 hours following the irradiation. Representative lines from one experiment is shown; experiment was performed by Dr. Stuart Sullivan. **B.** Biomass accumulation. The two phot2-V392L slow photocycle mutant lines, along with phot2-GFP (p2-GFP), and the *phot1phot2* (*p1p2*) double mutant were grown for four weeks under  $25 \mu\text{mol m}^{-2} \text{s}^{-1}$  red light and  $0.1 \mu\text{mol m}^{-2} \text{s}^{-1}$  blue light in long days for four weeks prior to weighing each plant. Data shown is from one representative experiments from of two independent repeats measuring 20 plants from each genotype. Representative images are shown; scale bar is 5 mm.

Since *phot2-V392L* showed increased sensitivity to both pulsed and continuous light, the biomass accumulation of this mutant was examined when grown under very low fluence rates of light ( $25 \mu\text{mol m}^{-2} \text{s}^{-1}$  red light,  $0.1 \mu\text{mol m}^{-2} \text{s}^{-1}$  blue light). Unlike the *phot1* slow photocycle mutant *phot1-L558I* compared to wild-type *phot1-GFP* (Figure 4.9), *phot2-V392L* accumulated nearly twice the biomass of wild-type *phot2-GFP* under these light conditions (Figure 6.1B). This enhanced growth seemed to be related to the increase in photosensitivity in *phot2-V392L*. The leaves of this mutant were visibly more expanded than those of wild-type *phot2-GFP*, which overall resembled *phot1phot2* mutants under these light conditions, making more surface area available for light capture in *phot2-V392L* than wild-type *phot2-GFP* (Figure 6.1B). Furthermore, the wild-type *phot2* lines appeared to be agravitropic, with a substantial proportion of the seedlings lying flat on the soil, while the *phot2-V392L* lines remained upright (observation not yet quantified). This possible difference in vertical orientation under low light also may have contributed to the success of *phot2-V392L* over wild-type *phot2-GFP* expressing plants. The increased activity for leaf flattening and gravitropic positioning in *phot2-V392L* in these conditions shows that the slow recovery of the photocycle in *phot2-V392L* likely increased the sensitivity of *phot2* for phot-mediated responses under low light. It would be interesting to assess whether carbon assimilation is increased in this mutant compared to wild-type *phot2-GFP* in order to evaluate whether stomatal opening was increased and potentially link the gain of *phot2* sensitivity to photosynthetic output. These results confirm the observation that phot activity is critical for plant growth and development under light-limiting conditions (Takemiya *et al.*, 2005) and demonstrate that the *phot2* photocycle is a major contributor to its sensitivity to low fluence rates of light.

It is interesting to consider why such marked gains in sensitivity under continuous light treatments were observed for the *phot2-V392L* photocycle mutant compared to wild-type *phot2-GFP* but not in the photocycle mutants of *phot1* relative to *phot1-GFP*. The most likely explanation for these differences seems to be that the photocycle of *phot2* is much faster than that of *phot1* to begin with (Kasahara *et al.*, 2002), thus making it more likely that slowing the *phot2* photocycle produces a noticeable effect under the fluence rates tested compared to *phot1*. This idea seems to be supported by domain swap experiments, where adding the LOV1+LOV2 photosensory region of *phot1* to the C-terminal region of *phot2* produced an increase in sensitivity that made this chimeric *phot2* apparently as photosensitive as *phot1* (Aihara *et al.* 2008). Slowing the *phot2* photocycle with the V392L mutation made this *phot2* variant more *phot1*-like due to its increased sensitivity, allowing this *phot2* mutant to complement phot responses under low light, which was not possible in the faster-cycling

wild-type phot2-GFP. However, even with this increase in sensitivity, it should be noted that phot2-V392L is still not as sensitive as phot1-GFP and only accumulates a fraction of the biomass of that transgenic line (compare Figure 4.9 and Figure 6.1B). Indeed, this would make it worthwhile to try to generate other, slower photocycle variants of phot2 to see if this increase in sensitivity can be taken even further and possibly allow phot2 slow photocycle mutants to complement low light responses to the same degree as wild-type phot1.

In wild-type plants, the lowered expression of phot2 in darkness and low-light conditions cannot be discounted in an evaluation of its sensitivity. The phot2 transgenic lines in this work are expressed on the *PHOT1* promoter and not the native *PHOT2* promoter. It is not certain that increased biomass accumulation under low light would be observed if the *PHOT2* promoter were used instead, since this would decrease the amount of phot2 protein available to signal under our low-light growth conditions. Still, driving phot2-V392L expression on the *PHOT2* promoter could confer other advantages. If its expression remains stable in higher light conditions, perhaps phot2-V392L would have an effect on phot2-specific responses such as influencing the development of palisade mesophyll cells (Kozuka *et al.*, 2011), where most photosynthesis in the leaf occurs, and increase plant growth through this pathway. Further investigations into the phot2 photocycle by expanding the number of slow photocycle variants and perhaps changing the promoter that drives its expression would likely continue to yield interesting results that could tell us more about phot2 function and how its photocycle evolved for its specific set of roles in plant physiology.

If slowing the phot2, but not phot1, photocycle is able to increase plant growth because phot2 has a faster photocycle than phot1 to begin with, then it is perhaps possible that the phot1 photocycle mutations studied here did not slow the photocycle enough to have a measurable effect on its sensitivity. One way to test this hypothesis could be to try to further slow the phot1 photocycle by introducing multiple photocycle mutations into LOV2 simultaneously, such as N476L-L558I, which showed a very slow photocycle *in vitro* (Figure 3.9). However, the two photocycle mutant combinations tested *in vitro* for this work were N476L-L558I and N476L-V525R, each of which contains the N476L variant, which as a single mutation proved to be slow to recover in LOV1+LOV2 *in vitro* but not in full-length phot1 *in vivo* (Figures 3.7 and 4.7). The N476L variant therefore may not be a good candidate to use to generate combinations of mutations to further slow the phot1 photocycle *in vivo*. Combining the V478I and L558I mutations may produce a very slow photocycle *in vivo*, as each of these mutants singly shows a slow rate of recovery of the phosphorylated state of NPH3 following a light treatment and return to darkness (Figure 4.7). One potential disadvantage of using

this particular combination may be that the V478I variant has pronounced functional defects for phototropism (Figure 4.8), and this may be exaggerated in the double mutant. Furthermore, since the V478L mutant appears to be non-functional in continuous light (Figure 4.10), it may be best to avoid modulating the photocycle by introducing any variations at that residue. If the phot1 photocycle could be further slowed by carefully selecting combinations of photocycle mutations, perhaps increases in activity could be observed using continuous light treatments.

Furthering the hypothesis that the phot1 photocycle may not have been slowed enough, it is possible that the introduction of mutations to the well-conserved LOV2 domain usually leads to a certain degree of signaling defects, but that in phot1, which is quite sensitive as a wild-type photoreceptor, these defects outweigh any increase in sensitivity. On the other hand, in the faster-cycling phot2, the effect of the introduced defects is ameliorated by the large increase in sensitivity resulting from slowing the dark reversion of phot2 (illustrated in Figure 6.2). In addition to making even slower photocycling phot1 variants, this hypothesis could be tested by introducing photocycle mutations into a mutant version of phot1 that is functional but less sensitive than wild type, such as L2K. If full-length phot1 is simply too sensitive to easily observe substantial benefits to a slower photocycle, then perhaps clear increases in sensitivity can be observed using L2K, which is ordinarily not very sensitive to low-intensity light (Sullivan *et al.*, 2008). A slower L2K photocycle would be likely to enhance its sensitivity for petiole positioning and phototropism under low light, perhaps leading to phenotypes similar to those observed in the 24B and 24C suppressor mutants.

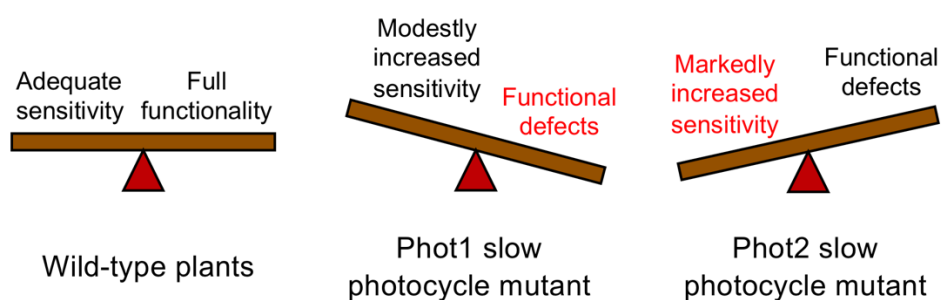


**Figure 6.2: Illustration of the compromise between increasing phot sensitivity and introducing functional defects.** It may be that the photocycle mutations introduced into LOV2 caused functional defects in both phot1 and phot2, but that the increase in sensitivity was much larger in phot2 than phot1, overcoming some of the defects brought on by the mutations in phot2. For phot1, the effects of the photocycle mutations may have negatively impacted functionality with very little benefit in terms in sensitivity.

Alternatively, the reason no increased sensitivity was observed in continuous light for the phot1 slow photocycle mutants could be that there are factors impacting the signal output of

phot1 but not phot2 *in vivo*, such as phot1-specific suppressors (see discussion in 4.3.2) or structural differences between phot1 and phot2 that causes the signaling defects to be more prevalent in phot1 than phot2. This possibility could be examined using the phot1-V478L transgenic line, which appears to be non-functional for phot1 responses under continuous light conditions (Figure 4.10). A genetic screen could be conducted on EMS-mutagenized seeds of phot1-V478L to try to isolate those possible suppressors. The screening conditions could simply be to look for signs of phot1 functionality, such as individuals with fully expanded leaves and wild-type-like petiole positioning under ordinary plant growth conditions, such as long days under  $100 \mu\text{mol m}^{-2} \text{s}^{-1}$  of white light. In addition to possible suppressors, any individuals with increased functionality could be reversion mutants that either mutate the V478L lesion back to the wild-type allele or possess a second mutation, likely also within LOV2, that reduces the signaling defects caused by introduction of the V478L variant. A similar approach was used with transgenic lines overexpressing phyB to identify EMS mutants that possessed lesions within phyB itself that reduced the high degree of sensitivity resulting from overexpression, hence identifying residues that were important for phyB signaling (Wagner and Quail, 1995). Though this would be a work-intensive tactic to answer the question of whether a suppressor acts on strongly active phot1 variants or to identify mutations that could be paired with V478L to increase function, if identified, these pieces of information would be very valuable to our understanding of phot1 activity.

Another aspect of the phot photocycle worth considering is whether activity of phot1 or phot2 photocycle mutants is substantially altered by temperature. PhyB was recently reported to be a thermosensor, with its dark reversion following light activation hastened by increased temperature such that phyB responses are modulated through the combined inputs of light and temperature (Legris *et al.*, 2016; Jung *et al.*, 2016). The single *Marchantia* phot was also reported to act as a thermosensor through its photocycle, with no activity for its chloroplast cold avoidance response observed in the fast photocycle mutant V478T (*Arabidopsis* phot1 amino acid numbering) at 4°C (Fujii *et al.* 2017). Whether the photocycle of phot1 or phot2 is affected by temperature changes in *Arabidopsis* has not yet been determined, though it is likely since LOV domain photocycles are strongly influenced by temperature *in vitro* (Harper *et al.*, 2004). It would be expected that slow phot photocycle mutants would sustain their activity better than wild type at high temperatures due to their slower rate of reversion. Phototropism would be a good response to study, because it is a relatively fast-acting response and would not require long-term growth at high temperature, which could produce many non-specific effects. However, it is not clear whether the slow photocycle mutants would show a stronger response, since none of them are fully functional

for phototropism at room temperature. Furthermore, because hypocotyl elongation is increased by high temperatures, the ability of the seedlings to easily bend toward the stimulus may be compromised by high temperature independent of phot activity. However, if an experiment can be devised that can separate phot responses from growth effects, it would be an interesting avenue of investigation, especially with phot2-V392L, since this mutant shows increased sensitivity that is easy to measure.

Through these investigations, we have been able to explore the role of the phot photocycle in plant growth and development. Under continuous light, all of the phot1 photocycle mutants generated except for the V478L variant, complemented phot1-mediated responses to varying degrees, though there was no clear gain in sensitivity for the slow photocycle mutants for phototropism (Figure 4.6). Unexpectedly, the fast photocycle mutants did not show decreased responsiveness for phototropism under continuous light (Appendix Figure 6.2B). However, when the sensitivity of these mutants to brief light pulses was tested, it was found that the slow photocycle mutant phot1-L558I was more responsive than phot1-GFP for chloroplast accumulation and that the fast photocycle mutants showed decreased chloroplast accumulation. Based on these results, it can be concluded that the phot1 photocycle is critical for sensitivity to pulsed light treatments. Hopefully, this result can be expanded to other responses, such as phototropism or stomatal opening in response to pulses. Nonetheless, the role of the phot1 photocycle under continuous light remains less clear and needs further investigation to see whether the phot1 photocycle can be further slowed or if there is a suppressor acting on phot1 activity in these mutants, limiting responses under continuous light. In contrast to phot1, the phot2 slow photocycle mutant phot2-V392L shows steady-state increases in phot activity, which allows these mutants to grow better than plants expressing wild-type phot2 under low light conditions. The result that the slow photocycle mutant phot2-V392L accumulates more biomass under low light than wild-type phot2, along with the increased chloroplast accumulation of phot1-L558I in response to pulsed blue light, affirms that the phot photocycle is central to sensitivity and modulates photoreceptor activity *in vivo*.

### **6.3 Examination of phot1-V478L functionality**

Investigations into the phot1-V478L slow photocycle mutant indicated that that it could not complement phot1 responses under continuous light (Figure 4.10). In spite of these severe deficiencies in phot1-mediated responses, phot1-V478L exhibits phot1 autophosphorylation and NPH3 dephosphorylation (Figure 4.10). Surprisingly, the phot1-V478L mutant has since

been found to be able to mediate chloroplast accumulation in response to pulses (Dr. Justyna Łabuz; Appendix Figure 6.3), indicating that some function could be retained under certain conditions. Given this result, it would be interesting to examine whether phot1-V478L has more functionality under very low light growth conditions, as observed for its phot2 equivalent, phot2-V392L (Figure 6.1).

Further investigations using the single LOV2 domain harboring the V478L mutation revealed structural perturbations that may contribute to its lack of functionality (Figure 4.11). When the structural studies were initially performed, we hypothesized that the position of V478 within LOV2 may be affecting signaling. This valine residue is located in a part of LOV2 crucial for signaling, lying between the photoactive cysteine, which forms the covalent photoadduct with FMN following light sensing, and Q575 (Figure 6.3). The glutamine at position 575 changes conformation to alter its hydrogen bonding pattern upon light sensing; this conformational change is thought to be crucial for translating the formation of the covalent photoadduct to the unfolding of the J $\alpha$  and A' $\alpha$  helices, eventually allowing the kinase domain to initiate signaling (Nozaki *et al.*, 2004; Jones *et al.*, 2007; Nash *et al.*, 2008; Peter *et al.*, 2010). Since the NMR data was not high-quality enough to assign most of the peaks in the spectra to specific amino acid residues, including Q575, this hypothesis could not be explored. Nonetheless, it is worth noting that introduction of the mutation Q575L to full-length phot1 was reported to reduce its autophosphorylation activity *in vitro*, which may be due to reduced conversion from photoadduct formation to conformational change in this mutant (Jones *et al.*, 2007). The V478L mutant, on the other hand, shows light-dependent autophosphorylation activity *in vitro* and *in vivo* (Jan Petersen, Stuart Sullivan, and John M. Christie, unpublished data) as well as NPH3 dephosphorylation *in vivo* (Figure 4.10), somewhat diminishing the possibility that the conformation of Q575 is somehow altered in V478L.

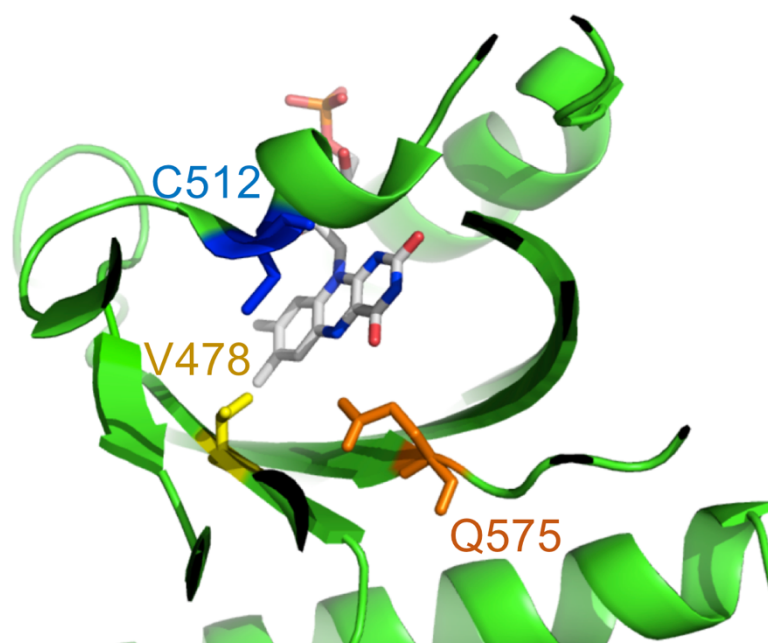


**Figure 6.3: Position of V478 within LOV2.** Halavaty and Moffat (2013) crystal structure of phot1 LOV2 with the photoactive cysteine C512, V478, and the glutamine Q575 residue, which is thought to be important for translating light perception to kinase activation, indicated.

When the NMR study was followed up with size-exclusion chromatography (SEC), it was found that a portion of the pool of LOV2-V478L was present as a dimer in darkness, which is generally not observed in wild-type LOV domains (Figure 4.11). Following these results, the dimerization of full-length phot1-V478L was investigated *in vivo* using a BiFC assay. The results indicated that the V478L variant could dimerize normally in the light, which matched the SEC data for light-treated LOV2-V478L (Figure 4.12). As discussed previously (Section 4.3.4), the dimerization of phot1-V478L in the dark could not be determined due to technical issues. It is still possible that the SEC data showing dimerization of LOV2-V478L in the dark potentially indicates the underlying reason that phot1-V478L is non-functional. However, though studies presented in Chapter Four delved into which phot1 domains are required for dimerization (Figures 4.13 and 4.14), it has not yet been established that light-dependent dimerization of phot1 is required for its activity, as it is, for example, for cryptochromes (Sang *et al.*, 2005; Rosenfeldt *et al.*, 2008). One of the first things that ought to be explored is whether “blind” phot1, in which both of the LOV domain cysteines are mutated (phot1-C234A-C512A) to eliminate photoadduct formation, can dimerize. It would be expected that, since phot1 dimerization is reported to be light-dependent (Kaiserli *et al.*, 2009; Xue *et al.*, 2018), blind phot1 would be unable to dimerize. Not only could this piece of data further establish that phot1 dimerization is light-dependent, but if this hypothesis is borne out, it would be an extremely valuable negative control for the BiFC studies and

provide a measure of the extent to which spurious dimerization occurs, laying the foundation for investigating whether phot1-V478L dimerizes in the dark *in planta*.

Aside from some of the indications of structural disturbances in LOV2-V478L that were observed in these studies, it remains possible that the non-functionality of phot1-V478L is related to its very slow photocycle. This hypothesis is supported by the fact that phot1-V478L autophosphorylates and triggers NPH3 dephosphorylation (Figure 4.10) and can complement chloroplast accumulation in response to pulses of blue light (Appendix Figure 6.3). That a very slow photocycle may cause low functionality under continuous light is supported by the observation that phot1-V478I also lacks complete functionality, but it is more functional than phot1-V478L (Figure 4.10) and also appears to possess a faster photocycle than phot1-V478L *in vivo* as inferred from NPH3 phosphorylation status (Figure 4.10). Furthering the possibility that function is tied to the photocycle, the fast photocycle mutant V478T, which is at the same position, appears to be fully functional for phot1-responses *in planta* (Appendix Figures 6.1 and 6.2). For these three variants, there is a correlation between how slow the photocycle is and how functional the mutant is for phot1 responses. The slow photocycle of V478L could render it near-constitutively active *in vivo*, with the pool of phot1 protein almost completely in its lit state under most light conditions, which, as discussed earlier, could somehow reduce its responsiveness. Indeed, constitutive variants of phot1 do not tend to signal constitutively *in planta*. For example, the phot1-R472H mutant, though constitutively autophosphorylated, requires strong light to drive its phototropic response (Petersen *et al.* 2017). Even taking this possibility into account, whether photocycle slowness belies functionality cannot be determined from our data. Although the photocycles of the three V478 mutants are quite different, the fast-cycling threonine variant has a polar side chain, while the leucine and isoleucine variants are aliphatic. These alterations in the chemical nature of the side chains at position 478 alone could be sufficient to explain the differences in functionality observed *in planta*.

All told, the possibilities for the deficiencies in phot1-V478L function are either that there is some sort of fundamental structural issue inhibiting efficient signaling, as inferred from the dimerization of LOV2-V478L in darkness, or that the photocycle is so slow in phot1-V478L that functionality is limited, perhaps through the activity of a suppressor. Structural studies of LOV2-V478L are still underway, including further NMR experiments to obtain data that can better resolve the position of specific amino acids within the domain. As mentioned in the previous section, identifying whether suppressors act on the phot1 photocycle mutants like phot1-V478L could be resolved with a suppressor screen.

Regardless of the mechanism of the disruption, it would seem that the V478 residue is important for normal phot1 activity and further investigation can help establish the basis of the non-functionality of phot1-V478L as well as provide some clues as to how phot1 functions on a molecular level.

## 6.4 Suppressors of phot1

When the EMS-mutagenized population of transgenic plants expressing L2K, a less-sensitive truncation of phot1, was screened for increased activity for petiole positioning under low light, three lines were identified that appeared to have greater sensitivity for this response than wild-type L2K. Two of the mutants, 24B and 24C, may be genuine suppressors of phot1 activity while the 21D line is mutated in *PHYB* and could exhibit increased petiole positioning through a pathway independent of L2K sensitivity. The 24C mutant appears to have increased sensitivity due to overexpression of the L2K protein, leading to greater activity than L2K for all of the phot1-mediated responses tested in this study. The 24B mutant, meanwhile, may contain a missense SNP within *SPL14*, a transcription factor that has not been well-characterized in *Arabidopsis*, occluding any obvious mechanism of suppressing phot1 activity. As a connection between *SPL14* and phot1 activity has not been made before this study, and phot1 (or its L2K truncation) has never been constitutively overexpressed, both of these putative suppressors act on phot1 activity through mechanisms that have not been previously identified.

It is interesting to consider the means by which the L2K protein is overexpressed in the 24C background. The level of *L2K* transcript levels is elevated four-fold in 24C relative to the L2K parent (Figure 5.8B), and it was established that this increase in transcript levels is not likely to be due to a lesion either within the 35S promoter driving L2K expression or downstream of the transgene insertion site (Appendix Figure 5.5). If there is a suppressor SNP acting in the 24C background, does not seem that it is acting to somehow influence transcript levels, since the four-fold increase in transcript is modest compared to the 14.6-fold enhancement in L2K protein expression in the 24C background. However, how the 24C SNP would alter L2K protein accumulation is not obvious, since L2K remains light-labile in the 24C background (Figure 5.9). It is possible that in addition to turnover induced by strong light, there is a second regulatory mechanism of phot1 protein levels that modulates expression independent of light conditions, and this is where the 24C SNP acts (modelled in Figure 6.4A), but there have been no reports of this kind of regulation of phot1 protein to our knowledge. However, that phot1 protein levels are subject to this sort of tight control is

supported both by the low protein expression of phot1 when it is driven by the constitutive 35S promoter as well as the reduced protein levels of constitutively active phot1 alleles (Sullivan *et al.*, 2008; Petersen *et al.*, 2017). It will be interesting to see whether the 24C lesion leads to overexpression of full-length phot1 as well as L2K, enabling overexpression studies on how increased phot1 protein levels affect plant growth, as has been performed for other plant photoreceptors (Boylan and Quail, 1991; Wagner *et al.* 1991; Lin *et al.* 1998). For this work to be performed, the causal gene needs to be identified. As discussed (Section 5.3.5), to identify a better set of candidate SNPs, the 24C background needs to be refined by eliminating its phyB lesion and then re-sequenced. Identifying the 24C suppressor is important, since it can aid in our understanding of how phot1 protein is regulated to modulate its activity.

In contrast to the 24C mutant, the 24B background has a reasonable candidate suppressor in *SPL14*. Since *SPL14* is a transcription factor and operates in the nucleus (Stone *et al.* 2005), while phot1 is localized to the plasma membrane, it seems likely that *SPL14* has an indirect effect on L2K activity, perhaps by transcribing genes that themselves act on phot1 (modelled in Figure 6.4B). Though the sequence to which *SPL14* binds has been identified (Liang *et al.*, 2008), no target genes have been identified as yet. Once the *SPL14* lesion is verified in the 24B background and complementation studies have been performed, it may be informative to perform chromatin immunoprecipitation followed by sequencing (ChIP-seq) to identify the target genes of this transcription factor. Because other SPL family members have been implicated in the shade avoidance pathway (Xie *et al.*, 2017), it seems plausible that the transcriptional activity of *SPL14* may relate to light signaling or phot1 activity.

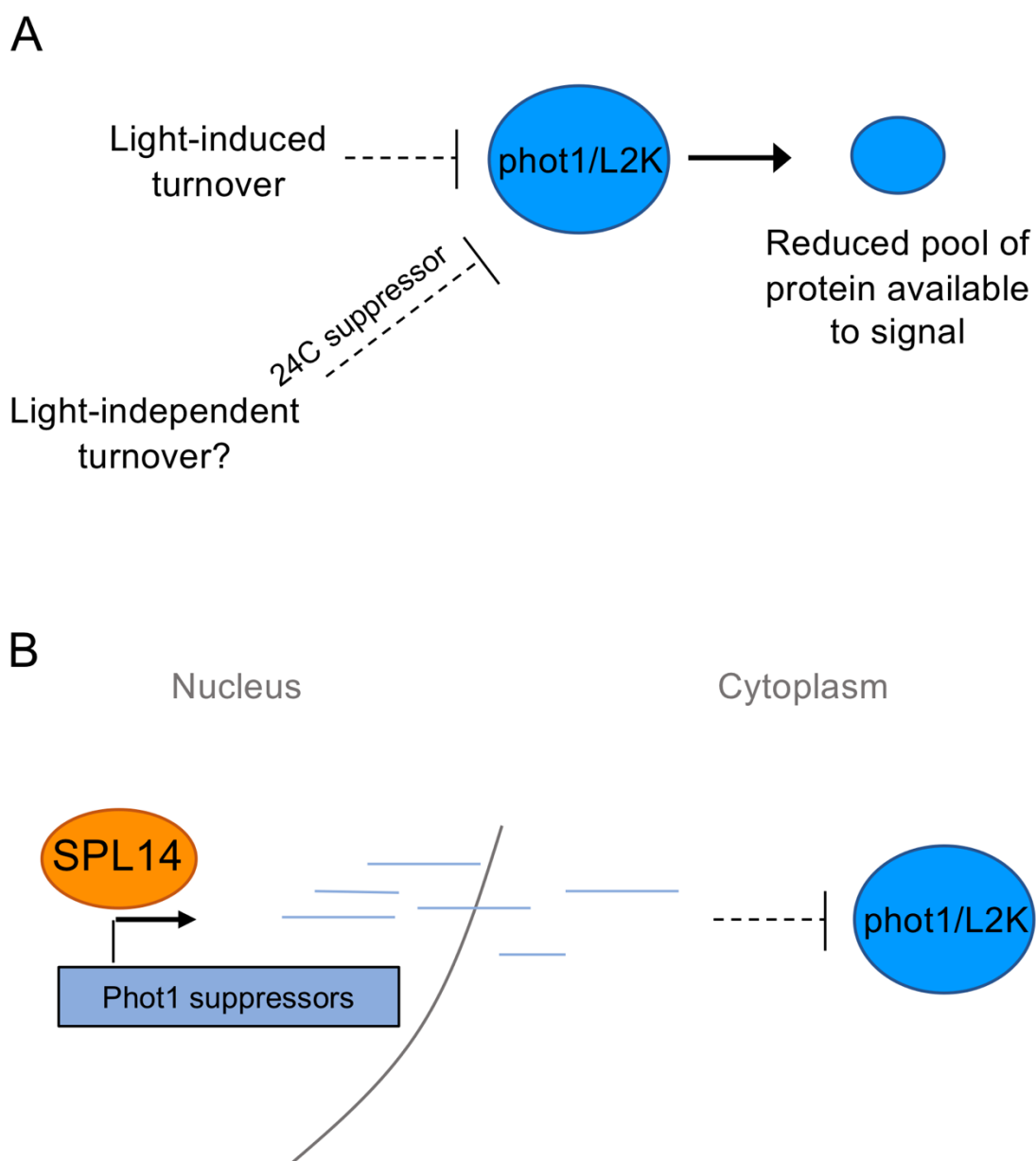


**Figure 6.4: Possible mechanisms of suppression in the 24C and 24B suppressor mutants. A.** In wild-type plants, the 24C suppressor may act to control phot1 or L2K protein accumulation independent of light condition, reducing the overall protein expression. In the 24C mutant background, mutation to this possible suppressor increases L2K protein levels, causing enhanced sensitivity. **B.** SPL14 may control the transcription of suppressors of phot1 activity, which in turn could negatively regulate L2K activity downstream. In the 24B mutant background, the putative mutation to *SPL14* may therefore lead to enhanced sensitivity for phot1-mediated responses.

Given the success of this EMS screen using the L2K background, it would be worthwhile to try to extend it, either by continuing with the petiole positioning screen, which was not performed to saturation, or by inspecting the population for a different phenotype. Since the studies performed here using the phot2 photocycle mutant V392L established that differences in biomass accumulation and leaf flattening under  $25 \mu\text{mol m}^{-2} \text{s}^{-1}$  red light and  $0.1 \mu\text{mol m}^{-2} \text{s}^{-1}$  blue light can be attributed to differences in sensitivity, the population could

be screened for individuals with flatter leaves than L2K, which would be expected to resemble a *phot1phot2* mutant under these conditions due to its lowered sensitivity. This could potentially help identify mutants in a phot pathway other than petiole positioning and possibly limit the identification of non-specific mutants by not screening for a response intimately involved in SAS.

#### 6.4.1 Possible signal integration between phyB and phot1

As examined earlier (Section 5.3.2), the identification of the 21D mutant in our screen, which encodes a mutant allele of the phyB red light receptor, raised the possibility that phyB and phot1 act antagonistically to determine petiole positioning in young plants. NPH3 may be a genetic link between phot1 and phyB. When it was reported that phyB suppresses phot1 activity for leaf flattening, leading to flatter leaves in *phyB* mutants than in wild-type plants, it was found that a *phyBnph3* double mutant partly recapitulated leaf curling, possibly demonstrating that phyB acts on NPH3 to influence phot1 activity (Kozuka *et al.*, 2012). There is a large degree of overlap between the leaf flattening and petiole positioning pathways (Inoue *et al.*, 2008B; de Carbonnel *et al.*, 2010), so it is perhaps possible that phyB acts on NPH3 in the same way to inhibit phot1 activity for petiole positioning (Figure 6.5A). It could be that phyB modulation of PIF transcriptional activity somehow indirectly influences NPH3. In addition to this possibility, whether NPH3 phosphorylation status or protein expression is altered in the *phyB* background should be explored to address the question of whether NPH3 represents a link between phyB and phot1 activity.

Another connection between phy and phot activity seems to exist in the gravitropic orientation of seedlings under low blue light, a response in which phyA is thought to repress the gravitropic pathway, with phot1 responsible for the maintenance of vertical growth (Lariguet and Fankhauser, 2004). This response is simple to assess, and the experiment can be performed on seedlings, making it another good starting point for investigating how phy and phot signaling integrate. Candidate genes can be rationally identified and then tested to see whether they are involved in the interaction between phot and phy for this response or if phy and phot activity can be uncoupled. PKS proteins would be good contenders, since PKS4 has already been implicated in gravitropic orientation under red light (Schepens *et al.*, 2008). Furthering our understanding of this response, the studies conducted here have shown that phot1 activity to maintain growth against the gravity gradient does not depend on NPH3 or RPT2, though the presence of these proteins does enhance the response (Appendix Figure 5.3; modelled in Figure 6.5B). It would be interesting to see whether combining *nph3* and

*rpt2* mutations with mutants of *PKS* genes, such as a *nph3pks4* double mutant, further reduces phot activity for this response. Further dissection of gravitropic orientation under low blue light could help us understand how phys and phots work together to influence seedling establishment.

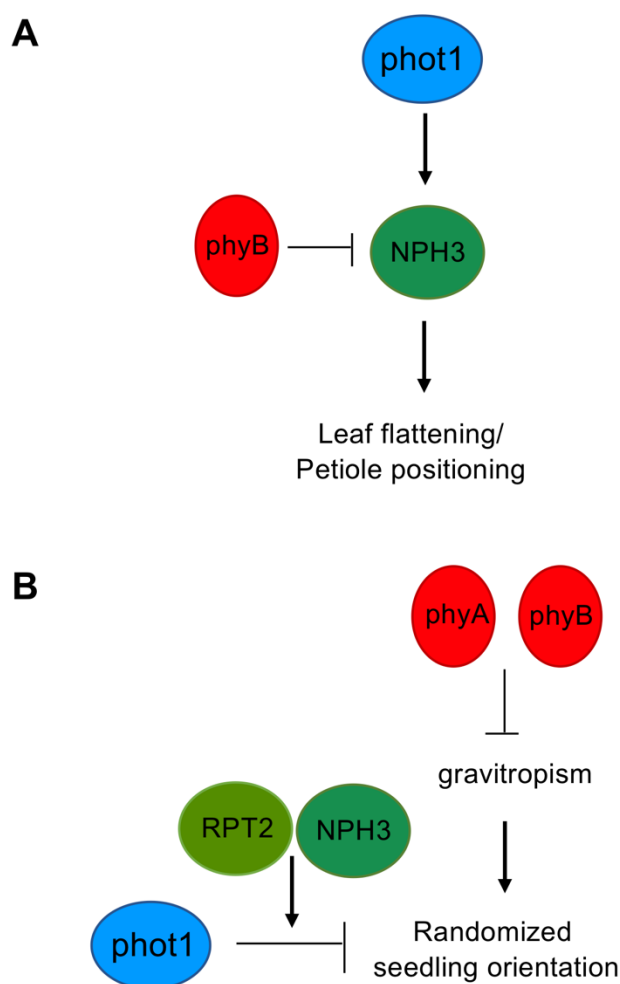


**Figure 6.5: Hypothesized mechanisms for phy and phot1 interactions.** **A.** phyB may act on NPH3 to suppress phot1 activity for some responses. As proposed in Kozuka *et al.* (2012), phyB may suppress NPH3 transduction of phot1 activity for leaf flattening. We suggest a similar mechanism may be in place for the petiole positioning response as well, leading the *phyB* mutation found in the 21D EMS mutant to have enhanced sensitivity for this response. **B.** Proposed relationship between phot1, RPT2, NPH3, phyA, and phyB for upward growth of seedlings under low blue light. PhyA, and secondarily phyB, inhibits gravitropic growth under low blue light, while phot1 antagonizes randomization by acting to maintain upward seedling growth. The work here suggests that, unusually, while RPT2 and NPH3 are not required for this response, they enhance phot1 activity for it.

## 6.5 Perspectives on phot1 sensitivity

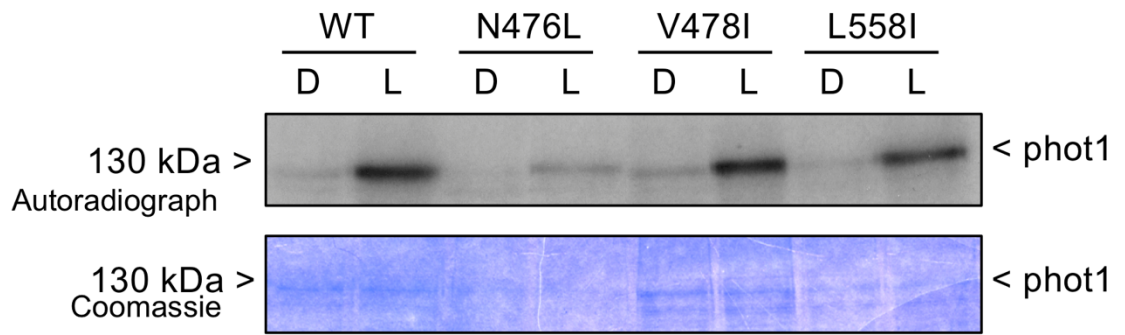
From the work undertaken here, we have learned the sensitivity of phot1 and phot2 can be successfully altered. Modifying the phot1 photocycle increased the sensitivity of the phot1-

L558I slow photocycle mutant, though this enhanced responsiveness appears to be limited to brief irradiations with blue light. Additionally, through identifying putative suppressors that seem to act on phot1 to regulate its activity, we observed increased sensitivity for phot1 responses in transgenic plants expressing the phot1 truncation L2K, which is normally insensitive to low-intensity blue light. From an engineering perspective, this project accomplished its intended goal of altering phot1 activity *in planta*.

Whether increasing phot1 sensitivity is beneficial for plant growth and development remains an open question. Unlike the phy photoreceptors, which exhibit definite increases in sensitivity as well as crop yield with approaches like receptor overexpression (Boylan and Quail, 1991; Wagner *et al.*, 1991; Thiele *et al.*, 1999; Garg *et al.*, 2005), modulating the sensitivity of phot1 has not led to clear-cut benefits to plant growth. Perhaps the most straightforward example of this is the 24C mutant, in which constitutive overexpression of a phot1 variant was observed for the first time. As reported for the overexpression of phys, the 24C mutant had increased sensitivity for all of the phot1-mediated responses tested, including phototropism and petiole positioning. In spite of this, the 24C mutant is a very small plant that does not accumulate as much biomass as the L2K parent (Figure 5.5), an observation that was also made for plants overexpressing the phot2 kinase domain on its own (Kong *et al.*, 2007). Even though sensitivity was increased in this mutant, its limited growth reduces the likelihood that translating the putative 24C suppressor into crop plants would provide any advantage or yield increases. Likewise, the slow photocycle mutants of phot1 demonstrate that there may be limitations to the extent to which phot1 sensitivity can be increased by altering dark reversion kinetics. It seems that, as for ztl (Pudasaini *et al.* 2017) and VVD (Dasgupta *et al.* 2015), the LOV photocycle of phot1 is already exquisitely tuned for its role in modulating plant growth. However, related work modulating the phot2 photocycle showed clear increases in sensitivity relative to wild-type phot2 (Figure 6.1), making phot2 perhaps a better target for future studies on sensitivity than phot1.

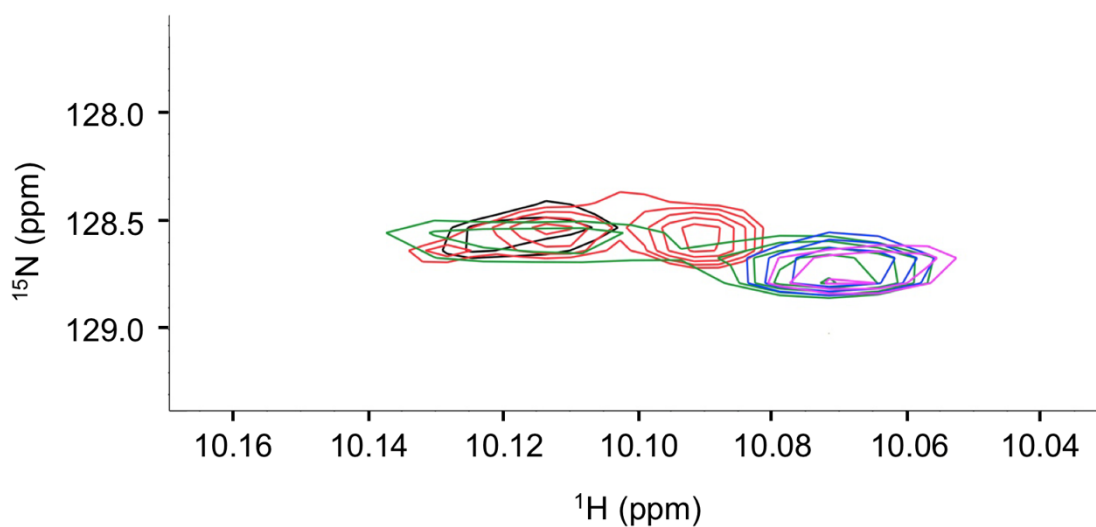
Apart from plant growth, this work has made advances in understanding how phot1 sensitivity is related to its activity and signal transduction by introducing photocycle mutations into phot1 to change its sensitivity, investigating how phot1 is likely to dimerize *in planta*, and how suppressors may interact with phot1 to modulate its activity. If these studies are continued, new frameworks for understanding phot1 signaling can be created, enabling future work.

## Appendix to Chapter 3

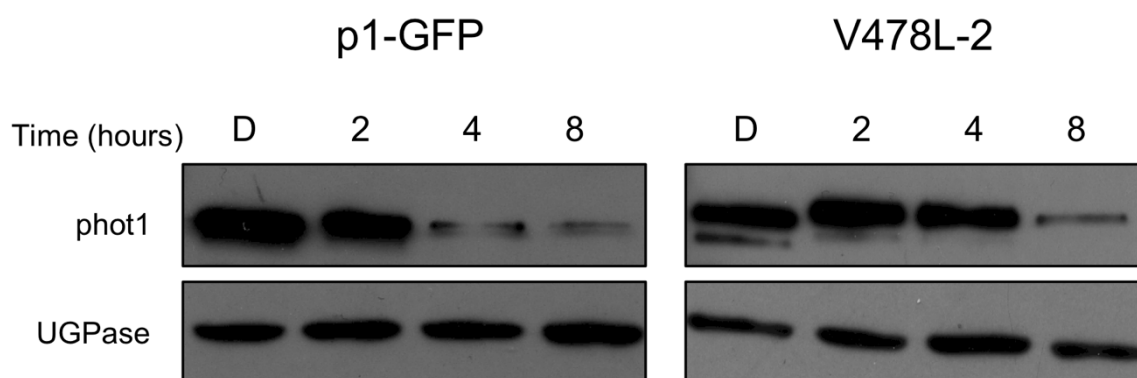


**Appendix 3.1: Alternative autoradiogram demonstrating the autophosphorylation activity of the photocycle mutants *in vitro*.** This experiment is an independent replicate and was performed as described in Figure 3.11

## Appendix to Chapter 4



**Appendix 4.1: Comparison of NMR contours of W553 between wild-type LOV2 and LOV2-V478L.** The black contours represent W553 in LOV2-V478L the dark state, and red contours the lit state; the magenta contours are for W553 in wild-type LOV2 in the dark state, and the blue contours the lit state. The green contours are for the LOV2-R586A mutant which mutates an arginine that was hypothesized to be related to the altered conformation of W553 in the LOV2-V478L mutant.

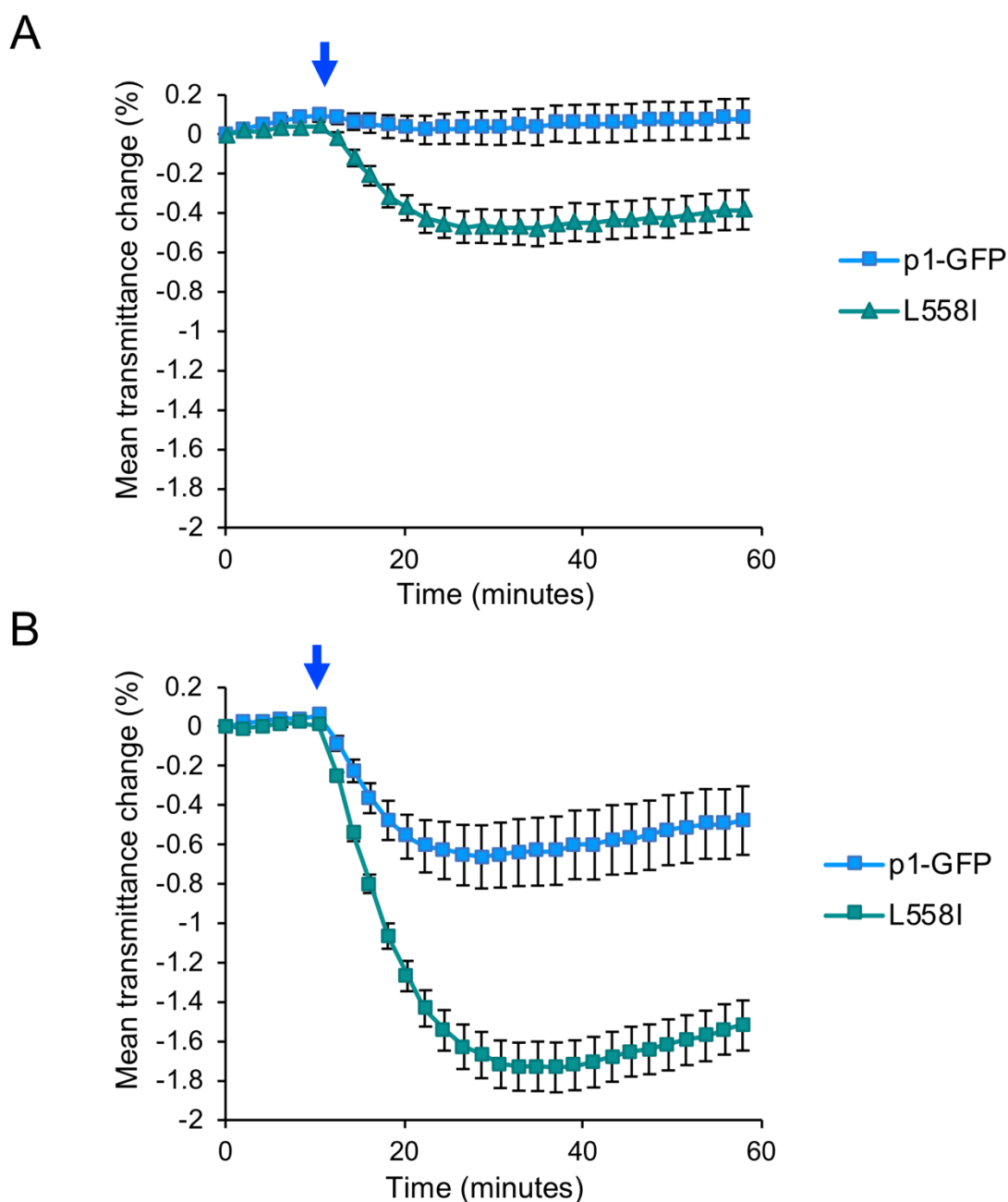


**Appendix 4.2: Protein stability of phot1-V478L.** Western blots of phot1-GFP expression over the course of blue light treatment. Protein extracts were either harvested from 3-day-old etiolated seedlings in the dark (D) or after two, four, or eight hours of illumination with  $150 \mu\text{mol m}^{-2} \text{s}^{-1}$  of blue light from above. Representative results from three independent repeats are shown.



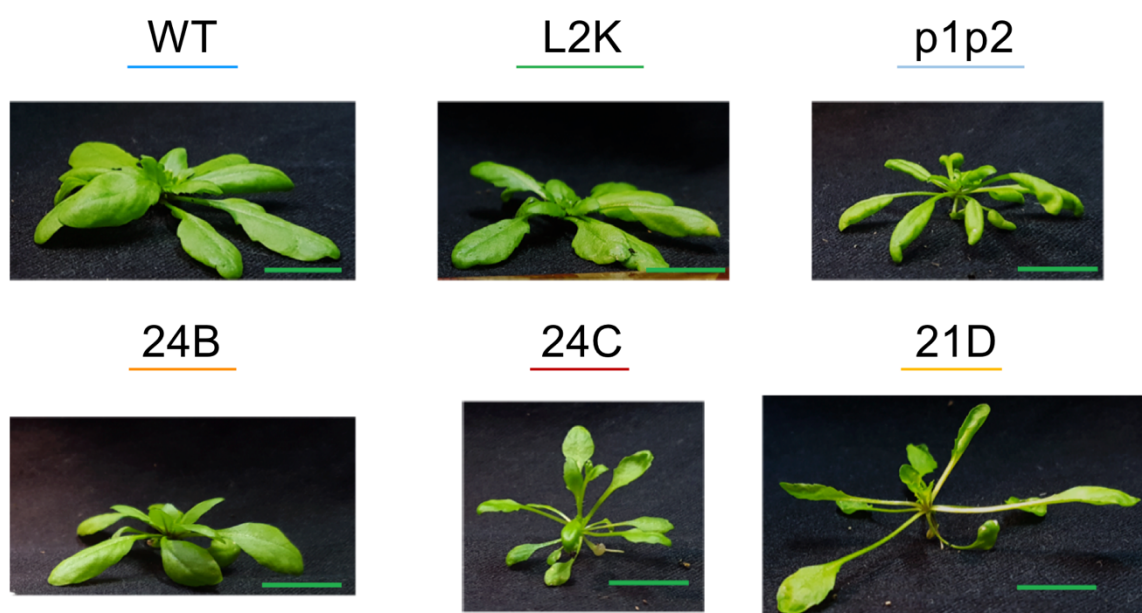


**Appendix 4.4: Phot1-W553L is functional for phototropism and leaf flattening.** The *phot1*-W553L construct was generated as for the photocycle mutants (see Figure 4.1). Three separate pots of *phot1phot2* mutant plants were used for transforming *Arabidopsis* by floral dip. The T<sub>1</sub> seeds obtained were sowed on sand moistened with quarter-strength MS media containing 100 mg/mL kanamycin. Three-day-old etiolated seedlings were given a phototropic light stimulus of  $0.5 \mu\text{mol m}^{-2} \text{s}^{-1}$  blue light for eight hours. Individuals that had a phototropic response were noted. Following phototropism, the plants were left to de-etiolate in white light over night to test for kanamycin selection. Only phototropic individuals were resistant to kanamycin treatment. Arrows indicate two independent transformants exhibiting phototropism. When the kanamycin resistant *phot1*-W553L seedlings were rescued and grown on soil, it was clear that they complemented the leaf flattening response; a representative image is shown.

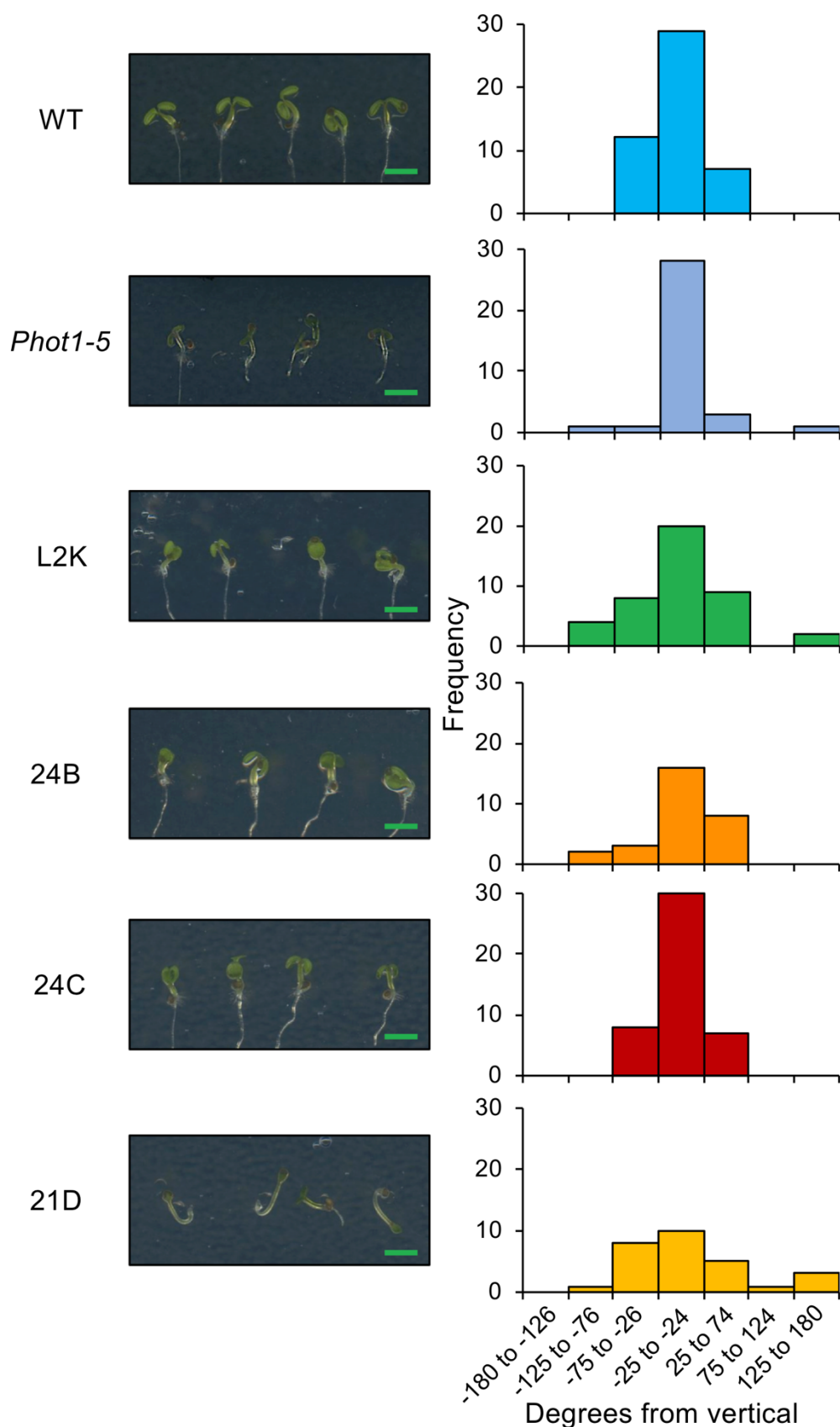


**Appendix 4.5: Chloroplast accumulation of phot1-GFP and phot1-L558I in response to a pulse of blue light.** **A.** Adult plants were dark adapted and then given a 0.1 second pulse of blue light at  $20 \mu\text{mol m}^{-2} \text{s}^{-1}$  ten minutes after the onset of measurement of transmittance of light through a single leaf (indicated by blue arrow). Transmittance was examined using a beam of red light administered at a fluence rate of  $0.1 \mu\text{mol m}^{-2} \text{s}^{-1}$ . A negative change in transmittance indicates chloroplast accumulation, and a positive change chloroplast avoidance. **B.** Adult plants were given a 0.1 second pulse of blue light at  $120 \mu\text{mol m}^{-2} \text{s}^{-1}$  ten seconds after the onset of measurements as above. Both experiments were conducted by Dr. Justyna Łabuz.

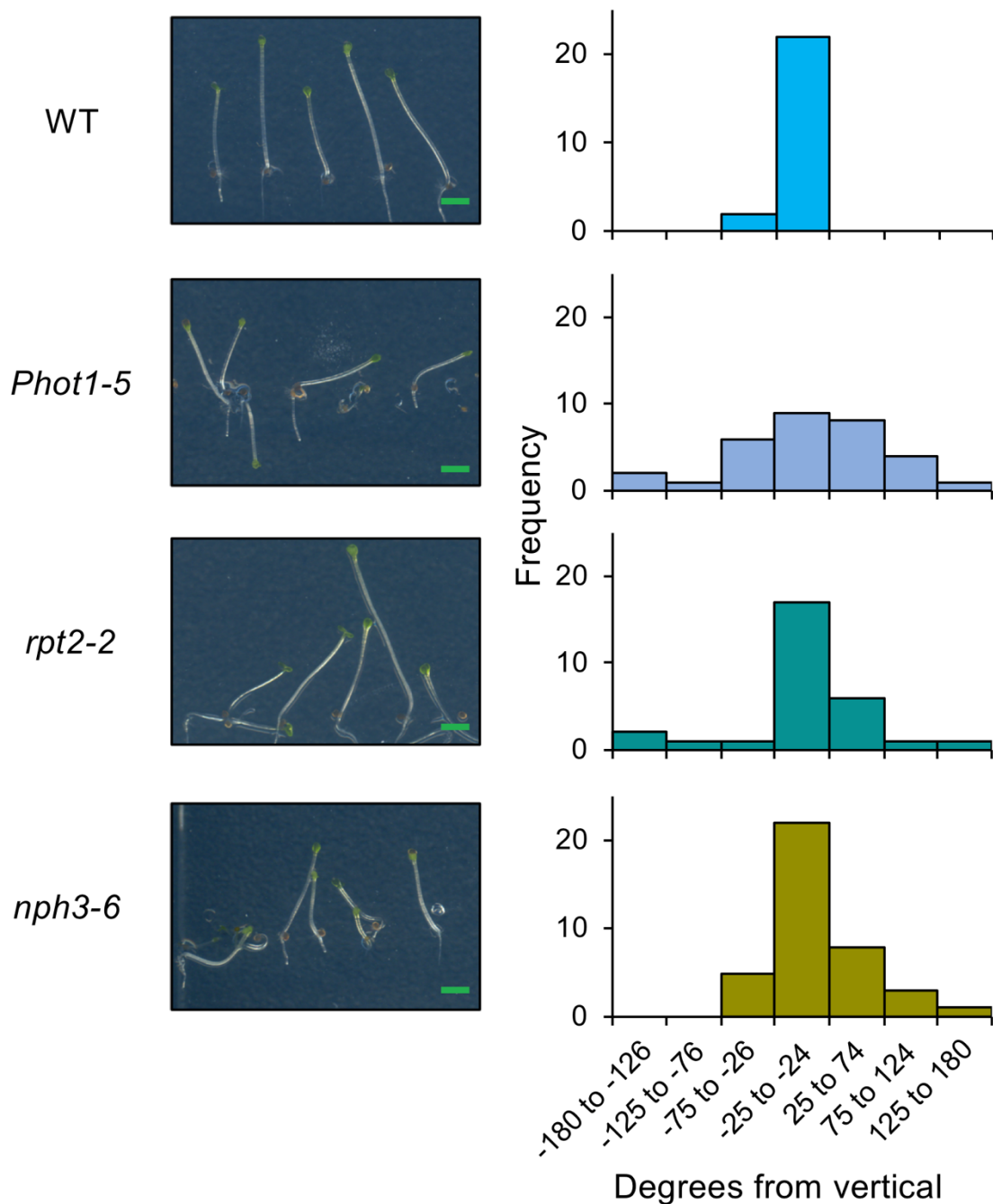
## Appendix to Chapter 5



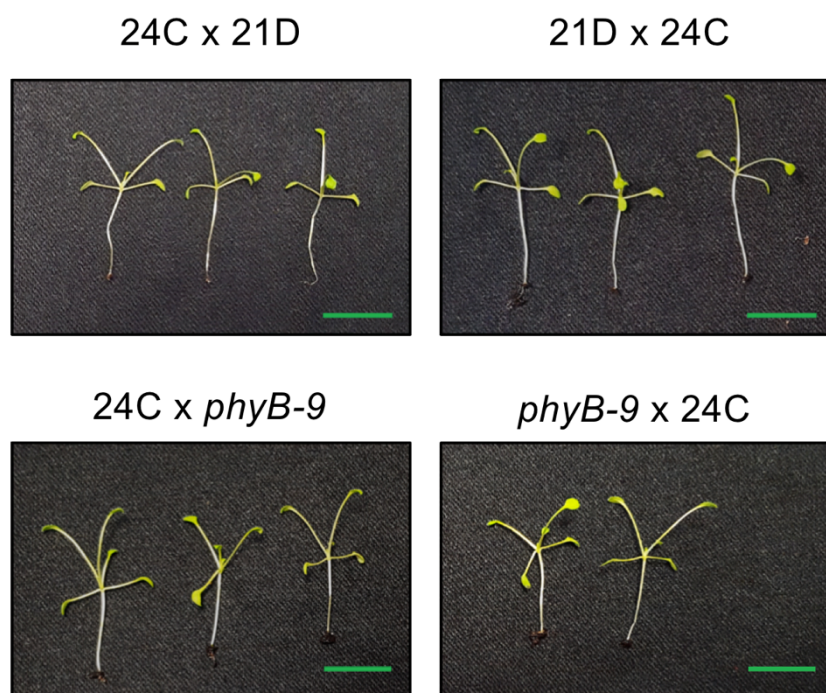
**Appendix 5.1: EMS mutants in profile.** The 4-week-old plants shown in Figure 5.6 viewed from the side. The scale bar is 1 cm.



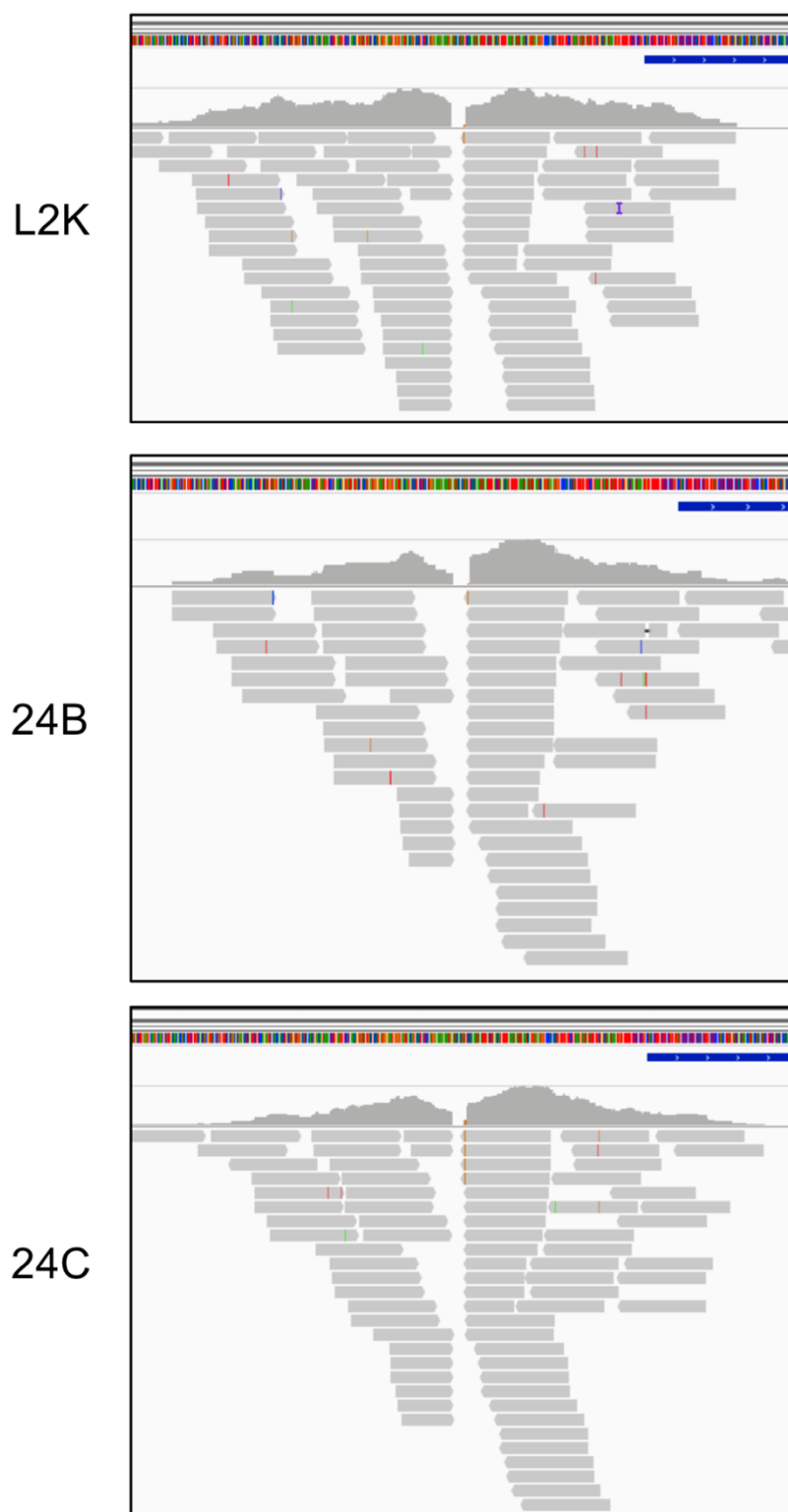
**Appendix 5.2: Gravity sensing is restored in L2K, *phot1-5*, and the 24B mutant under higher light intensities.** Seedlings were grown on half-strength MS agar plates under  $20 \mu\text{mol m}^{-2} \text{s}^{-1}$  overhead blue light for four days and then scanned to quantify the angle of each seedling. The histograms show the distribution of seedling deviation from vertical for each genotype in one representative experiment from three independent repeats. Representative images are shown; scale bar is 2 mm.



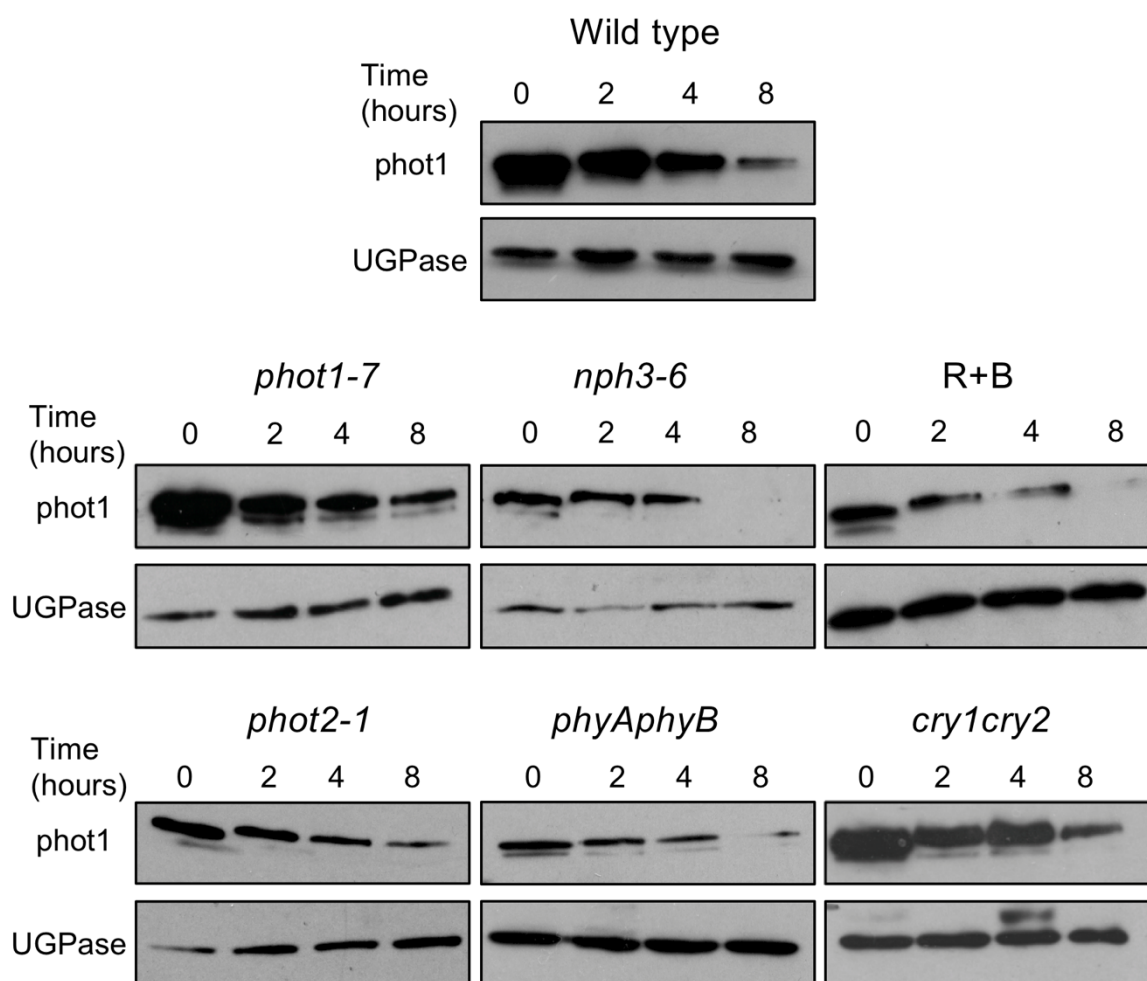
**Appendix 5.3: RPT2 and NPH3 are not required for vertical orientation in low blue light.** Seedlings were grown on half-strength MS agar plates under  $1 \mu\text{mol m}^{-2} \text{s}^{-1}$  overhead blue light for four days and then scanned to quantify the angle of each seedling. The histograms show the distribution of seedling deviation from vertical for each genotype in one representative experiment from two independent repeats. Representative images are shown; scale bar is 2 mm.



**Appendix 5.4: Allelism test of 24C and 21D.** The 24C and 21D mutants were crossed against each other, as was 24C mutants against *phyB-9* mutant. F<sub>1</sub> seedlings were grown for one week under 80  $\mu\text{mol m}^{-2} \text{s}^{-1}$  white light, after which the fluence rate was lowered to 10  $\mu\text{mol m}^{-2} \text{s}^{-1}$  white light for another week. The two-week-old seedlings were then imaged; scale bar is 1 cm.

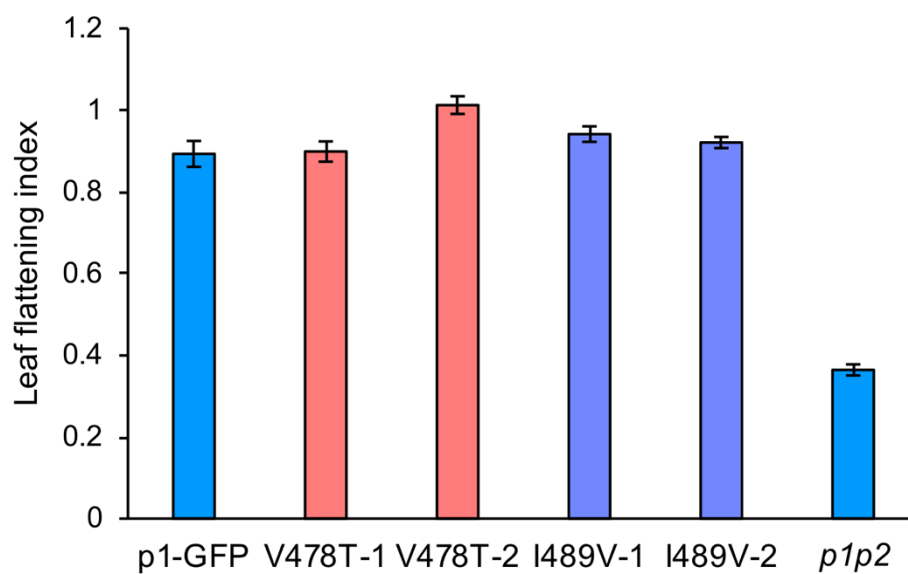


**Appendix 5.5: Comparison of the L2K transgene insertion site between the L2K parent, 24B, and 24C.** The images show the Integrated Genomics Viewer visualization of the deep sequencing reads aligned to the region approximately 500 base pairs up and downstream of the L2K transgene insertion site. The colorful band at the top of the image represents the *Arabidopsis* chromosome 2 sequence. The gray bars in the bottom two-thirds of the image are individual reads generated from sequencing that were mapped to the transgene insertion site. The insertion site is the central gap between the gray bars where no reads aligned due to the transgene insertion. The gray histograms are a visual readout of how many reads aligned to that region of the chromosome. The colored lines in the gray bars indicate polymorphisms in the read; if a true EMS-introduced SNP were present, it would be expected to be present in all of the reads aligning to that particular region.

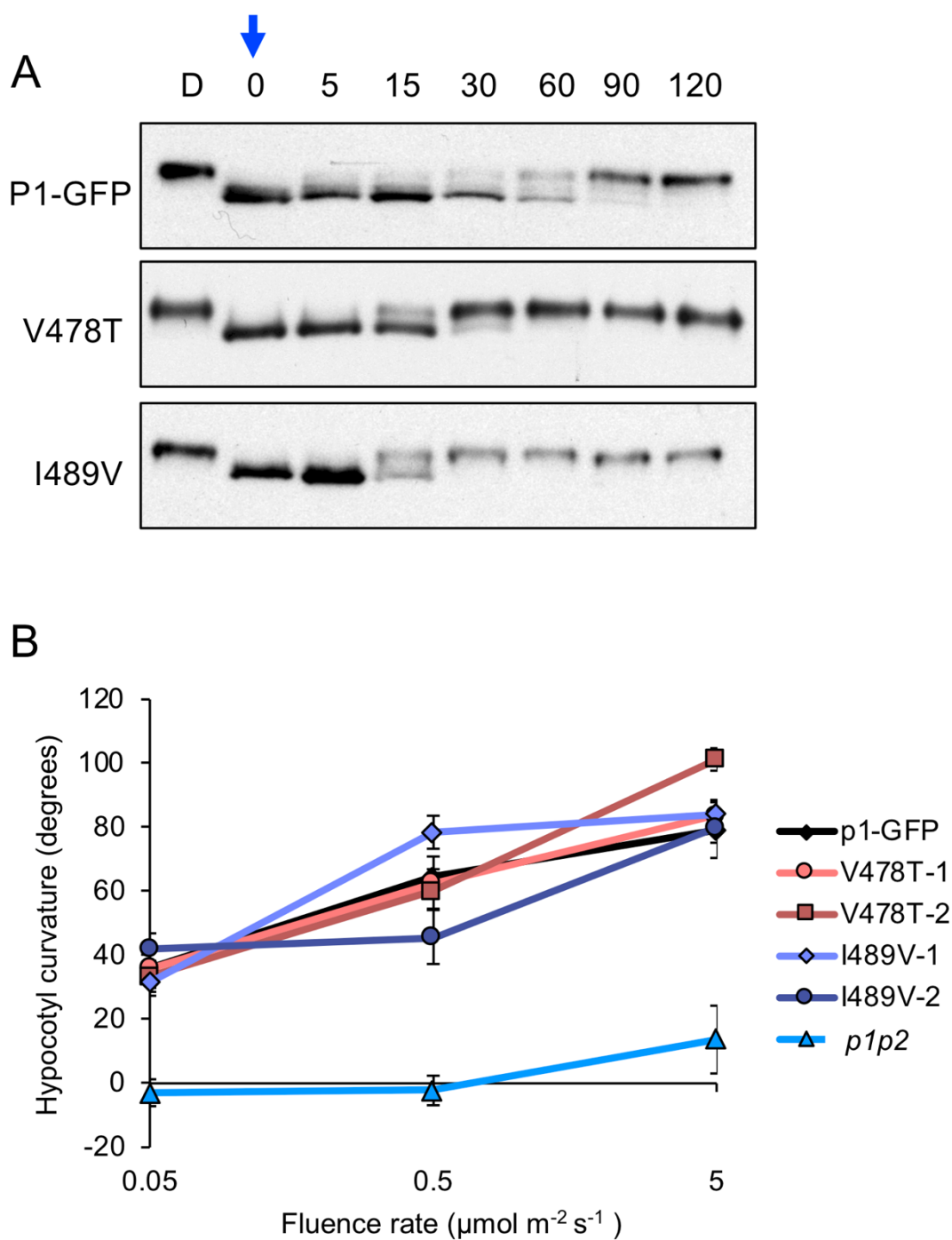


**Appendix 5.6: Protein stability of phot1.** Western blots of phot1 expression over the course of blue light treatment. Protein extracts were either harvested from 3-day-old etiolated seedlings in the dark (D) or after two, four, or eight hours of illumination with  $100 \mu\text{molm}^{-2}\text{s}^{-1}$  of blue light in the indicated mutant backgrounds. R+B is the same experiment in a wild-type genetic background but with simultaneous illumination with  $75 \mu\text{molm}^{-2}\text{s}^{-1}$  blue light and  $30 \mu\text{molm}^{-2}\text{s}^{-1}$  red light.

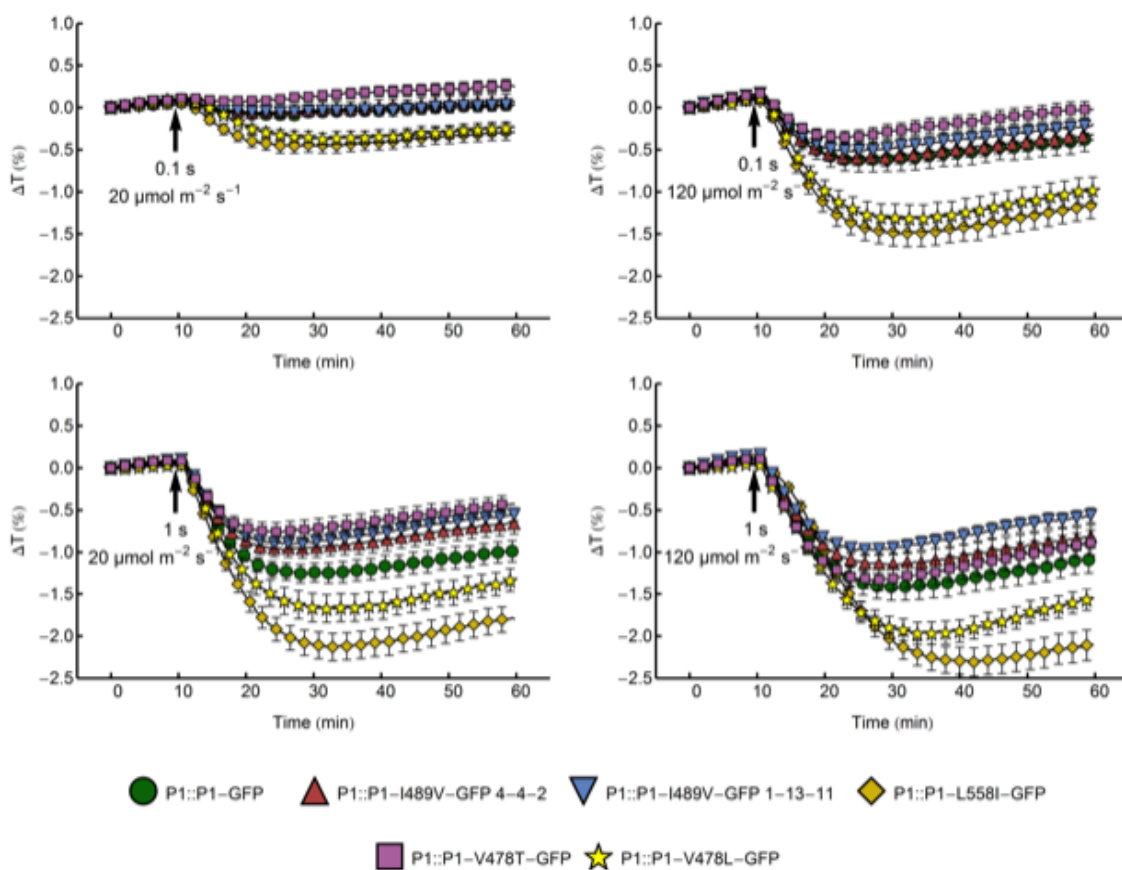
## Appendix to Chapter 6



**Appendix 6.1: Leaf flattening of the fast photocycle mutants *phot1-V478T* and *-I489V*.** Leaf flattening experiments were conducted on four-week-old *phot1*-GFP (*p1*-GFP), the fast photocycle mutant lines, and *phot1phot2* (*p1p2*) double mutant plants grown in long days under  $100 \mu\text{mol m}^{-2} \text{s}^{-1}$  white light for four weeks. The leaf flattening index was calculated as described in Figure 4.3.



**Appendix 6.2: NPH3 phosphorylation status and phototropic response in the fast photocycle mutants.** **A.** Western blots of NPH3 mobility shifts showing NPH3 phosphorylation status over time. Protein extracts were either harvested from 3-day-old etiolated seedlings of *phot1*-GFP (*p1*-GFP) or the fast photocycle mutant transgenic lines in the dark (D) or immediately following an overhead irradiation of blue light at 20  $\mu\text{mol m}^{-2} \text{s}^{-1}$  for 15 minutes (0; blue arrow). The seedlings were then returned to darkness and protein extracts were harvested at intervals of 5, 15, 30, 60, 90, and 120 minutes following the irradiation. Representative lines from three independent experiments are shown; these experiments were conducted by Dr. Stuart Sullivan. **B.** Phototropic response of the fast photocycle mutants at varying light intensities. Phototropism was conducted on three-day-old etiolated seedlings of the fast photocycle mutants, *phot1*-GFP (*p1*-GFP) and the *phot1phot2* (*p1p2*) double mutant as described in Figure 4.6 using the indicated fluence rate of blue light as the stimulus. Results show one representative experiment from three independent repeats using 18–36 seedlings per genotype for each experiment. Error bars are standard error of the mean.



**Appendix 6.3 Chloroplast accumulation of the photocycle mutants in response to a pulse of blue light.** A. Adult plants were dark adapted and then given a pulse of blue light at the noted duration and fluence rate ten seconds after the onset of measurement of transmittance of light through a single leaf (indicated by black arrow). A negative change in transmittance indicates chloroplast accumulation, and a positive change chloroplast avoidance. Dr. Justyna Łabuz conducted the experiment and generated the figure.

## List of References

- Ádám, É., Hussong, A., Bindics, J., Wüst, F., Viczián, A., Essing, M., Medzihradzsky, M., Kircher, S., Schäfer, E. and Nagy, F. (2011) 'Altered dark- and photoconversion of phytochrome B mediate extreme light sensitivity and loss of photoreversibility of the phyB-401 mutant', *PLoS ONE*, 6(11). doi: 10.1371/journal.pone.0027250.
- Ahmad, M. (1998) 'Chimeric Proteins between cry1 and cry2 Arabidopsis Blue Light Photoreceptors Indicate Overlapping Functions and Varying Protein Stability', *THE PLANT CELL ONLINE*. doi: 10.1105/tpc.10.2.197.
- Ahmad, M. (2016) 'Photocycle and signaling mechanisms of plant cryptochromes', *Current Opinion in Plant Biology*. Elsevier Ltd, 33, pp. 108–115. doi: 10.1016/j.pbi.2016.06.013.
- Ahmad, M. and Cashmore, A. R. (1993) 'HY4 gene of *A. thaliana* encodes a protein with characteristics of a blue-light photoreceptor', *Nature*. doi: 10.1038/366162a0.
- Aihara, Y., Tabata, R., Suzuki, T., Shimazaki, K. and Nagatani, A. (2008) 'Molecular basis of the functional specificities of phototropin 1 and 2', *The Plant Journal*. Wiley/Blackwell (10.1111), 56(3), pp. 364–375. doi: 10.1111/j.1365-313X.2008.03605.x.
- Al-Sady, B., Ni, W., Kircher, S., Schäfer, E. and Quail, P. H. (2006) 'Photoactivated Phytochrome Induces Rapid PIF3 Phosphorylation Prior to Proteasome-Mediated Degradation', *Molecular Cell*. doi: 10.1016/j.molcel.2006.06.011.
- Alexandre, M. T. a, Arents, J. C., Van Grondelle, R., Hellingwerf, K. J. and Kennis, J. T. M. (2007) 'A base-catalyzed mechanism for dark state recovery in the *Avena sativa* phototropin-1 LOV2 domain', *Biochemistry*, 46(11), pp. 3129–3137. doi: 10.1021/bi062074e.
- Ando, E., Ohnishi, M., Wang, Y., Matsushita, T., Watanabe, A., Hayashi, Y., Fujii, M., Ma, J. F., Inoue, S. -i. and Kinoshita, T. (2013) 'TWIN SISTER OF FT, GIGANTEA, and CONSTANS Have a Positive But Indirect Effect on Blue Light-Induced Stomatal Opening in *Arabidopsis*', *Plant Physiology*. doi: 10.1104/pp.113.217984.
- Banerjee, R., Schleicher, E., Meier, S., Viana, R. M., Pokorny, R., Ahmad, M., Bittl, R.

and Batschauer, A. (2007) 'The signaling state of Arabidopsis cryptochrome 2 contains flavin semiquinone', *Journal of Biological Chemistry*, 282(20), pp. 14916–14922. doi: 10.1074/jbc.M700616200.

Baudry, A., Ito, S., Song, Y. H., Strait, A. A., Kiba, T., Lu, S., Henriques, R., Pruneda-Paz, J. L., Chua, N. H., Tobin, E. M., Kay, S. A. and Imaizumi, T. (2010) 'F-Box Proteins FKF1 and LKP2 Act in Concert with ZEITLUPE to Control Arabidopsis Clock Progression', *The Plant Cell*, 22(3), pp. 606–622. doi: 10.1105/tpc.109.072843.

Bhattacharjee, N. and Biswas, P. (2010) 'Position-specific propensities of amino acids in the -strand', *BMC Structural Biology*, 10. doi: 10.1186/1472-6807-10-29.

Boccalandro, H. E., Ploschuck, E. L., Yanovsky, M. J., Sánchez, R. A., Gatz, C., Casal, J. J. (2003) 'Increased Phytochrome B Alleviates Density Effects on Tuber Yield of Field Potato Crops', *Plant Physiology*. doi: 10.1104/pp.103.029579.

Bouly, J. P., Schleicher, E., Dionisio-Sese, M., Vandenbussche, F., Van Der Straeten, D., Bakrim, N., Meier, S., Batschauer, A., Galland, P., Bittl, R. and Ahmad, M. (2007) 'Cryptochrome blue light photoreceptors are activated through interconversion of flavin redox states', *Journal of Biological Chemistry*, 282(13), pp. 9383–9391. doi: 10.1074/jbc.M609842200.

Boylan, M. T. and Quail, P. H. (1991) 'Phytochrome a overexpression inhibits hypocotyl elongation in transgenic Arabidopsis.', *Proceedings of the National Academy of Sciences of the United States of America*. doi: 10.1073/pnas.88.23.10806.

Bradley, J. M., Murphy, G., Whitlam, G. C. and Harberd, N. P. (1996) 'Identification of phytochrome B amino acid residues in three new phyB mutants of Arabidopsis thaliana', *Journal of Experimental Botany*, 47(302), pp. 1449–1455.

Briggs, W. R. (2007) 'The LOV domain: A chromophore module servicing multiple photoreceptors', in *Journal of Biomedical Science*. doi: 10.1007/s11373-007-9162-6.

Briggs, W. R. and Chon, H. P. (1966) 'The Physiological Versus the Spectrophotometric Status of Phytochrome in Corn Coleoptiles', *Plant Physiology*.

Brown, B. A., Cloix, C., Jiang, G. H., Kaiserli, E., Herzyk, P., Kliebenstein, D. J. and

- Jenkins, G. I. (2005) 'A UV-B-specific signaling component orchestrates plant UV protection', *Proceedings of the National Academy of Sciences*, 102(50), pp. 18225–18230. doi: 10.1073/pnas.0507187102.
- Van Buskirk, E. K., Reddy, A. K., Nagatani, A. and Chen, M. (2014) 'Photobody Localization of Phytochrome B Is Tightly Correlated with Prolonged and Light-Dependent Inhibition of Hypocotyl Elongation in the Dark', *Plant Physiology*, 165(2), pp. 595–607. doi: 10.1104/pp.114.236661.
- de Carbonnel, M., Davis, P., Roelfsema, M. R. G., Inoue, S. -i., Schepens, I., Lariguet, P., Geisler, M., Shimazaki, K. -i., Hangarter, R. and Fankhauser, C. (2010) 'The Arabidopsis PHYTOCHROME KINASE SUBSTRATE2 Protein Is a Phototropin Signaling Element That Regulates Leaf Flattening and Leaf Positioning', *Plant Physiology*, 152(3), pp. 1391–1405. doi: 10.1104/pp.109.150441.
- Cashmore, A. R., Jarillo, J. A., Wu, Y.-J. and Liu, D. (1999) 'Cryptochromes: blue-light receptors for plants and animals.', *Science*, 284(5415), pp. 760–765. doi: 10.1126/science.284.5415.760.
- Cenis, J. L. (1992) 'Rapid extraction of fungal DNA for PCR amplification', *Nucleic Acids Research*. doi: 10.1093/nar/20.9.2380.
- Chaves, I., Pokorny, R., Byrdin, M., Hoang, N., Ritz, T., Brettel, K., Essen, L.-O., van der Horst, G. T. J., Batschauer, A. and Ahmad, M. (2011) 'The cryptochromes: blue light photoreceptors in plants and animals.', *Annual review of plant biology*, 62, pp. 335–364. doi: 10.1146/annurev-arplant-042110-103759.
- Chen, M. (2008) 'Phytochrome nuclear body: an emerging model to study interphase nuclear dynamics and signaling', *Current Opinion in Plant Biology*, 11(5), pp. 503–508. doi: 10.1016/j.pbi.2008.06.012.
- Chen, M., Schwab, R. and Chory, J. (2003) 'Characterization of the requirements for localization of phytochrome B to nuclear bodies.', *Proceedings of the National Academy of Sciences of the United States of America*, 100(24), pp. 14493–14498. doi: 10.1073/pnas.1935989100.
- Cho, H.-Y., Tseng, T.-S., Kaiserli, E., Sullivan, S., Christie, J. M. and Briggs, W. R.

- (2006) 'Physiological Roles of the Light, Oxygen, or Voltage Domains of Phototropin 1 and Phototropin 2 in Arabidopsis', *Plant Physiology*, 143(1), pp. 517–529. doi: 10.1104/pp.106.089839.
- Christie, J. M. (2007) 'Phototropin Blue-Light Receptors', *Annual Review of Plant Biology*, 58(1), pp. 21–45. doi: 10.1146/annurev.arplant.58.032806.103951.
- Christie, J. M., Arvai, A. S., Baxter, K. J., Heilmann, M., Pratt, A. J., O'Hara, A., Kelly, S. M., Hothorn, M., Smith, B. O., Hitomi, K., Jenkins, G. I. and Getzoff, E. D. (2012) 'Plant UVR8 photoreceptor senses UV-B by tryptophan-mediated disruption of cross-dimer salt bridges', *Science*. doi: 10.1126/science.1218091.
- Christie, J. M., Blackwood, L., Petersen, J. and Sullivan, S. (2015) 'Plant flavoprotein photoreceptors', *Plant and Cell Physiology*, 56(3), pp. 401–413. doi: 10.1093/pcp/pcu196.
- Christie, J. M., Corchnoy, S. B., Swartz, T. E., Hokenson, M., Han, I. S., Briggs, W. R. and Bogomolni, R. a. (2007) 'Steric interactions stabilize the signaling state of the LOV2 domain of phototropin 1', *Biochemistry*, 46(32), pp. 9310–9319. doi: 10.1021/bi700852w.
- Christie, J. M. and Murphy, A. S. (2013) 'Shoot phototropism in higher plants: New light through old concepts', *American Journal of Botany*, 100(1), pp. 35–46. doi: 10.3732/ajb.1200340.
- Christie, J. M., Reymond, P., Powell, G. K., Bernasconi, P., Raibekas, A. A., Liscum, E. and Briggs, W. R. (1998) 'Arabidopsis NPH1: A flavoprotein with the properties of a photoreceptor for phototropism', *Science*. doi: 10.1126/science.282.5394.1698.
- Christie, J. M., Swartz, T. E., Bogomolni, R. a. and Briggs, W. R. (2002) 'Phototropin LOV domains exhibit distinct roles in regulating photoreceptor function', *Plant Journal*, 32(2), pp. 205–219. doi: 10.1046/j.1365-313X.2002.01415.x.
- Christie, J. M., Yang, H., Richter, G. L., Sullivan, S., Thomson, C. E., Lin, J., Titapiwatanakun, B., Ennis, M., Kaiserli, E., Lee, O. R., Adamec, J., Peer, W. A. and Murphy, A. S. (2011) 'Phot1 inhibition of ABCB19 primes lateral Auxin Fluxes in the Shoot Apex required for Phototropism', *PLoS Biology*, 9(6). doi: 10.1371/journal.pbio.1001076.

Christie, J., Suetsugu, N., Sullivan, S. and Wada, M. (2017) 'Shining Light on the Function of NPH3/RPT2-like Proteins in Phototropin Signalling', *Plant Physiology*, 176(February), pp. pp.00835.2017. doi: 10.1104/pp.17.00835.

Circolone, F., Granzin, J., Jentsch, K., Drepper, T., Jaeger, K. E., Willbold, D., Krauss, U. and Batra-Safferling, R. (2012) 'Structural basis for the slow dark recovery of a full-length LOV protein from *Pseudomonas putida*', *Journal of Molecular Biology*. Elsevier Ltd, 417(4), pp. 362–374. doi: 10.1016/j.jmb.2012.01.056.

Clough, R. C. and Vierstra, R. D. (1997) 'Phytochrome degradation', *Plant, Cell and Environment*. doi: 10.1046/j.1365-3040.1997.d01-107.x.

Dasgupta, A., Chen, C. H., Lee, C. H., Gladfelter, A. S., Dunlap, J. C. and Loros, J. J. (2015) 'Biological Significance of Photoreceptor Photocycle Length: VIVID Photocycle Governs the Dynamic VIVID-White Collar Complex Pool Mediating Photo-adaptation and Response to Changes in Light Intensity', *PLoS Genetics*, 11(5), pp. 1–23. doi: 10.1371/journal.pgen.1005215.

Davis, A. M., Hall, A., Millar, A. J., Darrah, C. and Davis, S. J. (2009) 'Protocol: Streamlined sub-protocols for floral-dip transformation and selection of transformants in *Arabidopsis thaliana*', *Plant Methods*. doi: 10.1186/1746-4811-5-3.

DeBlasio, S. L., Mullen, J. L., Luesse, D. R. and Hangarter, R. P. (2003) 'Phytochrome modulation of blue light-induced chloroplast movements in *Arabidopsis*.' , *Plant physiology*. doi: 10.1104/pp.103.029116.

Demarsy, E., Goldschmidt-Clermont, M. and Ulm, R. (2018) 'Coping with "Dark Sides of the Sun" through Photoreceptor Signaling', *Trends in Plant Science*. Elsevier Ltd, 23(3), pp. 260–271. doi: 10.1016/j.tplants.2017.11.007.

Demarsy, E., Schepens, I., Okajima, K., Hersch, M., Bergmann, S., Christie, J., Shimazaki, K. I., Tokutomi, S. and Fankhauser, C. (2012) 'Phytochrome Kinase Substrate 4 is phosphorylated by the phototropin 1 photoreceptor', *EMBO Journal*. doi: 10.1038/emboj.2012.186.

Ding, Z., Galván-Ampudia, C. S., Demarsy, E., Langowski, Ł., Kleine-Vehn, J., Fan, Y., Morita, M. T., Tasaka, M., Fankhauser, C., Offringa, R. and Friml, J. (2011) 'Light-

mediated polarization of the PIN3 auxin transporter for the phototropic response in *Arabidopsis*', *Nature Cell Biology*. doi: 10.1038/ncb2208.

Dornbusch, T., Lorrain, S., Kuznetsov, D., Fortier, A., Liechti, R., Xenarios, I. and Fankhauser, C. (2012) 'Measuring the diurnal pattern of leaf hyponasty and growth in *Arabidopsis* a novel phenotyping approach using laser scanning', *Functional Plant Biology*. doi: 10.1071/FP12018.

Dornbusch, T., Michaud, O., Xenarios, I. and Fankhauser, C. (2014) 'Differentially Phased Leaf Growth and Movements in *Arabidopsis* Depend on Coordinated Circadian and Light Regulation', *The Plant Cell*, 26(10), pp. 3911–3921. doi: 10.1105/tpc.114.129031.

Dowson-Day, M. J. and Millar, A. J. (1999) 'Circadian dysfunction causes aberrant hypocotyl elongation patterns in *Arabidopsis*', *Plant Journal*. doi: 10.1046/j.1365-313X.1999.00353.x.

Dubeaux, G. and Vert, G. (2017) 'Zooming into plant ubiquitin-mediated endocytosis', *Current Opinion in Plant Biology*. doi: 10.1016/j.pbi.2017.07.005.

Edwards, K., Johnstone, C. and Thompson, C. (1991) 'A simple and rapid method for the preparation of plant genomic DNA for PCR analysis', *Nucleic Acids Research*, 19(6), p. 1349. doi: 10.1093/nar/19.6.1349.

Elich, T. D. and Chory, J. (1997) 'Biochemical characterization of *Arabidopsis* wild-type and mutant phytochrome B holoproteins.', *The Plant Cell*, pp. 2271–2280. doi: 10.1105/tpc.9.12.2271.

Enderle, B., Sheerin, D. J., Paik, I., Kathare, P. K., Schwenk, P., Klose, C., Ulbrich, M. H., Huq, E. and Hiltbrunner, A. (2017) 'PCH1 and PCHL promote photomorphogenesis in plants by controlling phytochrome B dark reversion', *Nature Communications*. Springer US, 8(1). doi: 10.1038/s41467-017-02311-8.

Esmon, C. A., Tinsley, A. G., Ljung, K., Sandberg, G., Hearne, L. B. and Liscum, E. (2006) 'A gradient of auxin and auxin-dependent transcription precedes tropic growth responses.', *Proceedings of the National Academy of Sciences of the United States of America*, 103(1), pp. 236–241. doi: 10.1073/pnas.0507127103.

- Faigon-Soverna, A., Harmon, F. G., Storani, L., Karayekov, E., Staneloni, R. J., Gassmann, W., Mas, P., Casal, J. J., Kay, S. A. and Yanovsky, M. J. (2006) 'A Constitutive Shade-Avoidance Mutant Implicates TIR-NBS-LRR Proteins in Arabidopsis Photomorphogenic Development', *The Plant Cell*. doi: 10.1105/tpc.105.038810.
- Fankhauser, C., Yeh, K. C., Lagarias, J. C., Zhang, H., Elich, T. D. and Chory, J. (1999) 'PKS1, a substrate phosphorylated by phytochrome that modulates light signaling in Arabidopsis', *Science*. doi: 10.1126/science.284.5419.1539.
- Favory, J. J., Stec, A., Gruber, H., Rizzini, L., Oravec, A., Funk, M., Albert, A., Cloix, C., Jenkins, G. I., Oakeley, E. J., Seidlitz, H. K., Nagy, F. and Ulm, R. (2009) 'Interaction of COP1 and UVR8 regulates UV-B-induced photomorphogenesis and stress acclimation in Arabidopsis', *EMBO Journal*. doi: 10.1038/emboj.2009.4.
- Folta, K. M. and Kaufman, L. S. (2003) 'Phototropin 1 is required for high-fluence blue-light-mediated mRNA destabilization', *Plant Molecular Biology*. doi: 10.1023/A:1022393406204.
- Folta, K. M., Lieg, E. J., Durham, T. and Spalding, E. P. (2003) 'Primary Inhibition of Hypocotyl Growth and Phototropism Depend Differently on Phototropin-Mediated Increases in Cytoplasmic Calcium Induced by Blue Light', 133(December), pp. 1464–1470. doi: 10.1104/pp.103.024372.ways.
- Folta, K. M. and Spalding, E. P. (2001) 'Unexpected roles for cryptochrome 2 and phototropin revealed by high-resolution analysis of blue light-mediated hypocotyl growth inhibition', *Plant Journal*, 26(5), pp. 471–478. doi: 10.1046/j.1365-313X.2001.01038.x.
- Fornara, F., Panigrahi, K. C. S., Gissot, L., Sauerbrunn, N., Rühl, M., Jarillo, J. A. and Coupland, G. (2009) 'Arabidopsis DOF Transcription Factors Act Redundantly to Reduce CONSTANS Expression and Are Essential for a Photoperiodic Flowering Response', *Developmental Cell*, 17(1), pp. 75–86. doi: 10.1016/j.devcel.2009.06.015.
- Franklin, K. A. (2008) 'Shade avoidance', *New Phytologist*, 179(4), pp. 930–944. doi: 10.1111/j.1469-8137.2008.02507.x.
- Franklin, K. a. and Quail, P. H. (2010) 'Phytochrome functions in Arabidopsis development', *Journal of Experimental Botany*, 61(1), pp. 11–24. doi: 10.1093/jxb/erp304.

- Friml, J., Wiśniewska, J., Benková, E., Mendgen, K. and Palme, K. (2002) 'Lateral relocation of auxin efflux regulator PIN3 mediates tropism in Arabidopsis', *Nature*. doi: 10.1038/415806a.
- Fujii, Y., Tanaka, H., Konno, N., Ogasawara, Y., Hamashima, N., Tamura, S., Hasegawa, S., Hayasaki, Y., Okajima, K. and Kodama, Y. (2017) 'Phototropin perceives temperature based on the lifetime of its photoactivated state', *Proceedings of the National Academy of Sciences*, p. 201704462. doi: 10.1073/pnas.1704462114.
- Fujiwara, S., Wang, L., Han, L., Suh, S. S., Salomé, P. A., McClung, C. R. and Somers, D. E. (2008) 'Post-translational regulation of the Arabidopsis circadian clock through selective proteolysis and phosphorylation of pseudo-response regulator proteins', *Journal of Biological Chemistry*, 283(34), pp. 23073–23083. doi: 10.1074/jbc.M803471200.
- Ganesan, M., Lee, H. Y., Kim, J. Il and Song, P. S. (2017) 'Development of transgenic crops based on photobiotechnology', *Plant Cell and Environment*, 40(11), pp. 2469–2486. doi: 10.1111/pce.12887.
- Gangappa, S. N. and Botto, J. F. (2016) 'The Multifaceted Roles of HY5 in Plant Growth and Development', *Molecular Plant*. Elsevier Ltd, 9(10), pp. 1353–1365. doi: 10.1016/j.molp.2016.07.002.
- Gao, J., Wang, X., Zhang, M., Bian, M., Deng, W., Zuo, Z., Yang, Z., Zhong, D. and Lin, C. (2015) 'Trp triad-dependent rapid photoreduction is not required for the function of Arabidopsis CRY1', *Proceedings of the National Academy of Sciences*, 112(29), pp. 9135–9140. doi: 10.1073/pnas.1504404112.
- Garg, A. K., Sawers, R. J. H., Wang, H., Kim, J. K., Walker, J. M., Brutnell, T. P., Parthasarathy, M. V., Vierstra, R. D. and Wu, R. J. (2006) 'Light-regulated overexpression of an Arabidopsis phytochrome A gene in rice alters plant architecture and increases grain yield', *Planta*, 223(4), pp. 627–636. doi: 10.1007/s00425-005-0101-3.
- Giliberto, L., Perrotta, G., Pallara, P., Weller, J. L., Fraser, P. D., Bramley, P. M., Fiore, A., Tavazza, M. and Giuliano, G. (2005) 'Manipulation of the blue light photoreceptor cryptochrome 2 in tomato affects vegetative development, flowering time, and fruit antioxidant content.', *Plant physiology*, 137(1), pp. 199–208. doi: 10.1104/pp.104.051987.

- Glantz, S. T., Carpenter, E. J., Melkonian, M., Gardner, K. H., Boyden, E. S., Wong, G. K.-S. and Chow, B. Y. (2016) 'Functional and topological diversity of LOV domain photoreceptors', *Proceedings of the National Academy of Sciences*, 113(11), pp. E1442–E1451. doi: 10.1073/pnas.1509428113.
- Goyal, A., Karayekov, E., Galvão, V. C., Ren, H., Casal, J. J. and Fankhauser, C. (2016) 'Shade Promotes Phototropism through Phytochrome B-Controlled Auxin Production', *Current Biology*. doi: 10.1016/j.cub.2016.10.001.
- Gruber, H., Heijde, M., Heller, W., Albert, A., Seidlitz, H. K. and Ulm, R. (2010) 'Negative feedback regulation of UV-B-induced photomorphogenesis and stress acclimation in Arabidopsis', *Proceedings of the National Academy of Sciences*, 107(46), pp. 20132–20137. doi: 10.1073/pnas.0914532107.
- Guo, H., Duong, H., Ma, N. and Lin, C. (1999) 'The Arabidopsis blue light receptor cryptochrome 2 is a nuclear protein regulated by a blue light-dependent post-transcriptional mechanism', *Plant Journal*, 19(3), pp. 279–287. doi: 10.1046/j.1365-313X.1999.00525.x.
- Guo, H., Kottke, T., Hegemann, P. and Dick, B. (2005) 'The phot LOV2 domain and its interaction with LOV1', *Biophysical Journal*. doi: 10.1529/biophysj.104.058230.
- Guo, H., Yang, H., Mockler, T. C. and Lin, C. (1998) 'Regulation of flowering time by Arabidopsis photoreceptors', *Science*. doi: 10.1126/science.279.5355.1360.
- Haga, K., Frank, L., Kimura, T., Schwechheimer, C. and Sakai, T. (2018) 'Roles of AGCVIII Kinases in the Hypocotyl Phototropism of Arabidopsis Seedlings', *Plant and Cell Physiology*. doi: 10.1093/pcp/pcy048.
- Haga, K., Takano, M., Neumann, R. and Iino, M. (2005) 'The Rice COLEOPTILE PHOTOTROPISM1 gene encoding an ortholog of Arabidopsis NPH3 is required for phototropism of coleoptiles and lateral translocation of auxin.', *The Plant Cell*, 17(1), pp. 103–115. doi: 10.1105/tpc.104.028357.
- Haga, K., Tsuchida-Mayama, T., Yamada, M. and Sakai, T. (2015) 'Arabidopsis ROOT PHOTOTROPISM2 Contributes to the Adaptation to High-Intensity Light in Phototropic Responses', *The Plant Cell*, 27(4), pp. 1098–1112. doi: 10.1105/tpc.15.00178.

- Halavaty, A. S. and Moffat, K. (2013) 'Coiled-coil dimerization of the LOV2 domain of the blue-light photoreceptor phototropin 1 from *Arabidopsis thaliana*', *Acta Crystallographica Section F: Structural Biology and Crystallization Communications*. International Union of Crystallography, 69(12), pp. 1316–1321. doi: 10.1107/S1744309113029199.
- Halliday, K. J. and Fankhauser, C. (2003) 'Phytochrome-hormonal signalling networks', *New Phytologist*. doi: 10.1046/j.1469-8137.2003.00689.x.
- Halliday, K. J., Martínez-García, J. F. and Josse, E. M. (2009) 'Integration of light and auxin signaling.', *Cold Spring Harbor perspectives in biology*. doi: 10.1101/cshperspect.a001586.
- Han, I. S., Tseng, T.-S., Eisinger, W. and Briggs, W. R. (2008) 'Phytochrome A Regulates the Intracellular Distribution of Phototropin 1-Green Fluorescent Protein in *Arabidopsis thaliana*', *The Plant Cell*, 20(10), pp. 2835–2847. doi: 10.1105/tpc.108.059915.
- Harada, A., Takemiya, A., Inoue, S. I., Sakai, T. and Shimazaki, K. I. (2013) 'Role of RPT2 in leaf positioning and flattening and a possible inhibition of phot2 signaling by phot1', *Plant and Cell Physiology*, 54(1), pp. 36–47. doi: 10.1093/pcp/pcs094.
- Harper, S. M., Christie, J. M. and Gardner, K. H. (2004) 'Disruption of the LOV-J $\alpha$  helix interaction activates phototropin kinase activity', *Biochemistry*, 43(51), pp. 16184–16192. doi: 10.1021/bi048092i.
- Harper, S. M., Neil, L. C., Day, I. J., Hore, P. J. and Gardner, K. H. (2004) 'Conformational Changes in a Photosensory LOV Domain Monitored by Time-Resolved NMR Spectroscopy', *Journal of the American Chemical Society*. doi: 10.1021/ja038224f.
- Hart, J. W. and MacDonald, I. R. (1981) 'Phototropism and geotropism in hypocotyls of cress (*Lepidium sativum* L.)', *Plant, Cell & Environment*. doi: 10.1111/1365-3040.ep11610972.
- Hasegawa, K., Noguchi, H., Tanoue, C., Sando, S., Takada, M., Sakoda, M. and Hashimoto, T. (1987) 'Phototropism in Hypocotyls of Radish: IV. Flank Growth and Lateral Distribution of cis- and trans-Raphanusanins in the First Positive Phototropic

Curvature.’, *Plant Physiology*.

Hayashi, M., Inoue, S. I., Ueno, Y. and Kinoshita, T. (2017) ‘A Raf-like protein kinase BHP mediates blue light-dependent stomatal opening’, *Scientific Reports*. doi: 10.1038/srep45586.

Hayes, S., Sharma, A., Fraser, D. P., Trevisan, M., Cragg-Barber, C. K., Tavridou, E., Fankhauser, C., Jenkins, G. I. and Franklin, K. A. (2017) ‘UV-B Perceived by the UVR8 Photoreceptor Inhibits Plant Thermomorphogenesis’, *Current Biology*. Elsevier Ltd., 27(1), pp. 120–127. doi: 10.1016/j.cub.2016.11.004.

Hayes, S., Velanis, C. N., Jenkins, G. I. and Franklin, K. A. (2014) ‘UV-B detected by the UVR8 photoreceptor antagonizes auxin signaling and plant shade avoidance’, *Proceedings of the National Academy of Sciences*, 111(32), pp. 11894–11899. doi: 10.1073/pnas.1403052111.

Heijde, M. and Ulm, R. (2013) ‘Reversion of the Arabidopsis UV-B photoreceptor UVR8 to the homodimeric ground state’, *Proceedings of the National Academy of Sciences*. doi: 10.1073/pnas.1214237110.

Heintz, U. and Schlichting, I. (2016) ‘Blue light-induced LOV domain dimerization enhances the affinity of aureochrome 1a for its target DNA sequence’, *eLife*. doi: 10.7554/eLife.11860.

Hennig, L., Buche, C. and Schafer, E. (2000) ‘Degradation of phytochrome A and the high irradiance response in Arabidopsis: a kinetic analysis’, *Plant, Cell and Environment*. Wiley/Blackwell (10.1111), 23(7), pp. 727–734. doi: 10.1046/j.1365-3040.2000.00587.x.

Hisada, A., Hanzawa, H., Weller, J. L., Nagatani, A., Reid, J. B. and Furuya, M. (2000) ‘Light-induced nuclear translocation of endogenous pea phytochrome A visualized by immunocytochemical procedures.’, *The Plant cell*. doi: 10.1105/tpc.12.7.1063.

Hiyama, A., Takemiya, A., Munemasa, S., Okuma, E., Sugiyama, N., Tada, Y., Murata, Y. and Shimazaki, K. (2017) ‘Blue light and CO<sub>2</sub> signals converge to regulate light-induced stomatal opening’, *Nature Communications*. Springer US, 8(1), p. 1284. doi: 10.1038/s41467-017-01237-5.

- Hohm, T., Demarsy, E., Quan, C., Allenbach Petrolati, L., Preuten, T., Vernoux, T., Bergmann, S. and Fankhauser, C. (2014) 'Plasma membrane H<sup>+</sup> -ATPase regulation is required for auxin gradient formation preceding phototropic growth.', *Molecular Systems Biology*, 10(9), p. 751. doi: 10.15252/msb.20145247.
- Huang, H., Yoo, C. Y., Bindbeutel, R., Goldsworthy, J., Tielking, A., Alvarez, S., Naldrett, M. J., Evans, B. S., Chen, M. and Nusinow, D. A. (2016) 'PCH1 integrates circadian and light-signaling pathways to control photoperiod-responsive growth in Arabidopsis', *eLife*, pp. 1–26. doi: 10.7554/eLife.13292.
- Huang, X., Ouyang, X., Yang, P., Lau, O. S., Chen, L., Wei, N. and Deng, X. W. (2013) 'Conversion from CUL4-based COP1-SPA E3 apparatus to UVR8-COP1-SPA complexes underlies a distinct biochemical function of COP1 under UV-B', *Proceedings of the National Academy of Sciences*. doi: 10.1073/pnas.1316622110.
- Huq, E., Al-Sady, B. and Quail, P. H. (2003) 'Nuclear translocation of the photoreceptor phytochrome B is necessary for its biological function in seedling photomorphogenesis', *The Plant Journal*. Wiley/Blackwell (10.1111), 35(5), pp. 660–664. doi: 10.1046/j.1365-313X.2003.01836.x.
- Imaizumi, T., Shultz, T. F., Harmon, F. G., Ho, L. A., Kay S. A., (2005) 'F-Box protein mediates cyclic degradation of a repressor of CONSTANS', *Science*, 309(July), pp. 293–297. doi: 10.1126/science.1110586.
- Imaizumi, T., Tran, H. G., Swartz, T. E., Briggs, W. R. and Kay, S. A. (2003) 'FKF1 is essential for photoperiodic-specific light signalling in Arabidopsis', *Nature*. doi: 10.1038/nature02090.
- Inada, S., Ohgishi, M., Mayama, T., Okada, K. and Sakai, T. (2004) 'RPT2 is a signal transducer involved in phototropic response and stomatal opening by association with phototropin 1 in Arabidopsis thaliana', *The Plant Cell*, 16(4), pp. 887–896. doi: 10.1105/tpc.019901.
- Inoue, S. I., Kinoshita, T., Matsumoto, M., Nakayama, K. I., Doi, M. and Shimazaki, K. -i. (2008 A) 'Blue light-induced autophosphorylation of phototropin is a primary step for signaling', *Proceedings of the National Academy of Sciences*, 105(14), pp. 5626–5631. doi:

10.1073/pnas.0709189105.

Inoue, S. I., Kinoshita, T., Takemiya, A., Doi, M. and Shimazaki, K. I. (2008 B) 'Leaf positioning of Arabidopsis in response to blue light', *Molecular Plant*. 1(1), pp. 15–26. doi: 10.1093/mp/ssm001.

Inoue, S. I., Matsushita, T., Tomokiyo, Y., Matsumoto, M., Nakayama, K. I., Kinoshita, T. and Shimazaki, K. I. (2011) 'Functional Analyses of the Activation Loop of Phototropin2 in Arabidopsis', *Plant Physiology*. doi: 10.1104/pp.111.175943.

Inoue, S. I., Takemiya, A. and Shimazaki, K. I. (2010) 'Phototropin signaling and stomatal opening as a model case', *Current Opinion in Plant Biology*. doi: 10.1016/j.pbi.2010.09.002.

Inoue, S. and Kinoshita, T. (2017) 'Blue Light Regulation of Stomatal Opening and the Plasma Membrane H<sup>+</sup>-ATPase', *Plant Physiology*, 174(2), pp. 531–538. doi: 10.1104/pp.17.00166.

Ito, S., Song, Y. H. and Imaizumi, T. (2012) 'LOV domain-containing F-box proteins: Light-dependent protein degradation modules in Arabidopsis', *Molecular Plant*. 5(3), pp. 573–582. doi: 10.1093/mp/sss013.

Jaedicke, K., Lichtenthaler, a. L., Meyberg, R., Zeidler, M. and Hughes, J. (2012) 'A phytochrome-phototropin light signaling complex at the plasma membrane', *Proceedings of the National Academy of Sciences*, 109(30), pp. 12231–12236. doi: 10.1073/pnas.1120203109.

Jander, G. (2003) 'Ethylmethanesulfonate Saturation Mutagenesis in Arabidopsis to Determine Frequency of Herbicide Resistance', *Plant Physiology*, 131(1), pp. 139–146. doi: 10.1104/pp.102.010397.

Janoudi, A. K., Konjević, R., Whitelam, G., Gordon, W. and Poff, K. L. (1997) 'Both phytochrome A and phytochrome B are required for the normal expression of phototropism in Arabidopsis thaliana seedlings', *Physiologia Plantarum*, 101(2), pp. 278–282. doi: 10.1034/j.1399-3054.1997.1010204.x.

Jarillo, J. A., Gabrys, H., Capel, J., Alonso, J. M., Ecker, J. R. and Cashmore, A. R. (2001)

‘Phototropin-related NPL1 controls chloroplast relocation induced by blue light’, *Nature*, 410(6831), pp. 952–954. doi: 10.1038/35073622.

Jenkins, G. I. (2017) ‘Photomorphogenic responses to ultraviolet-B light’, *Plant Cell and Environment*, pp. 2544–2557. doi: 10.1111/pce.12934.

Jentzsch, K., Wirtz, A., Circolone, F., Drepper, T., Losi, A., Gärtner, W., Jaeger, K. E. and Krauss, U. (2009) ‘Mutual exchange of kinetic properties by extended mutagenesis in two short LOV domain proteins from *Pseudomonas putida*’, *Biochemistry*, 48(43), pp. 10321–10333. doi: 10.1021/bi901115z.

Jones, M. A., Feeney, K. A., Kelly, S. M. and Christie, J. M. (2007) ‘Mutational analysis of phototropin 1 provides insights into the mechanism underlying LOV2 signal transmission’, *Journal of Biological Chemistry*, 282(9), pp. 6405–6414. doi: 10.1074/jbc.M605969200.

Jung, J. H., Domijan, M., Klose, C., Biswas, S., Ezer, D., Gao, M., Khattak, A. K., Box, M. S., Charoensawan, V., Cortijo, S., Kumar, M., Grant, A., Locke, J. C. W., Schäfer, E., Jaeger, K. E. and Wigge, P. A. (2016) ‘Phytochromes function as thermosensors in *Arabidopsis*’, *Science*. doi: 10.1126/science.aaf6005.

Kagawa, T., Sakai, T., Suetsugu, N., Oikawa, K., Ishiguro, S., Kato, T., Tabata, S., Okada, K. and Wada, M. (2001) ‘*Arabidopsis* NPL1: A phototropin homolog controlling the chloroplast high-light avoidance response’, *Science*, 291(5511), pp. 2138–2141. doi: 10.1126/science.291.5511.2138.

Kaiserli, E., Sullivan, S., Jones, M. a, Feeney, K. a and Christie, J. M. (2009) ‘Domain swapping to assess the mechanistic basis of *Arabidopsis* phototropin 1 receptor kinase activation and endocytosis by blue light.’, *The Plant Cell*, 21(10), pp. 3226–3244. doi: 10.1105/tpc.109.067876.

Kami, C., Allenbach, L., Zourelidou, M., Ljung, K., Schütz, F., Isono, E., Watahiki, M. K., Yamamoto, K. T., Schwechheimer, C. and Fankhauser, C. (2014) ‘Reduced phototropism in pks mutants may be due to altered auxin-regulated gene expression or reduced lateral auxin transport’, *Plant Journal*. doi: 10.1111/tpj.12395.

Kami, C., Hersch, M., Trevisan, M., Genoud, T., Hiltbrunner, A., Bergmann, S. and

- Fankhauser, C. (2012) 'Nuclear phytochrome A signaling promotes phototropism in Arabidopsis.', *The Plant Cell*, 24(2), pp. 566–76. doi: 10.1105/tpc.111.095083.
- Kanegae, H., Tahir, M., Savazzini, F., Yamamoto, K., Yano, M., Sasaki, T., Kanegae, T., Wada, M. and Takano, M. (2000) 'Rice NPH1 homologues, OsNPH1a and OsNPH1b, are differently photoregulated', *Plant and Cell Physiology*, 41(4), pp. 415–423. doi: 10.1093/pcp/41.4.415.
- Kasahara, M., Kagawa, T., Oikawa, K., Suetsugu, N., Miyao, M. and Wada, M. (2002) 'Chloroplast avoidance movement reduces photodamage in plants', *Nature*. doi: 10.1038/nature01213.
- Kasahara, M., Swartz, T. E., Olney, M. a, Onodera, A., Mochizuki, N., Fukuzawa, H., Asamizu, E., Tabata, S., Kanegae, H., Takano, M., Christie, J. M., Nagatani, A. and Briggs, W. R. (2002) 'Photochemical properties of the flavin mononucleotide-binding domains of the phototropins from Arabidopsis, rice, and *Chlamydomonas reinhardtii*.', *Plant physiology*, 129(2), pp. 762–773. doi: 10.1104/pp.002410.
- Katsura, H., Zikihara, K., Okajima, K., Yoshihara, S. and Tokutomi, S. (2009) 'Oligomeric structure of LOV domains in Arabidopsis phototropin', *FEBS Letters*. Federation of European Biochemical Societies, 583(3), pp. 526–530. doi: 10.1016/j.febslet.2009.01.019.
- Kawano, F., Aono, Y., Suzuki, H. and Sato, M. (2013) 'Fluorescence imaging-based high-throughput screening of fast- and slow-cycling LOV proteins', *PLoS ONE*, 8(12). doi: 10.1371/journal.pone.0082693.
- Keller, M. M., Jaillais, Y., Pedmale, U. V., Moreno, J. E., Chory, J. and Ballaré, C. L. (2011) 'Cryptochrome 1 and phytochrome B control shade-avoidance responses in Arabidopsis via partially independent hormonal cascades', *Plant Journal*, 67(2), pp. 195–207. doi: 10.1111/j.1365-313X.2011.04598.x.
- Kiba, T., Henriques, R., Sakakibara, H. and Chua, N.-H. (2007) 'Targeted Degradation of PSEUDO-RESPONSE REGULATOR5 by an SCFZTL Complex Regulates Clock Function and Photomorphogenesis in Arabidopsis thaliana', *The Plant Cell*, 19(8), pp. 2516–2530. doi: 10.1105/tpc.107.053033.
- Kim, K., Shin, J., Lee, S.-H., Kweon, H.-S., Maloof, J. N. and Choi, G. (2011)

‘Phytochromes inhibit hypocotyl negative gravitropism by regulating the development of endodermal amyloplasts through phytochrome-interacting factors’, *Proceedings of the National Academy of Sciences*, 108(4), pp. 1729–1734. doi: 10.1073/pnas.1011066108.

Kinoshita, T., Doi, M., Suetsugu, N., Kagawa, T., Wada, M. and Shimazaki, K. I. (2001) ‘phot1 and phot2 mediate blue light regulation of stomatal opening’, *Nature*. doi: 10.1038/414656a.

Kinoshita, T., Ono, N., Hayashi, Y., Morimoto, S., Nakamura, S., Soda, M., Kato, Y., Ohnishi, M., Nakano, T., Inoue, S. I. and Shimazaki, K. I. (2011) ‘FLOWERING LOCUS T regulates stomatal opening’, *Current Biology*. doi: 10.1016/j.cub.2011.06.025.

Kircher, S., Kozma-Bognar, L., Kim L., Adam, E., Harter, K., Schäfer, E., Nagy, F. (1999) ‘Light Quality Dependent Nuclear Import of the Plant Photoreceptors Phytochrome A and B’, *The Plant Cell*. doi: 10.1105/tpc.11.8.1445.

Kircher, S., Gill, P., Kozma-Bognár, L., Fejes, E., Speth, V., Husselstein-Muller, T., Bauer, D., Ádám, E., Schäfer, E., Nagy, F. (2002) ‘Nucleocytoplasmic Partitioning of the Plant Photoreceptors Phytochrome A, B, C, D, and E Is Regulated Differentially by Light and Exhibits a Diurnal Rhythm’, *The Plant Cell*, 14(7), pp. 1541–1555. doi: 10.1105/tpc.001156.

Kiyosue, T. and Wada, M. (2000) ‘LKP1 (LOV kelch protein 1): a factor involved in the regulation of flowering time in Arabidopsis’, *The Plant Journal*. Wiley/Blackwell (10.1111), 23(6), pp. 807–815. doi: 10.1046/j.1365-313x.2000.00850.x.

Kleine, T., Lockhart, P. and Batschauer, A. (2003) ‘An Arabidopsis protein closely related to Synechocystis cryptochrome is targeted to organelles’, *Plant Journal*, 35(1), pp. 93–103. doi: 10.1046/j.1365-313X.2003.01787.x.

Kong, S. G., Kinoshita, T., Shimazaki, K. I., Mochizuki, N., Suzuki, T. and Nagatani, A. (2007) ‘The C-terminal kinase fragment of Arabidopsis phototropin 2 triggers constitutive phototropin responses’, *Plant Journal*. doi: 10.1111/j.1365-313X.2007.03187.x.

Kong, S. G., Suetsugu, N., Kikuchi, S., Nakai, M., Nagatani, A. and Wada, M. (2013) ‘Both phototropin 1 and 2 localize on the chloroplast outer membrane with distinct localization activity’, *Plant and Cell Physiology*. doi: 10.1093/pcp/pcs151.

Kong, S. G., Suzuki, T., Tamura, K., Mochizuki, N., Hara-Nishimura, I. and Nagatani, A. (2006) 'Blue light-induced association of phototropin 2 with the Golgi apparatus', *Plant Journal*. doi: 10.1111/j.1365-313X.2006.02667.x.

Kozuka, T., Kong, S.-G., Doi, M., Shimazaki, K. -i. and Nagatani, A. (2011) 'Tissue-Autonomous Promotion of Palisade Cell Development by Phototropin 2 in Arabidopsis', *The Plant Cell*, 23(10), pp. 3684–3695. doi: 10.1105/tpc.111.085852.

Kozuka, T., Suetsugu, N., Wada, M. and Nagatani, A. (2013) 'Antagonistic regulation of leaf flattening by phytochrome B and phototropin in Arabidopsis thaliana', *Plant and Cell Physiology*. doi: 10.1093/pcp/pcs134.

Kretsch, T., Poppe, C. and Schäfer, E. (2000) 'A new type of mutation in the plant photoreceptor phytochrome B causes loss of photoreversibility and an extremely enhanced light sensitivity', *Plant Journal*, 22(3), pp. 177–186. doi: 10.1046/j.1365-313X.2000.00715.x.

Łabuz, J., Hermanowicz, P. and Gabryś, H. (2015) 'The impact of temperature on blue light induced chloroplast movements in Arabidopsis thaliana', *Plant Science*. doi: 10.1016/j.plantsci.2015.07.013.

Laemmli, U. K. (1970) 'Cleavage of structural proteins during the assembly of the head of bacteriophage T4', *Nature*. doi: 10.1038/227680a0.

Lagarias, J. C. and Rapoport, H. (1980) 'Chromopeptides from Phytochrome. The Structure and Linkage of the PRForm of the Phytochrome Chromophore', *Journal of the American Chemical Society*. doi: 10.1021/ja00534a042.

Lariguet, P. and Fankhauser, C. (2004) 'Hypocotyl growth orientation in blue light is determined by phytochrome A inhibition of gravitropism and phototropin promotion of phototropism', *Plant Journal*, 40(5), pp. 826–834. doi: 10.1111/j.1365-313X.2004.02256.x.

Lariguet, P., Schepens, I., Hodgson, D., Pedmale, U. V, Trevisan, M., Kami, C., de Carbonnel, M., Alonso, J. M., Ecker, J. R., Liscum, E. and Fankhauser, C. (2006) 'PHYTOCHROME KINASE SUBSTRATE 1 is a phototropin 1 binding protein required for phototropism.', *Proceedings of the National Academy of Sciences of the United States*

*of America*. doi: 10.1073/pnas.0603799103.

Lee, B. D., Kim, M. R., Kang, M. Y., Cha, J. Y., Han, S. H., Nawkar, G. M., Sakuraba, Y., Lee, S. Y., Imaizumi, T., McClung, C. R., Kim, W. Y. and Paek, N. C. (2017) 'The F-box protein FKF1 inhibits dimerization of COP1 in the control of photoperiodic flowering', *Nature Communications*. Springer US, 8(1), pp. 1–10. doi: 10.1038/s41467-017-02476-2.

Legris, M., Klose, C., Burgie, E. S., Rojas, C. C., Neme, M., Hiltbrunner, A., Wigge, P. A., Schäfer, E., Vierstra, R. D. and Casal, J. J. (2016) 'Phytochrome B integrates light and temperature signals in Arabidopsis', *Science*. doi: 10.1126/science.aaf5656.

Leivar, P. and Monte, E. (2014) 'PIFs: Systems Integrators in Plant Development', *The Plant Cell*. doi: 10.1105/tpc.113.120857.

Li, F.W. and Mathews, S. (2016) 'Evolutionary aspects of plant photoreceptors', *Journal of Plant Research*. Springer Japan, 129(2), pp. 115–122. doi: 10.1007/s10265-016-0785-4.

Li, F. W., Melkonian, M., Rothfels, C. J., Villarreal, J. C., Stevenson, D. W., Graham, S. W., Wong, G. K. S., Pryer, K. M. and Mathews, S. (2015- **A**) 'Phytochrome diversity in green plants and the origin of canonical plant phytochromes', *Nature Communications*. Nature Publishing Group, 6, pp. 1–12. doi: 10.1038/ncomms8852.

Li, F.W., Rothfels, C. J., Melkonian, M., Villarreal, J. C., Stevenson, D. W., Graham, S. W., Wong, G. K.-S., Mathews, S. and Pryer, K. M. (2015- **B**) 'The origin and evolution of phototropins', *Frontiers in Plant Science*, 6(August), pp. 1–11. doi: 10.3389/fpls.2015.00637.

Li, X., Wang, Q., Yu, X., Liu, H., Yang, H., Zhao, C., Liu, X., Tan, C., Klejnot, J., Zhong, D. and Lin, C. (2011) 'Arabidopsis cryptochrome 2 (CRY2) functions by the photoactivation mechanism distinct from the tryptophan (trp) triad-dependent photoreduction', *Proceedings of the National Academy of Sciences*, 108(51), pp. 20844–20849. doi: 10.1073/pnas.1114579108.

Liang, T., Mei, S., Shi, C., Yang, Y., Peng, Y., Ma, L., Wang, F., Li, X., Huang, X., Yin, Y. and Liu, H. (2018) 'UVR8 Interacts with BES1 and BIM1 to Regulate Transcription and Photomorphogenesis in Arabidopsis', *Developmental Cell*, 44(4), p. 512–523.e5. doi: 10.1016/j.devcel.2017.12.028.

- Liang, X., Nazarenius, T. J. and Stone, J. M. (2008) 'Identification of a consensus DNA-binding site for the Arabidopsis thaliana SBP domain transcription factor, AtSPL14, and binding kinetics by surface plasmon resonance', *Biochemistry*. doi: 10.1021/bi701431y.
- Lin, C., Top, D., Manahan, C. C., Young, M. W. and Crane, B. R. (2018) 'Circadian clock activity of cryptochrome relies on tryptophan-mediated photoreduction', *Proceedings of the National Academy of Sciences*, p. 201719376. doi: 10.1073/pnas.1719376115.
- Lin, C., Yang, H., Guo, H., Mockler, T., Chen, J. and Cashmore, A. R. (1998) 'Enhancement of blue-light sensitivity of Arabidopsis seedlings by a blue light receptor cryptochrome 2', *Proceedings of the National Academy of Sciences*, 95(5), pp. 2686–2690. doi: 10.1073/pnas.95.5.2686.
- Lindbo, J. A. (2007). TRBO: a high-efficiency tobacco mosaic virus RNA-based overexpression vector. *Plant physiology*, 145(4), 1232-1240.
- Liscum, E. (2016) 'Blue Light-Induced Intracellular Movement of Phototropins: Functional Relevance or Red Herring?', *Frontiers in Plant Science*, 7(June), pp. 1–5. doi: 10.3389/fpls.2016.00827.
- Liscum, E. and Briggs, W. R. (1995) 'Mutations in the NPH1 locus of Arabidopsis disrupt the perception of phototropic stimuli.', *The Plant Cell*, 7(4), pp. 473–485. doi: 10.1105/tpc.7.4.473.
- Liu, H., Yu, X., Li, K., Klejnot, J., Yang, H., Lisiero, D. and Lin, C. (2008) 'Photoexcited CRY2 interacts with CIB1 to regulate transcription and floral initiation in Arabidopsis', *Science*. doi: 10.1126/science.1163927.
- Liu, J., Wang, W., Mei, D., Wang, H., Fu, L., Liu, D., Li, Y. and Hu, Q. (2016) 'Characterizing Variation of Branch Angle and Genome-Wide Association Mapping in Rapeseed (*Brassica napus* L.)', *Frontiers in Plant Science*, 7(February), pp. 1–10. doi: 10.3389/fpls.2016.00021.
- Liu, L.J., Zhang, Y.-C., Li, Q.-H., Sang, Y., Mao, J., Lian, H.-L., Wang, L. and Yang, H.-Q. (2008) 'COP1-Mediated Ubiquitination of CONSTANS Is Implicated in Cryptochrome Regulation of Flowering in Arabidopsis', *The Plant Cell*. doi: 10.1105/tpc.107.057281.

- Liu, Q., Wang, Q., Deng, W., Wang, X., Piao, M., Cai, D., Li, Y., Barshop, W. D., Yu, X., Zhou, T., Liu, B., Oka, Y., Wohlschlegel, J., Zuo, Z. and Lin, C. (2017) 'Molecular basis for blue light-dependent phosphorylation of Arabidopsis cryptochrome 2', *Nature Communications*. Nature Publishing Group, 8(May), pp. 1–12. doi: 10.1038/ncomms15234.
- Liu, Y., Li, X., Li, K., Liu, H. and Lin, C. (2013) 'Multiple bHLH Proteins form Heterodimers to Mediate CRY2-Dependent Regulation of Flowering-Time in Arabidopsis', *PLoS Genetics*. doi: 10.1371/journal.pgen.1003861.
- Lo, H. R. and Chao, Y. C. (2004) 'Rapid Titer Determination of Baculovirus by Quantitative Real-Time Polymerase Chain Reaction', *Biotechnology Progress*, 20(1), pp. 354–360. doi: 10.1021/bp034132i.
- Losi, A., Polverini, E., Quest, B. and Gärtner, W. (2002) 'First Evidence for Phototropin-Related Blue-Light Receptors in Prokaryotes', *Biophysical Journal*. Cell Press, 82(5), pp. 2627–2634. doi: 10.1016/S0006-3495(02)75604-X.
- Luesse, D. R., Deblasio, S. L. and Hangarter, R. P. (2010) 'Integration of phot1, phot2, and PhyB signalling in light-induced chloroplast movements', *Journal of Experimental Botany*, 61(15), pp. 4387–4397. doi: 10.1093/jxb/erq242.
- Ma, D., Li, X., Guo, Y., Chu, J., Fang, S., Yan, C., Noel, J. P. and Liu, H. (2016) 'Cryptochrome 1 interacts with PIF4 to regulate high temperature-mediated hypocotyl elongation in response to blue light', *Proceedings of the National Academy of Sciences*, 113(1), pp. 224–229. doi: 10.1073/pnas.1511437113.
- Más, P., Kim, W. Y., Somers, D. E. and Kay, S. A. (2003) 'Targeted ZTL modulates circadian function in Arabidopsis thaliana.', *Nature*, 426(6966), pp. 567–70. doi: 10.1038/nature02163.
- Mathews, S. (2010) 'Evolutionary Studies Illuminate the Structural-Functional Model of Plant Phytochromes', *The Plant Cell*. doi: 10.1105/tpc.109.072280.
- Mathews, S. and Sharrock, R. A. (1996) 'The phytochrome gene family in grasses (Poaceae): A phylogeny and evidence that grasses have a subset of the loci found in dicot angiosperms', *Molecular Biology and Evolution*, 13(8), pp. 1141–1150. doi:

10.1093/oxfordjournals.molbev.a025677.

Matsushita, T., Mochizuki, N. and Nagatani, A. (2003) 'Dimers of the N-terminal domain of phytochrome B are functional in the nucleus', *Nature*. doi: 10.1038/nature01837.

Millenaar, F. F., Van Zanten, M., Cox, M. C. H., Pierik, R., Voesenek, L. A. C. J. and Peeters, A. J. M. (2009) 'Differential petiole growth in *Arabidopsis thaliana*: Photocontrol and hormonal regulation', *New Phytologist*. doi: 10.1111/j.1469-8137.2009.02921.x.

Mutation Identification in Model Organism Genomes using Desktop PCs (MiModD). (n.d.). Retrieved September 1, 2018, from <https://celegans.de/mimodd/>

Möglich, A. and Moffat, K. (2007) 'Structural Basis for Light-dependent Signaling in the Dimeric LOV Domain of the Photosensor YtvA', *Journal of Molecular Biology*. doi: 10.1016/j.jmb.2007.07.039.

Moriconi, V., Binkert, M., Costigliolo Rojas, M. C., Sellaro, R., Ulm, R. and Casal, J. J. (2018) 'Perception of sunflecks by the UV-B photoreceptor UV RESISTANCE LOCUS 8', *Plant Physiology*. doi: 10.1104/pp.18.00048.

Motchoulski, A. and Liscum, E. (1999) 'Arabidopsis NPH3: A NPH1 photoreceptor-interacting protein essential for phototropism', *Science*. doi: 10.1126/science.286.5441.961.

Murashige, T. and Skoog, F. (1962) 'A Revised Medium for Rapid Growth and Bio Assays with Tobacco Tissue Cultures', *Physiologia Plantarum*, 15(3), pp. 473–497. doi: 10.1111/j.1399-3054.1962.tb08052.x.

Nagatani, A., Reed, J. W. and Chory, J. (1993) 'Isolation and Initial Characterization of Arabidopsis Mutants That Are Deficient in Phytochrome A.', *Plant physiology*. American Society of Plant Biologists, 102(1), pp. 269–277. doi: 10.1104/PP.102.1.269.

Nakasako, M., Zikihara, K., Matsuoka, D., Katsura, H. and Tokutomi, S. (2008) 'Structural Basis of the LOV1 Dimerization of Arabidopsis Phototropins 1 and 2', *Journal of Molecular Biology*, 381(3), pp. 718–733. doi: 10.1016/j.jmb.2008.06.033.

Nakasone, Y., Zikihara, K., Tokutomi, S. and Terazima, M. (2010) 'Kinetics of

- conformational changes of the FKF1-LOV domain upon photoexcitation', *Biophysical Journal*. Biophysical Society, 99(11), pp. 3831–3839. doi: 10.1016/j.bpj.2010.10.005.
- Nash, A. I., Ko, W. H., Harper, S. M. and Gardner, K. H. (2008) 'A conserved glutamine plays a central role in LOV domain signal transmission and Its duration', *Biochemistry*, 47(52), pp. 13842–13849. doi: 10.1021/bi801430e.
- Nelson, D. C., Lasswell, J., Rogg, L. E., Cohen, M. A. and Bartel, B. (2000) 'FKF1, a clock-controlled gene that regulates the transition to flowering in Arabidopsis', *Cell*. doi: 10.1016/S0092-8674(00)80842-9.
- Ni, W., Xu, S.-L., González-Grandío, E., Chalkley, R. J., Huhmer, A. F. R., Burlingame, A. L., Wang, Z.-Y. and Quail, P. H. (2017) 'PPKs mediate direct signal transfer from phytochrome photoreceptors to transcription factor PIF3', *Nature Communications*, 8(May), p. 15236. doi: 10.1038/ncomms15236.
- Ni, W., Xu, S.-L., Tepperman, J. M., Stanley, D. J., Maltby, D. a., Gross, J. D., Burlingame, a. L., Wang, Z.-Y. and Quail, P. H. (2014) 'A mutually assured destruction mechanism attenuates light signaling in Arabidopsis', *Science*, 344(6188), pp. 1160–1164. doi: 10.1126/science.1250778.
- Nozaki, D., Iwata, T., Ishikawa, T., Todo, T., Tokutomi, S. and Kandori, H. (2004) 'Role of Gln1029 in the photoactivation processes of the LOV2 domain in Adiantum phytochrome3', *Biochemistry*. doi: 10.1021/bi0494727.
- Oide, M., Okajima, K., Kashojiya, S., Takayama, Y., Oroguchi, T., Hikima, T., Yamamoto, M. and Nakasako, M. (2016) 'Blue Light-excited Light-Oxygen-Voltage-sensing Domain 2 (LOV2) Triggers a Rearrangement of the Kinase Domain to Induce Phosphorylation Activity in Arabidopsis Phototropin1.', *The Journal of Biological Chemistry*. American Society for Biochemistry and Molecular Biology, 291(38), pp. 19975–84. doi: 10.1074/jbc.M116.735787.
- Oikawa, K., Kasahara, M., Kiyosue, T., Kagawa, T., Suetsugu, N., Takahashi, F., Kanegae, T., Niwa, Y., Kadota, A., Wada, M. (2003) 'CHLOROPLAST UNUSUAL POSITIONING1 Is Essential for Proper Chloroplast Positioning', *The Plant Cell*. doi: 10.1105/tpc.016428.

- Oikawa, K., Yamasato, A., Kong, S.-G., Kasahara, M., Nakai, M., Takahashi, F., Ogura, Y., Kagawa, T. and Wada, M. (2008) 'Chloroplast Outer Envelope Protein CHUP1 Is Essential for Chloroplast Anchorage to the Plasma Membrane and Chloroplast Movement', *Plant Physiology*. doi: 10.1104/pp.108.123075.
- Oka, Y., Matsushita, T., Mochizuki, N., Suzuki, T. and Tokutomi, S. (2004) 'Functional Analysis of a 450 – Amino Acid N-Terminal Fragment of Phytochrome B in Arabidopsis', *The Plant Cell*. doi: 10.1105/tpc.104.022350.phytochrome.
- Okajima, K., Matsuoka, D. and Tokutomi, S. (2011) 'LOV2-linker-kinase phosphorylates LOV1-containing N-terminal polypeptide substrate via photoreaction of LOV2 in Arabidopsis phototropin1', *FEBS Letters*. doi: 10.1016/j.febslet.2011.10.003.
- Oravec, A. (2006) 'CONSTITUTIVELY PHOTOMORPHOGENIC1 Is Required for the UV-B Response in Arabidopsis', *The Plant Cell*, 18(8), pp. 1975–1990. doi: 10.1105/tpc.105.040097.
- Parks, B. M. and Quail, P. H. (1993) 'hy8, a new class of arabidopsis long hypocotyl mutants deficient in functional phytochrome A.', *The Plant Cell*. American Society of Plant Biologists, 5(1), pp. 39–48. doi: 10.1105/tpc.5.1.39.
- Parks, B. M., Quail, P. H. and Hangarter, R. P. (1996) 'Phytochrome A regulates red-light induction of phototropic enhancement in Arabidopsis.', *Plant Physiology*, 110(1), pp. 155–162. doi: 10.1104/pp.110.1.155.
- Pedmale, U. V., Huang, S. S. C., Zander, M., Cole, B. J., Hetzel, J., Ljung, K., Reis, P. A. B., Sridevi, P., Nito, K., Nery, J. R., Ecker, J. R. and Chory, J. (2016) 'Cryptochromes Interact Directly with PIFs to Control Plant Growth in Limiting Blue Light', *Cell*. Elsevier Inc., 164(1–2), pp. 233–245. doi: 10.1016/j.cell.2015.12.018.
- Pedmale, U. V. and Liscum, E. (2007) 'Regulation of phototropic signaling in Arabidopsis via phosphorylation state changes in the phototropin 1-interacting protein NPH3', *Journal of Biological Chemistry*, 282(27), pp. 19992–20001. doi: 10.1074/jbc.M702551200.
- Perrella, G. and Kaiserli, E. (2016) 'Light behind the curtain: photoregulation of nuclear architecture and chromatin dynamics in plants', *New Phytologist*, 212(4), pp. 908–919. doi: 10.1111/nph.14269.

- Peter, E., Dick, B. and Baeurle, S. A. (2010) 'Mechanism of signal transduction of the LOV2-J $\alpha$  photosensor from *Avena sativa*', *Nature Communications*. doi: 10.1038/ncomms1121.
- Petersen, J., Inoue, S. ichiro, Kelly, S. M., Sullivan, S., Kinoshita, T. and Christie, J. M. (2017) 'Functional characterization of a constitutively active kinase variant of Arabidopsis phototropin 1', *Journal of Biological Chemistry*. doi: 10.1074/jbc.M117.799643.
- Petroutsos, D., Tokutsu, R., Maruyama, S., Flori, S., Greiner, A., Magneschi, L., Cusant, L., Kottke, T., Mittag, M., Hegemann, P., Finazzi, G. and Minagawa, J. (2016) 'A blue-light photoreceptor mediates the feedback regulation of photosynthesis', *Nature*. doi: 10.1038/nature19358.
- Preston, J. C. and Hileman, L. C. (2013) 'Functional Evolution in the Plant SQUAMOSA-PROMOTER BINDING PROTEIN-LIKE (SPL) Gene Family', *Frontiers in Plant Science*, 4(April), pp. 1–13. doi: 10.3389/fpls.2013.00080.
- Preuten, T., Blackwood, L., Christie, J. M. and Fankhauser, C. (2015) 'Lipid anchoring of Arabidopsis phototropin 1 to assess the functional significance of receptor internalization : should I stay or should I go ?' *New Phytologist*, 206(3), pp.1038-1050.
- Pudasaini, A., El-Arab, K. K. and Zoltowski, B. D. (2015) 'LOV-based optogenetic devices: light-driven modules to impart photoregulated control of cellular signaling', *Frontiers in Molecular Biosciences*, 2(May), pp. 1–15. doi: 10.3389/fmolb.2015.00018.
- Pudasaini, A., Shim, J. S., Song, Y. H., Shi, H., Kiba, T., Somers, D. E., Imaizumi, T. and Zoltowski, B. D. (2017) 'Kinetics of the LOV domain of ZEITLUPE Determine its Circadian Function in Arabidopsis', *eLife*, 6(1), pp. 1–27. doi: 10.7554/eLife.21646.
- Pudasaini, A. and Zoltowski, B. D. (2013) 'Zeitlupe Senses Blue-Light Fluence to Mediate Circadian Timing In Arabidopsis Thaliana', *Biochemistry*, 52(40), pp. 7150–7158. doi: 10.1021/bi401027n.
- Qiu, Y., Pasoreck, E. K., Reddy, A. K., Nagatani, A., Ma, W., Chory, J. and Chen, M. (2017) 'Mechanism of early light signaling by the carboxy-terminal output module of Arabidopsis phytochrome B', *Nature Communications*. Springer US, 8(1). doi: 10.1038/s41467-017-02062-6.

- Raffelberg, S., Mansurova, M., Gärtner, W. and Losi, A. (2011) 'Modulation of the photocycle of a LOV domain photoreceptor by the hydrogen-bonding network', *Journal of the American Chemical Society*. doi: 10.1021/ja1097379.
- Rao, A. V. and Rao, L. G. (2007) 'Carotenoids and human health', *Pharmacological Research*. Academic Press, 55(3), pp. 207–216. doi: 10.1016/J.PHRS.2007.01.012.
- Reichel, M., Liao, Y., Rettel, M., Ragan, C., Evers, M., Alleaume, A.-M., Horos, R., Hentze, M. W., Preiss, T. and Millar, A. A. (2016) 'In Planta Determination of the mRNA-Binding Proteome of Arabidopsis Etiolated Seedlings', *The Plant Cell*. doi: 10.1105/tpc.16.00562.
- Rizzini, L., Favory, J. J., Cloix, C., Faggionato, D., O'Hara, A., Kaiserli, E., Baumeister, R., Schäfer, E., Nagy, F., Jenkins, G. I. and Ulm, R. (2011) 'Perception of UV-B by the arabidopsis UVR8 protein', *Science*, 332(6025), pp. 103–106. doi: 10.1126/science.1200660.
- Roberts, D., Pedmale, U. V., Morrow, J., Sachdev, S., Lechner, E., Tang, X., Zheng, N., Hannink, M., Genschik, P. and Liscum, E. (2011) 'Modulation of Phototropic Responsiveness in Arabidopsis through Ubiquitination of Phototropin 1 by the CUL3-Ring E3 Ubiquitin Ligase CRL3NPH3', *The Plant Cell*, 23(10), pp. 3627–3640. doi: 10.1105/tpc.111.087999.
- Rockwell, N. C., Su, Y.-S. and Lagarias, J. C. (2006) 'Phytochrome structure and signaling mechanisms.', *Annual Review of Plant Biology*, 57, pp. 837–858. doi: 10.1146/annurev.arplant.56.032604.144208.
- Rosenfeldt, G., Viana, R. M., Mootz, H. D., Von Arnim, A. G. and Batschauer, A. (2008) 'Chemically induced and light-independent cryptochrome photoreceptor activation', *Molecular Plant*, 1(1), pp. 4–14. doi: 10.1093/mp/ssm002.
- Sakai, T., Kagawa, T., Kasahara, M., Swartz, T. E., Christie, J. M., Briggs, W. R., Wada, M. and Okada, K. (2001) 'Arabidopsis *nph1* and *np11*: Blue light receptors that mediate both phototropism and chloroplast relocation', *Proceedings of the National Academy of Sciences*, 98(12), pp. 6969–6974. doi: 10.1073/pnas.101137598.
- Sakai, T., Wada, T., Ishiguro, S. and Okada, K. (2000) 'RPT2. A signal transducer of the

- phototropic response in Arabidopsis', *The Plant Cell*, 12(2), pp. 225–236. doi: 10.1016/S1369-5266(00)80033-3.
- Sakamoto, K. and Briggs, W. R. (2002) 'Cellular and subcellular localization of phototropin 1.', *The Plant Cell*, 14(8), pp. 1723–1735. doi: 10.1105/tpc.003293.
- Sakamoto, K. and Nagatani, A. (1996) 'Nuclear localization activity of phytochrome B.', *The Plant Journal*. doi: 10.1046/j.1365-313X.1996.10050859.x.
- Salomon, M., Christie, J. M., Knieb, E., Lempert, U. and Briggs, W. R. (2000) 'Photochemical and mutational analysis of the FMN-binding domains of the plant blue light receptor, phototropin', *Biochemistry*. doi: 10.1021/bi000585+.
- Salomon, M., Lempert, U. and Rüdiger, W. (2004) 'Dimerization of the plant photoreceptor phototropin is probably mediated by the LOV1 domain', *FEBS Letters*, 572(1–3), pp. 8–10. doi: 10.1016/j.febslet.2004.06.081.
- Salomon, M., Zacherl, M. and Rüdiger, W. (1997) 'Phototropism and protein phosphorylation in higher plants: Unilateral blue light irradiation generates a directional gradient of protein phosphorylation across the oat coleoptile', *Botanica Acta*. doi: 10.1111/j.1438-8677.1997.tb00631.x.
- Sang, Y., Li, Q., Rubio, V., Zhang, Y., Mao, J. and Deng, X. (2005) 'N-Terminal Domain – Mediated Homodimerization Is Required for Photoreceptor Activity of Arabidopsis', *The Plant Cell*, 17(May), pp. 1569–1584. doi: 10.1105/tpc.104.029645.strong.
- Schepens, I., Boccalandro, H. E., Kami, C., Casal, J. J. and Fankhauser, C. (2008) 'PHYTOCHROME KINASE SUBSTRATE4 Modulates Phytochrome-Mediated Control of Hypocotyl Growth Orientation', *Plant Physiology*, 147(2), pp. 661–671. doi: 10.1104/pp.108.118166.
- Schmidt Von Braun, S. and Schleiff, E. (2008) 'The chloroplast outer membrane protein CHUP1 interacts with actin and profilin', *Planta*. doi: 10.1007/s00425-007-0688-7.
- Schultz, T. F., Kiyosue, T., Yanovsky, M., Wada, M. and Kay, S. a (2001) 'A role for LKP2 in the circadian clock of Arabidopsis.', *The Plant Cell*, 13(12), pp. 2659–2670. doi: 10.1105/tpc.010332.

- Schumacher, P., Demarsy, E., Waridel, P., Petrolati, L. A., Trevisan, M. and Fankhauser, C. (2018) 'A phosphorylation switch turns a positive regulator of phototropism into an inhibitor of the process', *Nature Communications*. doi: 10.1038/s41467-018-04752-1.
- Selby, C. P. and Sancar, A. (2006) 'A cryptochrome/photolyase class of enzymes with single-stranded DNA-specific photolyase activity', *Proceedings of the National Academy of Sciences*, 103(47), pp. 17696–17700. doi: 10.1073/pnas.0607993103.
- Sellaro, R., Crepy, M., Trupkin, S. A., Karayekov, E., Buchovsky, A. S., Rossi, C. and Casal, J. J. (2010) 'Cryptochrome as a sensor of the blue/green ratio of natural radiation in Arabidopsis.', *Plant Physiology*, 154(1), pp. 401–409. doi: 10.1104/pp.110.160820.
- Sharrock, R. A., Clack T., (2002) 'Patterns of Expression and Normalized Levels of the Five Arabidopsis Phytochromes', *Plant Physiology*, 130(1), pp. 442–456. doi: 10.1104/pp.005389.
- Sharrock, R. A. and Quail, P. H. (1989) 'Novel phytochrome sequences in Arabidopsis thaliana: structure, evolution, and differential expression of a plant regulatory photoreceptor family.', *Genes & Development*, 3(11), pp. 1745–1757. doi: 10.1101/gad.3.11.1745.
- Shen, H., Zhu, L., Castillon, A., Majee, M., Downie, B. and Huq, E. (2008) 'Light-Induced Phosphorylation and Degradation of the Negative Regulator PHYTOCHROME-INTERACTING FACTOR1 from Arabidopsis Depend upon Its Direct Physical Interactions with Photoactivated Phytochromes', *The Plant Cell*. doi: 10.1105/tpc.108.060020.
- Shen, Y., Khanna, R., Carle, C. M. and Quail, P. H. (2007) 'Phytochrome Induces Rapid PIF5 Phosphorylation and Degradation in Response to Red-Light Activation', *Plant Physiology*. doi: 10.1104/pp.107.105601.
- Shin, A. Y., Han, Y. J., Baek, A., Ahn, T., Kim, S. Y., Nguyen, T. S., Son, M., Lee, K. W., Shen, Y., Song, P. S. and Kim, J. Il (2016) 'Evidence that phytochrome functions as a protein kinase in plant light signalling', *Nature Communications*. Nature Publishing Group, 7(May), pp. 1–13. doi: 10.1038/ncomms11545.
- Shinomura, T., Nagatani, a, Hanzawa, H., Kubota, M., Watanabe, M. and Furuya, M.

(1996) 'Action spectra for phytochrome A- and B-specific photoinduction of seed germination in *Arabidopsis thaliana*.' , *Proceedings of the National Academy of Sciences of the United States of America*, 93(15), pp. 8129–8133. doi: 10.1073/pnas.93.15.8129.

Smith, H. (2000) 'Phytochromes and light signal perception by plants - An emerging synthesis', *Nature*, 407(6804), pp. 585–591. doi: 10.1038/35036500.

Somers, D. E., Schultz, T. F., Milnamow, M. and Kay, S. A. (2000) 'ZEITLUPE encodes a novel clock-associated PAS protein from *Arabidopsis*' , *Cell*, 101(3), pp. 319–329. doi: 10.1016/S0092-8674(00)80841-7.

Somers, D., Sharrock, R., Tepperman, J. and Quail, P. (1991) 'The hy3 Long Hypocotyl Mutant of *Arabidopsis* Is Deficient in Phytochrome B.' , *The Plant cell*. American Society of Plant Biologists, 3(12), pp. 1263–1274. doi: 10.1105/tpc.3.12.1263.

Song, Y. H., Estrada, D. a., Johnson, R. S., Kim, S. K., Lee, S. Y., MacCoss, M. J. and Imaizumi, T. (2014) 'Distinct roles of FKF1, GIGANTEA, and ZEITLUPE proteins in the regulation of CONSTANS stability in *Arabidopsis* photoperiodic flowering' , *Proceedings of the National Academy of Sciences*, 111(49), pp. 17672–17677. doi: 10.1073/pnas.1415375111.

Song, Y. H., Ito, S. and Imaizumi, T. (2013) 'Flowering time regulation: Photoperiod- and temperature-sensing in leaves' , *Trends in Plant Science*. doi: 10.1016/j.tplants.2013.05.003.

Spalding, E. P. and Folta, K. M. (2005) 'Illuminating topics in plant photobiology' , *Plant, Cell and Environment*, 28(1), pp. 39–53. doi: 10.1111/j.1365-3040.2004.01282.x.

Stone, J. M., Liang, X., Nekl, E. R. and Stiers, J. J. (2005) 'Arabidopsis AtSPL14, a plant-specific SBP-domain transcription factor, participates in plant development and sensitivity to fumonisin B1' , *Plant Journal*, 41(5), pp. 744–754. doi: 10.1111/j.1365-313X.2005.02334.x.

Su, Y. and Lagarias, J. C. (2007) 'Light-independent phytochrome signaling mediated by dominant GAF domain tyrosine mutants of *Arabidopsis* phytochromes in transgenic plants.' , *The Plant Cell*, 19(7), pp. 2124–2139. doi: 10.1105/tpc.107.051516.

- Suetsugu, N., Kagawa, T., Wada, M. and Corporation, T. (2005) 'An Auxilin-Like J-Domain Protein, JAC1, Regulates Phototropin-Mediated Chloroplast Movement in Arabidopsis.' *Plant Physiology*, 139(1), pp.151-162.
- Suetsugu, N., Takemiya, A., Kong, S.-G., Higa, T., Komatsu, A., Shimazaki, K., Kohchi, T. and Wada, M. (2016) 'RPT2/NCH1 subfamily of NPH3-like proteins is essential for the chloroplast accumulation response in land plants', *Proceedings of the National Academy of Sciences*. doi: 10.1073/pnas.1602151113.
- Suetsugu, N. and Wada, M. (2012) 'Advances in Photosynthesis (Chapter 11): Chloroplast Photorelocation Movement: A Sophisticated Strategy for Chloroplasts to Perform Efficient Photosynthesis', *Advances in Photosynthesis: Fundamental Aspects*, pp. 215–234. doi: 10.5772/1385.
- Suetsugu, N., Yamada, N., Kagawa, T., Yonekura, H., Uyeda, T. Q. P., Kadota, A. and Wada, M. (2010) 'Two kinesin-like proteins mediate actin-based chloroplast movement in Arabidopsis thaliana', *Proceedings of the National Academy of Sciences*. doi: 10.1073/pnas.0912773107.
- Sullivan, S., Hart, J. E., Rasch, P., Walker, C. H. and Christie, J. M. (2016) 'Phytochrome A Mediates Blue-Light Enhancement of Second-Positive Phototropism in Arabidopsis', *Frontiers in Plant Science*, 7(March), pp. 1–12. doi: 10.3389/fpls.2016.00290.
- Sullivan, S., Kaiserli, E., Tseng, T.-S. and Christie, J. M. (2010) 'Subcellular localization and turnover of Arabidopsis phototropin 1.', *Plant Signaling & Behavior*, 5(2), pp. 184–186. doi: 10.4161/psb.5.2.11082.
- Sullivan, S., Thomson, C. E., Lamont, D. J., Jones, M. a and Christie, J. M. (2008) 'In vivo phosphorylation site mapping and functional characterization of Arabidopsis phototropin 1.', *Molecular Plant*, 1(1), pp. 178–194. doi: 10.1093/mp/ssm017.
- Swartz, T. E., Corchnoy, S. B., Christie, J. M., Lewis, J. W., Szundi, I., Briggs, W. R. and Bogomolni, R. A. (2001) 'The Photocycle of a Flavin-binding Domain of the Blue Light Photoreceptor Phototropin', *Journal of Biological Chemistry*, 276(39), pp. 36493–36500. doi: 10.1074/jbc.M103114200.
- Takakado, A., Nakasone, Y., Okajima, K., Tokutomi, S. and Terazima, M. (2017) 'Light-

Induced Conformational Changes of LOV2-Kinase and the Linker Region in Arabidopsis Phototropin2', *Journal of Physical Chemistry B*, 121(17), pp. 4414–4421. doi: 10.1021/acs.jpcc.7b01552.

Takemiya, A., Sugiyama, N., Fujimoto, H., Tsutsumi, T., Yamauchi, S., Hiyama, A., Tada, Y., Christie, J. M. and Shimazaki, K. I. (2013) 'Phosphorylation of BLUS1 kinase by phototropins is a primary step in stomatal opening', *Nature Communications*. Nature Publishing Group, 4(May), pp. 1–8. doi: 10.1038/ncomms3094.

Thiele, a, Herold, M., Lenk, I., Quail, P. H. and Gatz, C. (1999) 'Heterologous expression of Arabidopsis phytochrome B in transgenic potato influences photosynthetic performance and tuber development.', *Plant Physiology*, 120(1), pp. 73–82. doi: 10.1104/pp.120.1.73.

Thompson, C. (2008) *Investigation of phototropin blue light receptor function and signalling in arabidopsis*. University of Glasgow.

Tseng, T.-S. and Briggs, W. R. (2010) 'The Arabidopsis rcn1-1 Mutation Impairs Dephosphorylation of Phot2, Resulting in Enhanced Blue Light Responses', *The Plant Cell*, 22(2), pp. 392–402. doi: 10.1105/tpc.109.066423.

Tsuchida-Mayama, T., Nakano, M., Uehara, Y., Sano, M., Fujisawa, N., Okada, K. and Sakai, T. (2008) 'Mapping of the phosphorylation sites on the phototropic signal transducer, NPH3', *Plant Science*. doi: 10.1016/j.plantsci.2008.03.018.

Tsutsumi, T., Takemiya, A., Harada, A. and Shimazaki, K. ichiro (2013) 'Disruption of ROOT PHOTOTROPISM2 gene does not affect phototropin-mediated stomatal opening', *Plant Science*. Elsevier Ireland Ltd, 201–202(1), pp. 93–97. doi: 10.1016/j.plantsci.2012.11.012.

Turck, F., Fornara, F. and Coupland, G. (2008) 'Regulation and Identity of Florigen: FLOWERING LOCUS T Moves Center Stage', *Annual Review of Plant Biology*, 59(1), pp. 573–594. doi: 10.1146/annurev.arplant.59.032607.092755.

Valverde, F., Mouradov, A., Soppe, W., Ravenscroft, D., Samach, A. and Coupland, G. (2004) 'Photoreceptor Regulation of CONSTANS Protein in Photoperiodic Flowering', *Science*. doi: 10.1126/science.1091761.

- Vogt, J. H. M. and Schippers, J. H. M. (2015) 'Setting the PAS, the role of circadian PAS domain proteins during environmental adaptation in plants', *Frontiers in Plant Science*, 6(July), pp. 1–10. doi: 10.3389/fpls.2015.00513.
- Wada, M. and Kong, S.-G. (2018) 'Actin-mediated movement of chloroplasts', *Journal of Cell Science*, 131(2), p. jcs210310. doi: 10.1242/jcs.210310.
- Wagner, D. and Quail, P. H. (1995) 'Mutational analysis of phytochrome B identifies a small COOH-terminal-domain region critical for regulatory activity.', *Proceedings of the National Academy of Sciences of the United States of America*, 92(19), pp. 8596–8600. doi: 10.1073/pnas.92.19.8596.
- Wagner, D., Tepperman, J. and Quail, P. (1991) 'Overexpression of Phytochrome B Induces a Short Hypocotyl Phenotype in Transgenic Arabidopsis.', *The Plant Cell*. doi: 10.1105/tpc.3.12.1275.
- Walter, M., Chaban, C., Schütze, K., Batistic, O., Weckermann, K., Näke, C., Blazevic, D., Grafen, C., Schumacher, K., Oecking, C., Harter, K. and Kudla, J. (2004) 'Visualization of protein interactions in living plant cells using bimolecular fluorescence complementation', *Plant Journal*, 40(3), pp. 428–438. doi: 10.1111/j.1365-313X.2004.02219.x.
- Wan, Y., Jasik, J., Wang, L., Hao, H., Volkmann, D., Menzel, D., Mancuso, S., Baluska, F. and Lin, J. (2012) 'The Signal Transducer NPH3 Integrates the Phototropin1 Photosensor with PIN2-Based Polar Auxin Transport in Arabidopsis Root Phototropism', *The Plant Cell*, 24(2), pp. 551–565. doi: 10.1105/tpc.111.094284.
- Wang, Q., Zuo, Z., Wang, X., Gu, L., Yoshizumi, T., Yang, Z., Yang, L., Liu, Q., Liu, W., Han, Y. J., Kim, J. Il, Liu, B., Wohlschlegel, J. A., Matsui, M., Oka, Y. and Lin, C. (2016) 'Photoactivation and inactivation of Arabidopsis cryptochrome 2', *Science*. doi: 10.1126/science.aaf9030.
- Wang, Q., Zuo, Z., Wang, X., Liu, Q., Gu, L., Oka, Y. and Lin, C. (2018) 'Beyond the photocycle — how cryptochromes regulate photoresponses in plants?', *Current Opinion in Plant Biology*. Elsevier Ltd, 45, pp. 120–126. doi: 10.1016/j.pbi.2018.05.014.
- Wang, X., Wang, Q., Han, Y. J., Liu, Q., Gu, L., Yang, Z., Su, J., Liu, B., Zuo, Z., He, W., Wang, J., Liu, B., Matsui, M., Kim, J. Il, Oka, Y. and Lin, C. (2017) 'A CRY–BIC

negative-feedback circuitry regulating blue light sensitivity of Arabidopsis', *Plant Journal*, 92(3), pp. 426–436. doi: 10.1111/tpj.13664.

Wang, Y., Noguchi, K., Ono, N., Inoue, S. -i., Terashima, I. and Kinoshita, T. (2014) 'Overexpression of plasma membrane H<sup>+</sup>-ATPase in guard cells promotes light-induced stomatal opening and enhances plant growth', *Proceedings of the National Academy of Sciences*. doi: 10.1073/pnas.1305438111.

Whippo, C. W., Khurana, P., Davis, P. A., Deblasio, S. L., Desloover, D., Staiger, C. J. and Hangarter, R. P. (2011) 'THRUMIN1 is a light-regulated actin-bundling protein involved in chloroplast motility', *Current Biology*. doi: 10.1016/j.cub.2010.11.059.

Whitelam, G. C., Johnson, E., Peng J., Carol, P., Anderson, M. L., Cowl, J. S., Harberd, N. P. (1993) 'Phytochrome A Null Mutants of Arabidopsis Display a Wild-Type Phenotype in White Light', *the Plant Cell Online*, 5(7), pp. 757–768. doi: 10.1105/tpc.5.7.757.

Whitelam, G. C. and Johnson, C. B. (1982) 'Photomorphogenesis in *Impatiens parviflora* and other Plant Species Under Simulated Natural Canopy Radiations', *New Phytologist*, 90(4), pp. 611–618. doi: 10.1111/j.1469-8137.1982.tb03270.x.

Whitelam, G. C., Johnson, E., Peng, J., Carol, P., Anderson, M. L., Cowl, J. S. and Harberd, N. P. (1993) 'Phytochrome A null mutants of Arabidopsis display a wild-type phenotype in white light.', *The Plant Cell*. American Society of Plant Biologists, 5(7), pp. 757–68. doi: 10.1105/tpc.5.7.757.

Willige, B. C., Ahlers, S., Zourelidou, M., Barbosa, I. C. R., Demarsy, E., Trevisan, M., Davis, P. A., Roelfsema, M. R. G., Hangarter, R., Fankhauser, C. and Schwechheimer, C. (2013) 'D6PK AGCVIII Kinases Are Required for Auxin Transport and Phototropic Hypocotyl Bending in *Arabidopsis*', *The Plant Cell*. doi: 10.1105/tpc.113.111484.

Di Wu, Hu, Q., Yan, Z., Chen, W., Yan, C., Huang, X., Zhang, J., Yang, P., Deng, H., Wang, J., Deng, X. and Shi, Y. (2012) 'Structural basis of ultraviolet-B perception by UVR8', *Nature*. doi: 10.1038/nature10931.

Xie, Y., Liu, Y., Wang, H., Ma, X., Wang, B., Wu, G. and Wang, H. (2017) 'Phytochrome-interacting factors directly suppress MIR156 expression to enhance shade-avoidance syndrome in Arabidopsis', *Nature Communications*. doi: 10.1038/s41467-017-

00404-y.

Xue, Y., Xing, J., Wan, Y., Lv, X., Fan, L., Zhang, Y., Song, K., Wang, L., Wang, X., Deng, X., Baluška, F., Christie, J. M. and Lin, J. (2018) 'Arabidopsis Blue Light Receptor Phototropin 1 Undergoes Blue Light-Induced Activation in Membrane Microdomains', *Molecular Plant*. Cell Press, 11(6), pp. 846–859. doi: 10.1016/J.MOLP.2018.04.003.

Yamaguchi, R., Nakamura, M., Mochizuki, N., Kay, S. A. and Nagatani, A. (1999) 'Light-dependent translocation of a phytochrome B-GFP fusion protein to the nucleus in transgenic Arabidopsis', *Journal of Cell Biology*. doi: 10.1083/jcb.145.3.437.

Yamamoto, A., Iwata, T., Tokutomi, S. and Kandori, H. (2008) 'Role of Phe1010 in light-induced structural changes of the neo1-LOV2 domain of Adiantum', *Biochemistry*. doi: 10.1021/bi701851v.

Yang, H. Q., Wu, Y. J., Tang, R. H., Liu, D., Liu, Y. and Cashmore, A. R. (2000) 'The C termini of Arabidopsis cryptochromes mediate a constitutive light response', *Cell*. doi: 10.1016/S0092-8674(00)00184-7.

Yanovsky, M. J., Luppi, J. P., Kirchbauer, D., Ogorodnikova O.B., Sineshchekov, V.A., Adam, E., Kircher, S., Staneloni, R. J., Schäfer, E., Nagy, F., Casal, J. J. (2002) 'Missense Mutation in the PAS2 Domain of Phytochrome A Impairs Subnuclear Localization and a Subset of Responses', *The Plant Cell*, 14(7), pp. 1591–1603. doi: 10.1105/tpc.000521.

Yanovsky, M. J., Casal, J. J. and Whitelam, G. C. (1995) 'Phytochrome A, phytochrome B and HY4 are involved in hypocotyl growth responses to natural radiation in Arabidopsis: weak de-etiolation of the phyA mutant under dense canopies', *Plant, Cell and Environment*. Wiley/Blackwell (10.1111), 18(7), pp. 788–794. doi: 10.1111/j.1365-3040.1995.tb00582.x.

van Zanten, M., Pons, T. L., Janssen, J. A. M., Voeselek, L. A. C. J. and Peeters, A. J. M. (2010) 'On the relevance and control of leaf angle', *Critical Reviews in Plant Sciences*. doi: 10.1080/07352689.2010.502086.

Zayner, J. P., Antoniou, C. and Sosnick, T. R. (2012) 'The amino-terminal helix modulates light-activated conformational changes in AsLOV2', *Journal of Molecular Biology*. Elsevier Ltd, 419(1–2), pp. 61–74. doi: 10.1016/j.jmb.2012.02.037.

- Zayner, J. P. and Sosnick, T. R. (2014) 'Factors that control the chemistry of the LOV domain photocycle', *PLoS ONE*, 9(1). doi: 10.1371/journal.pone.0087074.
- Zeugner, A., Byrdin, M., Bouly, J. P., Bakrim, N., Giovani, B., Brettel, H. and Ahmad, M. (2005) 'Light-induced electron transfer in Arabidopsis cryptochrome-1 correlates with in vivo function', *Journal of Biological Chemistry*, 280(20), pp. 19437–19440. doi: 10.1074/jbc.C500077200.
- Zhang, J., Stankey, R. J. and Vierstra, R. D. (2013) 'Structure-guided engineering of plant phytochrome B with altered photochemistry and light signaling.', *Plant Physiology*, 161(3), pp. 1445–57. doi: 10.1104/pp.112.208892.
- Zhao, X., Zhao, Q., Xu, C., Wang, J., Zhu, J., Shang, B. and Zhang, X. (2018) 'Phot2-regulated relocation of NPH3 mediates phototropic response to high-intensity blue light in *Arabidopsis thaliana*', *Journal of Integrative Plant Biology*. Wiley/Blackwell (10.1111), 60(7), pp. 562–577. doi: 10.1111/jipb.12639.
- Zikihara, K., Iwata, T., Matsuoka, D., Kandori, H., Todo, T. and Tokutomi, S. (2006) 'Photoreaction cycle of the light, oxygen, and voltage domain in FKF1 determined by low-temperature absorption spectroscopy', *Biochemistry*, 45(36), pp. 10828–10837. doi: 10.1021/bi0607857.
- Zoltowski, B. D. and Crane, B. R. (2008) 'Light activation of the LOV protein vivid generates a rapidly exchanging dimer', *Biochemistry*. doi: 10.1021/bi8007017.
- Zoltowski, B. D., Schwerdtfeger, C., Widom, J., Loros, J. J., Bilwes, A. M., Dunlap, J. C. and Crane, B. R. (2007) 'Conformational switching in the fungal light sensor vivid', *Science*. doi: 10.1126/science.1137128.
- Zoltowski, B. D., Vaccaro, B. and Crane, B. R. (2009) 'Mechanism-based tuning of a LOV domain photoreceptor.', *Nature Chemical Biology*, 5(11), pp. 827–834. doi: 10.1038/nchembio.210.
- Zourelidou, M., Muller, I., Willige, B. C., Nill, C., Jikumaru, Y., Li, H. and Schwechheimer, C. (2009) 'The polarly localized D6 PROTEIN KINASE is required for efficient auxin transport in *Arabidopsis thaliana*', *Development*. doi: 10.1242/dev.028365.



